Attitude Control of Microsatellite

Luo Wencheng

School of Electrical & Electronic Engineering

A thesis submitted to the Nanyang Technological University

in fulfillment of the requirement for the degree of

Doctor of Philosophy

2005

Acknowledgement

I am deeply indebted to my supervisor Professor Chu Yun-Chung who has been taking care of me all the time since I came to NTU for study, both academically and personally, and shown understanding to my stupidity. It has been my pleasure to work with Professor Chu, and his perseverance with difficult problems, his strict and precise thinking over academic issues and his keen insights on researches have had a great influence on my work and researches.

I would also like to thank Professor Ling Keck-Voon at Nanyang Technological University (NTU) for his great help on my study and I would also like to thank distinguished Professor Keith Glover at Cambridge University for his valuable discussions and comments on my work during the time when he visited NTU in 2002.

I would like to express my gratitude to my former and present colleagues during the past three years at Instrumentation and System Engineering Laboratory at NTU for their valuable hints, supports, help and interests, and to all friends who help me and make my life at Singapore colorful and interesting. I would also like to thank technicians, Yock, Song Lee Sim, Joanna and Norriki, of Instrumentation and System Engineering Laboratory for their help.

My Ph.D. studies have been financially sponsored by Nanyang Technological University, and I would like to extend my sincere acknowledgements to NTU which enables me to complete my study at NTU.

Finally, I would like to thank my parents and specially appreciate my lovely wife, Li Shumei, for her continuous supports and encouragements to my study and my life at NTU. In the past three years, she has sacrificed her career and her time to support my study and to take care of our family. I hope to devote my gratitude with my heart to my lovely wife for her unselfish devotions to me and our family.

Luo Wencheng

School of Electrical & Electronic Engineering

Nanyang Technological University, Singapore

August 1, 2004

Contents

Summary

In this thesis, we study the robust optimal attitude control problem of microsatellites with disturbances and an uncertain inertia matrix. This is a nonlinear control problem.

As the emphasis is on the development of state-feedback attitude controllers that achieve optimality as well as disturbance attenuation, a brief survey is made of the Lyapunov stability and the disturbance attenuation problems of nonlinear systems.

Using the unit quaternion to represent the attitude of spacecraft and by introducing the concept of extended disturbances, the inverse optimal control method is applied to address the attitude tracking control problem with external disturbances. It is shown by the argument of Lyapunov's method that the proposed attitude feedback controller is optimal with respect to a meaningful cost functional and achieves H_∞ disturbance attenuation without solving the associated Hamilton-Jacobi-Isaacs partial differential equation explicitly. On the basis of the system performance analysis in terms of the performance limitation, guidelines for selecting the controller gains are also given.

For the attitude tracking problem with disturbances and an uncertain inertia matrix, it is addressed by combining the adaptive control method and the inverse optimal control approach. The method of backstepping is applied to construct the control Lyapunov function and a stabilizing control of a particular form. It is shown by the Lyapunov's method that the proposed adaptive feedback controllers are optimal with respect to a family of meaningful cost functionals and also achieve H_∞ disturbance attenuation. Moreover, if certain conditions of the disturbances are satisfied, it is shown that the inverse optimal adaptive controller could achieve asymptotic attitude tracking with a global convergence of tracking errors to zero for all initial conditions.

The proposed inverse optimal attitude control algorithms are demonstrated effective by numerical simulations, in which the input saturations are taken into account.

Finally, to investigate the effects of control saturations in the attitude regulation, local H_2- and H_∞-performance for linear systems with input saturations are analyzed and synthesized in the region of attraction using the linear matrix inequality approach. Using the LMI software, the proposed LMI algorithms are then applied to the linear attitude control problem with disturbances, structured parameter uncertainties and input saturations.

Keywords: Attitude control, spacecraft, nonlinear systems, inverse optimal control, adaptive control, H_∞ disturbance attenuation, extended disturbances, uncertainty, saturation nonlinearity, linear matrix inequalities, generalized H_2 performance.

List of Figures

List of Tables

Chapter 1

Introduction

1.1 Motivation of Research

Low earth orbit (LEO) satellites usually orbit close to the Earth with an altitude less than 1000km and are considered suitable for a number of applications such as mobile communications, remote sensing, earth observations and so on. Especially, due to their low orbit, LEO satellites provide an excellent platform for high-resolution imaging of the earth over a substantial field of view (FOV). Moreover, LEO satellites with large-angle maneuvering capabilities can take immediate actions to point at and observe some special regions.

The earliest satellites were very small and simple because of the limitations of satellite technology and launch vehicle capacity at that time. After late 1960s, more and more large satellites were built owing to gradually maturing technology and growing demands. Since about late 1980s, the following reasons have changed this trend and re-energized the developments of small satellites. First, in the foreseeable future, no launch technology breakthroughs appear to be on the horizon to afford larger satellites. Second, small satellite cluster is a new application suitable for many space missions and replaces part of the space missions usually taken by larger satellites. Third, from a risk-sharing point of view, a number of smaller satellites have a significant reliability advantage over a bigger one. Fourth, small satellite is low in cost, small in size and cheap to launch and thus would be an economical choice due to the limited budget. Therefore, as a kind of modern small satellites, a microsatellite with mass $\leq$ 100kg becomes a promising spacecraft for its advantages of reducing cost, risk and manufacturing time and for the abilities of incorporating newly developed technologies, especially microelectronics, micromachine, new materials, new design methods and new attitude control theory.

Due to these advantages mentioned, LEO microsatellites now play a more and more important role in various space missions, such as position location [2], earth observation [38], space science [75,133], communication [81], new technology demonstration [39] and so on, and are becoming a hotter research topic in universities and companies.

Following the successful launch of the small satellite UoSAT-12 and the commission-

Table 1.1: General Descriptions of NTU Microsatellite

Mission	(1) Hyper-spectral imaging for earth observation (2) Communication service
Mass	$\leq$ 100kg
Orbit	Equatorial orbit (the first choice) or Sun-synchronous orbit (the second choice)
Attitude control type	Three-axis attitude stabilizing control
Attitude actuators	Four reaction wheels, three magnetorquers
Attitude sensors	Three-axis magnetometer, sun sensor, earth sensor, star sensor, GPS (only for experiments), rate gryometers

ing of the Merlion payload system[1] on April 21, 1999, Nanyang Technological University (NTU) has planned to design and develop a fully owned microsatellite, X-Sat, and determined the hyper-spectral imaging for earth observations as its primary mission. It is also required to provide communication services. The preferred altitude of the microsatellite is therefore in the range of 700$\sim$900km. Since the location of Singapore is near the equator, an equatorial orbit is preferred. However, due to the fact that the launch opportunities of small satellite to low equatorial orbit are quite limited, the sun-synchronous orbit is an alternative. General descriptions of this microsatellite are listed in Table 1.1.

As part of the researches related to the NTU X-Sat microsatellite, the work presented in this thesis is fully devoted to the attitude control problem of microsatellites.

1.2 Object of Study

The functional block of a typical attitude determination and control system (ADCS) in a microsatellite is shown in Figure 1.1. The *satellite dynamics block* represents the attitude dynamics as well as the measurements from attitude sensors. The perturbation torques will inevitably affect the spacecraft attitude that will affect the measurements. The sensors data is the output of this block, while input excitations to this block are the torques provided by reaction wheels and magnetorquers. The sensors data is normally subject to sensors errors and noises and is refined by using the *extended Kalman filter block*. The filtered attitude is compared with the reference or target attitude in the *controller block* and then an appropriate control law is invoked to give the torque excitations to the attitude actuators (wheels and magnetorquers).

In order to meet the requirements on attitude acquisition, maneuver, tracking and high-accuracy pointing performance, three-axis attitude control technology is usually applied to a satellite, leading to a typical (nonlinear) multi-input-multi-output (MIMO) control system. For the attitude control of spacecraft in the normal mode, it suffices to assume that the variations of Euler angles at the working point are small and

[1]The small satellite UoSat-12 [39] was designed and manufactured by Surrey University, Britain. The communication payload Merlion subsystem [22] was developed by Nanyang Technological University.

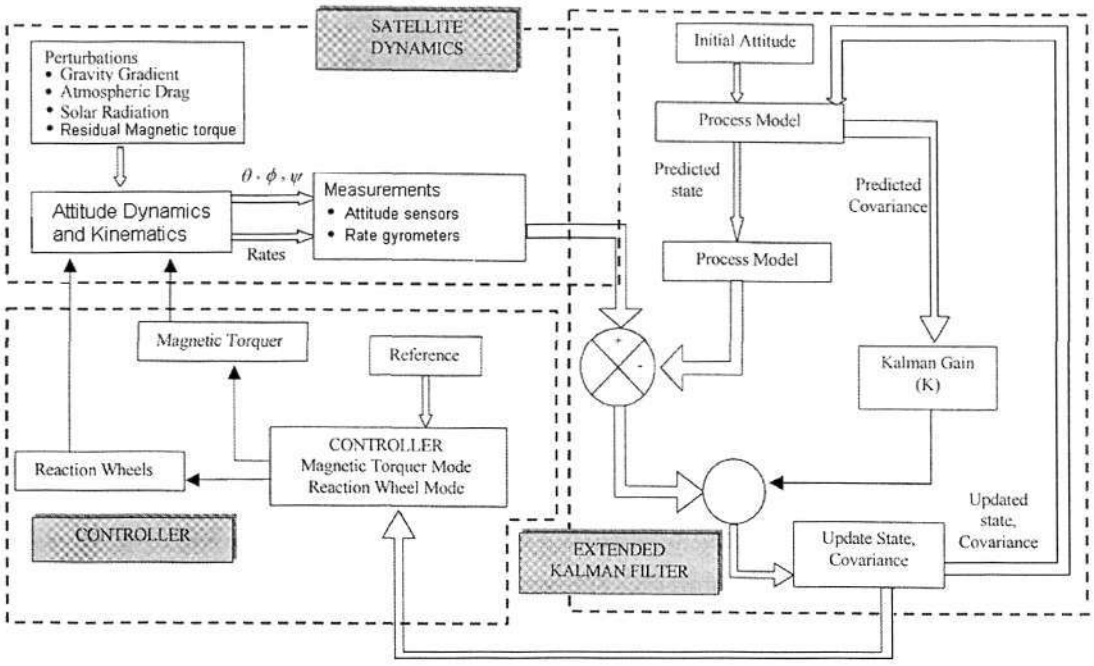

Figure 1.1: Attitude determination and control system

thus we can linearize the attitude equations near the working point and apply linear control theories to the design of attitude controllers. However, when the spacecraft is in large-angle maneuver or attitude tracking, attitude equations are highly nonlinear and coupled. As such, we must consider nonlinear control methods for the large-angle attitude maneuver control and for the attitude tracking control problem.

In the attitude control literature, the state-feedback design is quite common, for example, [1, 25, 57, 64, 65, 101, 125, 128]. There are many types of sensors that could be used to measure the attitude and the angular rate of a spacecraft. For instance, sun sensors and star trackers provide the attitude information and rate gyros provide rate information. Thus, the states (the attitude and the angular rate) of an attitude control system can be measured effectively and accurately by contemporary technologies if appropriate sensors are selected with well-designed filters. Moreover, the state-feedback control provides an equal basis to judge the performance of different types of controllers designed by various control methods.

It is recognized that observers or filters play an important role in ADCS. Although the measurements of attitude and angular rates are available for most satellites by using various sensors, there are indeed practical problems in processing these measurements data from various types of sensors. For instances, the gyrometers and star sensors provide measurements at different sampling frequencies with different accuracies, different delays and different drawbacks. One of the best solutions is to use some (extended) Kalman filters [13] to predict and correct measurements data from sensors. For example, [6] used a star tracker, a three-axis magnetometer and a Kalman filter to provide accurate attitude information. In [140], a Kalman filter was employed for attitude

determination that uses the sun sensor and magnetometer measurements to update a gyro propagated attitude solution. The attitude determination systems (ADS) of the MSX satellite [40] and the global imaging system 2000 satellite [131] contained star trackers for attitude information, ring-laser-gyros for rate information and other coarse sensors. The measurement data were processed within ADS in a double filter process, a measurement mixing filter and a Kalman filter, to minimize the long-term and short-term noise errors. The angular rate measurements from the rate gyros are sampled at a higher frequency while the attitude measurements from the star trackers and other coarse sensors are sampled at lower frequencies. The measurement-mixing filter provides an optimal mixture of attitude and rate measurements and the (extended) Kalman filter provides an optimal estimate of the attitude/rate from the measurements and the dynamics models prediction. The detailed discussions of and solutions to the problems of processing measurement data from various types of sensors using Kalman filters can be found in [40, 117, 118, 131]. Other filters for such an estimation include the state-dependent Riccati equation (SDRE) filter [23], in which the nonlinear attitude model predictions and the nonlinear measurements are parameterized into a linear structure with state-dependent coefficients. For example, this SDRE filter was used in [42] to estimate the angular velocity from attitude vector measurements.

Having understood the practical attitude determination problems and the remedies of using sensors and gyrometers, we could assume that all states including the attitude and the angular velocity are available and measured accurately, and thus this thesis will focus on the design of attitude control laws. The attitude determination problem and the design of filter algorithms are beyond the scope of this thesis.

Two other major problems in the attitude control of a microsatellite are the external disturbances caused by the space environment and the parametric uncertainties of spacecraft's moment-of-inertia matrix. For LEO spacecraft below 1000km, gravity-gradient torque, aerodynamic torque and residual magnetic torque are the major disturbances. On the other hand, the fuel consumption, the movement of payload and the rotation of appendages (such as camera and solar arrays) usually cause variations of moments of inertia, which are considered as parametric uncertainties. For a microsatellite with mass $\leq$ 100kg, its moments of inertia are usually less than 20kg$\cdot$m^2 [127, pp.336-337], thus its attitude is quite sensitive to disturbances and parametric uncertainties.

In the face of nonlinear dynamics, disturbances and parametric uncertainties, the robust control theory provides designers a systematic approach for the synthesis of an attitude controller. Attitude tracking control is a typical nonlinear control problem. Attitude stabilizing control and large-angle attitude maneuver control can be considered as two special cases of the attitude tracking control problem. As such, the primary objective of this thesis is to design state-feedback controllers that are robust to disturbances and parametric uncertainties of the inertia matrix for the attitude tracking control problem and the attitude stabilizing control problem. Also, the optimality of these attitude controllers with respect to some meaningful (quadratic) cost functionals including control efforts and system errors is another important concern.

1.3 An Overview

In this thesis, the attitude tracking control of a rigid spacecraft with disturbances and parametric uncertainties is addressed. For such a problem, the variable structure control, nonlinear H_∞ control and inverse optimal control method are good choices for the controller design. Adaptive control method is also suitable for addressing the parametric uncertainties. The linear attitude control problem subject to input saturations, disturbances and uncertainties is also considered in this thesis. Therefore, we will briefly survey the literature on these topics in this section.

1.3.1 Variable Structure Control

It is well-known that variable structure control (VSC) [54, 102] is robust to disturbances and parametric uncertainties. The main idea behind the variable structure control is to design suitable algorithms for changing the structure of the control system during the course of operation to exploit the desirable features of different structures. Under certain conditions a new behavior, known as sliding mode, can arise in such systems as a result of infinitely frequent switching between different structures. Sliding mode can occur under certain conditions in a dynamical system with discontinuous inputs. Such inputs can force the solution of the system to a hypersurface in the state space where the behavior of the system is dominated by lower-order dynamics and is invariant to external disturbances and parameter variations. In the case when the existence of a sliding mode cannot be guaranteed, the discontinuous control is referred to as the variable structure control algorithm. The use of both sliding mode and variable structure controllers also results in finite time responses. These properties have been extensively applied to design robust controllers for a wide variety of systems [54, 102, 119].

Since the variable structure controllers use highly frequent switchings to achieve the objective of maintaining the solution of the system on the sliding surface and because of the imperfection of switching devices, chattering of the signals in the system occurs in practice. This unexpected feature would be removed by replacing the sign function used in VSC with either a saturation function [27] or an approximate sign function [10]. This action leads to the solution of the closed-loop system being confined into a thin boundary layer around the switching surface, which was clearly stated in [102].

VSC has been successfully applied to spacecraft attitude control problems by many researchers. Authors of [24,32] developed nonglobal VSC algorithms using the minimal attitude representation. Vadali [119] was the first to design a global VSC algorithm for the attitude maneuver control, in which the sliding surface was determined by the use of optimal control theory for a special performance index. However, the analysis appears incomplete as the nonlinear attitude dynamics was neglected. When the input saturation nonlinearity was considered explicitly, a global VSC algorithm [10] was designed for the attitude maneuver problem. Attitude tracking control is more difficult. Among those based on the attitude representation using unit quaternions, the VSC algorithm developed in [73] is not global because the scalar part of the unit quaternion

was restricted to be nonnegative so that the reciprocal of the vector part of the quaternion was used to implement the control law. A global VSC attitude tracking algorithm with input saturation was designed in [9] and the adaptive approach was used to tune the control gain. It is also simulated in Chapter 5 to make a brief comparison between the VSC algorithm in [9] and the H_∞ inverse optimal controller proposed in this thesis.

1.3.2 H_∞ Optimal Attitude Control

Optimal control of rigid bodies has a long history stemming from the interest in the control of rigid spacecraft and aircraft [26,104,121]. The main thruster of this research had been motivated by the time-optimal and fuel-optimal control problems [14,28,98]. The optimal regulation problem over a finite or infinite time horizon was treated in the past mainly for the attitude dynamics subsystem and for special quadratic costs [11,31]. The case of general quadratic costs had also been addressed in [116]. The main obstruction in constructing feedback control laws for optimal regulation control problem stems from the difficulty in solving the Hamilton-Jacobi equation, especially when the cost includes a penalty term on the control effort. In [90], the authors obtained closed-form optimal solutions for special cases of quadratic costs without penalty on the control effort. These control laws asymptotically recover the optimal cost for the kinematics but may lead to high-gain control. When the control penalty is included in the performance index, linear control laws have been constructed which provide an upper bound for a quadratic cost in some specified compact set of initial conditions. Suboptimal results can be obtained by minimizing this upper bound [90]. Alternatively, one can penalize only the high-gain portion of the control input. This approach is based on the optimal results of [58] and was used for both axis-symmetric [115] and nonsymmetric bodies [114].

Time-optimal attitude maneuver control was comprehensively surveyed in [98]. In theory, time-optimal control is a Bang-Bang control. To smoothen the control effort, a smoothing factor was introduced in [7] to design a smooth time-suboptimal control law. Quadratic optimal attitude maneuver control for the complete attitude problem, i.e., including the attitude kinematics, is more difficult and has been addressed in terms of trajectory planning [120] or feedback form [15,16,120]. All works mentioned above on the optimal attitude (maneuver) control is mainly for zero-disturbance attitude control system and these results are sensitive to disturbances and uncertainties. In the face of disturbances and uncertainties, the most advanced efforts towards designing stable optimal attitude controller have been made in [25,57,135] in the framework of nonlinear H_∞ control theory [123] and in [18,83] in robotics in the framework of inverse optimal control theory [35,61].

Nonlinear state-feedback H_∞ suboptimal control

Consider an affine nonlinear system

$$\dot{x} = f(x) + g_2(x)u + g_1(x)d, \quad z = h(x) + D(x)u \tag{1.1}$$

where $x \in \mathcal{R}^n$, $u \in \mathcal{R}^m$, $d \in \mathcal{R}^l$; $f(x)$, $g_1(x)$, $g_2(x)$, $h(x)$ and $D(x)$ are smooth.

The *nonlinear H_∞ suboptimal control problem* is to find a continuous state-feedback control $u = \alpha(x)$ for (1.1) such that the $\mathcal{L}_2$ gain of the closed-loop system from the disturbance d to the output z is $\leq \gamma$, i.e., $\int_0^T ||z(t)||^2 dt \leq \gamma^2 \int_0^T ||d(t)||^2 dt + K(x_0)$ is satisfied for all $T \geq 0$ and for any initial condition $x(0) = x_0$ of (1.1), where $K(x)$ is positive definite in x.

By the work [123], the state-feedback control $u = -g_2^T(\frac{\partial V}{\partial x})^T$ that is synthesized from the solution $V(x)$ to the Hamilton-Jacobi-Isaacs (HJI) partial differential inequality

$$\frac{\partial V}{\partial x} f(x) + \frac{1}{2}\frac{\partial V}{\partial x}\Big[\frac{1}{\gamma^2} g_1(x) g_1(x)^T - g_2(x) g_2(x)^T\Big]\frac{\partial^T V}{\partial x} + \frac{1}{2} h(x)^T h(x) \leq 0 \qquad (1.2)$$

solves the nonlinear H_∞ control problem for the system (1.1). The nonlinear H_∞ control problem and its characterizations will be reviewed in Section 3.4 in Chapter 3.

The most challenging task in nonlinear H_∞ control is to solve the HJI inequality (1.2). Unfortunately, it is very difficult to do so and there are no general solutions to (1.2), and thus the applications of nonlinear H_∞ control remain open. Various methods have been proposed in an attempt to solve the HJI equation. For some particular choices of a control Lyapunov function candidate $V(x)$ and an output z, nonlinear H_∞ suboptimal control had been applied to the spacecraft attitude control problem [25,57, 65,135], in which algebraic and geometric tools were employed to study a particular H_∞ suboptimal control problem by solving the associated HJI partial differential inequality. However, the H_∞ suboptimal control laws derived in [25, 57, 65, 135] were designed to solve the attitude stabilizing control problem and the $\mathcal{L}_2$ gain γ was restricted to be larger than a certain value. Furthermore, these attitude controls were obtained by solving the Hamilton-Jacobi-Isaacs partial differential inequality (1.2), which, in general, only guarantees an upper bound of the cost for zero initial conditions. A power series solution [100] of the HJI inequality was proposed for the H_∞ suboptimal control of wing rock motions by representing the state vector as a series of closed-loop Lyapunov functions. The concept of extended disturbances, including system error dynamics, was introduced in robotic attitude control system by [83,84] to solve the HJI equation for Euler-Lagrange systems. The state-dependent Riccati equation method [23,36] was also proposed to provide an approximate solution to the HJI equation in a local domain as details below.

State-dependent Riccati equation (SDRE) method

When it is impossible to get an exact analytic solution $V(x)$ to the HJI (1.2), an approximate solution is obtained by the SDRE method in a local domain. Motivated by the linear H_∞ control [93, 138], which is characterized by the algebraic Riccati equation, the state-dependent Riccati equation method was proposed [23, 36] as an approximation of nonlinear optimal control and summarized as follows.

Use the parametrization method to represent (1.1) as a system with state-dependent

coefficients

$$\dot{x} = A(x)x + B_1(x)d + B_2(x)u, \qquad y = C(x)x + D(x)u$$

where $f(x) = A(x)x$, $h(x) = C(x)x$. It is required that $\{A, B_1\}$ and $\{A, B_2\}$ are stabilizable and $\{A, C\}$ is detectable for all x in some local region. Then, the nonlinear state-feedback controller

$$u(x) = -R^{-1}(x)[B(x)^T P(x) + D(x)^T C(x)]x \tag{1.3}$$

is synthesized from the solution, $P(x) = P(x)^T \geq 0$, to the frozen state-dependent Riccati equation

$$A^T P(x) + P(x)A + P(x)\left[\gamma^{-2} B_1 B_1^T - B_2 R^{-1} B_2^T\right] P(x) + \hat{C}^T \hat{C} = 0. \tag{1.4}$$

where $R(x) = R(x)^T > 0$ and $\hat{C}(x) = (I - DR^{-1}D^T)C$. When let γ in (1.4) be $\gamma = \infty$, the H_∞ problem is transformed into a quadratic optimal control problem. Although in theory the control law (1.3) only guarantees the local asymptotic stability of the origin and the suboptimality of a cost function, it turns out to be quite effective in a number of practical applications [42, 74, 80, 85, 113]. Since the state-dependent Riccati equation (1.4) depends on the current state, the computation will be carried out online. However, this will increase the burden of on-board computer. Furthermore, complete information of attitude models is required and therefore the SDRE control is sensitive to parametric uncertainties of system model.

Numerical approaches

Besides these attempts to find analytical solutions, a numerical approach [49–51] was proposed by J. Huang as a more systematic way to find numerical solutions to the HJI equation or the HJI inequality. This method is based on the Taylor-series expansion and the Kronecker product mathematics [138]. Huang [51] applied this numerical approach to the H_∞ control of the pitch dynamics of a missile autopilot. The main obstruction of applications of this method in practice lies in its complex structure of the iterative algorithm and the fact that it requires a large amount of computations.

1.3.3 Inverse Optimal Attitude Control

Inverse optimal control approach is another alternative approach that was systematically proposed to derive nonlinear (robust) optimal feedback control laws in the past few years. Compared with the nonlinear H_∞ control, the inverse optimality approach circumvents the hard task of solving a Hamilton-Jacobi equation and results in a state-feedback controller optimal with respect to a family of meaningful cost functionals. This approach, originated by Kalman to establish certain gain and phase margin of linear quadratic regulators [3], was introduced into nonlinear control in [79], and had been long dormant until it was revived in [35] to develop a methodology for designing

robust nonlinear controllers. While [79] established a certain nonlinear "return difference" inequality which implies robustness to some input nonlinearities, the full analogy to linear stability margins was established in [99].

In parallel to nonlinear H_∞, the framework of input-to-state stability (ISS) introduced by Sontag [106] has triggered efforts towards designing input-to-state stabilizing controllers. ISS and its characterizations will be surveyed in Section 3.3 in Chapter 3. It was shown in [63] that input-to-state stabilizability is both necessary and sufficient condition for the solvability of an inverse optimal control problem. [63] also established a relationship between the inverse optimal control and the nonlinear H_∞ control. The inverse optimal control for the disturbance attenuation problem will be surveyed again in Section 3.5 in Chapter 3. Inverse optimal adaptive control was systematically formulated in [61] for nonlinear systems with uncertainties.

The first application of this approach to the attitude control problem was presented in [64], in which a nonlinear inverse optimal feedback controller based on Rodriguez parameters was proposed for the attitude stabilizing control problem of a rigid spacecraft without exogenous disturbances. The optimal feedback control law [64] is a regional solution because the attitude representation using Rodriguez parameters has a singularity. Also, only the stabilizing control problem but not the attitude tracking problem was considered in [64]. For the trajectory tracking control of Euler-Lagrange systems, inverse optimal state-feedback controllers were designed in robotics [18,83,84] with the help of the introduction of the concept of extended disturbances.

1.3.4 Adaptive attitude control

Researches in adaptive control started in the early 1950's in a connection with the design of autopilots for high-performance aircraft, which operate in a wide range of speeds and altitudes and thus experience large parameter variations. These researches had been dormant for a long time until 1980's when a coherent adaptive control theory was developed. With the help of advances of the computer technology, these theoretical advances have lead to many practical applications. Good introductory texts on adaptive control include [45,62,66,102] and many references therein.

Adaptive control has been applied successfully to the attitude tracking control problem of spacecraft by many authors, for examples, [1,9,10,33,34,56,103,125]. Authors of [34,103] developed adaptive control schemes for the attitude tracking problem; however, due to the use of Rodriguez parameters, attitude representation singularities appear in the description of the physical orientation and therefore global results were not obtained. Based on the attitude representation using singularity-free modified Rodriguez parameters, an adaptive control algorithm was developed in [56] for attitude maneuvers. Using the singularity-free unit quaternion to represent the attitude of spacecraft, [1,33,125] presented adaptive controllers. It was shown by Lyapunov functions that these adaptive controllers achieved global convergence of the attitude tracking errors to zero. In [125], only scalar control gains could be used. Also, it is not straightforward to extend the result [125] to other adaptive control schemes. In [33],

a control scheme was designed using the passivity theory and it allowed the control gain to be a matrix form. Applying nonlinearity cancellation technique, adaptive controller [1] was designed to identify the inertia matrix and to achieve asymptotic attitude tracking. These adaptive tracking controllers above-mentioned were designed for spacecraft without external disturbances. Moreover, the degree of quadratic optimality of these adaptive controllers was not stated explicitly.

In the presence of external disturbances, the adaptive control is more complicated. Using Euler angles to represent the attitude of spacecraft, an H_2/H_∞ suboptimal adaptive controller was presented in [134] for the attitude regulation problem with external disturbances. It is nonglobal due to the use of Euler angles to represent the attitude. Also, it is not for the attitude tracking problem. A global VSC adaptive attitude tracking algorithm was designed in [9] in which the adaptive approach was used to tune the control gain. Krstić [61] proposed a systematical design methodology on inverse optimal adaptive tracking control for nonlinear affine systems without disturbances. In Chapter 6, the results in [61,63] are extended to the design of inverse optimal adaptive control for nonlinear systems with disturbances and then the results are applied to the attitude tracking problem with disturbances and an uncertain inertia matrix.

1.4 Contributions of the Thesis

The thesis focuses on the design of robust state-feedback attitude controllers of microsatellites. The main results are presented in Chapters 4, 5, 6 and 7.

In Chapter 4, complete attitude models are presented. Based on the attitude representation using unit quaternions, the attitude tracking control problem is formulated.

In Chapter 5, the attitude tracking control problem subject to external disturbances is addressed using the inverse optimal control method. The main contributions of this chapter relative to other related works are:

- With the introduction of the concept of extended disturbance, the inverse optimality approach is applied to solve the attitude tracking control problem subject to exogenous disturbances. This approach was used in robot control [18, 83, 84] for the trajectory tracking problem of Euler-Lagrangian systems but not in the attitude control literature for the attitude tracking problem of spacecraft with external disturbances.

- The proposed inverse optimal controller is also H_∞ optimal with respect to the extended disturbance, thus achieving H_∞ disturbance attenuation. By comparison, the H_∞ suboptimal controllers in [25, 57, 65, 135] were designed for the attitude stabilizing problem but not the attitude tracking problem. Furthermore, the $\mathcal{L}_2$-gains γ of those H_∞ suboptimal controllers were restricted to be larger than certain values. Under the H_∞ inverse optimal controller in this thesis, the $\mathcal{L}_2$-gain γ of the closed-loop system is only required to be positive and can be chosen sufficiently small so as to achieve any level of H_∞ disturbance attenuation by a proper control effort. Moreover, the H_∞ inverse optimal controller for the

attitude tracking problem is indeed robust to a certain amount of parametric uncertainties because complete information of the inertia matrix is not required in the controller.

- The proposed controller is a PD controller, and tuning guidelines for selecting the controller gains are established in Chapter 5 based on the performance analysis. PD controllers were designed in [25,57,65,125,135] and conditions were given for the PD control gains. However, how to tune the control gains on the basis of performance analysis was not analytically studied.

In Chapter 6, the attitude tracking problem with disturbances and parametric uncertainties is addressed explicitly by using the inverse optimal control method and the adaptive control approach. An adaptive term is added in the state-feedback controller. The contributions of this chapter are:

- The adaptive control method and the inverse optimal control approach are combined to account for the parametric uncertainties in the inertia matrix of the spacecraft and the optimality of the attitude controller for the attitude tracking control problem. The method of backstepping [35] is used to construct a control Lyapunov function and stabilizing control laws of particular forms.

- For the zero-disturbance case, the proposed inverse optimal adaptive controller achieves global asymptotic attitude tracking for all initial conditions. In a comparison with the results reported in [1,33,103,125], the adaptive feedback control laws in Chapter 6 are inverse optimal with respect to a set of meaningful cost functionals involving tracking errors and control efforts.

- When external disturbances are considered in the attitude tracking control problem, an adaptive attitude tracking controller is proposed that is inverse optimal and achieves H_∞ disturbance attenuation without solving the associated HJI partial differential equation explicitly.

In Chapter 7, robust attitude control with actuator's saturation nonlinearity is addressed via LMIs in a local region of attraction. The main contributions are:

- Analysis and synthesis of general linear control systems with saturated inputs under the considerations of local H_2- and H_∞-performance are formulated in terms of linear matrix inequalities (LMIs).

- Using the LMI software, the local H_2- and H_∞-performance are analyzed and synthesized for the linear attitude control system with disturbances, uncertainties of moments of inertia and saturated controls.

1.5 Outline of the Thesis

The contents of the thesis are organized as follows.

Chapter 2: Mathematical Preliminaries

In Chapter 2, we will present the basic mathematical materials and introduce the fundamental notations used throughout the thesis.

Chapter 3: Stability and Robust Control

In Chapter 3, we will survey some Lyapunov stability results and then the disturbance attenuation problem for nonlinear systems. Input-to-state stabilization framework and (direct or inverse) differential optimal game approach are two disturbance attenuation methods that have received considerable attention. We first review the results on input-to-state stability and input-to-state stabilization. Then, the nonlinear H_∞ state-feedback control is reviewed. Compared with the nonlinear H_∞ control, the inverse optimal control approach achieves optimality without solving the associated Hamilton-Jacobi-Isaacs partial differential equation explicitly and is also reviewed in details.

Chapter 4: Attitude Dynamic Models

In Chapter 4, the kinematic and dynamic equations of the attitude motion are derived for a wheel-based attitude control system. Using the unit quaternion to represent the attitude orientation of spacecraft, the attitude tracking control problem is formulated for a rigid spacecraft with disturbances.

Chapter 5: H_∞ Inverse Optimal Attitude Tracking Control

In Chapter 5, the attitude tracking control problem with external disturbances is addressed using the inverse optimal control method and by introducing the concept of extended disturbance. An H_∞ suboptimal controller is introduced first for the attitude tracking problem. Inverse optimal control approach is then applied to design a state-feedback control law that is optimal with respect to a meaningful cost functional involving tracking errors, control efforts and extended disturbances. The associated Lyapunov function satisfies a Hamilton-Jacobi-Isaacs partial differential equation. Hence, the controller also achieves H_∞ disturbance attenuation. System performance of the inverse optimal controller is analyzed in terms of performance limitation and guidelines for the selection of the controller gains are established on the basis of the performance analysis. Finally, numerical simulations are carried out to demonstrate the effectiveness of the proposed control algorithm and the tuning guidelines.

Chapter 6: H_∞ Inverse Optimal Adaptive Attitude Tracking Control

In Chapter 6, the attitude tracking control problem with disturbances and an uncertain inertia matrix is addressed using the adaptive control method and the inverse optimal control approach. Some theoretical results on inverse optimal adaptive control are presented and then applied to the attitude tracking control problem. The design of the feedback controller is separated into two stages by means of integrator backstepping. The resulting adaptive feedback controllers are optimal with respect to a family of meaningful cost functionals. For the zero-disturbance tracking problem, a control Lyapunov argument is constructed to show that the inverse optimal adaptive controller achieves asymptotic attitude

tracking with a global convergence. An inverse optimal adaptive controller is also designed for the attitude tracking problem with external disturbances and H_∞ disturbance attenuation is achieved. Numerical simulations illustrate the performance of the proposed control algorithms.

Chapter 7: Linear Attitude Control with Saturated Inputs

Chapter 7 is devoted to the analysis and the synthesis of local H_2 and H_∞ performance of the linear attitude control with input saturations, external disturbances and structured uncertainties of moments of inertia. These local performance are formulated via LMIs. With the small-angle assumption, the nonlinear attitude models are linearized to derive a linear input-output synthesis model with structured uncertainties of the moments of inertia. Then, using the LMI software, local H_2 and H_∞ performance of the linear attitude control system are analyzed and synthesized in a local region of attraction via convex LMI optimizations.

Chapter 8: Conclusions

We conclude this thesis with a summary of the contributions, and propose several suggestions for future work which are interesting and important topics but have not been investigated in this thesis.

Several supplementary results can be found in the appendices.

Chapter 2

Mathematical Preliminaries

This chapter sets forth the basic mathematical tools and fundamental definitions that are used throughout this thesis. It is not self-contained as it is assumed that the reader will be familiar with most of these mathematic preliminaries. General references are cited which contains fuller explorations of these related topics.

In Section 2.1, some norms and normed spaces are defined. Section 2.2 presents some important definitions and conceptions. Section 2.3 gives the system definitions in terms of operators. Section 2.4 describes a class of saturation functions. Finally, linear matrix inequalities are briefly reviewed in Section 2.5.

2.1 Signals and Spaces

The set of all n-dimensional vectors $x = [x_1, \cdots, x_n]^T$, where $x_1, \cdots, x_n$ are real numbers, defines the n-dimensional Euclidean space denoted by $\mathcal{R}^n$. The one-dimensional Euclidean space consists of all real numbers and is denoted by $\mathcal{R}$. The subset $\{x : x \in \mathcal{R},\ x \geq 0\}$ is denoted by $\mathcal{R}_+$. Similarly, if $x_1, \cdots, x_n$ are complex numbers, complex spaces $\mathbb{C}^n$ and $\mathbb{C}$ are defined accordingly. The integers are denoted by $\mathcal{Z}$, with the subset $\{x : x \in \mathcal{Z}, x \geq 0\}$ denoted by $\mathcal{Z}_+$.

The inner product of two vectors $x \in \mathcal{R}^n$ and $y \in \mathcal{R}^n$ is $x^T y = \sum_{i=1}^{n} x_i y_i$, where the superscript "T" denotes the transpose[1].

Let $X \subset \mathcal{R}^n$ be a vector space and let $x \in X$, a real-valued function $||x||$ defined on X is called the norm of x if it satisfies the following properties:

- $||x|| \geq 0$ for all $x \in \mathcal{R}^n$, $||x|| = 0$ if and only if $x = 0$ (positive definiteness);
- $||x + y|| \leq ||x|| + ||y||$ for all $x,\ y \in \mathcal{R}^n$ (triangle inequality);
- $||\alpha x|| = |\alpha|\ ||x||$ for all $\alpha \in \mathcal{R}$ and $x \in \mathcal{R}^n$ (homogeneity).

A generic definition of signal sets is not sufficient for any non-trivial theory to be developed and there are many classes of such signal sets. We will only define the signal spaces and sets used in this thesis.

[1] In the complex spaces $\mathbb{C}^n$, we often use the superscript "$*$" to denote the conjugate transpose.

Definition 2.1. *Let $x \in \mathcal{R}^n$. The* vector p-norm *of x is defined as*

$$||x||_p=(|x_1|^p + |x_2|^p + \cdots + |x_n|^p)^{1/p}, \qquad 1 \le p \le \infty. \tag{2.1}$$

In particular, when $p = 1, 2, \infty$, we have

$$||x||_1 = \sum_{i=1}^{n} |x_i|, \qquad ||x||_2 = \sqrt{x^T x}, \qquad ||x||_\infty = \max_{1\le i\le n} |x_i|,$$

which are the three most commonly used vector norms in control theory. The norm $||x||_2$ is often called the Euclidean norm of the vector x. In fact, the norm of a vector is a measure of the vector's "length". For example, $||x||_2$ is the Euclidean distance of x from the origin. Similarly, we can introduce some kind of measure for a matrix.

Definition 2.2. *An $m \times n$ matrix $A = [a_{ij}]$ of real elements defines a linear mapping $y = Ax$ from $\mathcal{R}^n$ into $\mathcal{R}^m$. The* induced p-norm *of A is defined by*[2]

$$||A||_p = \sup \frac{||Ax||_p}{||x||_p} = \max_{||x||_p=1} ||Ax||_p \tag{2.2}$$

In particular, when $p = 1, 2, \infty$, it follows that

$$||A||_1 = \max_{1\le j\le n} \sum_{i=1}^{m} |a_{ij}|, \quad ||A||_2 = \sqrt{\lambda_{\max}(A^T A)}, \quad ||A||_\infty = \max_{1\le i\le m} \sum_{j=1}^{n} |a_{ij}|,$$

where $\lambda_{\max}(A^T A)$ is the maximum eigenvalue of the square matrix $A^T A$.

Hereafter, we shall adopt $||\cdot||$ throughout the remainder of this thesis to denote the *Euclidean 2-norm* of the vector x by $||x|| \triangleq ||x||_2$ and the *induced 2-norm* of the matrix A by $||A|| \triangleq ||A||_2$. The following important properties of the induced $p-$norms of matrices are easy to show [59, 138]:

Lemma 2.1. *Let A be an $m \times n$ real matrix and B be an $n \times q$ real matrix. Then,*

- $||A||^2 \le ||A||_1 ||A||_\infty$, $\frac{1}{\sqrt{n}}||A||_\infty \le ||A|| \le \sqrt{m}||A||_\infty$, $\frac{1}{\sqrt{m}}||A||_1 \le ||A|| \le \sqrt{n}||A||_1$.
- $||AB||_p \le ||A||_p ||B||_p$ *for $p \ge 1$. In particular, this gives $||A^{-1}||_p \ge ||A||_p^{-1}$ if A is invertible.*
- $||UAV|| = ||A||$ *for any appropriately dimensioned unitary matrices U and V.*

Definition 2.3. *For $p \in \mathcal{Z}_+$ with $1 \le p < \infty$, the $\mathcal{L}_p$-norm is defined as:*

$$||x||_{L_p} = \Big(\int_0^\infty ||x(t)||^p dt \Big)^{1/p}, \qquad 1 \le p < \infty \tag{2.3}$$

with $x(t) \in \mathcal{R}^m$, and with the integral in (2.3) being the Lebesgue integral. The linear space $\mathcal{L}_p^m[0, \infty)$ is the set of all functions $x : \mathcal{R}_+ \to \mathcal{R}^m$ such that the $\mathcal{L}_p$-norm of x is

[2] sup denotes supremum, the least upper bound; inf denotes infimum, the greatest lower bound.

finite. The most commonly used space is $\mathcal{L}_2^m[0,\infty)$ *which consists all square integrable* $\mathcal{R}^m$*-valued functions. When* $p=\infty$*, the* $\mathcal{L}_\infty$-norm *is defined as:*

$$||x||_{L_\infty} = \text{ess sup}_{t\in\mathcal{R}_+}\{||x(t)||\}.$$

The sets $\mathcal{W}_{p,q}(N)$ will now be introduced, which are bounded subsets of $\mathcal{L}_p^m[0,\infty)$. Although they are somewhat nonstandard, their use seems to be necessary for the synthesis of a system, with motivation coming from the analysis in Chapter 7.

Definition 2.4. *The set* $\mathcal{W}_{p,q}(N)$ *is the intersection of two sets,* $\mathcal{L}_p^m[0,\infty) \cap \{w : ||w||_q \le N\}$.

Another important signal set to be defined here is the *extended space*. In order to define such signal sets, the *truncation operator* is needed and defined first.

Definition 2.5. *The truncation operator at time* T*, denoted by* P_T*, is defined by*

$$(P_T f)(t) = \begin{cases} f(t), & 0 \le t \le T, \\ 0, & t \ge T. \end{cases} \tag{2.4}$$

Definition 2.6. *The extended space* $\mathcal{L}_{pe}^m[0,\infty)$ *consists of members* $x : \mathcal{R}_+ \to \mathcal{R}^m$ *such that for all* $T \ge 0$*, the* $\mathcal{L}_p$ *norm of* $P_T x$ *is finite, that is,*

$$\mathcal{L}_{pe}^m[0,\infty) = \{x : \mathcal{R}_+ \to \mathcal{R}^m \big|\ P_T x \in \mathcal{L}_p^m[0,\infty)\}.$$

One of the most commonly referred such spaces is the set $\mathcal{L}_{2e}^m[0,\infty)$, which is a weaker condition of the set $\mathcal{L}_2^m[0,\infty)$ and can be applied to define and analyze the $\mathcal{L}_2$-gain for a nonlinear system even with bounded and persistent exogenous disturbances.

2.2 Preliminary Definitions

A subset $S \subset \mathcal{R}^n$ is said to be *open* if, for every vector $x \in S$, one can find an ε-neighborhood of x, denoted by $N(x,\varepsilon) = \{z \in \mathcal{R}^n | \ ||z-x|| < \varepsilon\}$, such that $N(x,\varepsilon) \subset S$. A set S is *closed* if and only if its complement in $\mathcal{R}^n$ is open. A set S is *bounded* if there is $r > 0$ such that $||x|| \le r$ for all $x \in S$. A set S is *compact* if it is closed and bounded. A set S is *convex* if, for every $x, y \in S$ and every real number θ, $0 < \theta < 1$, the point $\theta x + (1-\theta)y \in S$. If $x \in X \subset \mathcal{R}^n$ and $y \in Y \subset \mathcal{R}^m$, we say that (x,y) belongs to the product set $X \times Y \subset \mathcal{R}^n \times \mathcal{R}^m$.

Continuity concepts are heavily used throughout. A function $f : \mathcal{R}^n \to \mathcal{R}^m$ is said to be *continuous* at a point x if $f(x_k) \to f(x)$ whenever $x_k \to x$. Equivalently, f is continuous at x if, given $\varepsilon > 0$, there is $\delta > 0$ such that

$$||x-y|| < \delta \Longrightarrow ||f(x) - f(y)|| < \varepsilon.$$

A function f is continuous on a set S if it is continuous at every point of S, and it is *uniformly continuous* on S if, given $\varepsilon > 0$, there is $\delta > 0$ such that the inequality holds

for all $x, y \in S$. If S_1, S_2 and S_3 are any sets, and $f_1 : S_1 \to S_2$ and $f_2 : S_2 \to S_3$ are functions, the function $f_2 \circ f_1 : S_1 \to S_3$, defined by

$$(f_2 \circ f_1)(\cdot) = f_2(f_1(\cdot))$$

is called the *composition* of f_1 and f_2. The composition of two continuous functions is continuous. If $S \subset \mathcal{R}^n$ and $f : S \to \mathcal{R}^m$, then the set of $f(x)$ such that $x \in S$ is called the image of S under f and is denoted by $f(S)$. If f is a continuous function defined on a compact set S, then $f(S)$ is compact. A function f defined on a set S is said to be one-to-one on S if whenever $x, y \in S$ and $x \neq y$, then $f(x) \neq f(y)$. If $f : S \to \mathcal{R}^m$ is continuous and one-to-one function on a compact set $S \subset \mathcal{R}^n$, then f has a continuous inverse function f^{-1} on $f(S)$. A function $f : \mathcal{R} \to \mathcal{R}^m$ is said to be *piecewise continuous* on an interval $N \subset R$ if for every bounded subinterval $N_0 \subset N$, f is continuous for all $x \in N_0$ except, possibly, at a finite number of points where f may have discontinuous.

An important lemma, known as *Barbalat's lemma* [59, 102], states the convergence of an integrable uniformly continuous function to zero.

Lemma 2.2 (Barbalat). *Let $f : \mathcal{R} \to \mathcal{R}$ be a uniformly continuous function on $[0, \infty)$. Suppose that $\lim_{t\to\infty} \int_0^t f(\tau)d\tau$ exists and is finite. Then $f(t) \to 0$ as $t \to \infty$.*

Proof. If it is not true, then there is a positive constant k_1 such that for every $T > 0$ we can find $T_1 \geq T$ with $|f(T_1)| \geq k_1$. Since $f(t)$ is uniformly continuous, there is a positive constant k_2 such that $|f(t+\tau) - f(t)| < k_1/2$ for all $t \geq 0$ and all $0 \leq \tau \leq k_2$. Hence, for all $t \in [T_1, T_1 + k_2]$,

$$|f(t)| = |f(t) + f(T_1) - f(T_1)| \geq |f(T_1)| - |f(t) - f(T_1)| > \tfrac{1}{2}k_1.$$

Therefore, $|\int_{T_1}^{T_1+k_2} f(t)dt| = \int_{T_1}^{T_1+k_2} |f(t)|dt > \frac{1}{2}k_1k_2$, where the equality holds since $f(t)$ retains the same sign for all $t \in [T_1, T_1 + k_2]$. Thus, the integral $\int_0^t f(\tau)d\tau$ cannot converge to a finite limit as $t \to \infty$, a contradiction. □

A function $f : \mathcal{R} \to \mathcal{R}$ is said to be *differentiable* at a point x if the limit

$$f'(x) = \lim_{h\to 0} \frac{f(x+h) - f(x)}{h}$$

exists. Such a limit $f'(x)$ is called the derivative of f at the point x. A function $f : \mathcal{R}^n \to \mathcal{R}^m$ is said to be *continuously differentiable* at the point x_0 if the partial derivatives $\partial f_i/\partial x_j$ exist and are continuous at x_0 for $1 \leq i \leq m$, $1 \leq j \leq n$. A function f is continuously differentiable on a set S if it is continuously differentiable at every point of S. A function which is continuous on its domain is said to lie in $\mathcal{C}^0$, and if it is continuously differentiable k times, it lies in $\mathcal{C}^k$ with $k \in \mathcal{Z}_+$. For a given smooth function $f(x) : \mathcal{R}^n \to \mathcal{R}$, the *gradient vector* of f, denoted as $\nabla f(x)$ and defined by

$$\nabla f(x) = \left[\frac{\partial f}{\partial x}\right]^T = \left[\frac{\partial f}{\partial x_1}, \quad \cdots, \quad \frac{\partial f}{\partial x_n}\right]^T,$$

is represented as a column vector of elements of $\frac{\partial f}{\partial x_i}$ for $1 \leq i \leq n$. Similarly, for a smooth function $f : \mathcal{R}^n \to \mathcal{R}^m$, the *Jacobian matrix* $\frac{\partial f}{\partial x}$ is an $m \times n$ matrix whose element in the ith row and jth column is $\frac{\partial f_i}{\partial x_j}$, for $i = 1, \cdots, m$ and $j = 1, \cdots, n$.

Definition 2.7 (Lie Derivative). *Let $V : \mathcal{R}^n \to \mathcal{R}$ be a smooth scalar function, and $f : \mathcal{R}^n \to \mathcal{R}^n$ be a smooth vector field on $\mathcal{R}^n$, then the Lie derivative of V with respect to f, written as $L_f V$, is a scalar function defined by*

$$L_f V(x) = \frac{\partial V}{\partial x} f(x) = [\nabla V(x)]^T f(x). \tag{2.5}$$

The Lipschitz condition is an important conception used in nonlinear control.

Definition 2.8 (Lipschitz Condition). *Let $\mathcal{D} \subset \mathcal{R}^m$. A function $f : \mathcal{R} \times \mathcal{D} \to \mathcal{R}$ satisfying*

$$|f(t, x) - f(t, y)| \leq L||x - y||$$

is said to be locally Lipschitz in x, and the positive constant L is called a Lipschitz constant. If $\mathcal{D} = \mathcal{R}^m$, we shall say that $f(t, x)$ is globally Lipschitz in x.

Basic linear algebra is used in this thesis for the analysis and synthesis of an attitude controller. A real symmetric matrix $P \in \mathcal{R}^{n \times n}$ is called positive definite, denoted by $P > 0$, if $x^T P x > 0$ for all nonzero $x \in \mathcal{R}^n$. It is called positive semi-definite if the preceding strict inequality is relaxed to a non-strict one, i.e., $x^T P x \geq 0$ for all nonzero $x \in \mathcal{R}^n$. For a positive definite symmetric matrix P, let $||x||_P^2$ denote the quadratic form $x^T P x$. A matrix $P = [p_{ij}] \in \mathcal{R}^{n \times n}$, where p_{ij} is the (i, j)-entry of P, is said to be positive diagonally dominant (pdd for short) if P is positive definite and (row) diagonally dominant $|p_{ii}| \geq \sum_{j \neq i} |p_{ij}|$ for all $1 \leq i \leq n$. A matrix is called Hurwitz if all its eigenvalues lie in the open left half plane. A matrix is neutrally stable if all its eigenvalues lie in the closed left half plane, without repeated eigenvalues on the imaginary axis or eigenvalues at the origin. A matrix is said to be unstable if at least one of eigenvalues lies in the open right half plane. A matrix B is called skew-symmetric if $B^T = -B$.

2.3 System Definitions

In the operator theoretic (or input/output-based) approach, the signals are examined as inputs and outputs in some signal sets, while the actual system dynamics (expressed as differential or difference equations) are not the point of concern. As such, systems are thought of as operators on signal sets and not in terms of their state-space realizations.

Definition 2.9. *A system is an operator which maps a signal set $\mathcal{U}$ (the input set) into a signal set $\mathcal{Y}$ (the output set).*

Definition 2.10. *A system is said to be input/output stable if its domain of definition is the entire input set.*

This definition of stability is a weaker condition than finite gain stability, which takes into account signal size. Then, we can define the extremely important concept of operator norms, which are a measure of "signal magnitude throughout" and can be used in stability analysis of the closed-loop control systems.

Definition 2.11. *The induced $\mathcal{L}_p$-norm of a stable system Υ from a space $\mathcal{L}_p^m[0,\infty)$ to another space $\mathcal{L}_p^n[0,\infty)$, denoted by $||\Upsilon||_{L_p}$, is defined by*

$$||\Upsilon||_{L_p} = \sup_{w \in \mathcal{L}_p^m[0,\infty)} \frac{||\Upsilon w||_{L_p}}{||w||_{L_p}}. \tag{2.6}$$

The most commonly referred one is the induced $\mathcal{L}_2$-gain. Hereafter, we will focus on the induced $\mathcal{L}_2$-gain of continuous time systems. We will now give some properties of system operators.

An operator $\Upsilon : \mathcal{L}_{2e}^l[0,\infty) \to \mathcal{L}_{2e}^m[0,\infty)$ is called *causal* if $P_T\Upsilon = P_T\Upsilon P_T$ for all $T \geq 0$. A causal operator Υ is *bounded* if there exists a constant $c > 0$ such that $||P_T\Upsilon(v)||_{\mathcal{L}_2} \leq c||P_T v||_{\mathcal{L}_2}$ for all $T \geq 0$ and $v \in \mathcal{L}_{2e}^l[0,\infty)$. Finally, a system operator Υ is *memoryless* if it is causal and if $(I-P_T)\Upsilon(I-P_T) = (I-P_T)\Upsilon$ for all T. Formally, a system operator is *linear* if for all x, y in an input set, and for all α, $\beta \in \mathcal{R}$, we have that $\Upsilon(\alpha x + \beta y) = \alpha\Upsilon x + \beta\Upsilon y$ if $\alpha x + \beta y$ also lies in the input set.

In fact, many system operators are generated by a state space realization. This is extremely useful for nonlinear systems with memory, as it is then possible to generate the system outputs via simulations on a computer. Formally, *a realization of a continuous time system* $\Upsilon : w \to z$ is a set of differential equations over $\mathcal{R}_+$ as

$$\begin{aligned} \dot{x}(t) &= f(x(t), w(t), t), \quad x(t_0) = x_0, \\ z(t) &= h(x(t), w(t), t), \end{aligned} \tag{2.7}$$

with $x(t) \in \mathcal{R}^n$, $w(t) \in \mathcal{R}^l$ and $z(t) \in \mathcal{R}^m$. It is assumed that $f(0,0,t) = 0$ and $h(0,0,t) = 0$ for all $t \in \mathcal{R}_+$. The operator defined by (2.7) with initial conditions $x(t_0)$ is said to be *finite dimensional*.

The following is a well known statement regarding the system properties of the operators generated by a finite-dimensional state space realizations.

Proposition 2.3. *A system operator Υ generated by a finite dimensional realization will be causal. In addition, if the functions f and h in (2.7) are independent of time t, Υ is shift invariant.*

Quite often when we study the state equation $\dot{x} = f(t,x)$, we expect to compute bounds of the solution $x(t)$ without computing the solution itself explicitly. The Gronwall-Bellman inequality [59, Lemma 2.1] is one of such tools that can reach that goal. Another one is the comparison lemma [59, Lemma 2.5] that compares the solution of the differential inequality $\dot{v} \leq f(t, v(t))$ with that of the differential equation $\dot{u} = f(t,u)$. The lemma applies even when $v(t)$ is not differentiable, but has an upper-hand derivative $D^+v(t)$ which satisfies a differential inequality.

Lemma 2.4 (Comparison Lemma). *Consider the scalar differential equation*

$$\dot{u} = f(t,u), \quad u(t_0) = u_0$$

where $f(t,u)$ is continuous in t and locally Lipschitz in u, for all $t \geq 0$ and for all $u \in N \subset R$. Let $[t_0, T)$ (T could be infinite) be the maximal interval of existence of the solution $u(t)$, and suppose $u(t) \in N$ for $t \in [t_0, T)$. Let $v(t)$ be a continuous function whose upper right-hand derivative $D^+v(t)$ satisfies the differential inequality

$$D^+v(t) \leq f(t,v(t)), \quad v(t_0) = u_0$$

with $v(t) \in N$ for all $t \in [t_0, T)$. Then, $v(t) \leq u(t)$ for all $t \in [t_0, T)$.

Proof. See Appendix A.1 in [59] for details. We omit it here. □

2.4 Saturation Nonlinearity

Due to the capabilities of actuators, the output characteristics of the control efforts is always with a saturation nonlinearity. In Chapters 5 and 6 the saturation nonlinearity of reaction wheels (attitude actuators) will be considered only in numerical simulations; in Chapter 7 the local performance analysis and synthesis will be carried out for the linearized attitude control system subject to saturated inputs.

The single-input saturation operator σ is a memoryless operator with 1-dimensional input and output spaces, which is defined by

$$(\sigma u)(t) = \sigma(u(t)), \quad t \in \mathcal{R}_+,$$

with σ being a member of the class of saturation functions, which map $\mathcal{R}$ to a subset of $\mathcal{R}$. The generic definition of the class of saturation functions is given as follows [17, 71, 72, 89, 94].

Definition 2.12. *A function $\sigma : \mathcal{R} \to \mathcal{R}$ is a saturation function if the following conditions hold:*

1. *σ is continuous, bounded and $(1 + |x|)|\sigma'(x)|$ is bounded for almost all $x \in \mathcal{R}$;*
2. *$x\sigma(x) > 0$ if $x \neq 0$, $\liminf_{x \to 0} \frac{\sigma(x)}{x} > 0$, and $\liminf_{|x| \to \infty} |\sigma(x)| > 0$.*

It is possible to show that these conditions are equivalent to some others, allowing other equivalent definitions of the saturation functions. The following characterization is taken from [17, 71, 72].

Lemma 2.5. *A function σ satisfies Condition 1 of Definition 2.12 if and only if it satisfies the following two conditions:*

1. *σ is globally Lipschitz;*

2. *there exists a constant* c_1 *such that for all* $x, y \in \mathcal{R}$, $|x||\sigma(x+y) - \sigma(x)| \leq c_1|y|$.

Definition 2.13. *The constant* $k > 0$ *is an* S*-bound for the saturation function* σ *if there exist* $a, b > 0$ *and a measurable function* $\tau : \mathcal{R} \to [a, b]$ *such that*

1. $|\sigma(t) - \sigma(s)| \leq k|t - s|$;
2. $|t||\sigma(t+s) - \sigma(s)| \leq k|s|$;
3. $|\sigma(t) - \tau(t)\sigma(s)| \leq kt\sigma(t)$.

(It was shown in [71,72] that such a bound always exists for a saturation function.) Among the class of saturation functions, the standard saturation function, denoted by σ_0, is defined by

$$\sigma_0(x) = \text{sgn}(x) \min\{|x|, 1\}. \tag{2.8}$$

The usefulness of this standard saturation function is that it represents one of the simplest definitions of saturation functions in its class, and it is possible to exploit the fact that it is piecewise linear. It is non-differentiable, and sometimes it can be approximated by some smooth functions, for example, the function tanh(x).

A nonlinear function $\phi : \mathcal{R} \to \mathcal{R}$ is said to be monotonically non-decreasing if $(\phi(x) - \phi(y))(x - y) \geq 0$ for all $x, y \in \mathcal{R}$. The function $\phi \in$ sector$[0, k]$ if $\phi(0) = 0$ and $0 \leq x\phi(x) \leq kx^2$ for all x. The stronger assumption $\phi \in$ slope$[0, k]$ means that $\phi(0) = 0$ and it satisfies $0 \leq \frac{\phi(y_1)-\phi(y_2)}{y_1-y_2} \leq k$ for all $y_1 \neq y_2$. The operator ϕ is odd if $\phi(-x) = -\phi(x)$.

If the saturation function σ satisfies $|\sigma(s)| \leq k|s|$, then it has an S-bound. Hence, the standard saturation $\sigma_0(s)$ defined in (2.8) is obviously with an S-bound 1. Clearly, it is odd and also belongs to sector$[0, 1]$ and slope$[0, 1]$.

2.5 Linear Matrix Inequality

In Chapter 7, we shall use the tools of linear matrix inequalities (often abbreviated as LMI's) to estimate local performance of the linearized attitude control system with saturated inputs. Linear matrix inequalities and LMI techniques had become an area of intense research interest, as they are believed to be an extension of the quite useful algebraic Riccati equation. Analytic solutions to the linear matrix inequalities generally do not exist, but the numerical schemes to find feasible solutions to these inequalities have been a hot subject of current research activities. In summary, three factors make the LMI techniques appealing and a powerful design tool:

- a variety of design specifications and constraints can be expressed as LMIs;
- once formulated in terms of LMIs, a problem can be solved exactly by efficient convex optimization algorithms;

- while most problems with multiple constraints or objectives lack analytical solutions in terms of matrix equations, they often remain tractable in the LMI framework. This makes LMI-based design a valuable alternative to classical "analytical" methods.

A very useful reference, which is a good introduction to the LMI's problem, is the one written by Boyd [12]. The authors of [12] stressed that as long as analytic solutions are not necessarily demanded or not achievable, reduction of an analysis problem to a linear matrix inequality is sufficient in some sense to have "solved" the problem.

A *linear matrix inequality* (LMI) is of the form:

$$F(x) = F_0 + \sum_{i=1}^{m} x_i F_i(x) > 0 \tag{2.9}$$

where $x \in \mathcal{R}^m$ is the variable and the matrices $F_i = F_i^T \in \mathcal{R}^{n\times n}$ are given for all $i = 0,1,\cdots,m$. The inequality symbol in (2.9) means that $F(x)$ is positive definite. A *non-strict linear matrix inequality* is of the form $F(x) \geq 0$, which is the result of the relaxation of the condition on $F(x)$ to be positive semidefinite.

The LMI (2.9) is a convex constraint on x, i.e., the set $\{x : F(x) > 0\}$ is convex. As a result, its solution set, called the feasible set, is a convex subset of $\mathcal{R}^m$, and finding a solution x to (2.9), if any, is a convex optimization problem. Convexity guarantees that an LMI optimization problem can be solved numerically with a unique solution when one exists.

It is possible to express the multiple linear matrix inequalities $F^{(1)}(x) > 0, \cdots, F^{(p)}(x) > 0$ as a single LMI $\text{diag}\{F^{(1)}(x), \cdots, F^{(p)}(x)\} > 0$. As such, multiple coupled LMIs are treated as a single LMI without any difficulties.

An important manipulation upon linear matrix inequalities is the use of *Schur complements*, by which nonlinear (convex) inequalities are converted into an LMI form. A simple formulation is that the LMI

$$\begin{bmatrix} Q(x) & S(x) \\ S(x)^T & R(x) \end{bmatrix} > 0$$

with $Q(x) = Q(x)^T$, $R(x) = R(x)^T$, and $S(x)$ dependent in an affine fashion upon x, is equivalent to:

$$R(x) > 0, \qquad Q(x) - S(x)R(x)^{-1}S(x)^T > 0.$$

For example, the famous inequality

$$A^TP + PA + PBR^{-1}B^TP + Q < 0$$

is equivalent to the LMI

$$\begin{bmatrix} PA + A^TP + Q & PB \\ B^TP & -R \end{bmatrix} < 0$$

with the variable $P = P^T$ and the given matrices $Q = Q^T > 0$, $R = R^T > 0$.

Four generic LMI problems are listed as follows. Finding a solution x to the LMI system (2.9) is called the *feasibility problem*. Minimizing a convex objective under LMI constraints is also a *convex optimization problem*. In particular, the linear objective minimization problem

$$\begin{array}{ll} \text{minimize} & c^T x \\ \text{subject to} & F(x) > 0 \end{array} \tag{2.10}$$

plays an important role in LMI-based design. The *eigenvalue problem*

$$\begin{array}{ll} \text{minimize} & \lambda \\ \text{subject to} & \lambda I - A(x) > 0, \quad B(x) > 0 \end{array} \tag{2.11}$$

where A and B are symmetric matrices that depend affinely on the optimization variable x, is a convex optimization problem. Finally, the *generalized eigenvalue minimization problem*

$$\begin{array}{ll} \text{minimize} & \lambda \\ \text{subject to} & \lambda B(x) - A(x) > 0, \quad B(x) > 0, \quad C(x) > 0 \end{array} \tag{2.12}$$

where A, B and C are symmetric matrices dependent affinely on the optimization variable x, is quasi-convex and can be solved by similar techniques.

Discussion of the computational aspects of LMIs is beyond the scope of this thesis. However, their solution appears to be computationally tractable. Algorithms exist that have been shown to be of polynomial complexity, and in fact seem to be quite efficient in practice. The simplest one in principle is the *ellipsoid algorithm*. Since late 1980's, the *interior-point methods* have been proposed which are much more efficient. For more details on the computational algorithms, the reader is referred to [12,37] and the references therein.

Chapter 3

Stability and Robust Control

This chapter is fully devoted to the preliminaries of robust stability/stabilizing theory and the disturbance attenuation problem of nonlinear systems with exogenous disturbances. It is a survey of some results taken from the literature [4, 35, 55, 59, 61, 63, 93, 99, 102, 106, 108, 123] on stability and robust control.

One of the oldest and most generic methods to analyze the stability of a nonlinear system is via the use of Lyapunov functions, which is variously referred to as Lyapunov's Direct Method, and is summarized in Section 3.1 and intensively applied throughout this thesis. For nonlinear control systems, it often requires to search for both a Lyapunov function and a feedback control. This brings the concept of a control Lyapunov function, which will be briefly reviewed in Section 3.2. For the disturbance attenuation problem, two methods have attained considerable attention, and been heavily developed in recent years. One is the framework of input-to-state stability (ISS), which relates the peak values of the disturbance and the system state. Some standard results on ISS and input-to-state stabilization are surveyed in Section 3.3. Another approach for the disturbance attenuation is the (direct or inverse) nonlinear differential game assignment method, which relates integral penalties on the disturbance and the state/control pair. In this thesis, we will focus on two well-developed robust optimal control methods, nonlinear H_∞ control and inverse optimal control, which are reviewed respectively in Sections 3.4 and 3.5.

3.1 Lyapunov Stability and LaSalle Theorems

Consider the nonautonomous system

$$\dot{x} = f(x, t) \tag{3.1}$$

where $f : \mathcal{X} \times \mathcal{R}_+ \to \mathcal{R}^n$ with $\mathcal{X} \subseteq \mathcal{R}^n$ is locally Lipschitz in x and piecewise continuous in t. If f does not depend explicitly on the time t, that is, $\dot{x} = f(x)$, the system is said to be autonomous.

Definition 3.1. *$x_e \in \mathcal{X}$ is an equilibrium point of (3.1) if $f(x_e, t) = 0$ for all $t \geq 0$; the origin $x = 0$ is the equilibrium point for (3.1) if $f(0, t) = 0$ for all $t \geq 0$.*

In this thesis, the following *comparison functions* are important and frequently used.

Definition 3.2. *A continuous function $\alpha : [0, a) \to \mathcal{R}^+$ is of class $\mathcal{K}$ if it is positive definite, strictly increasing and $\alpha(0) = 0$. It is said to belong to class $\mathcal{K}_\infty$ if $a = \infty$ and $\alpha(r) \to \infty$ as $r \to \infty$.*

Definition 3.3. *A continuous function $\beta : [0, a) \times \mathcal{R}^+ \to \mathcal{R}^+$ is said to belong to class $\mathcal{KL}$ if, for each fixed $t \geq 0$, the mapping $\beta(s, t)$ is of class $\mathcal{K}$ with respect to s, and for each fixed $s \geq 0$, the mapping $\beta(s, t)$ is decreasing with respect to t and $\beta(s, t) \to 0$ as $t \to \infty$.*

Our goal is to characterize and study the stability of the equilibrium point x_e of the nonlinear system (3.1). Without loss of generality, we shall assume that the origin $x = 0$ is the equilibrium point and thus study the Lyapunov stability[1] of the origin. First, we present definitions of Lyapunov stability.

Definition 3.4. *The equilibrium point $x = 0$ of (3.1) is stable if, for any $\varepsilon > 0$, there exists $\delta(\varepsilon, t_0) > 0$ such that if $||x(t_0)|| < \delta(\varepsilon, t_0)$ then $||x(t)|| < \varepsilon$ for all $t \geq t_0$. Otherwise, it is unstable.*

Definition 3.5. *The equilibrium point $x = 0$ of (3.1) is uniformly stable[2] if and only if there exist a class $\mathcal{K}$ function $\gamma(\cdot)$ and a constant $c > 0$, independent of t_0, such that*

$$||x(t)|| \leq \gamma(||x(t_0)||), \quad \forall t \geq t_0 \geq 0, \quad \forall ||x(t_0)|| < c.$$

If the equilibrium point $x = 0$ is uniformly stable for all $c > 0$ i.e., for all $x(t_0)$, then it is globally uniformly stable.

Definition 3.6. *The equilibrium point $x = 0$ of (3.1) is uniformly asymptotically stable[3] if and only if there exist a class $\mathcal{KL}$ function $\beta(\cdot, \cdot)$ and a positive constant c, independent of t_0, such that*

$$||x(t)|| \leq \beta(||x(t_0)||, t - t_0), \quad \forall t \geq t_0 \geq 0, \quad \forall ||x(t_0)|| < c.$$

If the equilibrium point $x = 0$ is uniformly asymptotically stable for all $c > 0$, it is then globally uniformly asymptotically stable.

Definition 3.7. *The equilibrium point $x = 0$ of (3.1) is exponentially stable if there exist two positive numbers α and λ, such that $||x(t)|| \leq \alpha ||x(t_0)|| e^{-\lambda(t-t_0)}$ for sufficiently small $x(t_0)$ and for all $t \geq t_0$. It is globally exponentially stable if it is exponentially stable for all $x(t_0) \in \mathcal{R}^n$.*

---

[1] Lyapunov stability and Lyapunov theory for nonautonomous systems are well documented in literature. Nice references on these topics include [59, 93, 102, 108].

[2] It was shown in [59] that Definition 3.5 is an equivalence of the definition of uniform stability in [93, 102]: the equilibrium point $x = 0$ is uniformly stable if, for any $\varepsilon > 0$, there exists $\delta(\varepsilon) > 0$ independent of t_0 such that if $||x(t_0)|| < \delta(\varepsilon)$ then $||x(t)|| < \varepsilon$ for all $t \geq t_0$.

[3] It was also shown in [59] that Definition 3.6 is an equivalence of the definition of uniform asymptotic stability in [93, 102]: the equilibrium point $x = 0$ is asymptotically stable if it is stable and there exists $\delta(t_0) > 0$ such that $x(t) \to 0$ as $t \to \infty$ for $||x(t_0)|| < \delta(t_0)$.

The Lyapunov/LaSalle stability theorems that follow are standard and can be found in many references on stability theory, for instance, the texts [55, 59, 62, 93, 102, 108]. We start with a theorem on uniform asymptotic stability, and present two theorems on global uniform stability and global uniform asymptotic stability.

Theorem 3.1. *Let $x = 0$ be an equilibrium point for (3.1) and $\mathcal{X} \subset \mathcal{R}^n$ be a domain containing the origin $x = 0$. Suppose that $V : \mathcal{X} \times \mathcal{R}_+ \to \mathcal{R}_+$ be a continuously differentiable function such that*

$$W_1(x) \leq V(x,t) \leq W_2(x) \tag{3.2}$$

$$\frac{\partial V}{\partial t} + \frac{\partial V}{\partial t} f(t,x) \leq -W_3(x) \leq 0 \tag{3.3}$$

$\forall t \geq 0$ and $\forall x \in \mathcal{X}$, where $W_1(x)$, $W_2(x)$ and $W_3(x)$ are continuous positive definite functions on $\mathcal{X}$. Then the equilibrium $x = 0$ is uniformly asymptotically stable.

Proof. See [59, Theorem 3.8, Lemma 3.4 and Lemma 3.5] for details. □

When $W_1(x)$ and $W_2(x)$ are class $\mathcal{K}_\infty$ functions and $W_3(x)$ is relaxed to be a continuous function, it follows the well-known LaSalle-Yoshizawa theorem on global uniform stability. Furthermore, if $W_3(x)$ is a class $\mathcal{K}$ function, then the LaSalle-Yoshizawa theorem becomes the well-known Lyapunov theorem on global uniform asymptotic stability.

Theorem 3.2 (LaSalle-Yoshizawa). *Let $x = 0$ be an equilibrium point for (3.1). Suppose that $V : \mathcal{R}^n \times \mathcal{R}_+ \to \mathcal{R}_+$ be a continuously differentiable function such that*

$$\gamma_1(||x||) \leq V(x,t) \leq \gamma_2(||x||)$$
$$\frac{\partial V}{\partial t} + \frac{\partial V}{\partial t} f(t,x) \leq -W_3(x) \leq 0$$

for all $t \geq 0$ and for all $x \in \mathcal{R}^n$, where $\gamma_1(\cdot)$ and $\gamma_2(\cdot)$ are class $\mathcal{K}_\infty$ functions and $W_3(x)$ is a continues function. Then the equilibrium $x = 0$ is globally uniformly stable and $\lim_{t\to\infty} W_3(x(t)) = 0$.

Proof. It is a standard result on global uniform stability. For a complete proof, see [59, Theorems 4.4 and 4.5] (see also [61, Theorem 1.5]). The convergence of $W_3(x)$ to zero is attained by Barbalat's Lemma 2.2. □

Theorem 3.3 (Lyapunov Theorem). *Let $x = 0$ be an equilibrium point for (3.1). Suppose that $V : \mathcal{R}^n \times \mathcal{R}_+ \to \mathcal{R}_+$ be a continuously differentiable function such that*

$$\gamma_1(||x||) \leq V(x,t) \leq \gamma_2(||x||)$$
$$\frac{\partial V}{\partial t} + \frac{\partial V}{\partial t} f(t,x) \leq -\gamma_3(||x||)$$

$\forall t \geq 0$ and $\forall x \in \mathcal{R}^n$, where $\gamma_1(\cdot)$ and $\gamma_2(\cdot)$ are class $\mathcal{K}_\infty$ functions and $\gamma_3(\cdot)$ is a class $\mathcal{K}$ function. Then the equilibrium $x = 0$ is globally uniformly asymptotically stable.

Proof. It is a standard result on the global uniform asymptotic stability. For a proof, see [102, Theorem 4.1] (see also [59, Theorem 3.8 and Corollary 3.3]). □

A function $V(x,t)$ satisfying the left inequality of (3.2) is said to be *positive definite*. A function $V(x,t)$ satisfying the right inequality of (3.2) is said to be *decrescent*. If, in a certain neighborhood of the equilibrium point, $V(x,t)$ is continuously differentiable, positive definite and $\dot{V}(x,t)$, its derivative along the trajectories of the system, is negative semi-definite, then $V(x,t)$ is called a *Lyapunov function*.

Note that Theorems 3.1, 3.2 and 3.3 are only sufficient conditions for the Lyapunov stability, that is, if a given Lyapunov function candidate fails the Lyapunov stability test, it tells us nothing. However, converse Lyapunov theorem [59,102] tells us that such a function necessarily exists if the system is stable. These results are also applicable to autonomous nonlinear systems.

3.2 Control Lyapunov Function

The seemingly obvious concept of a *control Lyapunov function* (CLF), introduced by Artstein [5] and Sontag [105], made a tremendous impact on stabilization theory. It converted stability descriptions into tools for solving stabilization tasks. Artstein [5] also showed that *the existence of a control Lyapunov function is a necessary and sufficient condition for the stabilization of a nonlinear control system.*

Consider two finite-dimensional Euclidean spaces: the state space $\mathcal{X}$ and the control space $\mathcal{U}$. Consider a nonlinear system of the form

$$\dot{x} = f(x,u,t) \tag{3.4}$$

where $x \in \mathcal{X}$ is the state vector, $u \in \mathcal{U}$ is the control input and f is a smooth function. Let $x(t) = \varphi(t;t_0,x(t_0),u)$ denote the trajectories of (3.4) with the control u, starting at t_0. For a given Lyapunov function candidate $V(x,t)$, its time derivative for the system (3.4) is written as $\dot{V}(x,t) = \frac{\partial V}{\partial t} + \frac{\partial V}{\partial x} f(x,u,t)$.

One way to stabilize this control problem is to select a Lyapunov function $V(x,t)$ and then try to search for a feedback control $u = \alpha(x,t)$ that renders $\dot{V}(x,t)$ negative. This search of both $V(x,t)$ and $u(x,t)$ brings the concept of a *control Lyapunov function*.

Definition 3.8. *A smooth positive definite radially unbounded function $V(x,t) : \mathcal{X} \times \mathcal{R}_+ \to \mathcal{R}_+$ is called a control Lyapunov function (CLF) for (3.4) if*

$$\inf_{u \in \mathcal{U}} \left\{ \frac{\partial V}{\partial t} + \frac{\partial V}{\partial x} f(x,u,t) \right\} < 0, \qquad \forall x \in \mathcal{X},\ x \neq 0.$$

For the nonlinear systems affine in the control u

$$\dot{x} = f(x) + g(x)u, \quad f(0) = 0 \tag{3.5}$$

where $g(x)$ is also a smooth function. For a given CLF candidate $V(x)$, it follows that $\dot{V}(x,t) = L_f V + L_g V u$. There are nice properties for such nonlinear affine systems.

Lemma 3.4. *A smooth positive definite radially unbounded function $V(x)$ is a CLF for (3.5) if and only if $L_gV = 0 \Rightarrow L_fV < 0$ whenever $x \neq 0$.*

From this lemma, the set where $L_gV = 0$ is significant, because in it the uncontrolled system has the property $L_fV < 0$. However, if $L_fV > 0$ when $L_gV = 0$, then $V(x)$ is not a CLF and cannot be used for a feedback stabilization design.

When $V(x)$ is indeed a CLF, there are many control laws that render $\dot{V}(x,t)$ negative definite, one of which is called a "universal" formula proposed by Sontag [107]:

$$u = \alpha_s(x) = \begin{cases} -\frac{L_fV + \sqrt{(L_fV)^2 + ||L_gV||^4}}{||L_gV||^2}(L_gV)^T, & L_gV \neq 0 \\ 0 & L_gV = 0 \end{cases} \tag{3.6}$$

By Theorem 3.3, this formula $\alpha_s(x)$ is globally asymptotically stabilizing the system (3.5) because it gives $\dot{V} = -\sqrt{(L_fV)^2 + ||L_gV||^4}$, which is negative definite by Lemma 3.4. A further characterization of the stabilizing control law $\alpha_s(x)$ is that it is smooth away from $x = 0$; moreover, $\alpha_s(x)$ is continuous on the whole $\mathcal{R}^n$ if and only if the CLF $V(x)$ satisfies the small control property; see [61, 107] for details.

Definition 3.9 (Small control property). *A CLF $V(x)$ is said to satisfy the small control property if, for each $\varepsilon > 0$ there exists a $\delta(\varepsilon) > 0$ such that, if $x \neq 0$ satisfies $||x|| < \delta$, then there is some control law $u = \alpha_c(x)$ with $||\alpha_c(x)|| < \varepsilon$ such that*

$$L_fV(x) + L_gV\alpha_c(x) < 0, \qquad \forall x \neq 0.$$

By standard converse Lyapunov theorem, if (3.5) is stabilizable, a CLF exists. The construction of a CLF is a hard problem, which has been solved for special classes of systems. There is still no general CLF formula for any general systems. For a larger class of systems, CLF's may be constructed by *backstepping* [35, 62].

The following theorem establishes the equivalent relationship between the existence of a CLF which satisfies the small control property and the stabilizability by a continuous control law which is smooth away from the origin. See [35, 62, 107].

Theorem 3.5 (Sontag). *The system (3.5) is stabilizable by a feedback continuous at the origin and smooth away from the origin if and only if there exists a CLF with a small control property.*

3.3 Input-to-State Stabilization

To formulate a nonlinear disturbance attenuation problem, we need an appropriate definition for the "gain" of a nonlinear system. One might consider using standard input/output definitions for the gain of an operator between signals spaces (such as $\mathcal{L}_2$ or $\mathcal{L}_\infty$), but such definitions may be inadequate for several reasons: 1)the gain definition should reflect the fact that, for nonlinear systems, relationships between inputs and outputs depend on signal sizes, 2)the definition should also incorporate the nonlinear effects of initial conditions, and, 3)methods should exist for completing the

defined quantities. Motivated by such considerations, Sontag introduced input-to-state stability (ISS) in his landmark paper [106].

For a general autonomous nonlinear system

$$\dot{x}(t) = f(x, d), \tag{3.7}$$

where x is the system state, d is a locally essentially bounded disturbance and f is continuous with $f(0,0) = 0$ and locally Lipschitz in x and d.

Definition 3.10. *The system (3.7) is input-to-state stable (ISS) with respect to d if there exist functions $\gamma \in \mathcal{K}_\infty$ and $\beta \in \mathcal{KL}$ such that for all initial states $x(t_0)$ and for all $d \in \mathcal{L}_\infty$, every solution $x(t)$ of (3.7) starting from t_0 satisfies*

$$||x(t)|| \leq \beta(||x(t_0)||, t - t_0) + \gamma(||d_t||) \tag{3.8}$$

for all $t \geq t_0$, where $||d_t|| = \text{ess sup}\{||d(s)|| : s \in [t_0, t]\}$.

It was showed in [59, 69, 111] that a necessary and sufficient condition[4] for the ISS property is the existence of an ISS-Lyapunov function for the autonomous system (3.7), that is, there is a positive definite radially unbounded smooth function $V : R^n \to R$ with

$$\alpha_1(||x||) \leq V(x) \leq \alpha_2(||x||)$$

such that

$$\nabla V(x)^T f(x, d) \leq -\alpha_3(||x||) + \chi(||d||), \qquad \forall x, d \tag{3.9}$$

for some $\mathcal{K}_\infty$ functions $\alpha_1(\cdot)$, $\alpha_2(\cdot)$, $\alpha_3(\cdot)$ and $\chi(\cdot)$. An alternative characterizations using $\alpha_4(c\cdot), \rho(\cdot) \in \mathcal{K}$ is

$$||x|| \geq \rho(||d||) \Rightarrow \nabla V(x)^T f(x, d) \leq -\alpha_4(||x||).$$

Then, the ISS-gain $\gamma(\cdot)$ in (3.8) is the composition $\gamma(\cdot) = \alpha_1^{-1} \circ \alpha_2 \circ \rho(\cdot)$.

An important situation not covered by (3.8) is when the input $d(t)$ is unbounded, but has a finite energy. Motivated by this problem, Sontag [109] introduced the concept of integral input-to-state stability (IISS).

Definition 3.11. *The system (3.7) is integral input-to-state stable (IISS) with respect to d if for some functions α, $\gamma \in \mathcal{K}_\infty$ and $\beta \in \mathcal{KL}$, for all initial states $x(t_0)$ and all d, the following estimate holds:*

$$\alpha(||x(t)||) \leq \beta(||x(t_0)||, t) + \int_0^t \gamma(||d(s)||)ds, \qquad \forall t \geq 0.$$

Definition 3.12. *The system (3.7) is 0-GAS if the 0-disturbance system $\dot{x} = f(x, 0)$ is globally asymptotically stable (GAS).*

[4] For non-autonomous nonlinear systems $\dot{x}(t) = f(x, d, t)$, it was shown in [59] that the existence of an ISS-Lyapunov function $V(x, t)$ is only a sufficient condition for the ISS property.

Definition 3.13. *The system (3.7) is zero-output dissipative if there exist a positive definite radially unbounded smooth function $V : R^n \to R$ and a class $\mathcal{K}_\infty$ function $\nu(\cdot)$ such that $\nabla V(x)^T f(x,d) \leq \nu(||d||)$ for all x and d.*

Remark 3.1. It was showed in [4,68,69,109] that the IISS property is equivalent to the existence of an IISS-Lyapunov function which differs from the ISS Lyapunov function in that $\alpha_3(\cdot)$ in (3.9) is only positive definite but not necessarily of class $\mathcal{K}_\infty$. Another sufficient and necessary condition stated in [4] is that the system (3.7) is IISS if and only if it is 0-GAS and zero-output dissipative. While ISS implies IISS, the converse is not true. ⊗

The ISS (and IISS) concept of stability is rapidly becoming standard in the nonlinear control community, and many alternative stability definitions proposed in the literature have recently been shown equivalent to ISS. Moreover, Lyapunov functions are the powerful tools for computing the functions γ, β in Definition 3.10 and α, γ, β in Definition 3.11. Therefore ISS is the framework of choice for the formulation of nonlinear disturbance attenuation problems. Other frameworks that have received considerable attention in the literature include the differential game assignment problems formulated by nonlinear H_∞ control [59,123,124,138] and inverse optimal control [35,61,63], which will be surveyed in the next two sections. Now, we proceed to consider the input-to-state stabilization for the disturbance attenuation problem with control inputs. For the integral input-to-state stabilization, the readers could refer to [4,68,69].

Consider a nonlinear system of the form

$$\dot{x} = f(x) + g_1(x)d + g_2(x)u \tag{3.10}$$

where $x \in \mathcal{R}^n$ is the state vector, $d \in \mathcal{R}^q$ is the exogenous disturbance to be rejected and $u \in \mathcal{R}^m$ is the control input. We assume that $f(x)$, $g_1(x)$ and $g_2(x)$ are smooth functions and $x = 0$ is the equilibrium point of the nonlinear system, i.e., $f(0) = h(0) = 0$. Let the solution to (3.10) be $x(t) = \varphi(t; t_0, x_0, u)$ resulting from $u = k(x)$ for the initial state $x_0 = x(t_0)$. We say that (3.10) is input-to-state stabilizable if there exists a control law $u = \alpha(x)$ continuous everywhere with $\alpha(0) = 0$, such that the closed-loop system is ISS with respect to d.

Definition 3.14. *A smooth positive definite radially unbounded function $V : R^n \to R$ is called an ISS-control Lyapunov function (ISS-CLF) for (3.10) if there exists a class $\mathcal{K}_\infty$ function $\rho(\cdot)$ such that the following estimate holds for all $x \neq 0$ and all $d \in \mathcal{R}^r$:*

$$||x|| \geq \rho(||d||) \Rightarrow \inf_{u \in \mathcal{R}^m} \{L_f V + L_{g_1} V d + L_{g_2} V u\} < 0. \tag{3.11}$$

From Definition 3.14, it is noted that the set $L_{g_2}V(x) = 0$ is critical because in it we require that $L_f V + ||L_{g_1}V||\rho^{-1}(||x||) < 0$, which means that $L_f V$ must be negative enough to overcome the effect of disturbances bounded by $||d|| < \rho^{-1}(||x||)$.

The following theorem [59, 61, 63, 69, 111] establishes the equivalence between the input-to-state stabilization and the existence of an ISS-CLF.

Theorem 3.6. *The system (3.10) is input-to-state stabilizable if and only if there exists an ISS-CLF with small control property.*

3.4 Nonlinear H_∞ Optimal Control

In the previous section, we have reviewed briefly the definitions and some results on the input-to-state stability and the input-to-state stabilization for nonlinear systems. Another approach that has attained considerable considerations for disturbance attenuation is the so-called "nonlinear H_∞ control" [55, 112, 123, 124]. Both input-to-state stabilization and nonlinear H_∞ control fall under the general theory of dissipative systems [132]. Sontag [110] discussed the connection between ISS and dissipativity. Van de Schaft [123] systematically formulated the L_2-gain analysis and the nonlinear H_∞ control for a class of nonlinear systems within the framework of dissipativity.

Consider the system (3.10) with an output signal y

$$\begin{aligned} \dot{x} &= f(x) + g_1(x)d + g_2(x)u, \qquad x \in \mathcal{X}, d \in \mathcal{R}^q, u \in \mathcal{R}^m \\ y &= h(x), \end{aligned} \tag{3.12}$$

where $h(x)$ is smooth and $f(x_e) = h(x_e) = 0$ where $x_e = 0$ is an equilibrium point.

Definition 3.15. *The **nonlinear state-feedback H_∞ control problem** is to find a smooth state-feedback control*

$$u = \alpha(x), \quad \alpha(x_e) = 0 \tag{3.13}$$

for (3.12) such that the $\mathcal{L}_2$-gain of the closed-loop system from the disturbance d to the block vector of the output $y = h(x)$ and the input $u = \alpha(x)$ is not larger than γ, i.e., there exist a smooth matrix $R(x)$ such that $R(x) = R(x)^T > 0$ for all x, and a positive function $K(x)$, $0 \le K(x) < \infty$ with $K(x_e) = 0$, such that

$$\int_0^T \left(||y(t)||^2 + ||u(t)||_R^2 \right) dt \le \gamma^2 \int_0^T ||d(t)||^2 dt + K(x_0) \tag{3.14}$$

is satisfied for all $T \ge 0$ and for any initial condition $x(t_0) = x_0$ of (3.12).

Analogous to the linear state-space H_∞ optimal control theory, the nonlinear state-feedback H_∞ optimal control problem was stated in [123] as follows.

Definition 3.16. *The **nonlinear state feedback H_∞ optimal control problem** is to find, if exists, the smallest value $\gamma^* \ge 0$ such that for $\gamma > \gamma^*$ there exists a state feedback (3.13) such that the $\mathcal{L}_2$-gain from d to $\begin{bmatrix} y \\ R^{1/2}u \end{bmatrix}$ is less than or equal to γ.*

The definition is somewhat different from the definition used in linear H_∞ control where it is required that the closed-loop system is asymptotically stable. In the nonlinear case, the asymptotic stability is often implied by the finite gain property of the

closed-loop system, and we will find it easier to consider first the H_∞ problem formulated in Definition 3.16 without any priori conditions on the closed-loop stability. We start with the following theorem [123, 124].

Theorem 3.7. *Consider the nonlinear system (3.12) with disturbances. Given $\gamma > 0$ and a smooth matrix $R(x) = R(x)^T > 0$ for all $x \in \mathcal{X}$. Suppose that there exists a $\mathcal{C}^r$ ($k \geq r \geq 1$) solution $V : \mathcal{X} \to \mathcal{R}^+$, with $V(x) \geq 0$ for all x, to the Hamilton-Jacobi-Isaacs partial differential equation*

$$\frac{\partial V}{\partial x} f + \frac{1}{2}\frac{\partial V}{\partial x}\Big(\frac{1}{\gamma^2} g_1 g_1^T - g_2 R^{-1} g_2^T\Big)\Big(\frac{\partial V}{\partial x}\Big)^T + \frac{1}{2} h^T h = 0, \quad V(x_e) = 0, \tag{3.15}$$

or to the Hamilton-Jacobi-Isaacs partial differential inequality

$$\frac{\partial V}{\partial x} f + \frac{1}{2}\frac{\partial V}{\partial x}\Big(\frac{1}{\gamma^2} g_1 g_1^T - g_2 R^{-1} g_2^T\Big)\Big(\frac{\partial V}{\partial x}\Big)^T + \frac{1}{2} h^T h \leq 0, \quad V(x_e) = 0. \tag{3.16}$$

Then, the closed-loop system for the $\mathcal{C}^{r-1}$ state-feedback

$$u = -R(x) L_{g_2}^T V(x) \tag{3.17}$$

solves the state feedback H_∞-suboptimal control problem with $\mathcal{L}_2$-gain $\leq \gamma$. Moreover, $K(x) = 2V(x)$ satisfies the conditions given in Definition 3.16.

Proof. By "completing the squares" and using (3.15) or (3.16), we have [123]

$$\begin{aligned}
\dot{V} &= \frac{\partial V}{\partial x} f(x) + \frac{\partial V}{\partial x} g_1(x) d + \frac{\partial V}{\partial x} g_2(x) u \\
&\leq \frac{1}{2}\Big|\Big| R^{-1/2}\big(L_{g_2} V\big)^T - R^{1/2} u \Big|\Big|^2 - \frac{1}{2}\gamma^2 \Big|\Big| d - \frac{1}{\gamma^2}\big(L_{g_1} V\big)^T \Big|\Big|^2 \\
&\quad - \frac{1}{2}||y||^2 - \frac{1}{2} u^T R u + \frac{1}{2}\gamma^2 ||d||^2,
\end{aligned}$$

where $y = h(x)$. Choosing u as in (3.17) and integrating with respect to t from $t = 0$ to $t = T$, we obtain

$$\int_0^T \Big(||y(t)||^2 + u(t)^T R u(t) \Big) dt \leq \int_0^T \gamma^2 ||d(t)||^2 dt + 2V(x_0) - 2V(x(T)), \quad \forall T \geq 0,$$

and the worst-case disturbance $d^* = \frac{1}{\gamma^2}\big(L_{g_1} V\big)^T$. Since $V(x) \geq 0$, we conclude that (3.14) is satisfied with $K(x) = 2V(x)$ and the $\mathcal{L}_2$ gain of the closed-loop system from d to $\binom{y}{R^{1/2}u}$ is not larger than γ. □

With minor modifications on Theorem 3.7, we obtain the following corollary that is very useful to the analysis of H_∞ inverse optimal control in later sections.

Corollary 3.8. *Consider the nonlinear affine system (3.12). Let the constant $\gamma > 0$ and the matrix $R(x) = R^T(x) > 0$ for all x. Suppose that there exists a smooth solution*

$V(x) \geq 0$ to the Hamilton-Jacobi-Isaacs partial differential inequality

$$\frac{\partial V}{\partial x} f + \frac{\partial V}{\partial x}\Big[\frac{1}{\gamma^2} g_1 g_1^T - g_2 R^{-1} g_2^T\Big]\Big(\frac{\partial V}{\partial x}\Big)^T + \frac{1}{4} h^T h \leq 0, \quad V(x_e) = 0, \tag{3.18}$$

then the closed-loop system with the feedback

$$u = -2R^{-1}(x)(L_{g_2} V)^T \tag{3.19}$$

has the $\mathcal{L}_2$-gain less than or equal to γ from d to $\binom{y}{R^{1/2}u}$. The "worst-case" disturbance is given by $d^* = \frac{2}{\gamma^2}(L_{g_1} V)^T$.

Proof. The proof is analogous to that of Theorem 3.7 and therefore is omitted. Note that (3.14) is satisfied with $K(x) = 4V(x)$. □

With regard to the (global) asymptotic stability of the closed-loop system, the next theorem summarizes it as follows.

Theorem 3.9. [123] *Suppose there exists a solution $V \geq 0$ to (3.15) or (3.16). Assume that the system $\dot{x} = f(x)$ with outputs $y = h(x)$ and $u = -g^T(x)(\partial V/\partial x)^T(x)$ is zero-state observable[5]. Then $V(x) > 0$ for all $x \neq x_e$ and the closed-loop system (3.12)(3.17) (with $d \equiv 0$) is locally asymptotically stable. Assume additionally that V is proper[6], then the closed-loop system is globally asymptotically stable.*

The converse of Theorem 3.7 and Corollary 3.8 is formulated as follows [43, 123]. Suppose that there exist a smooth matrix $R(x) = R(x)^T > 0$ and a smooth feedback control $u = l(x)$ with $l(x_e) = 0$ such that the $\mathcal{L}_2$-gain of the closed-loop system

$$\begin{aligned} \dot{x} &= f(x) + g_1(x)d + g_2(x)l(x), \\ y &= h(x), \qquad u = l(x) \end{aligned} \tag{3.20}$$

[from d to $\binom{y}{R^{1/2}u}$] is $\leq \gamma$. Assume additionally that (3.20) is reachable[7] from x_0. Then the storage function $V_a(x)$ and supply function $V_r(x)$ of the forms

$$V_a(x) = -\inf_{\substack{u \in \mathcal{L}_{2e}[0,T),\ T \geq 0 \\ x(0)=x}} \frac{1}{2}\int_0^T \big(\gamma^2 ||u||^2 - ||y||^2 - ||u||_R^2\big) dt, \tag{3.21}$$

$$V_r(x) = \inf_{\substack{u \in \mathcal{L}_{2e}(t_{-1},0),\ t_{-1} \leq 0 \\ x = \varphi(0, t_{-1}, x_0, u)}} \frac{1}{2}\int_{t_{-1}}^0 \big(\gamma^2 ||u||^2 - ||y||^2 - ||u||_R^2\big) dt. \tag{3.22}$$

[5] The definition of zero-state observability can be found in [43,123] and the references therein. The system $\dot{x} = f(x) + g(x)u$ with output $y = h(x)$ is *zero-state observable* if for any trajectory such that $u(t) \equiv 0$, $y(t) \equiv 0$ implies $x(t) \equiv x_0$.

[6] A positive function V is called proper if, for each $c > 0$, the set $\{x \in \mathcal{X} | 0 \leq V(x) \leq c\}$ is compact.

[7] The system $\dot{x} = f(x, u, t)$, $x \in \mathcal{X}$, is reachable if for any $\bar{x} \in \mathcal{X}$ there exist a $\bar{t} \geq 0$ and an input $\bar{u}$ such that $\bar{x} = \varphi(\bar{t}, t_0, x_0, \bar{u})$, where $\varphi(t, t_0, x_0, u)$ denote the solutions to $\dot{x} = f(x, u, t)$ with the input u and the initial condition x_0.

for (3.20) are well defined. Assume that V_a or V_r is smooth. Then $V \triangleq V_a$ or $V \triangleq V_r$ satisfies the HJI inequality (3.16). Furthermore, the closed-loop system for the feedback $u = -R(x)^{-1}(L_{g_2}V)^T$ also has $\mathcal{L}_2$-gain $\leq \gamma$.

In general, the HJI partial differential inequality (3.16) only guarantees a suboptimal solution. In order to find an optimal controller, we always expect to solve the HJI partial differential equation (3.15). Then, the work remains is to find an appropriate control Lyapunov function (CLF) $V(x)$ to solve the HJI equation (3.15) or the HJI inequality (3.16), which is the most challenging task in solving the nonlinear H_∞ control problem for a nonlinear system. Unfortunately, there is no general analytical formula on how to construct a CLF $V(x)$ to solve (3.15) or (3.16), and the applications of nonlinear H_∞ control have been studied only for some special nonlinear systems. If we hope to use V_a or V_r to design the H_∞ control, we must face two challenging tasks: the smoothness of V_a and V_r is not readily given; also, verifying the reachability is generally a difficult task. The state-dependent Riccati equation (SDRE) method is reviewed in Section 1.3.2 in Chapter 1 as an approximation result of (3.15) with a locally asymptotic stability. Alternatively, the numerical algorithm developed by Huang [49–51] is a more systematic approach to (3.15).

However, it was shown in [122, 123] that there exists at least one locally smooth solution $V \geq 0$ to (3.15) if the $\mathcal{L}_2$-gain is less than γ. Denote the linearization of (3.12) at the equilibrium point x_e as

$$\begin{aligned} \dot{\bar{x}} &= A\bar{x} + B_1\bar{d} + B_2\bar{u}, \qquad \bar{x} \in \mathcal{R}^n, \bar{u} \in \mathcal{R}^m, \bar{d} \in \mathcal{R}^q, \\ \bar{y} &= C\bar{x}, \qquad \bar{y} \in \mathcal{R}^p, \end{aligned} \tag{3.23}$$

where

$$A = \frac{\partial f}{\partial x}(x_e), \quad B_1 = g_1(x_e), \quad B_2 = g_2(x_e), \quad C = \frac{\partial h}{\partial x}(x_e).$$

From linear H_∞ theory [30, 138, 139], the following two theorems [122, 123] are quite standard and establish the local existence of a smooth solution V to (3.15).

Theorem 3.10. *Assume that (C, A) is detectable. Let $\gamma > 0$. Then there exist a real matrix $R = R^T > 0$ and a linear feedback*

$$\bar{u} = F\bar{x} \tag{3.24}$$

such that the closed-loop system (3.23)(3.24) [with inputs $\bar{d}$ to outputs $\begin{pmatrix} \bar{y} \\ R^{1/2}\bar{u} \end{pmatrix}$] is asymptotically stable and has L_2-gain $\leq \gamma$ if and only if there exists a solution $P \geq 0$ to the algebraic Riccati equation

$$A^TP + PA + P\left[\gamma^{-2}B_1B_1^T - B_2R^{-1}B_2^T\right]P + C^TC = 0. \tag{3.25}$$

Furthermore, the L_2-gain is less than γ if and only if there exists a solution $P \geq 0$ to (3.25) such that all the eigenvalues of $A - B_2R^{-1}B_2^TP + \gamma^{-2}B_1B_1^TP$ lie in the open left-half of the complex plane, denoted by $\sigma\left(A - B_2R^{-1}B_2^TP + \gamma^{-2}B_1B_1^TP\right) \in \mathbb{C}^-$.

Moreover, if $P \geq 0$ is a solution to (3.25), then if we choose

$$F = -R^{-1}B_2^T P \tag{3.26}$$

the closed-loop system (3.23)(3.24) is asymptotically stable and has L_2-gain $\leq \gamma$ [respectively $< \gamma$ if there exists a solution P to (3.25) and $\sigma\big(A - B_2R^{-1}B_2^TP + \gamma^{-2}B_1B_1^TP\big) \in \mathbb{C}^-$].

Theorem 3.11. *Consider the system (3.23) and assume that (C, A) is detectable. Let $\gamma > 0$. Suppose there exist a real matrix $R = R^T > 0$ and a feedback $\bar{u} = F\bar{x}$ such that the L_2-gain of the closed-loop system [from $\bar{d}$ to $\begin{pmatrix} \bar{y} \\ R^{1/2}\bar{u} \end{pmatrix}$] is less than γ and the closed-loop system is asymptotically stable. Then there exists a neighborhood $\bar{\mathcal{X}}$ of x_e and a smooth function $V \geq 0$ defined on $\bar{\mathcal{X}}$ such that V is a solution to HJI partial differential equation (3.15). Furthermore, the feedback $u = -R^{-1}g_2^T(x)(\frac{\partial^T V}{\partial x})^T$ for (3.12) has the property that the closed-loop system has locally L_2-gain $\leq \gamma$ in the sense that*

$$\int_0^T (||y(t)||^2 + ||u(t)||_R^2)dt \leq \gamma^2 \int_0^T ||d(t)||^2 dt \qquad \text{with } x_0 = x_e$$

for all $T \geq 0$ and all $d \in \mathcal{L}_2^p(0,T)$ such that the state-space trajectories $x(t)$ starting from $x_0 = x_e \in \bar{\mathcal{X}}$ do not leave $\bar{\mathcal{X}}$ (i.e., the state-feedback H_∞ control problem for γ is solved on the local region $\bar{\mathcal{X}}$).

3.5 Inverse Optimal Gain Assignment

Compared with the nonlinear H_∞ control, the inverse optimal method [35,63] solves the nonlinear optimal gain-assignment problem with respect to a family of meaningful cost functionals without solving the associated HJI partial differential equation explicitly. Moreover, Krstić showed in [63] that the input-to-state stabilization problem and the inverse optimal gain-assignment problem are equivalent. Precisely, an inverse optimal control problem for a nonlinear system is solvable if and only if the nonlinear system is input-to-state stabilizable. These nice properties make the inverse optimal control method also appealing for the disturbance attenuation problem.

Definition 3.17. *The **inverse optimal gain-assignment problem** for the system (3.10) is solvable if there exist a positive constant β, a class $\mathcal{K}_\infty$ function ρ whose derivative ρ' is also a class $\mathcal{K}_\infty$ function, a positive definite symmetric matrix $R(x)$, a positive semidefinite radially unbounded functions $l(x)$, a smooth nonnegative function $E(x)$, and a feedback control $u = \alpha(x)$ which minimizes the cost functional*

$$J_a(u) = \sup_{d \in \mathcal{D}} \Big\{ \lim_{t \to \infty} \Big[E(x(t)) + \int_0^t \big(l(x) + u^T R(x) u - \rho(||d||) \big) d\tau \Big] \Big\} \tag{3.27}$$

where $\mathcal{D}$ is the set of locally bounded functions of x.

The cost functional (3.27) puts penalties on both the state and the control as well as the disturbance. The state weight $l(x)$ may be positive semidefinite and the control

weight $R(x)$ is not allowed to vanish anywhere in $\mathcal{R}^n$. The penalty on the disturbance $\rho(||d||)$ is allowed to be non-quadratic. However, when $\rho(||d||)$ is quadratic, for example, $\rho(||d||) = \gamma^2||d||^2$ for $\gamma > 0$, it is possible to establish a relationship between the inverse optimal control method and the nonlinear H_∞ control approach. In fact, this is what we will do for the nonlinear attitude control problem in Chapters 5 and 6.

Before further development of the main results on inverse optimal control [63], the following notations are needed: For a class $\mathcal{K}_\infty$ function $\rho(\cdot)$ whose derivative exists and is also a class $\mathcal{K}_\infty$ function, $\ell\rho$ denotes the transform

$$\ell\rho(r) = r(\rho')^{-1}(r) - \rho((\rho')^{-1}(r)) \tag{3.28}$$

where $(\rho')^{-1}(r)$ stands for the inverse function of $\frac{d\rho(r)}{dr}$. Using integration, it is easy to show that $\ell\rho$ is equivalent to the Legendre-Fenchel transform $\ell\rho(r) = \int_0^r (\rho')^{-1}(s)ds$. See Appendix C for more properties of the Legendre-Fenchel transform $\ell\rho(r)$.

Krstić [63] provided a sufficient condition for the solvability of the inverse optimal gain assignment problem by the following theorem. Since the theorem is heavily applied to our attitude control problem, we repeat the proof here for comprehension.

Theorem 3.12. [63] *Consider the auxiliary system of (3.10)*

$$\dot{x} = f(x) + g_1(x)\ell\rho(2||L_{g_1}V||)\frac{(L_{g_1}V)^T}{||L_{g_1}V||^2} + g_2(x)u, \tag{3.29}$$

where $V(x)$ is a control Lyapunov function candidate; ρ is a class $\mathcal{K}_\infty$ function whose derivative ρ' is also a class $\mathcal{K}_\infty$ function. Suppose that there exists a matrix-valued function $R_2(x) = R_2^T(x) > 0$ such that the control law

$$u = \alpha(x) = -R_2^{-1}(x)(L_{g_2}V)^T \tag{3.30}$$

globally asymptotically stabilizes (3.29) with respect to $V(x)$. Then the control law

$$u = \alpha^*(x) = -\beta R_2^{-1}(x)(L_{g_2}V)^T \tag{3.31}$$

with $\beta \geq 2$ solves the inverse optimal gain assignment problem for the nonlinear system (3.10) by minimizing the cost functional

$$J_a(u) = \sup_{d\in\mathcal{D}}\left\{\lim_{t\to\infty}\left[2\beta V(x(t)) + \int_0^t \left(l(x) + u^T R_2(x)u - \beta\lambda\rho(\frac{||d||}{\lambda})\right)d\tau\right]\right\} \tag{3.32}$$

for any $\lambda \in (0, 2]$, where

$$l(x) = -2\beta L_f V - 2\beta\lambda\ell\rho(2||L_{g_1}V||) + \beta^2 L_{g_2}V R_2^{-1}(L_{g_2}V)^T. \tag{3.33}$$

Proof. Since the feedback control law $u = \alpha(x)$ in (3.30) stabilizes the auxiliary system (3.29), there exists a continuous positive definite function $W(x)$ such that

$$L_f V + \ell\rho(2||L_{g_1}V||) - L_{g_2}V R_2^{-1}(L_{g_2}V)^T \leq -W(x,\theta) \leq 0,$$

which brings

$$l(x) \geq W(x) + \beta(2-\lambda)\ell\rho(2||L_{g_1}V||) + \beta(\beta-2)L_{g_2}VR_2^{-1}\big(L_{g_2}V\big)^T.$$

Since $\beta \geq 2$, $R_2(x) > 0$ and $W(x)$ is positive definite, $l(x)$ is also positive definite. Therefore, the cost functional $J_a(u)$ defined in (3.32) with $l(x)$ given by (3.33) is a meaningful cost functional, which puts penalties on $x(t)$, $u(t)$ and $d(t)$. Substituting $l(x)$ into (3.32), letting $v = (u - \alpha^*)$ and applying the transform (3.28), we have

$$\begin{aligned}
J_a(u) &= \sup_d \Big\{ \lim_{t\to\infty} \Big[2\beta V(x(t)) - 2\beta \int_0^t \big(L_f V + L_{g_1}Vd + L_{g_2}Vu\big)d\tau \\
&\quad + \int_0^t \Big(\beta^2 L_{g_2}VR_2^{-1}(L_{g_2}V)^T + 2\beta L_{g_2}Vu + u^T R_2 u\Big)d\tau \\
&\quad + \int_0^t \Big(2\beta L_{g_1}Vd - \beta\lambda\ell\rho(2||L_{g_1}V||) - \beta\lambda\rho(\frac{||d||}{\lambda})\Big)d\tau\Big]\Big\} \\
&= \sup_d \Big\{ \lim_{t\to\infty} \Big[2\beta V(x(t)) - 2\beta \int_0^t dV + \int_0^t v^T R_2 v d\tau + \beta \int_0^t \Big(2L_{g_1}Vd \\
&\quad - 2\lambda||L_{g_1}V||(\rho')^{-1}(2||L_{g_1}V||) + \lambda\rho((\rho')^{-1}(2||L_{g_1}V||)) - \lambda\rho(\frac{||d||}{\lambda})\Big)d\tau\Big]\Big\} \\
&= 2\beta V(x_0) + \int_0^\infty (u-\alpha^*)^T R_2 (u-\alpha^*)dt + \beta\lambda \sup_d \int_0^\infty \Pi(d,d^*)dt,
\end{aligned}$$

where d^* is the "worst-case" disturbance given by $d^* = \lambda(\rho')^{-1}(2||L_{g_1}V||)\frac{(L_{g_1}V)^T}{||L_{g_1}V||}$ and the notation $\Pi(d,d^*)$ is defined as

$$\Pi(d,d^*) = \rho\Big(\frac{||d^*||}{\lambda}\Big) - \rho\Big(\frac{||d||}{\lambda}\Big) - \rho'\Big(\frac{||d^*||}{\lambda}\Big)\frac{(d^*)^T}{\lambda||d^*||}(d^*-d)$$

By $\ell\rho(\rho'(r)) = r(\rho')(r) - \rho(r)$ (shown in Appendix C), it follows that

$$\Pi(d,d^*) = -\rho\Big(\frac{||d||}{\lambda}\Big) - \ell\rho\Big(\rho'\Big(\frac{||d^*||}{\lambda}\Big)\Big) + \rho'\Big(\frac{||d^*||}{\lambda}\Big)\frac{(d^*)^T}{||d^*||}\frac{d}{\lambda}.$$

By the Young's Inequality (shown in Appendix C), we have that

$$\Pi(d,d^*) \leq -\rho\Big(\frac{||d||}{\lambda}\Big) - \ell\rho\Big(\rho'\Big(\frac{||d^*||}{\lambda}\Big)\Big) + \rho\Big(\frac{||d||}{\lambda}\Big) + \ell\rho\Big(\rho'\Big(\frac{||d^*||}{\lambda}\Big)\Big) = 0$$

and $\Pi(d,d^*) = 0$ if and only if $d = d^*$. Thus $\sup_d \int_0^\infty \Pi(d,d^*)dt = 0$. Hence, the minimum of the cost functional $J_a(u)$ defined in (3.32) is reached with $u = \alpha^*(x)$, and the feedback control law (3.31) minimizes the cost functional (3.32). The value function[8] of (3.32) is $J_a^*(x) = 2\beta V(x)$. □

Remark 3.2. The parameter $\beta \geq 2$ in Theorem 3.12 represents a design degree of freedom. The parameter $\lambda \in (0,2]$ indicates that the same control law is inverse

[8]The "value function" [61,62] is a function of the state x and is valued as the minimum of the cost functional $J_a(u)$ when the initial time is set as t, instead of t_0, for all $t \geq 0$.

optimal with respect to an entire family of different cost functionals. Implicitly, the associated Lyapunov function $V(x)$ solves a family of HJI partial equations

$$L_f V - \frac{\beta}{2} L_{g_2} V R_2^{-1} (L_{g_2} V)^T + \frac{\lambda}{2} \ell\rho(2||L_{g_1} V||) + \frac{l(x)}{2\beta} = 0.$$

A nice characterization proved by Krstić [63] on the inverse optimal control is that the solvability of the inverse optimal gain assignment problem for the nonlinear system (3.10) is equivalent to the input-to-state stabilizability of (3.10).

Theorem 3.13. *If the system (3.10) is input-to-state stabilizable, then the inverse optimal gain assignment problem is solvable.*

Proof. See [63, Theorem 3.2] (see also [61, Theorem 2.10]). (Theorem 3.13 tells us how to construct a stabilizing control (3.30) in Theorem 3.12 using the Sontag's formula for any nonlinear systems that is input-to-state stabilizable.) □

Theorem 3.14. *If the inverse optimal gain assignment problem for the system (3.10) is solvable, then the system is input-to-state stabilizable.*

Proof. See [63, Theorem 3.3] (see also [61, Theorem 2.12]). □

Another nice characterization is that an inverse optimal controller has infinite gain margin, which implies that the controller remains stable in the presence of a certain class of input uncertainties. Without proof, we recall the following theorem [63, Theorem 4.2] on stability margin.

Theorem 3.15. *If a controller solves the inverse optimal gain assignment problem for (3.10) with $R_2(x) = I$, then it is input-to-state stabilizing for the system*

$$\begin{aligned} \dot{x} &= f(x) + g_1(x)d + g_2(x)a(u + \hat{y}) \\ \dot{\chi} &= \hat{f}(\chi) + \hat{g}(\chi)u, \qquad \hat{y} = \hat{h}(\chi) \end{aligned}$$

where $a \in [1/2, \infty)$ and the χ-system is strictly passive.

Chapter 4

Dynamic Models of Attitude Control System

4.1 Introduction

In this chapter, the models of attitude kinematics and dynamics are presented for the attitude control system (ACS) of a wheel-controlled satellite, and subsequently the attitude tracking control problem is formulated. The structure of the attitude control system is shown as in Figure 4.1. This chapter contains only the dynamic models that will be applied in this thesis. More comprehensive explorations can be found in the texts [53, 88, 101, 117, 118, 126] and the references therein.

It is known that the basis for modelling attitude kinematics and dynamics is the reference coordinate frames and the orientation vectors. The definitions of several coordinate frames will be presented in Section 4.2. The mathematical representations of the attitude vector using the Euler angles and the unit quaternions will be presented in Section 4.3, in which the attitude kinematics is derived correspondingly. Based on the Euler theorem, attitude dynamics is presented for the wheel-controlled attitude control system in Section 4.4, in which the models of wheels and geomagnetic field are also briefly introduced and a magnetic unloading algorithm is then designed for managing angular momentum of the wheels. In Section 4.5, nonlinear attitude tracking control problem is formulated using the unit quaternions to represent the attitude.

Before formulating the dynamic models for the attitude control system, some basic notations are required to be introduced first. Let $SO(3)$ be the Lie group of orthogonal matrices of order 3 and determinant 1, where the direction cosine matrix lies, i.e., $C \in SO(3)$ if and only if $C^T C = I_3$ and $\det(C) = 1$. Let $S(3)$ be unit sphere in R^4, where the unit quaternion lies, and $TS(3)$ be the tangent bundle of $S(3)$. Let $\mathbf{V}$ be a normed linear vector space of dimension 3 and be endowed with an inner product, in which the reference frames are defined. Another important linear operator, the cross-product matrix, denoted by $a^\times$, is heavily applied throughout this thesis and defined as follows.

Definition 4.1. *A linear operator* $a^\times : \mathcal{R}^3 \to \mathcal{R}^{3\times 3}$ *induced by the real vector* $a =$

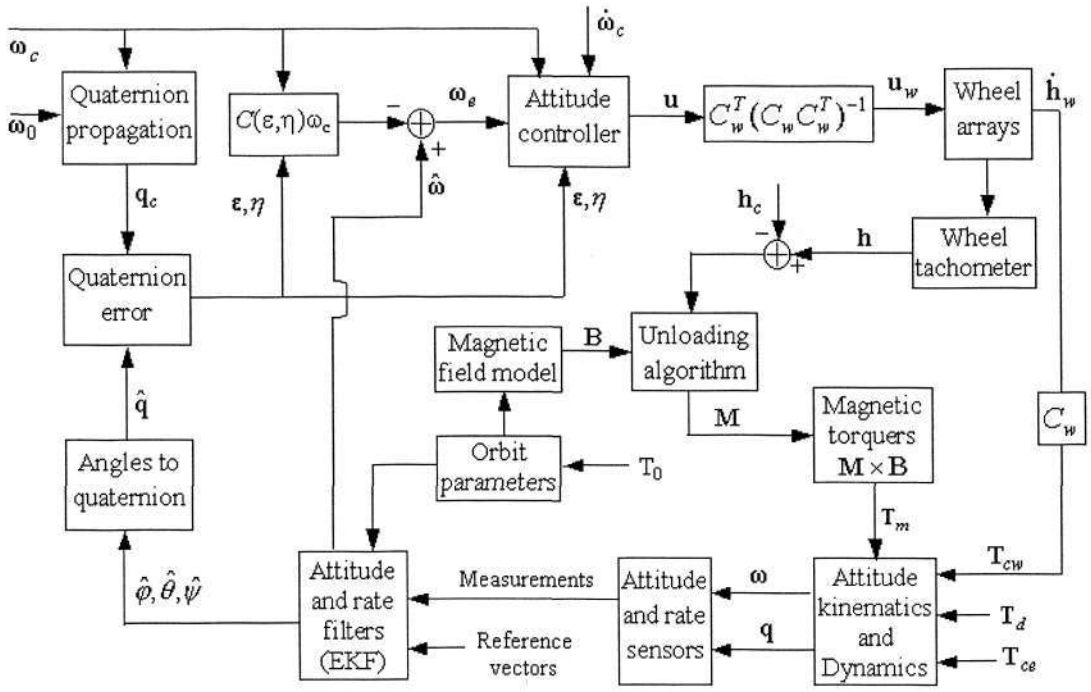

Figure 4.1: The structure of the attitude control system

$[a_1, a_2, a_3]^T$ *is called a cross-product matrix and defined as*

$$a^{\times} = \begin{bmatrix} 0 & -a_3 & a_2 \\ a_3 & 0 & -a_1 \\ -a_2 & a_1 & 0 \end{bmatrix}. \tag{4.1}$$

The name "cross-product matrix" comes from the fact that the cross product of two 3-dimensional vectors $a \in \mathcal{R}^3$ and $b \in \mathcal{R}^3$ is expressed as a linear operation $a \times b = a^{\times} b$. The linear operator $a^{\times}$ is a skew-symmetric matrix and has the following important properties listed in the lemma below:

Lemma 4.1. *For all $a \in \mathcal{R}^3$ and $b \in \mathcal{R}^3$, it follows that:*

Property 1: $(a^{\times})^T = -a^{\times}$;
Property 2: $a^{\times} b = -b^{\times} a$, $a^{\times} a = 0$;
Property 3: $a^T b^{\times} a = 0$;
Property 4: $(a+b)^{\times} = a^{\times} + b^{\times}$;
Property 5: $a^{\times} b^{\times} = b a^T - a^T b I_3$;
Property 6: $(a^{\times} b)^{\times} = b a^T - a b^T$;
Property 7: $||a^{\times}|| = ||a|| = \sqrt{a^T a}$.

Proof. Property 1 follows from $a^{\times}$ being skew symmetric; property 2 is obtained from the facts that $a \times b = -b \times a$ and $a \times a = 0$; property 3 is due to the result that the quadratic form of a skew-symmetric matrix is identically zero; property 4 is due to the linearity of the operator $a^{\times}$ in a; property 5 follows from the cross-product implication

that

$$a \times (b \times c) = a^{\times} b^{\times} c = (a \cdot c)b - (a \cdot b)c = (ba^T - a^T b I_3)c$$

for all $c \in \mathcal{R}^3$; property 6 is obtained from the fact that

$$(a \times b) \times c = (a^{\times} b)^{\times} c = (a \cdot c)b - (b \cdot c)a = (ba^T - ab^T)c$$

for all $c \in \mathcal{R}^3$; from Definitions 2.1 and 2.2, property 7 can be easily verified for the induced 2-norm of the matrix $a^{\times}$ and the vector norm of a. □

4.2 Reference Coordinate Frames

To make a difference, we use symbols in bold to denote coordinate frames and the vectors related to these coordinate frames. A coordinate frame system in $\mathbf{V}$ is given by a set of *orthonormal basis vectors* that obey the right hand rule, say, $\{\boldsymbol{e}_{rx}, \boldsymbol{e}_{ry}, \boldsymbol{e}_{rz}\}$, and can be considered as a linear operator $\mathcal{F}_r : \mathcal{R}^3 \rightarrow \mathbf{V}$ (a row of three vectors) defined by $\mathcal{F}_r = [\boldsymbol{e}_{rx}, \boldsymbol{e}_{ry}, \boldsymbol{e}_{rz}]^T$. In this thesis, there are three reference coordinate frames of interest, namely, an inertial reference frame $\mathcal{F}_I$, an orbital reference frame $\mathcal{F}_o$ and a body reference frame $\mathcal{F}_b$, which are defined as follows:

- **Orbital reference frame $\mathcal{F}_o$:** A local vertical local horizontal (LVLH) reference frame is defined with the center of mass of the spacecraft as its origin. The LVLH frame has a set of unit vectors $\{\boldsymbol{x}_o, \boldsymbol{y}_o, \boldsymbol{z}_o\}$, with $\boldsymbol{z}_o$ pointing toward the center of mass of the earth, $\boldsymbol{x}_o$ along the velocity direction of the spacecraft, and $\boldsymbol{y}_o$ completing an orthogonal right-handed Cartesian frame system, shown as in Figure 4.2(a).

- **Inertial reference frame $\mathcal{F}_I$:** For an earth-orbiting spacecraft, an inertial coordinate system is commonly defined with the center of mass of the earth as its origin and whose direction in space is fixed relative to the solar system. Its basic directions $\{\mathbf{X}, \mathbf{Y}, \mathbf{Z}\}$ in space is inertial with respect to the solar system, where $\mathbf{X}$ points toward the Vernal Equinox, $\mathbf{Z}$ is the axis of rotation of the earth in a positive direction (north) and $\mathbf{Y}$ completes an orthogonal right-handed frame system, shown as in Figure 4.2(b).

- **Body reference frame $\mathcal{F}_b$:** It is an orthogonal right-handed frame system with its origin located at the center of mass of the spacecraft and with a set of mutually perpendicular unit vectors $\{\boldsymbol{x}_b, \boldsymbol{y}_b, \boldsymbol{z}_b\}$. The frame $\mathcal{F}_b$ is fixed to the spacecraft and commonly used to represent the attitude of the spacecraft with respect to other reference frames, such as $\mathcal{F}_o$ and $\mathcal{F}_I$.

Discussion of the orbit control problem is beyond the scope of this thesis. However, for the attitude control problem, it suffices to assume that the spacecraft is moving in a Keplerian orbit [53, 101] for simplicity of analysis. With this assumption, the location of the satellite in orbit can be perfectly determined by six *classical orbit parameters* $[a_o, e_o, i_o, \Omega_o, \omega_o, \theta_o]^T$, as illustrated in Figure 4.2(b). In the inertial reference frame $\mathcal{F}_I$,

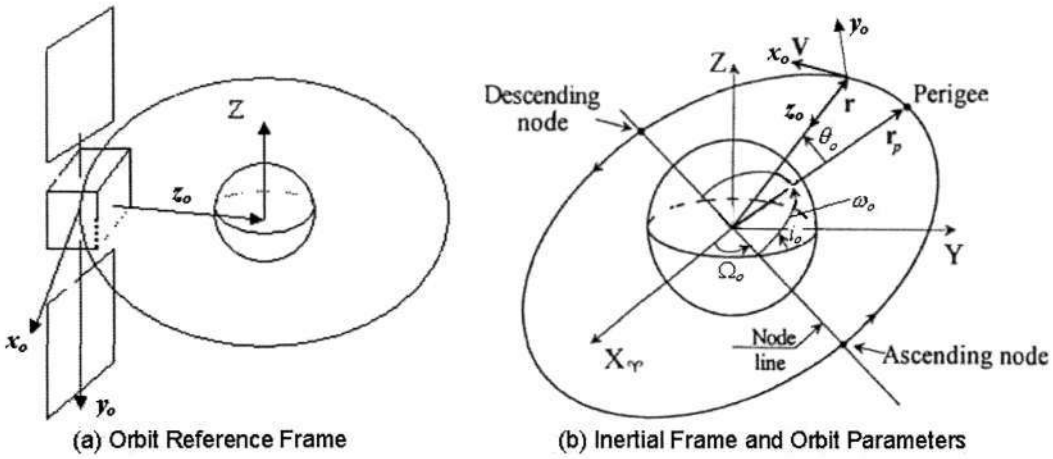

Figure 4.2: Orbit reference frame $\mathcal{F}_o$ and inertial frame $\mathcal{F}_I$

the orbit plane is defined by the *right ascension* of the ascending node, denoted Ω_o, and the *orbit inclination* i_o. On an elliptic orbit with a *large semi-radius* a_o and with an *eccentricity* e_o, position of the spacecraft mass center O_o is defined by the radius vector $\boldsymbol{r}$ and the true anomaly θ_o, which is combined with ω_o into the *orbit argument* $u_o = \omega_o + \theta_o$, where ω_o is the *argument of perigee*, the angle between the ascending node and the orbit perigee $\boldsymbol{r}_p$ in the orbit plane. More detailed interpretations can be found in the textbooks [53, 101].

4.3 Kinematic Equations of Attitude Motion

The attitude operator is defined as a linear transformation bringing a given reference frame $\mathcal{F}_r$ to a body fixed frame $\mathcal{F}_b$. This transformation is of the form

$$C_{br} = \mathcal{F}_b \mathcal{F}_r^*, \tag{4.2}$$

where $*$ denotes the adjoint of a linear transform. It follows from the definition that $C_{br}^T = C_{br}^*$ and $||C_{br}|| = 1$. The orthonormality of the basis vectors implies that C_{br} is orthogonal, i.e., $C_{br}^* C_{br} = I_3$. There are three eigenvalues for C_{br} : $\{1, e^{j\Phi}, e^{-j\Phi}\}$. Let the eigenvector corresponding to the eigenvalue 1 be $\boldsymbol{e} = [e_1, e_2, e_3]$. By the Euler theorem, C_{br} is equivalent to an angular rotation about the axis $\boldsymbol{e}$ over the angle Φ. This equivalence will be applied later to define a unit quaternion q.

This coordinate frame representation C_{br} is known as the attitude matrix, which has 9 elements subject to 6 constraints imposed by the orthogonality. We may need simpler representations. The minimal number needed to represent attitude orientations is 3 without constraints. The commonly used minimal-parameter representations include Euler angles, Rodriguez parameters and Euler axis/angle parameters. However, minimal-parameter representations are only a locally one-to-one and onto mapping of an attitude matrix, and there are always singularities at some spacial orientations. The

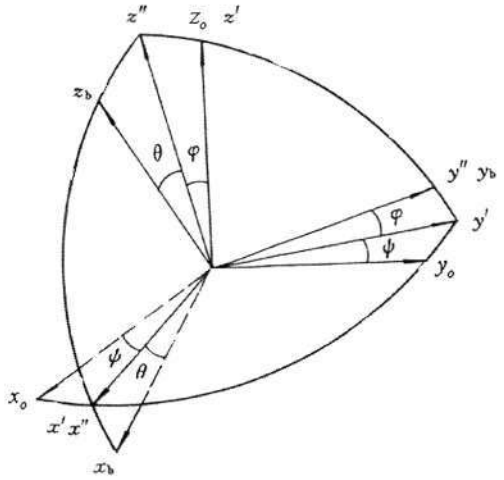

Figure 4.3: Euler angles and coordinate transformation

minimal number of parameters that can globally represent attitude without singularities is 4 with one constraint, such as the unit quaternion (also called Euler parameters).

Among those mathematical representations of the spacecraft attitude, the most efficient and commonly used ones are based on the Euler angles and the unit quaternion. Attitude representation using the Euler angles is simpler and has a more obvious geometrical interpretation but also has singularities. Compared to the Euler angles, the attitude representation using the unit quaternion is free of singularities but has no clear geometric meanings.

4.3.1 Attitude Kinematics in terms of Euler Angles

The Euler angles, known as the roll angle φ, the pitch angle ϑ and the yaw angle ψ, are in general defined by three successive angular rotations from the orbital reference frame $\mathcal{F}_o$ to the body frame $\mathcal{F}_b$. In this thesis, we perform the angular transformations $\psi \rightarrow \varphi \rightarrow \vartheta$ successively, shown as in Figure 4.3:

1. Rotate the frame $\{\boldsymbol{x}_o, \boldsymbol{y}_o, \boldsymbol{z}_o\}$ about $\boldsymbol{z}_o$ through the yaw angle ψ to the frame $\{\boldsymbol{x}', \boldsymbol{y}', \boldsymbol{z}'\}$.

2. Rotate the frame $\{\boldsymbol{x}', \boldsymbol{y}', \boldsymbol{z}'\}$ about $\mathbf{x}'$ through the roll angle φ to the frame $\{\boldsymbol{x}'', \boldsymbol{y}'', \boldsymbol{z}''\}$.

3. Rotate the frame $\{\boldsymbol{x}'', \boldsymbol{y}'', \boldsymbol{z}''\}$ about $\boldsymbol{y}''$ through the pitch angle ϑ to the frame $\{\boldsymbol{x}_b, \boldsymbol{y}_b, \boldsymbol{z}_b\}$.

Then, the resulting complete coordinate transformation can be expressed as

$$\begin{bmatrix} \boldsymbol{x}_b \\ \boldsymbol{y}_b \\ \boldsymbol{z}_b \end{bmatrix} = C_{bo}(\varphi, \vartheta, \psi) \begin{bmatrix} \boldsymbol{x}_o \\ \boldsymbol{y}_o \\ \boldsymbol{z}_o \end{bmatrix}, \qquad \text{or} \qquad \begin{bmatrix} \boldsymbol{x}_o \\ \boldsymbol{y}_o \\ \boldsymbol{z}_o \end{bmatrix} = C_{bo}^{-1}(\varphi, \vartheta, \psi) \begin{bmatrix} \boldsymbol{x}_b \\ \boldsymbol{y}_b \\ \boldsymbol{z}_b \end{bmatrix}$$

where the rotation matrix $C_{bo}(\varphi, \vartheta, \psi)$ (also called the direction cosine matrix) in terms of three Euler angles is given by

$$C_{bo} = \begin{bmatrix} \cos\vartheta\cos\psi - \sin\vartheta\sin\varphi\sin\psi & \cos\vartheta\sin\psi + \sin\vartheta\sin\varphi\cos\psi & -\sin\vartheta\cos\varphi \\ -\cos\varphi\sin\psi & \cos\varphi\cos\psi & \sin\varphi \\ \sin\vartheta\cos\psi + \cos\vartheta\sin\varphi\sin\psi & \sin\vartheta\sin\psi - \cos\vartheta\sin\varphi\cos\psi & \cos\vartheta\cos\varphi \end{bmatrix}. \quad (4.3)$$

As a consequence of three successive angular rotations, the Euler angular velocity of the body frame $\mathcal{F}_b$ relative to the LVLH frame $\mathcal{F}_o$ is given by

$$\begin{aligned} \omega_{bo} &= \begin{bmatrix} 0 \\ \dot{\vartheta} \\ 0 \end{bmatrix} + \begin{bmatrix} \cos\vartheta & 0 & -\sin\vartheta \\ 0 & 1 & 0 \\ \sin\vartheta & 0 & \cos\vartheta \end{bmatrix} \begin{bmatrix} \dot{\varphi} \\ 0 \\ 0 \end{bmatrix} + \begin{bmatrix} \cos\vartheta & 0 & -\sin\vartheta \\ 0 & 1 & 0 \\ \sin\vartheta & 0 & \cos\vartheta \end{bmatrix} \begin{bmatrix} 1 & 0 & 0 \\ 0 & \cos\varphi & s\varphi \\ 0 & -\sin\varphi & c\varphi \end{bmatrix} \begin{bmatrix} 0 \\ 0 \\ \dot{\psi} \end{bmatrix} \\ &= \begin{bmatrix} \cos\vartheta & 0 & -\sin\vartheta\cos\varphi \\ 0 & 1 & \sin\varphi \\ \sin\vartheta & 0 & \cos\vartheta\cos\varphi \end{bmatrix} \begin{bmatrix} \dot{\varphi} \\ \dot{\vartheta} \\ \dot{\psi} \end{bmatrix}. \end{aligned} \quad (4.4)$$

Let ω and ω_{oi} denote the angular velocities of the body frame $\mathcal{F}_b$ and the orbital frame $\mathcal{F}_o$, respectively, with respect to the inertia frame $\mathcal{F}_I$ and let both of them be expressed in the body frame $\mathcal{F}_b$. By the definition of the orbital frame $\mathcal{F}_o$ in a circular orbit, the angular velocity of $\mathcal{F}_o$ with respect to $\mathcal{F}_I$ is expressed in the frame $\mathcal{F}_o$ by

$$\omega_0 = [0, -n_0, \ 0]^T, \quad (4.5)$$

where n_0 is the mean motion given by $n_0 = \frac{2\pi}{T_o}$ and T_o is the period of the orbit motion of the spacecraft.

By the differential equation of a rotation matrix C, it follows that $\dot{C}_{bo} = -\omega_{bo}^{\times} C_{bo}$ and $\dot{C}_{oi} = -\omega_{oi}^{\times} C_{oi}$, (see Appendix C). Since $C_{bi} = C_{bo}C_{oi}$, it follows that

$$\omega :\equiv \omega_{bi} = \omega_{bo} + \omega_{oi} = \omega_{bo} + C_{bo}\omega_0 \quad (4.6)$$

Thus, substituting Eqs.(4.3) and (4.4) into Eq.(4.6) yields

$$\begin{bmatrix} \omega_1 \\ \omega_2 \\ \omega_3 \end{bmatrix} = \begin{bmatrix} \dot{\varphi}\cos\vartheta - \dot{\psi}\sin\vartheta\cos\varphi - n_0(\cos\vartheta\sin\psi + \sin\vartheta\sin\varphi\cos\psi) \\ \dot{\vartheta} + \dot{\psi}\sin\varphi - n_0\cos\varphi\cos\psi \\ \dot{\varphi}\sin\vartheta + \dot{\psi}\cos\vartheta\cos\varphi - n_0(\sin\vartheta\sin\psi - \cos\vartheta\sin\varphi\cos\psi) \end{bmatrix}. \quad (4.7)$$

Conversely, it follows the attitude kinematics in terms of the three Euler angles

$$\begin{bmatrix} \dot{\varphi} \\ \dot{\vartheta} \\ \dot{\psi} \end{bmatrix} = \begin{bmatrix} w_1\cos\vartheta + w_3\sin\vartheta + n_0\sin\psi \\ w_2 + \tan\varphi(w_1\sin\vartheta - w_3\cos\vartheta) + n_0\cos\psi/\cos\varphi \\ (w_3\cos\vartheta - w_1\sin\vartheta - n_0\sin\varphi\cos\psi)/\cos\varphi \end{bmatrix}, \quad (4.8)$$

from which we see that singularities occur at $\varphi = \pm 90°$. Precisely, the Euler angles ϑ and ψ lie in the same plane when $\varphi = \pm 90°$, resulting in the difficulty in determining ϑ and ψ validly. Having singularities is the main disadvantage of the attitude repre-

sentation using the Euler angles. When the angles φ, ϑ and ψ are assumed small, we can linearize the equations of the attitude kinematics as

$$C_{bo} = \begin{bmatrix} 1 & \psi & -\vartheta \\ -\phi & 1 & \varphi \\ \vartheta & -\varphi & 1 \end{bmatrix}, \qquad \begin{bmatrix} \omega_1 \\ \omega_2 \\ \omega_3 \end{bmatrix} = \begin{bmatrix} \dot{\varphi} - n_0\psi \\ \dot{\vartheta} - n_0 \\ \dot{\psi} + n_0\varphi \end{bmatrix}. \tag{4.9}$$

4.3.2 Attitude Kinematics in terms of Quaternion

Compared with the Euler angles, attitude representation using the unit quaternion is free of singularities and has a constraint. It has been stated that the rotation matrix C_{br} in (4.2) is equivalent to an angular rotation about $\boldsymbol{e} = [e_1, e_2, e_3]^T$ over an angle Φ, which transforms the reference frame $\mathcal{F}_r$ ($\mathcal{F}_r$ may be either $\mathcal{F}_o$ or $\mathcal{F}_I$) to the body frame $\mathcal{F}_b$. Then, elements of the quaternion $q = [q_1, q_2, q_3, q_4]^T$ can be defined as

$$q_i = e_i \sin(\frac{\Phi}{2}), \qquad q_4 = \cos(\frac{\Phi}{2}), \qquad i = 1, 2, 3,$$

where $q_v = [q_1, q_2, q_3]^T$ is called the vector part of q and q_4 is the scalar part of q. Clearly, the quaternion $[q_v^T, q_4]^T$ is a redundant system with a nonlinear algebraic constraint

$$q_v^T q_v + q_4^2 = 1. \tag{4.10}$$

The rotation matrix C_{br} associated with the angular displacement $q = [q_v^T, q_4]^T$ is now expressed as

$$C_{br}(q) = (q_4^2 - q_v^T q_v) I_3 + 2 q_v q_v^T - 2 q_4 q_v^{\times}. \tag{4.11}$$

Differentiating the quaternion vector q brings the attitude kinematics in terms of the unit quaternion q (cf. Appendix A):

$$\begin{aligned} \dot{q}_v &= \frac{1}{2}(q_4 I_3 + q_v^{\times})\omega_{br} = \frac{1}{2}(q_4 I_3 + q_v^{\times})(\omega - C_{br}(q)\omega_{ri}), \\ \dot{q}_4 &= -\frac{1}{2} q_v^T \omega_{br} = -\frac{1}{2} q_v^T (\omega - C_{br}(q)\omega_{ri}), \end{aligned} \tag{4.12}$$

where ω_{br} is the angular velocity of the body frame $\mathcal{F}_b$ with respect to a reference frame $\mathcal{F}_r$; ω_{ri} is the angular velocity of the reference frame $\mathcal{F}_r$ with respect to the inertial frame $\mathcal{F}_I$; both of them are expressed in the body frame $\mathcal{F}_b$.

If $\mathcal{F}_r$ is chosen as $\mathcal{F}_I$, then ω_{ri} in Eq.(4.12) is absolutely zero, $\omega_{ri} = 0$. If $\mathcal{F}_r$ is chosen as $\mathcal{F}_o$, then ω_{ri} is given by $\omega_{ri} = C_{bo}(q)\omega_0$ and the attitude kinematics Eq.(4.12) can be finally represented as (See Appendix B for the detailed derivations)

$$\begin{aligned} \dot{q}_v &= \frac{1}{2}(q_4 I_3 + q_v^{\times})\omega - \tfrac{1}{2}(q_4 I_3 - q_v^{\times})\omega_0, \\ \dot{q}_4 &= -\frac{1}{2} q_v^T (\omega - \omega_0). \end{aligned} \tag{4.13}$$

With the choice of $\mathcal{F}_r$ being $\mathcal{F}_o$, there exists a rather direct relationship between the unit quaternion $q = [q_1, q_2, q_3, q_4]^T$ and three Euler angles (in the 3-1-2 rotation sequence):

$$\begin{aligned}
q_1 &= \cos\frac{\vartheta}{2}\sin\frac{\varphi}{2}\cos\frac{\psi}{2} - \sin\frac{\vartheta}{2}\cos\frac{\varphi}{2}\sin\frac{\psi}{2},\\
q_2 &= \sin\frac{\vartheta}{2}\cos\frac{\varphi}{2}\cos\frac{\psi}{2} + \cos\frac{\vartheta}{2}\sin\frac{\varphi}{2}\sin\frac{\psi}{2},\\
q_3 &= \sin\frac{\vartheta}{2}\sin\frac{\varphi}{2}\cos\frac{\psi}{2} + \cos\frac{\vartheta}{2}\cos\frac{\varphi}{2}\sin\frac{\psi}{2},\\
q_4 &= \cos\frac{\vartheta}{2}\cos\frac{\varphi}{2}\cos\frac{\psi}{2} - \sin\frac{\vartheta}{2}\sin\frac{\varphi}{2}\sin\frac{\psi}{2}.
\end{aligned}$$

At this point, we may ask: What single angular displacement $q = [q_v^T, q_4]^T$ corresponds to two successive angular transformations, first $q' = [(q'_v)^T, q'_4]^T$ and then $q'' = [(q''_v)^T, q''_4]^T$? These two transformations can be expressed in the quaternion terminology by $C(q')$ for the first rotation and by $C(q'')$ for the second one. Then, the following expression holds

$$C(q) = C(q'')C(q'). \tag{4.14}$$

The resulting quaternion q can be extracted from $C(q)$. Fortunately, it is much easier to perform a direct quaternion multiplication, resulting in the answer being

$$\begin{aligned}
q_v &= [q''_4 I_3 - (q''_v)^\times]q'_v + q'_4 q''_v\\
q_4 &= -(q'_v)^T q''_v + q'_4 q''_4.
\end{aligned} \tag{4.15}$$

4.4 Dynamic Equations of Attitude Motion

4.4.1 Dynamic Equations of Attitude Motion [53, 101, 126]

A typical spacecraft structure consists of two principal parts: rigid center body and flexible solar panels. The solar panels are appended to the center body by gimbals, so that the panels could be rotated toward the sun from any orbit location. To gain satisfactory control accuracy, three or more reaction wheels – known as *momentum exchange devices* – are mounted in the satellite as attitude actuators to provide almost continuous torques for controlling the attitude.

Attitude dynamical equations of a spacecraft can be established by *Euler's momentum equation*

$$\left.\frac{dH_s}{dt}\right|_I = \left.\frac{dH_s}{dt}\right|_B + \omega \times H_s = T_c + T_d, \tag{4.16}$$

where the subscripts "I" and "B" denote the derivatives with respect to the inertial frame $\mathcal{F}_I$ and the body frame $\mathcal{F}_B$, respectively; H_s denotes the total angular momentum $H_s \in \mathcal{R}^3$ of the spacecraft system in the body frame $\mathcal{F}_b$; $\omega \in \mathcal{R}^3$ is the angular velocity of the spacecraft with respect to the inertial frame $\mathcal{F}_I$; $T_d \in \mathcal{R}^3$ and $T_c \in \mathcal{R}^3$

are the external disturbance torques and the external control torques respectively. For simplicity of analysis, we assume that the spacecraft's transitional and rotational dynamics are decoupled and addressed independently. With this assumption, we have the total angular momentum H_s of the spacecraft as

$$H_s = H_b + H_w + H_p = J\omega + C_w J_w \Omega_w + \delta_p^T \dot{\eta}_p,$$

where the subscripts "w" and "p" denote the wheel and the solar panel respectively. Then, we obtain the Euler's equations of motion for spacecraft attitude as

$$J\dot{\omega} + C_w J_w \dot{\Omega}_w + \delta^T \ddot{\eta}_p + \omega^\times (J\omega + C_w J_w \Omega_w + \delta_p^T \dot{\eta}_p) = T_c + T_d, \tag{4.17}$$

$$\ddot{\eta}_p + 2\xi_p \sigma_p \dot{\eta}_p + \sigma_p^2 \eta_p = \delta_p \dot{\omega}, \tag{4.18}$$

where $\Omega_w \in \mathcal{R}^{n_w}$ is the angular velocity of the wheels with respect to the body of spacecraft; η_i of $\eta_p \in \mathcal{R}^{n_\eta}$ is the amplitude of the ith flexible mode of the solar panels. With regard to vector dimensions, n_w denotes the number of reaction wheels, n_η is the number of flexible modes of the solar panels. Formal definitions of the different matrices are as follows:

$J \in \mathcal{R}^{3\times 3}$	– overall inertia matrix of the integrated satellite system;
$J_w \in \mathcal{R}^{n_w \times n_w}$	– inertia matrix of the wheel arrays;
$C_w \in \mathcal{R}^{3\times n_w}$	– configuration matrix of the wheel arrays;
$\delta_p \in \mathcal{R}^{n_\eta \times 3}$	– flexible modes coupling matrix;
$\xi_p \in \mathcal{R}^{n_\eta \times n_\eta}$	– flexible modes damping matrix, diagonal;
$\sigma_p \in \mathcal{R}^{n_\eta \times n_\eta}$	– flexible modes frequency matrix, diagonal.

4.4.2 Model of Reaction Wheels [101]

Inside a spacecraft, a symmetric rotating body produces an angular torque when accelerated about its axis of rotation. Since the momentum caused by the rotation is internal to the spacecraft, its increase does not change the overall momentum of the system but merely transfers the momentum changes to the spacecraft. This is the principle of *conservation of angular momentum.*

The reaction wheels may be mounted in the satellite with its rotational axis in any direction relative to the body frame $\mathcal{F}_b$. For controlling attitude in space, at least three reaction wheels are required and we assume that the number is m ($m \geq 3$). Let C_w denote the configuration matrix of the wheels. Then, the momentum vector of all wheels inside the satellite can be expressed in the body frame as

$$H_w = [H_{wx}, H_{wy}, H_{wz}]^T = C_w J_w \Omega_w$$

where $J_w = \text{diag}[J_{w_1}, \cdots, J_{w_m}]$ and $\Omega_w = \text{diag}[\Omega_1, \cdots, \Omega_m]$. The complete dynamical model of a reaction wheel in torque command mode is shown as in Figure 4.4. To enable the linear transfer function analysis, the blocks describing the dry friction F_f and the saturation nonlinearity are omitted. Then, the transfer function from the commanded

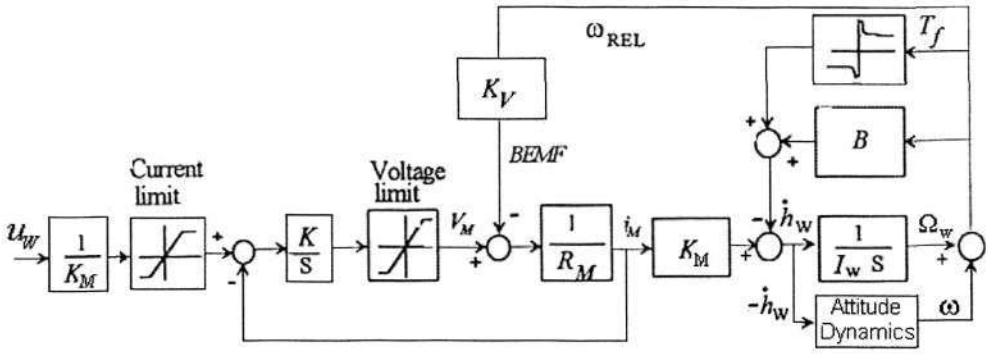

Figure 4.4: Wheel model in torque command mode

torque u_w to the reactional torque $\dot{h}_w$ can be written as

$$G_w(s) = \frac{\dot{h}_w(s)}{u_w(s)} = \frac{(K/R_M)s}{(s + \frac{K}{R_M})[s + \frac{1}{J_w}(B + \frac{K_V K_M}{R_M})]}$$

With the valid assumption that $B \to 0$ and by choosing $K \gg K_V K_M / J_w$, the transfer function $G_w(s)$ is simplified to

$$G_w(s) = \frac{\dot{h}_w(s)}{u_w(s)} = \frac{1}{\tau_w s + 1} \tag{4.19}$$

where $\tau_w = R_M/K$ is called the time constant, which is small. For a good reaction wheel assembly, τ_w may be of the order of milliseconds and can be neglected if necessary. Then, the dynamic equation of the wheels can be rewritten as

$$J_w \dot{\Omega} = u_w - \tau_w J_w \Omega.$$

Let u_c be the control torque vector computed from the control laws and u_w be the input signal to drive the reaction wheels. Let T_{cw} denote the control torque input to the attitude control system for controlling the spacecraft attitude. Then, we can set up the following allocation implications for the wheel array assemblies

$$T_{cw} = C_w \dot{h}_w, \qquad u_w = C_w^T (C_w C_w^T)^{-1} u_c.$$

4.4.3 Environmental Disturbances

An analysis of external disturbances which are caused by space environment and have serious effects on the satellite's attitude is a prior to the design of an attitude control system. In general, gravity-gradient torque, aerodynamic torque, solar radiation torque and magnetic torque are the primary environmental disturbances considered in the attitude control system of a spacecraft. Here, we only present the results taken from the texts [53, 101, 118, 126] and readers can refer to these texts for more details.

Gravity-Gradient Torque

Gravitational torque is generated when the vector of gravity, which depends mainly on the satellite's attitude and mass properties, does not pass through the center of mass of the spacecraft. Under the assumption that the spacecraft is moving in a Keplerian orbit and the earth is spherical, the gravity-gradient torque can be expressed as

$$T_{gd} = \frac{3\mu}{r^5}\, \boldsymbol{r} \times J\boldsymbol{r}$$

where $\boldsymbol{r}$ indicates the position of the spacecraft and $r = ||\boldsymbol{r}||$ is the disturbance from the center of mass of the earth to that of the spacecraft; $\mu = 398600.5\text{km}^3/s^2$ is a constant, and J is the inertia matrix. In the LVLH frame $\mathcal{F}_o$, $\boldsymbol{r}$ is given by $\boldsymbol{r} = [0,\ 0, -r]^T$. By the rotation matrix (4.3), we can estimate the gravity-gradient torque T_{gd} in the body frame $\mathcal{F}_b$ in terms of the three Euler angles as

$$\begin{aligned} T_{g1} &= \tfrac{3\mu}{r^3}(J_3 - J_2)\cos\vartheta \sin\varphi\cos\varphi, \\ T_{g2} &= \tfrac{3\mu}{r^3}(J_3 - J_1)\sin\vartheta\cos\vartheta\cos^2\varphi, \\ T_{g3} &= \tfrac{3\mu}{r^3}(J_1 - J_2)\sin\vartheta\sin\varphi\cos\varphi, \end{aligned} \tag{4.20}$$

in which those terms related to the off-diagonal elements of J are ignored.

Aerodynamic Torque

The rapid spacecraft motion through the tenuous upper atmosphere causes the aerodynamic torque. For an LEO spacecraft with altitude less than 500km, the aerodynamic toque is predominant among all external disturbances caused by the space environment. Between the altitude of 120km and 800km, we can consider atmospheric air as a flow of free molecules that generates atmospheric drag when spacecraft is moving on its orbit. Atmospheric drag causes a satellite to slow down and thus the satellite altitude will lower to gain velocity. The aerodynamic drag is assumed to be proportional to air density and the square of the relative air velocity

$$F_a = \tfrac{1}{2}\rho v^2 C_d A V_0.$$

Then, the aerodynamic torque can be estimated as

$$T_{ad} = L_{cp} \times F_a, \tag{4.21}$$

where C_d and ρ are the drag coefficient and the atmosphere density respectively; V_0 is the unit vector along the air flowing velocity; L_{cp} is the vector offset from the center of mass of the spacecraft to the center of aerodynamic pressure; A is the spacecraft's area perpendicular to V_0; v is the flight rate of the spacecraft.

Residual Magnetic Torque

This torque arises from the interaction of the residual magnetic moments of the spacecraft with the earth's magnetic field. The primary sources generating such mag-

netic torques are the onboard residual magnetic moments, eddy currents and hysteresis. Among these, the onboard residual magnetic moment is usually the predominant source of the magnetic torques. Assume that the residual magnetic moment is ΔM and the geomagnetic field in body reference frame is expressed by B. (The geomagnetic field model will be introduced later.) Then the residual magnetic torque T_{md} is given by

$$T_{md} = \Delta M \times B. \tag{4.22}$$

Solar Radiation Torque

The solar radiation torque is generated by the exchange of moments between radiation particles and satellite surfaces. The total radiation force acting on the whole surfaces of the satellite can be written as [53]

$$F_s = p(c_a + c_{rd})A_p S_0 + p(2c_{rs}A_{pp} + \frac{2}{3}c_{rd}A_p)N_0 \tag{4.23}$$

where p is the incident momentum flux, $p \approx 4.51 \times 10^{-6} N/s^2$ for LEO satellites; c_a is the absorption coefficient of surface under sun shining, c_{rd} the diffuse reflection coefficient, c_{rs} the specular reflection coefficient, $c_a + c_{rs} + c_{rd} = 1$; S_0 is the unit energy flux vector from the Sun to the satellite, N_0 is the unit inward surface normal vector. $A_p = \oint_A H(\cos\alpha)\cos\alpha dA$ and $A_{pp} = \oint_A H(\cos\alpha)\cos^2\alpha dA$ are two integrating functions with respect to the whole surface area A, where α is the angle of incidence of the solar radiation, measured with respect to the normal; $H(x)$ is the Heaviside function, $H(x) = 1$ if $x \geq 0$, else $H(x) = 0$.

Let L_{sp} denote the vector offset from the center of mass of the satellite to the center of solar radiating pressure. Then, the solar radiation torque can be estimated as

$$T_{sd} = L_{sp} \times F_s. \tag{4.24}$$

4.4.4 Geomagnetic Field and Magnetic Unloading

In the attitude control system, the geomagnetic field affects the system performance in a dual way: the interaction with the residual magnetic dipolar moment of the spacecraft generates disturbance torque, which will deteriorate the system performance; on the other hand, with a well-designed algorithm, the interaction with three magnetorquers will generate beneficial torques to remove part of the unexpected excess angular momentum of the wheels, which will improve the system performance.

Geomagnetic Field Model

The predominant portion of the geomagnetic field, B, can be expressed as the gradient of a scalar potential function V,

$$B = -\nabla V, \tag{4.25}$$

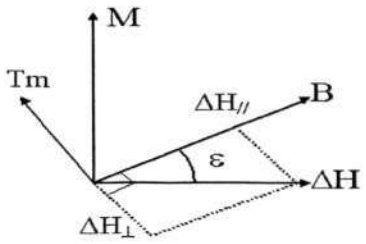

Figure 4.5: Analysis of magnetic momentum unloading

where V is represented by a series of spherical harmonics

$$V(r,\lambda,\theta_e) = R_0 \sum_{n=1}^{\infty}\sum_{m=0}^{n} P_n^m(\cos\theta_e)\Big\{\Big[C_{1n}^m\Big(\frac{r}{R_0}\Big)^n + (1-C_{1n}^m)\Big(\frac{R_0}{r}\Big)^{n+1}\Big]g_n^m\cos m\lambda + \Big[C_{2n}^m\Big(\frac{r}{R_0}\Big)^n + (1-C_{2n}^m)\Big(\frac{R_0}{r}\Big)^{n+1}\Big]h_n^m\sin m\lambda\Big\}$$

where R_0 is the equatorial radius of the earth, $R_0 = 6378.15$km; n is the order of the magnetic field model to be calculated; $P_n^m(\cos\theta_e)$ is the Legendre function (Schmidit normalized); g_n^m and h_n^m are Gaussian coefficients of the IGRF model, $m \le n$; r is the geocentric distance from the earth center to the spacecraft; θ_e is the co-elevation of the satellite (south positive); λ is the east longitude from Greenwich; C_{1n}^m and C_{2n}^m are small correcting coefficients. In practice, the correcting coefficients C_{1n}^m and C_{2n}^m are very small. Hence, it is reasonable to simplify the analysis of V to

$$V(r,\lambda,\theta_e) = R_0 \sum_{n=1}^{\infty}\Big(\frac{R_0}{r}\Big)^{n+1}\sum_{m=0}^{n}\Big(g_n^m\cos m\lambda + h_n^m\sin m\lambda\Big)P_n^m(\cos\theta_e). \tag{4.26}$$

In general, the larger the order n is, the more accurate the model is with respect to the actual magnetic field B; see [126, Appendix H] for the detailed computations of the model of the magnetic field. Actually, the magnetic field B changes nearly periodically as the spacecraft orbits the earth. For simplicity of analysis, the magnetic field B can be approximated by a dipole [126] and thus its magnitude is approximated by

$$||B|| = \frac{\mu_E}{r^3}(1+3\sin^2\theta_m)^{1/2} \tag{4.27}$$

where $\mu_E = 8.1\times 10^{15}\text{Tm}^3$ and θ_m is the magnetic latitude measured from the geomagnetic equator.

Momentum Management of the Wheels

External disturbances acting on the spacecraft induce an accumulation of momentum in the momentum exchange devices such as wheels. This excess momentum might bring the wheels to improper working conditions. Moreover, the existence of excess angular momentum in the satellite might cause control difficulties when attitude maneuvers in

space are executed, because this superfluous momentum provides the spacecraft with unwanted gyroscopic stability. For these reasons, three-axis stabilized spacecraft with a capacity of maneuvering are basically zero-bias-momentum systems and the excess momentum must be unloaded when it exceeds some predetermined limiting values.

We assume that three magnetorquers are installed along the three axes of the body frame $\mathcal{F}_b$ as actuators to dump the wheel. Magnetorquers generate magnetic moments whose interaction with the geomagnetic field produces necessary torques to remove the excess momentum. The strategy for this momentum unloading approach is quite simple, as shown in Figure 4.5.

Let $M_{\max}$ denote the maximal magnetic moment of a magnetorquer and k_m be the unloading control gain. Suppose that h is the actual wheels' momentum vector, h_c is the desired momentum vector and B is the magnetic field vector. Then, $\Delta H_w = C_w(h - h_c)$ is the additional momentum to be removed in the frame $\mathcal{F}_b$ and a momentum-unloading algorithm is designed as

$$\begin{aligned} M &= k_m(\Delta H_w \times B)/||B||^2 \\ T_m &= M \times B = -k_m[B^2 \Delta H_w - B(B \cdot \Delta H_w)]/||B||^2 \end{aligned} \tag{4.28}$$

where T_m is the magnetic torque provided for unloading the excess momentum. If $M_i \geq M_{\max}$, let $M_i = M_{\max}$ for $i = 1, 2, 3$, the elements of M. The control gain k_m is often obtained by the trial-and-error method.

Physically, with the unloading algorithm (4.28), the magnetic torque T_m can only unload the momentum error component $\Delta H_\perp$ that is perpendicular to the magnetic field B at a given time, shown as in Figure 4.5. Fortunately, the component $\Delta H_\parallel$ paralleling to B at this given time can be removed at some other time because the magnetic field B in the body frame changes almost periodically when the satellite is moving around the earth. Thus, an average removal of the excess momentum takes place. The effectiveness of magnetic momentum unloading depends very much on the specific orbit in which the satellite is moving. For equatorial orbits, the efficiency is quite low. Also, when the angle ε in Figure 4.5 is small, the effectiveness of magnetic momentum-unloading is low in the sense that the magnetorquers may produce larger disturbances in the direction of $\Delta H_\parallel$ than the useful unloading torques in the direction of $\Delta H_\perp$. In practice, we often take the following remedy: if the angle ε is larger than a predetermined value, such as 45 degrees, the magnetic unloading algorithm is activated; otherwise, it is not activated. Moreover, such a remedy helps to improve the effectiveness of the power that is to drive the magnetoquers.

4.5 Attitude Tracking Control Problem

In Section 4.4, we have presented complete dynamic models for a wheel-based attitude control system. The attitude control problem for microsatellites is unlike that for large satellites. For large satellites with large flexible appendages, the lightly damped flexible modes should be a major concern. For a microsatellite, the solar panels are

in general small with a considerable rigidity. Hence, it suffices to assume that the microsatellite is compact and to model it as a rigid body at the initial design stage for simplicity of analysis. With the rigid-body assumption and by letting

$$u = -\dot{H}_w + T_c + T_m - \omega^\times H_w,$$
$$d = T_{gd} + T_{ad} + T_{md} + T_{sd},$$

we can simplify the attitude dynamics (4.17) into a rigid body as

$$J\dot{\omega} = -\omega^\times J\omega + u + d \tag{4.29}$$

with the constant, positive definite inertia matrix of the form

$$J = \begin{bmatrix} J_{11} & J_{12} & J_{13} \\ J_{12} & J_{22} & J_{23} \\ J_{13} & J_{23} & J_{33} \end{bmatrix}. \tag{4.30}$$

In attitude control systems, the reference frame $\mathcal{F}_r$ in Eq.(4.12) is commonly chosen to be the orbit (LVLH) frame $\mathcal{F}_o$ to maintain the attitude of spacecraft stable with respect to the LVLH frame. With such a choice, the attitude kinematics is represented by (4.13) (see Appendix B). To formulate the attitude control problem, we let $\mathcal{F}_{bc}$ denote the body frame in which the desired attitude motion of the spacecraft is described. Then, the attitude tracking control is to assure that the two frames $\mathcal{F}_b$ and $\mathcal{F}_{bc}$ coincide eventually, that is, $\mathcal{F}_b \to \mathcal{F}_{bc}$ as $t \to \infty$.

Let the unit quaternion $q_c = [q_{cv}^T, q_{c4}]^T$ satisfying $q_{cv}^T q_{cv} + q_{c4}^2 = 1$ represent the target attitude of the spacecraft in the body frame $\mathcal{F}_{bc}$ with respect to the orbital frame $\mathcal{F}_o$, and let $\omega_c \in \mathcal{R}^3$ be the desired angular velocity of the body frame $\mathcal{F}_{bc}$ with respect to the inertia frame $\mathcal{F}_I$ and be expressed in the frame $\mathcal{F}_{bc}$. From (4.13) we have the following differential equations of the desired attitude motion

$$\begin{aligned} \dot{q}_{cv} &= \tfrac{1}{2}(q_{c4}I_3 + q_{cv}^\times)\omega_c - \tfrac{1}{2}(q_{c4}I_3 - q_{cv}^\times)\omega_0, \\ \dot{q}_{c4} &= -\tfrac{1}{2}q_{cv}^T(\omega_c - \omega_0). \end{aligned} \tag{4.31}$$

Remark 4.1. Conversely, if the desired attitude quaternion q_c is known, then we can obtain the desired angular velocity ω_c of $\mathcal{F}_{bc}$ with respect to $\mathcal{F}_I$ by

$$\omega_c = 2(q_{c4} - q_{cv}^\times)\dot{q}_{cv} - 2q_{cv}\dot{q}_{c4} + C_{co}(q_c)\omega_0,$$

and its time derivative $\dot{\omega}_c$ by

$$\dot{\omega}_c = 2(q_{c4}\ddot{q}_{cv} - \ddot{q}_{c4}q_{cv}) - 2q_{cv}^\times\ddot{q}_{cv} - \omega_c^\times C_{co}(q_c)\omega_0,$$

where the direction cosine matrix $C_{co}(q_c) = (q_{c4}^2 - q_{cv}^T q_{cv})I_3 + 2q_{cv}q_{cv}^T - 2q_{c4}q_{cv}^\times$ relates the frame $\mathcal{F}_{bc}$ to the frame $\mathcal{F}_I$. (See Appendix A.) ⊗

At this point, we can define a quaternion error q_e to express the attitude orientation

error between the spacecraft quaternion q and the target quaternion q_c. According to (4.14), we can write

$$C(q_e) = C_{bo}(q)[C_{co}(q_c)]^{-1}. \tag{4.32}$$

By the quaternion multiplication (4.15), Eq. (4.32) leads to the quaternion error vector $q_e = [\epsilon^T, \eta]^T$ being expressed as

$$\begin{aligned} \epsilon &= q_{c4}q_v - q_{cv}^{\times}q_v - q_4 q_{cv}, \\ \eta &= q_{cv}^T q_v + q_4 q_{c4}. \end{aligned} \tag{4.33}$$

Clearly, the quaternion error $q_e = [\epsilon^T, \eta]^T$ satisfies the nonlinear algebraic constraint

$$\epsilon^T\epsilon + \eta^2 = 1, \quad \epsilon \in \mathcal{R}^3, \eta \in \mathcal{R} \tag{4.34}$$

and corresponds to the direction cosine matrix $C(q_e) = C(\epsilon, \eta) \in SO(3)$ that relates the frame $\mathcal{F}_b$ to the frame $\mathcal{F}_{bc}$

$$C(\epsilon, \eta) = (1 - 2\epsilon^T\epsilon)I_3 + 2\epsilon\epsilon^T - 2\eta\epsilon^{\times}. \tag{4.35}$$

It is observed that both (ϵ, η) and $(-\epsilon, -\eta)$ stand for exactly the same physical attitude orientation, resulting in the same $C(\epsilon, \eta) \in SO(3)$. Note that

$$\begin{aligned} \epsilon = 0 &\Longleftrightarrow C(\epsilon, \eta) = I_3, \\ \epsilon = 0 &\Longleftrightarrow \eta = \pm 1. \end{aligned} \tag{4.36}$$

Hence, $(\epsilon, \eta) = (0, 1)$ and $(\epsilon, \eta) = (0, -1)$ both correspond to $C(\epsilon, \eta) = I_3$.

The angular velocity error ω_e is defined as

$$\omega_e = \omega - C(\epsilon, \eta)\omega_c, \tag{4.37}$$

which represents the relative angular velocity of $\mathcal{F}_b$ with respect to $\mathcal{F}_{bc}$ and is expressed in the frame $\mathcal{F}_b$. It follows from [101, Chapter 4] that

$$C^T C = 1, \quad ||C|| = 1, \quad \dot{C} = -\omega_e^{\times} C.$$

To state the attitude tracking control problem in Definition 4.2, the following assumption is required.

Assumption 4.1. *The target angular velocity $\omega_c(t)$ and its derivative $\dot{\omega}_c(t)$ are bounded for all $t \geq 0$ with known bounds, that is, there exist some known, finite constants $\bar{c}_{w1} > 0$ and $\bar{c}_{w2} > 0$ such that $\bar{c}_{w1} = \sup\{||\omega_c(t)||\}$ and $\bar{c}_{w2} = \sup\{||\dot{\omega}_c(t)||\}$ for all $t \geq 0$.*

Definition 4.2. *With Assumption 4.1, the **attitude tracking control problem** is to find a continuous feedback control*

$$u = \alpha(\epsilon, \eta, \omega_e, \omega_c, \dot{\omega}_c)$$

such that $C(\epsilon,\eta) \to I_3$ *and* $\omega_e \to 0$ *as* $t \to \infty$.

Lemma 4.2. [137] *Two coordinate systems* $\mathcal{F}_b$ *and* $\mathcal{F}_{bc}$, *corresponding to* q *and* q_c *respectively, coincide if and only if the error vector* ϵ *in (4.33) is zero, i.e.,* $\epsilon = 0$.

From (4.36) it follows that $C(\epsilon,\eta) \to I_3$ if and only if $\epsilon \to 0$. By Lemma 4.2, the attitude tracking control problem is solved if and only if $\epsilon \to 0$ and $\omega_e \to 0$ as $t \to \infty$. Note that $\eta \to \pm 1$ when $\epsilon \to 0$ as $t \to \infty$.

Substituting (4.31)–(4.37) into (4.13) and (4.29) and applying $\dot{C} = -\omega_e^{\times} C$ and Lemma 4.1, we obtain the following differential error equations for the attitude tracking control problem (see Appendix B)

$$\dot{\epsilon} = \tfrac{1}{2}(\eta I_3 + \epsilon^{\times})\omega_e, \tag{4.38}$$

$$\dot{\eta} = -\tfrac{1}{2}\epsilon^T \omega_e, \tag{4.39}$$

$$J\dot{\omega} = -(\omega_e + C\omega_c)^{\times} J(\omega_e + C\omega_c) + J(\omega_e^{\times} C\omega_c - C\dot{\omega}_c) + u + d. \tag{4.40}$$

The attitude tracking control problem is thus transformed into the problem of stabilizing the error system (4.38–4.40).

Remark 4.2. With Assumption 4.1, if a controller stabilizes the error system (4.38–4.40), then it makes the original system (4.13) and (4.29) stable. ⊗

Remark 4.3. For the attitude stabilizing control problem, we wish to keep the Euler angles and the Euler rates near zeros, thus we can let $\varphi_c = \vartheta_c = \psi_c = 0$ and $\dot{\varphi}_c = \dot{\vartheta}_c = \dot{\psi}_c = 0$, that is, $\omega_c \equiv \omega_0$, $\dot{\omega}_c \equiv 0$ and $q_c = 0$, where ω_0 is defined by (4.5). ⊗

Remark 4.4. For the large-angle attitude maneuver problem, it follows that $\dot{\omega}_c \equiv 0$, $\omega_c = C_{co}(q_c)\omega_0$ and $q_c = \textit{constant}$, where $C_{co}(q_c)$ is defined in Remark 4.1. Thus, both the attitude stabilizing control and the large-angle attitude maneuver control can indeed be considered as special cases of the attitude tracking control problem. ⊗

Summary

We have presented the attitude kinematics and dynamics for the attitude control system shown in Figure 4.1, which can be used for the attitude maneuver/tracking control and for the attitude stabilizing control. In practice, the attitude determination and the attitude control are two decoupled tasks. Hence, in the attitude control, precise attitude information is assumed available from well-designed attitude sensors and attitude determination algorithms, and state feedback will be used for the attitude control. This simplifies the design problem in practice. Also, it is quite common not to consider the attitude determination problem in the design of attitude controllers. Our major concerns of the thesis are the design of attitude controllers and the corresponding performance analysis, which will be presented in the next few chapters.

Chapter 5

H_∞ Inverse Optimal Attitude Tracking Control

5.1 Introduction

The present generation of space missions requires attitude control systems to provide capabilities of attitude maneuver, tracking and pointing, while the equations that govern large-angle attitude maneuvers or tracking in the presence of exogenous disturbances are nonlinear and highly coupled. As such, control system design must consider the nonlinear dynamic models.

Based on the direct use of nonlinear system model and nonlinear control theory, various nonlinear control algorithms have been proposed for solving the attitude control problem. These include nonlinear feedback control [102, 125, 128], feedback linearization [78], variable structure sliding control [119], linearly bound control [8], nonlinear adaptive control [1] and nonlinear H_∞ control [57], etc. Due to its inherent robust property with respect to disturbances and model uncertainties, nonlinear H_∞ optimal control method [123] is a potential approach for solving the nonlinear attitude control problem. However, the practical application of nonlinear H_∞ optimal control still remains open due to the difficulty in solving the associated Hamilton-Jacobi-Isaacs (HJI) partial differential equation. Various methods have been proposed in an attempt to solve the HJI equation. One of the methods that provides approximate solutions is the state-dependent Riccati equation (SDRE) method [23, 52], albeit only suboptimality and local stability can be guaranteed. Algebraic and geometric tools [25, 65, 135] were employed to study a particular H_∞ suboptimal control problem by solving the associated HJI partial differential inequality. Note that the derived H_∞ suboptimal control laws [25, 65, 135] were designed to solve the attitude stabilizing control problem and the $\mathcal{L}_2$ gain γ was restricted to be larger than a certain value. A power series solution [100] to the HJI inequality was proposed for the H_∞ suboptimal control of wing rock motions by representing the state vector as a series of closed-loop Lyapunov functions. The concept of extended disturbances, including system error dynamics, was introduced in robotics by [83, 84] to solve the HJI equation. Besides these attempts to find analytical solutions, a numerical approach [49–51] based on Taylor-series expan-

sion was proposed as a more systematic way to find the numerical solution to the HJI equation or the HJI inequality.

As stated in Chapter 2, the inverse optimality approach is another approach to achieve robust optimal control without solving the associated Hamilton-Jacobi-Isaacs partial differential equation in a direct way. In this chapter we follow the inverse optimal control method [35, 63] to derive an H_∞ optimal control law for the nonlinear attitude tracking problem of a rigid spacecraft with external disturbances. The first application of this approach to the attitude control problem was presented in [64], in which a nonlinear inverse optimal feedback controller based on Rodriguez parameters was proposed for the attitude stabilizing control problem of a rigid spacecraft in the absence of exogenous disturbances. The optimal feedback control in [64] is a regional solution because the attitude representation using Rodriguez parameters has a singularity. Also, only the stabilizing control problem but not the attitude tracking problem was considered in [64]. An H_∞ inverse optimal PID controller [18] was designed for the trajectory tracking control problem of robotic manipulators that are described by Lagrangian equations.

Using the singularity-free unit quaternion to represent the attitude of spacecraft, in this chapter we apply the inverse optimal control method and introduce the concept of extended disturbances to solve the attitude tracking control problem. The robust inverse optimality approach requires the knowledge of a control Lyapunov function and a stabilizing control law for an auxiliary nonlinear system. The proposed controller is inverse optimal with respect to a set of cost functionals involving tracking errors, control efforts and extended disturbances. We present an inverse optimal feedback controller which is also H_∞ optimal with respect to extended disturbances. Compared with [25,57,65,135], the $\mathcal{L}_2$ gain γ for this H_∞ inverse optimal controller is only required to be positive and can be chosen sufficiently small instead of γ being larger than certain values, thus the feedback controller can achieve any disturbance attenuation level. Also, the performance analysis is carried out for the H_∞ inverse optimal attitude controller in terms of performance limitation, and tuning rules are presented for selecting the control gains.

This chapter is organized as follows. In Section 5.2, the concept of extended disturbances is introduced to formulate the nonlinear H_∞ inverse optimal control problem. In Section 5.3, results in [25, 57] are extended to the attitude tracking control problem to design a nonlinear H_∞-suboptimal controller by solving the HJI inequality explicitly for a given $\gamma > 1$ and some special choices of the output function. In Section 5.4, an H_∞ inverse optimal feedback controller is derived using the inverse optimal control method. Performance estimates of the inverse optimal controller are analyzed and guidelines are established in Section 5.5 for selecting controller gains. Numerical simulations in Section 5.6 illustrate the control algorithms in this chapter. Finally, conclusions for this chapter follow in Section 5.7.

5.2 Formulation of Nonlinear H_∞ Inverse Optimal Control Problem

In formulating the H_∞ disturbance attenuation problem, we will apply the concept of extended disturbances, which includes system error dynamics, to simplify the synthesis of the attitude control problem. The concept of extended disturbances was developed in robotics in [18,83,84] to solve the HJI partial differential equation for the trajectory tracking problem of Euler-Lagrange systems of the form:

$$M(q)\ddot{q} + C(q,\dot{q})\dot{q} + g(q) + d(t) = \tau,$$

where $q \in \mathcal{R}^n$ is the generalized coordinates of Euler-Lagrange systems; $\tau \in \mathcal{R}^n$ is the input; $d \in \mathcal{R}^n$ is the disturbances; $g(q)$ denotes the gravity forces; $M(q) \in \mathcal{R}^{n\times n}$ is the generalized inertia matrix, which is symmetric and positive definite; $C(q,\dot{q}) \in \mathcal{R}^{n\times n}$. For such a Euler-Lagrange system, the associated HJI partial differential equation can be transformed into a differential Riccati equation.

For attitude representations using minimal parameters such as the Euler angles and the Euler-Rodriguez vector, it was shown in [96,102,134] that the attitude control system can be represented as a Euler-Lagrange system. However, there are singularities at some special orientations for the attitude representation using minimal parameters and hence global results are not available. For attitude representations using the unit quaternion, it is not suitable to reformulate the attitude control system as a Euler-Lagrange equation because the unit quaternion is a redundant system with a nonlinear algebraic constraint. Therefore, we could not expect to design a controller by solving the differential Riccati equation as done in [18,83,84]. However, with the introduction of the concept of extended disturbances into the attitude control and by applying extensively the properties of the matrix $a^\times$ given in Lemma 4.1, it is still possible for us to design an optimal controller for the attitude tracking control problem.

In Chapter 4, we derived the following differential error equations for the attitude tracking problem

$$\begin{aligned} J\dot{\omega}_e &= -\omega_e^\times J\omega_e + u + [d + J\omega_e^\times C\omega_c - JC\dot{\omega}_c - (C\omega_c)^\times J\omega_e - (\omega_e + C\omega_c)^\times JC\omega_c], \\ \dot{\epsilon} &= \frac{1}{2}[\eta I_3 + \epsilon^\times]\omega_e, \\ \dot{\eta} &= -\frac{1}{2}\epsilon^T\omega_e. \end{aligned} \tag{5.1}$$

Define the extended disturbance $\hat{d}(C,\omega_e,\omega_c,\dot{\omega}_c)$ as

$$\hat{d} :\equiv d + J\omega_e^\times C\omega_c - JC\dot{\omega}_c - (C\omega_c)^\times J\omega_e - (\omega_e + C\omega_c)^\times JC\omega_c \tag{5.2}$$

and denote the state vector x as

$$x = \begin{bmatrix} \epsilon^T & \eta & \omega_e^T \end{bmatrix}^T. \tag{5.3}$$

Then, we can rewrite the nonlinear error differential equation (5.1) as

$$\dot{x} = f(x) + g_1(x)\hat{d} + g_2(x)u \tag{5.4}$$

with the following smooth matrix functions

$$f(x) = \begin{bmatrix} \frac{1}{2}(\eta I_3 + \epsilon^\times)\omega_e \\ -\frac{1}{2}\epsilon^T\omega_e \\ -J^{-1}\omega_e^\times J\omega_e \end{bmatrix}, \quad g_2(x) = \begin{bmatrix} 0_{33} \\ 0_{13} \\ J^{-1} \end{bmatrix}, \quad g_1(x) = \begin{bmatrix} 0_{33} \\ 0_{13} \\ J^{-1} \end{bmatrix},$$

where 0_{33} and 0_{13} are the zero matrices of the indicated dimensions. Thus, the attitude tracking problem is transformed into the problem of stabilizing the error system (5.4) with respect to the extended disturbance $\hat{d}(C, \omega_e, \omega_c, \dot{\omega}_c)$.

Note that x is not an independent state vector due to the fact $\epsilon^T\epsilon + \eta^2 = 1$. Therefore, our control goal is to let $\epsilon \to 0$ and $\omega_e \to 0$ as $t \to \infty$, instead of that $x \to 0$ as $t \to \infty$.

In Chapter 3, the nonlinear H_∞ control problem is defined in Definition 3.15 and the inverse optimal control problem is defined in Definition 3.17. Analogously, we can define the nonlinear H_∞ inverse optimal control problem for the system:

$$\begin{aligned} &\dot{x} = f(x) + g_1(x)d + g_2(x)u, \quad x \in \mathcal{X} \subset \mathcal{R}^n, d \in \mathcal{R}^r, u \in \mathcal{R}^m, \\ &z = \begin{bmatrix} h(x) \\ R_2(x)^{1/2}u(x) \end{bmatrix}, \quad z \in \mathcal{R}^p, \end{aligned} \tag{5.5}$$

where $f(x)$, $g_1(x)$, $g_2(x)$ and $h(x)$ are all C^k functions with $k \geq 2$; the continuous matrix $R(x)$ is positive definite and symmetric, $R(x)^T = R(x) > 0$ for all x.

Definition 5.1. *[63] The H_∞* ***inverse optimal control problem*** *for the nonlinear system (5.5) is solvable if there exist two continuous matrices $R_1(x)$ and $R_2(x)$ such that $R_1(x) = R_1^T(x) > 0$ and $R_2(x) = R_2^T(x) > 0$ for all x, positive semi-definite radially unbounded functions $l(x)$ and $E(x)$, and a feedback control $u = \alpha(x)$ that is continuous with $\alpha(x_e) = 0$ and minimizes the cost functional,*

$$J_a(u) = \sup_{d \in \mathcal{D}} \left\{ \lim_{t \to \infty} \left[E(x(t)) + \int_0^t \left(l(x) + u^T R_2(x) u - d^T R_1 d \right) d\tau \right] \right\}$$

where $\mathcal{D}$ is the set of locally bounded functions of x.

The state-dependent weight $R_1(x)$ is required to take finite values for all finite values of the state x. Also, a smaller $R_1(x)$ means a better disturbance attenuation. It is obvious that when $R_1(x) = \gamma^2 I_r$ and $J_a(u) \geq 0$, Definition 5.1 covers the nonlinear H_∞ control problem in Definition 3.15. The function $E(x(t))$ is to avoid imposing explicitly an additional constraint that $x \to 0$ as $t \to \infty$. For the attitude tracking problem, since η and ϵ are not independent of each other, we can use this $E(x)$ to avoid imposing the assumption that $\eta \to 1$ as $t \to \infty$ because $(\eta, \epsilon) = (\pm 1, 0)$ stands for the same physical attitude. We only require the asymptotic convergence of ϵ to zero.

5.3 An H_∞ Suboptimal Attitude Controller

As formulated in Chapter 3, the H_∞ disturbance attenuation problem of nonlinear systems can be formulated as an H_∞-suboptimal control problem in the sense of Definition 3.15. In this section, by applying Theorem 3.7 and using the extended disturbance (5.2), we extend the results in [25, 57] for the attitude regulation problem to design an H_∞-suboptimal control law by solving the HJI inequality (3.16) explicitly for the attitude tracking control problem (5.4).

Define the output function for the attitude tracking problem (5.4) as

$$z = \begin{bmatrix} \frac{1}{2}\rho_1 \omega_e^T J \omega_e + \rho_2 (2 \arccos |\eta|)^2]^{1/2} \\ -L_{g_2}^T V(x) \end{bmatrix} \tag{5.6}$$

with some positive constants ρ_1 and ρ_2. Using the Lyapunov function candidate

$$V = \frac{1}{2} a \omega_e^T J \omega_e + b \omega_e^T J \epsilon + c(1-\eta)^2 + c\epsilon^T \epsilon$$

to solve the HJI partial differential inequality (3.16), we obtain the following theorem that establishes an H_∞-suboptimal control law for solving the attitude tracking control problem with respect to the extended disturbance $\hat{d}(C, \omega_e, \omega_c, \dot{\omega}_c)$ in the sense of Definition 3.15.

Theorem 5.1. *Let $\gamma > 1$ and*

$$b \geq \sqrt{\frac{\pi^2 \gamma^2 \rho_2}{\gamma^2 - 1}}, \tag{5.7}$$

$$a \geq \sqrt{\frac{(b + \frac{1}{2}\rho_1)\gamma^2 ||J||}{\gamma^2 - 1}}, \tag{5.8}$$

then, the state-feedback control

$$u = -a\omega_e - b\epsilon \tag{5.9}$$

solves the nonlinear state-feedback H_∞-suboptimal control problem (defined in Definition 3.15) for the system described by (5.4) and (5.6) on $TS(3)$ with respect to the extended disturbance $\hat{d}(C, \omega_e, \omega_c, \dot{\omega}_c)$ in (5.2).

In addition, the closed-loop system (5.4), (5.9) is locally asymptotically stable at the equilibrium point $(\epsilon, \eta, \omega_e)_e = (0, 1, 0)$ when $\hat{d}(C, \omega_e, \omega_c, \dot{\omega}_c) = 0$ for all $t \geq 0$.

Proof. Theorem 5.1 is analogous to [25, Theorem 2], but it is extended to address the attitude tracking problem and has a minor improvement to get the condition (5.8). It should be noted that Lemma 4.1 and the inequality $|\omega_e^T J(\eta I_3 - \epsilon^\times)\omega_e| \leq ||J|| ||\omega_e||^2$ are applied such that the constraint $a \geq \sqrt{\frac{(3b+\rho_1/2)\gamma^2||J||}{(\gamma^2-1)}}$ in [25] is relaxed to (5.8). Readers can easily follow [25] to complete the proof. Therefore, we omit it here. □

Furthermore, since both $(\epsilon, \eta, \omega_e) = (0, 1, 0)$ and $(\epsilon, \eta, \omega_e) = (0, -1, 0)$ stand for the

same physical orientation in space, the control law proposed in (5.9) is global for the attitude tracking problem presented in Definition 4.2.

If we use the nonlinear system (5.1) directly to design a controller, we have the following derivative of V:

$$\begin{aligned}\dot{V} &= \frac{\partial V}{\partial \epsilon}\dot{\epsilon} + \frac{\partial V}{\partial \eta}\dot{\eta} + \frac{\partial V}{\partial \omega_e}\dot{\omega}_e \\ &= c\epsilon^T\omega_e + \frac{1}{2}b\omega_e^T J(\eta I + \epsilon^\times)\omega_e + (a\epsilon + b\omega_e)^T(u+d) \\ &\quad + (a\epsilon + b\omega_e)^T\left[J\omega_e^\times C\omega_c - JC\dot{\omega}_c - (\omega_e + C\omega_c)^\times J(\omega_e + C\omega_c)\right],\end{aligned}$$

from which it is observed that the presence of the reference signals $\omega_c(t)$ and $\dot{\omega}_c(t)$ makes it very difficult to solve the HJI partial differential inequality (3.16) using a static feedback control law $u = -(L_{g_2}V(x))^T = -a\omega_e - b\epsilon$. Therefore, we conclude that the introduction of the extended disturbance $\hat{d}(C, \omega_e, \omega_c, \dot{\omega}_c)$ helps us to alleviate greatly the difficulty in solving the HJI partial differential inequality (3.16) and makes it possible for an H_∞-suboptimal control problem to be solvable in such a manner.

From Theorem 5.1 it is also noted that the $\mathcal{L}_2$-gain from the extended disturbance $\hat{d}$ to the output vector z is required to be $\gamma > 1$ and only suboptimality is achieved. The constraint $\gamma > 1$ is imposed by the solvability of the HJI inequality (3.16) with the output penalty vector (5.6). In next section, an H_∞ inverse optimal state-feedback control law will be designed, in which the limitation of $\gamma > 1$ will be removed and thus the proposed inverse optimal controller is also less restrictive.

The effects of the extended disturbance $\hat{d}(C, \omega_e, \omega_c, \dot{\omega}_c)$ on the system performance under the state-feedback H_∞ control (5.9) can be analogously analyzed as the performance analysis of an H_∞ inverse optimal attitude controller in Section 5.5.

5.4 H_∞ Inverse Optimal Control for the Attitude Tracking Problem

As stated in [35,61–63], the inverse optimality approach circumvents the task of solving the Hamilton-Jacobi-Isaacs partial differential equation and results in the proposed controller inverse optimal with respect to a family of meaningful cost functionals. Now we proceed to apply the inverse optimal control method to the design of an inverse optimal control law for the attitude tracking control problem.

The main tool for stability analysis and synthesis is the Lyapunov direct method [59,62,102] with a judicious choice of the Lyapunov function candidate. Motivated by the consideration of the total energy of the attitude control system (5.1), we choose the control Lyapunov function V of the form:

$$V(x) = \tfrac{1}{2}\omega_e^T J\omega_e + b\omega_e^T J\epsilon + 2c(1-\eta), \tag{5.10}$$

where b should be small enough to ensure that V is positive definite, and $c > 0$. The

energy candidate V consists of three parts: the kinetic energy $\frac{1}{2}\omega_e^T J\omega_e$, an artificial potential energy $c(1-\eta)$ and an inner-product term of the angular momentum $J\omega_e$ and the position error ϵ. The purpose of this cross term is to establish a locally exponential convergence and to facilitate the adaptive control in next chapter. Without this product term, stability can still be shown by using the LaSalle invariance principle [59, Section 3.2], but the locally exponential stability is lost. Also, if without the product term, it seems impossible to design a robust control of the static feedback form $u = -R_2^{-1}(L_{g_2}V)^T$ for the attitude tracking problem with disturbances.

Since $2(1-\eta) = ||\epsilon||^2 + (1-\eta)^2$ and $\epsilon^T\epsilon + \eta^2 = 1$, therefore it follows that

$$V(x) = \frac{1}{2}\omega_e^T J\omega_e + b\omega_e^T J\epsilon + c\epsilon^T\epsilon + c(1-\eta)^2 = \frac{1}{2}\tilde{x}^T Q_V \tilde{x} + c(1-\eta)^2$$

for the notations

$$\tilde{x} = \begin{bmatrix} \epsilon \\ \omega_e \end{bmatrix}, \qquad Q_V = \begin{bmatrix} 2cI_3 & bJ \\ bJ & J \end{bmatrix}. \tag{5.11}$$

Standard matrix analysis then gives a sufficient condition for V to be positive definite

$$2cI_3 > b^2 J, \tag{5.12}$$

which ensures that $Q_V > 0$.

Therefore, applying the properties of the matrix $a^\times$ in Lemma 4.1, we have the following Lie derivatives of V of (5.10) along the solutions of the system (5.4):

$$\begin{aligned} L_f V &= \frac{b}{2}\omega_e^T J(\eta I_3 + \epsilon^\times)\omega_e + c\epsilon^T\omega_e - b\epsilon^T\omega_e^\times J\omega_e \\ &= \frac{b}{2}\omega_e^T J(\eta I_3 - \epsilon^\times)\omega_e + c\epsilon^T\omega_e, \\ L_{g_1}V &= \omega_e^T + b\epsilon^T, \\ L_{g_2}V &= \omega_e^T + b\epsilon^T. \end{aligned} \tag{5.13}$$

Also, let λ_j denote the maximum eigenvalue of the inertia matrix J of the spacecraft, and $||J||$ denote the induced 2-norm of J. It follows that

$$\lambda_j = \lambda_{\max}(J) = ||J||.$$

Before presenting an inverse optimal control law in Theorem 5.3, we first propose a PD controller that stabilizes an auxiliary system of the nonlinear attitude system (5.4) on $(\mathcal{S}(3) \times \mathcal{R}^3) \setminus (0, -1, 0)$ by the following theorem.

Theorem 5.2. *The PD control law*

$$u = -R_2^{-1}(x)(L_{g_2}V)^T = -\Big(k_1 + \frac{1}{\gamma^2}k_2\Big)(\omega_e + b\epsilon) \tag{5.14}$$

with the matrix $R_2(x)$ *being*

$$R_2^{-1}(x) = \Big(k_1 + \frac{1}{\gamma^2}k_2\Big)I_3 \tag{5.15}$$

globally asymptotically stabilizes the auxiliary system

$$\begin{bmatrix} \dot{\epsilon} \\ \dot{\eta} \\ \dot{w}_e \end{bmatrix} = \begin{bmatrix} \frac{1}{2}(\eta I_3 + \epsilon^\times)\omega_e \\ -\frac{1}{2}\epsilon^T\omega_e \\ -J^{-1}\omega_e^\times J\omega_e \end{bmatrix} + \frac{1}{\gamma^2}\begin{bmatrix} 0_{33} \\ 0_{13} \\ J^{-1} \end{bmatrix}(L_{g_1}V)^T + \begin{bmatrix} 0_{33} \\ 0_{13} \\ J^{-1} \end{bmatrix}u \tag{5.16}$$

about the equilibrium point $(\epsilon, \eta, \omega_e) = (0, 1, 0)$ *on* $(\mathcal{S}(3)\times\mathcal{R}^3)\backslash(0, -1, 0)$ *if the controller gains in (5.10) and (5.14) satisfy the following conditions:*

$$b > 0, \quad c = 2b\Big(k_1 + \frac{k_2 - 1}{\gamma^2}\Big), \quad k_1 > \frac{b}{2}\lambda_j - \frac{k_2 - 1}{\gamma^2}, \quad k_2 \geq 1. \tag{5.17}$$

Furthermore, if the initial condition at $t_0 = 0$ *satisfies*

$$\eta(0) \geq -1 + \frac{1}{2c}\Big[\frac{1}{2}\omega_e^T(0)J\omega_e(0) + b\omega_e^T(0)J\epsilon(0)\Big] + \frac{1}{2c}\delta_\eta, \tag{5.18}$$

where δ_η *is a sufficiently small constant,* $\delta_\eta > 0$, *then* ϵ *and* $\omega_e \to 0$ *exponentially.*

Proof. If we consider a class $\mathcal{K}_\infty$ function $\rho(r) = \gamma^2 r^2$, it follows that $\rho'(r) = 2\gamma^2 r$, $(\rho')^{-1}(r) = \frac{r}{2\gamma^2}$, $\ell\rho(r) = \int_0^r (\rho')^{-1}(s)ds = \frac{r^2}{4\gamma^2}$ and $\ell\rho(2r) = \frac{r^2}{\gamma^2}$. We can then construct an auxiliary system as follows:

$$\dot{x}(t) = f(x) + \tfrac{1}{\gamma^2}g_1(x)(L_{g_1}V)^T + g_2(x)u, \tag{5.19}$$

which is the state representation of (5.16).

Since $\epsilon^T\epsilon + \eta^2 = 1$, it can be shown by Definition 2.2 and Lemma 2.1 that

$$\begin{aligned} &||\eta I_3 - \epsilon^\times|| = ||\eta I_3 + \epsilon^\times|| = 1, \\ &|w^T J(\eta I_3 - \epsilon^\times)w| \leq ||J||||w||^2. \end{aligned} \tag{5.20}$$

Applying the inequality (5.20) and Lemma 4.1, we have the following derivative of V along the solution of the system (5.16):

$$\begin{aligned} \dot{V} &= L_f V + \frac{1}{\gamma^2}(L_{g_1}V)(L_{g_1}V)^T + L_{g_2}Vu \\ &= \frac{b}{2}\omega_e^T J(\eta I_3 - \epsilon^\times)\omega_e + c\epsilon^T\omega_e + \frac{1}{\gamma^2}\big|\big|\omega_e + b\epsilon\big|\big|^2 + (\omega_e + b\epsilon)^T u \\ &\leq \frac{b}{2}\lambda_j||\omega_e||^2 + \Big(c + \frac{2b}{\gamma^2}\Big)\epsilon^T\omega_e + \frac{1}{\gamma^2}\Big(||\omega_e||^2 + b^2||\epsilon||^2\Big) + (\omega_e + b\epsilon)^T u \\ &= \Big(\frac{b}{2}\lambda_j + \frac{1}{\gamma^2}\Big)||\omega_e||^2 + \frac{b^2}{\gamma^2}||\epsilon||^2 + \Big(c + \frac{2b}{\gamma^2}\Big)\epsilon^T\omega_e + (\omega_e + b\epsilon)^T u. \end{aligned} \tag{5.21}$$

We design the control law $u(x)$ to be of a PD form, given by (5.14), and select

the controller parameters b, c, k_1, k_2 satisfying the constraint (5.17). Clearly, such parameters guarantee (5.12) such that the Lyapunov function V in (5.10) is positive definite since

$$2cI_3 = 4b\big(k_1 + \frac{k_2 - 1}{\gamma^2}\big)I_3 > 2b^2||M||I_3 > b^2 M.$$

Hence,

$$\begin{aligned}\dot{V} &\leq \Big(\frac{b}{2}\lambda_j + \frac{1}{\gamma^2}\Big)||\omega_e||^2 + \frac{b^2}{\gamma^2}||\epsilon||^2 + \Big(c + \frac{2b}{\gamma^2}\Big)\epsilon^T\omega_e - \Big(k_1 + \frac{k_2}{\gamma^2}\Big)||\omega_e + b\epsilon||^2 \\ &\leq -\lambda_b||\tilde{x}||^2,\end{aligned}$$

where the vector $\tilde{x} = [\epsilon^T, \omega_e^T]^T$ is given as in (5.11) and $\lambda_b > 0$ is defined by

$$\lambda_b = \min\Big\{k_1 - \frac{b}{2}\lambda_j + \frac{k_2 - 1}{\gamma^2},\ \ \frac{b^2(k_2 - 1)}{\gamma^2} + k_1 b^2\Big\}.$$

It follows from Lemma 2.2 that $\tilde{x}(t) \to 0$ as $t \to \infty$, i.e., $\epsilon \to 0$ and $\omega_e \to 0$ as $t \to \infty$. By Lemma 4.2, this corresponds to zero attitude error and zero rate error for the auxiliary system (5.16).

Since $||\epsilon||^2 + \eta^2 = 1$, the derivative value $\dot{V} = 0$ implies two equilibrium points $(\epsilon, \eta, \omega_e)_e = (0, \pm 1, 0)$ on $\mathcal{S}(3) \times \mathcal{R}^3$, standing for exactly the same physical attitude orientation. However, it is clear that $(0, -1, 0)$ is an unstable equilibrium point [125], because it is a local maximum of $V(\epsilon, \eta, \omega_e)$ on $\mathcal{S}(3) \times \mathcal{R}^3$ and $\dot{V} < 0$ whenever $||\tilde{x}|| \neq 0$. We therefore conclude that $\eta \to 1$ as $t \to \infty$ whenever the initial condition $x(0) \neq (0, -1, 0)$ and the PD control law (5.14) results in the global asymptotic stability of the auxiliary system (5.16) on $(\mathcal{S}(3) \times \mathcal{R}^3) \setminus (0, -1, 0)$.

If the initial condition (5.18) is satisfied, we have

$$V(x(t)) \leq V(x(0)) \leq 4c - \delta_\eta = V((0, -1, 0)) - \delta_\eta,$$

implying that $x(t)$ is bounded away from the unstable equilibrium point $(0, -1, 0)$ for all $t \geq 0$. Then there exist finite coefficients $c_\eta > 0$, $\lambda_1 > 0$ and $\lambda_2 > 0$ such that

$$(1 - \eta)^2 \leq c_\eta \epsilon^T \epsilon,$$

$$V(x) \geq \lambda_1 ||\tilde{x}||^2,$$

$$V(x) \leq \frac{1}{2}\omega_e^T J \omega_e + b\omega_e^T J\epsilon + (c + c_\eta)||\epsilon||^2 \leq \lambda_2 ||\tilde{x}||^2.$$

Therefore, it follows

$$\dot{V} \leq -\frac{\lambda_b}{\lambda_2} V.$$

Hence, by the comparison Lemma 2.4 and from $V(x) \geq \lambda_1 ||\tilde{x}||^2$, we can conclude that $\epsilon \to 0$ and $\omega_e \to 0$ exponentially. □

Remark 5.1. Given any initial conditions, the control law (5.14) will make the errors ϵ and ω_e of the auxiliary system (5.16) converge to zeros asymptotically, but $x(t)$ might

be arbitrarily close to $(\epsilon, \eta, \omega_e)_e = (0, -1, 0)$ for some t before it converges to the desired equilibrium point $(0, 1, 0)$. On the other hand, $(0, -1, 0)$ corresponds to an unstable equilibrium point as any small perturbation will cause a rotation of 360° to $\eta = +1$. This situation is avoided if (5.18) is satisfied by choosing k_1 large enough (because $c = 2bk_1$ if $k_2 = 1$) or $\omega_e(0) = 0$. In fact, in most attitude tracking control applications, the initial angular velocity $\omega_e(0)$ is zero or sufficiently small (by choosing the initial velocity $\omega_c(0)$ to be the actual initial velocity $\omega(0)$), which brings the system (5.16) to converge to $(\epsilon, \eta, \omega_e)_e = (0, 1, 0)$ exponentially. ⊗

It may appear that the control laws presented here create a continuous, globally asymptotically stable vector field on $SO(3) \times \mathcal{R}^3$. This is not possible, as pointed out in [60, 125]. Indeed, their implementation would require memory since the sign ambiguity in the unit quaternion q cannot be solved from the attitude matrix and the attitude kinematic equation (4.8). This means that the control law does not generate a vector field on $SO(3) \times \mathcal{R}^3$. However, on $S(3) \times \mathcal{R}^3$, then we do have a globally asymptotically stable vector field in the closed-loop when the kinematics in (5.16) in terms of q is used instead of that in terms of Euler angles in (4.8).

Note that the state penalty function $l(x)$ in Theorem 3.12 can be positive semidefinite, which also corresponds to a meaningful cost functional without loss of the inverse optimality. Applying Theorem 3.12 and Theorem 5.2, we will obtain the following theorem on designing the inverse optimal attitude tracking control law.

Theorem 5.3. *If we let $\beta = \lambda = 2$, then the state feedback PD control law*

$$u = \beta\alpha(x) = -2\Big(k_1 + \frac{k_2}{\gamma^2}\Big)(\omega_e + b\epsilon) \tag{5.22}$$

with the parameters b, c, k_1, k_2 and $R_2(x)$ being given in Theorem 5.2, solves the inverse optimal gain assignment problem for the attitude tracking control problem with respect to the extended disturbance $\hat{d}(C, \omega_e, \omega_c, \dot{\omega}_c)$ by minimizing the cost functional

$$J_a(u) = \sup_{\hat{d}\in\mathcal{D}} \Big\{ \lim_{t\to\infty} \Big[4V(x(t)) + \int_0^t \Big(l(x) + u^T R_2(x) u - \gamma^2 ||\hat{d}||^2\Big) d\tau\Big]\Big\}, \tag{5.23}$$

where $l(x)$ is a positive semidefinite state penalty function defined by

$$l(x) = -4L_f V - \frac{4}{\gamma^2}||L_{g_1} V||^2 + 4L_{g_2} V R_2^{-1} (L_{g_2} V)^T. \tag{5.24}$$

Furthermore, the control law (5.22) is also H_∞ optimal for the closed-loop attitude system with respect to the extended disturbance $\hat{d}(C, \omega_e, \omega_c, \dot{\omega}_c)$ and the H_∞ performance index (5.23).

Proof. This theorem is a consequence of Theorem 3.12 and Theorem 5.2. From the derivations in Theorem 5.2, we observe that $R_2(x)$ is positive definite and

$$l(x) \geq 4\Big(k_1 - \frac{b}{2}\lambda_j + \frac{k_2 - 1}{\gamma^2}\Big)||\omega_e||^2 + 4b^2\Big(k_1 + \frac{k_2 - 1}{\gamma^2}\Big)||\epsilon||^2, \tag{5.25}$$

which shows that $l(x)$ is positive semidefinite on $\mathcal{S}(3) \times \mathcal{R}^3$ (precisely, $l(x)$ is positive definite in ϵ and ω_e). Therefore, $J_a(u)$ is a meaningful cost functional for the attitude tracking control problem, penalizing the tracking errors ϵ and ω_e as well as the control effort u and the extended disturbance $\hat{d}(C, \omega_e, \omega_c, \dot{\omega}_c)$.

Substituting $l(x)$ into the cost functional $J_a(u)$ in (5.23), we have the optimal cost $J_a(u) = 4V(x(0))$ and the "worse-case" extended disturbance

$$\hat{d}^*(x) = \lambda(\rho')^{-1}(2||L_{g_1}V||)\frac{(L_{g_1}V)^T}{||L_{g_1}V||} = \frac{2}{\gamma^2}(L_{g_1}V(x))^T \tag{5.26}$$

(see Theorem 3.12 for the detailed computations). The class $\mathcal{K}_\infty$ function ρ whose derivative ρ' is also a class $\mathcal{K}_\infty$ function is defined in the same way as in the proof of Theorem 5.2, i.e., $\rho(r) = \gamma^2 r^2$, $(\rho')^{-1}(r) = \frac{r}{2\gamma^2}$.

From $J_a(u) = 4V(x(0))$, it follows that

$$\int_0^T \Big(l(x) + u^T R_2(x) u\Big) dt \leq \gamma^2 \int_0^T ||\hat{d}||^2 dt + 4V(x(0)) \tag{5.27}$$

for all $T \geq 0$, which implies that the closed-loop system for the feedback control law (5.22) has $\mathcal{L}_2$ gain less than or equal to γ from the extended disturbance $\hat{d}(C, \omega_e, \omega_c, \dot{\omega}_c)$ to the block vector of tracking errors $\tilde{x}(t)$ and control inputs u, thus H_∞ disturbance attenuation is achieved.

In addition, the Lyapunov function candidate $V(x)$ solves the following Hamilton-Jacobi-Isaacs partial differential equation

$$\frac{\partial V}{\partial x} f(x) + \frac{\partial V}{\partial x}\Big[\frac{1}{\gamma^2} g_1(x) g_1^T(x) - g_2(x) R_2^{-1} g_2^T(x)\Big]\Big(\frac{\partial V}{\partial x}\Big)^T + \frac{1}{4} l(x) = 0.$$

Therefore we conclude that the inverse optimal PD control law (5.22) shows H_∞ optimality with respect to the extended disturbance $\hat{d}(C, \omega_e, \omega_c, \dot{\omega}_c)$ and minimizes the H_∞ performance index (5.23).

Furthermore, if the extended disturbance $\hat{d}(C, \omega_e, \omega_c, \dot{\omega}_c) \in \mathcal{L}_2[0, \infty)$, it follows from (5.27) that $\epsilon \in \mathcal{L}_2[0, \infty)$, $\omega_e \in \mathcal{L}_2[0, \infty)$, $\omega_c \in \mathcal{L}_2[0, \infty)$ and $\dot{\omega}_c \in \mathcal{L}_2[0, \infty)$. We conclude that $\epsilon \to 0$ and $\omega_e \to 0$ as $t \to \infty$, thus asymptotic attitude tracking is achieved with a global convergence of tracking errors to zero for all initial conditions. □

Remark 5.2. When $k_2 = 1$, by applying (5.13), (5.15) and (5.17), it is observed that the state penalty function $l(x)$ in (5.24) can be rewritten as

$$l(x) = 4k_1||L_{g_2}V||^2 - 4L_f V = \tilde{x}^T Q(x)\tilde{x}$$

with the weighting matrices $Q(x)$ and $R_2(x)$,

$$Q(x) = \begin{bmatrix} 4k_1 b^2 & 0 \\ 0 & 4k_1 - 2b\eta J + bJ\epsilon^\times - b\epsilon^\times J \end{bmatrix}, \qquad R_2(x) = (k_1 + \frac{1}{\gamma^2})^{-1} I_3,$$

being positive definite for each $x = [\epsilon^T, \eta, \omega_e^T]^T$. Note that $\tilde{x} = [\epsilon^T, \omega_e^T]^T$. ⊗

Therefore, the system error certainly depends on the gains k_1, b and γ. As shown in the performance analysis in Section 5.5, the error is approximately proportional to the magnitude of k_1 and a smaller γ brings a smaller system error. Therefore, if we are to reduce the system error, we can enlarge k_1 in the weight $Q(x)$ and decrease γ in the weight $R_2(x)$, producing a bigger control effort. Conversely, if k_1 is reduced, then a smaller control effort and a bigger error will be produced.

Remark 5.3. Compared with the feedback linearization approach [78] or the feedforward compensation [125, Theorem 2] where complete information of the inertia matrix J is always required, the H_∞ inverse optimal control (5.22) is not model-sensitive because it does not employ feedforward compensations to cancel the quadratic nonlinearities regarding w_c in the model, namely $S(w_e)Jw_c$, $S(w_c)Jw_e$ and $S(w_c)Jw_c$. Instead, they are considered as parts of the extended disturbance $\hat{d}(C, \omega_e, \omega_c, \dot{\omega}_c)$ given by (5.2) and will be analyzed in Section 5.5. Therefore, the control law (5.22) does not require complete information of the inertia matrix J, ensuring that the controller is fairly robust to parametric uncertainties. Note that the controller gains of (5.22) only require the largest eigenvalue of the inertia matrix J, which is always available or can be easily estimated in practice even when the complete inertia matrix is unknown. $\otimes$

For nonlinear systems with disturbances or in the case of the trajectory tracking problem, IISS [4,67,109] is a useful theoretical tool to analyze the stability of the closed-loop system; recall Section 3.3 for some preliminaries and see [4, 109] for examples. The stability of the closed-loop attitude tracking control system (5.4) with the inverse optimal control law (5.22) is summarized within the framework of IISS by the following Lemma.

Lemma 5.4. *The attitude trajectory tracking full-state $(\epsilon, \eta, \omega_e)$-system under the inverse optimal PD control law of (5.22) is integral-input-to-state stable (IISS) on $(\mathcal{S}(3) \times \mathcal{R}^3) \setminus (0, -1, 0)$ with respect to the extended disturbance $\hat{d}(C, \omega_e, \omega_c, \dot{\omega}_c)$.*

Proof. Employing the state-feedback control law (5.22) into the error differential equation (5.4), we obtain the derivative value $\dot{V}(x,t)$ by

$$\begin{aligned}\dot{V} &= L_f V(x) + L_{g_1} V \hat{d} - 2L_{g_2} V R_2^{-1}(x)(L_{g_2}V)^T \\ &= -\tfrac{1}{4} l(x) - \tfrac{1}{\gamma^2}||L_{g_1}V(x)||^2 + L_{g_1}V(x)\hat{d}(t) - L_{g_2}V(x)R_2^{-1}(x)(L_{g_2}V(x))^T.\end{aligned}$$

Using the Young's inequality [41], it follows that

$$L_{g_1} V \hat{d} \leq \frac{\gamma^2}{4}||\hat{d}||^2 + \frac{1}{\gamma^2}||L_{g_1}V||^2,$$

where the equal sign "=" is satisfied only when $\hat{d}(C, \omega_e, \omega_c, \dot{\omega}_c) = \hat{d}^*(x) = \frac{2}{\gamma^2}(L_{g_1}V)^T$. Therefore,

$$\dot{V} \leq -\frac{1}{4} l(x) - L_{g_2} V R_2^{-1}(x)(L_{g_2}V)^T + \frac{\gamma^2}{4}||\hat{d}||^2. \tag{5.28}$$

Note that $R_2(x)$ is positive definite symmetric and $l(x)$ is positive definite on $(\mathcal{S}(3) \times \mathcal{R}^3) \setminus (0, -1, 0)$. As analyzed in the proof of Theorem 5.2, the full-state system is 0-GAS on $(\mathcal{S}(3) \times \mathcal{R}^3) \setminus (0, -1, 0)$ if the extended disturbance $\hat{d} = 0$. It is zero-output dissipative because, if we let the output be $h(x) = 0$, then $\dot{V} < \frac{\gamma^2}{4}||\hat{d}||^2$. Hence, it is IISS with respect to the extended disturbance $\hat{d}(C, \omega_e, \omega_c, \dot{\omega}_c)$. □

5.5 Performance of Inverse Optimal Control

Although the inverse optimal control law (5.22) guarantees the property of IISS of the closed-loop attitude control system, it does not provide a global asymptotical stability due to the presence of external disturbances and the tracking references. The static state-feedback control law in Theorem 5.1 establishes the H_∞ optimality with respect to the extended disturbance $\hat{d}(C, \omega_e, \omega_c, \dot{\omega}_c)$. Therefore, it is necessary to analyze the effects of $\hat{d}(C, \omega_e, \omega_c, \dot{\omega}_c)$ on the system performance. In this section, we will introduce the concept of performance limitation in [18] to analyze the performance of the inverse optimal attitude tracking controller (5.22). The performance analysis of the controller in Theorem 5.1 can be done similarly, thus omitted here.

5.5.1 Performance Analysis

The extended disturbance $\hat{d}(C, \omega_e, \omega_c, \dot{\omega}_c)$ defined by (5.2) can be divided into two parts regarding the tracking error ω_e:

$$\hat{d}(C, \omega_e, \omega_c, \dot{\omega}_c) = h_1(C, \omega_c, \dot{\omega}_c)\omega_e + h_2(C, d, \omega_c, \dot{\omega}_c), \tag{5.29}$$

where

$$h_1(C, \omega_c, \dot{\omega}_c) = (JC\omega_c)^\times - (C\omega_c)^\times J - J(C\omega_c)^\times,$$
$$h_2(C, d, \omega_c, \dot{\omega}_c) = d - JC\dot{\omega}_c - (C\omega_c)^\times JC\omega_c.$$

To formulate an upper bound of the Euclidian norm of the extended disturbance in (5.29), we need an additional assumption besides Assumption 4.1:

Assumption 5.1. *The external disturbance $d(t)$ is bounded with a known bound for all $t \geq 0$, that is, there exists a known, finite and positive constant c_d such that $c_d = \sup_{t\geq 0}\{||d(t)||\}$.*

Satisfying assumption 4.1 is important if the proposed control can solve the attitude tracking control problem. The requirement of the external disturbance $d(t)$ in Assumption 5.1 is rather minimal. We emphasize that the H_∞ inverse optimal control (5.22) is not restricted to disturbances with $\int_0^\infty ||d(t)||^2 dt < \infty$ and $\int_0^\infty ||\hat{d}(\omega_e, t)||^2 dt < \infty$ because any bounded (and persistent) extended disturbance, consisting of the external disturbance d and the tracking reference signals w_c and $\dot{w}_c$, is allowed in the H_∞ inverse optimality approach [63] and the IISS analysis [4]. The control law (5.22) guarantees

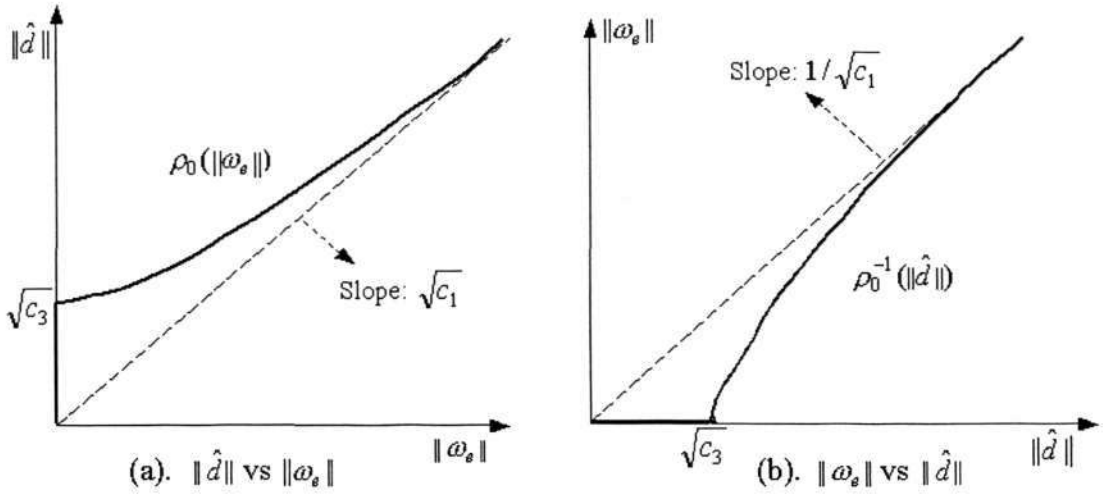

Figure 5.1: Functions $\rho_0(||\omega_e||)$ and $\rho_0^{-1}(||\hat{d}||)$.

the boundedness of the tracking errors ϵ and w_e for any bounded extended disturbance $\hat{d}(C, w_e, \omega_c, \dot{\omega}_c)$.

With Assumptions 4.1 and 5.1, there must exist some finite, positive, time-varying coefficients c_1, c_2 and c_3 such that

$$\begin{aligned} ||\hat{d}(C, \omega_e, \omega_c, \dot{\omega}_c)||^2 &= \omega_e^T(h_1^T h_1)\omega_e + 2\omega_e^T(h_1^T h_2) + h_2^T h_2 \\ &\leq c_1||\omega_e||^2 + c_2||\omega_e|| + c_3 \end{aligned} \tag{5.30}$$

or some finite, positive, time-varying coefficients β_1 and β_2 such that

$$||\hat{d}(C, \omega_e, \omega_c, \dot{\omega}_c)||^2 = \omega_e^T(h_1^T h_1)\omega_e + 2\omega_e^T(h_1^T h_2) + h_2^T h_2 \leq \beta_1||\omega_e||^2 + \beta_2. \tag{5.31}$$

Such coefficients can be chosen as

$$\begin{aligned} c_1 &= ||h_1^T h_1|| \leq 9\lambda_j^2||\omega_c||^2, \\ c_2 &= 2||h_1^T h_2|| \leq 6\lambda_j||\omega_c||||d_c|| = 6\lambda_j||\omega_c||\sqrt{3||d||^2 + 3\lambda_j^2||\dot{\omega}_c||^2 + 3\lambda_j^2||\omega_c||^4}, \\ c_3 &= ||h_2^T h_2|| \leq 3||d||^2 + 3\lambda_j^2||\dot{\omega}_c||^2 + 3\lambda_j^2||\omega_c||^4, \quad \text{(by Schwartz inequality [41])} \\ \beta_1 &= 2||h_1^T h_1|| \leq 18\lambda_j^2||\omega_c||^2 \\ \beta_2 &= 2||h_2^T h_2|| \leq 6||d||^2 + 6\lambda_j^2||\dot{\omega}_c||^2 + 6\lambda_j^2||\omega_c||^4. \end{aligned}$$

The inequality (5.30) or (5.31) implies a relation between the Euclidian norm of the extended disturbance $\hat{d}$ and that of the error ω_e, shown as in Figure 5.1(a):

$$||\hat{d}(C, \omega_e, \omega_c, \dot{\omega}_c)|| \leq \rho_o(||\omega_e||),$$

which implies that the norm of the extended disturbance $\hat{d}$ is bounded below by a function of the norm of the tracking error ω_e. It is clear that $\rho_0(||\omega_e||)$ is an increasing

and monotone function, which implies an inverse relationship

$$\rho_o^{-1}(||\hat{d}(C,\omega_e,\omega_c,\dot{\omega}_c)||) \leq ||\omega_e||$$

where $\rho_0^{-1}(||\hat{d}||)$ is not a class $\mathcal{K}_\infty$ function in the case of the trajectory tracking control or in the presence of the external disturbance because $\rho_0^{-1}(\cdot)$ is increasing but not strictly increasing when $c_3 \neq 0$ or $\beta_2 \neq 0$, as shown in Figure 5.1(b).

If there exists no external disturbance, $d(t) = 0$, then the 0-GAS property holds for the regulation control problem (corresponding to $\dot{\omega}_c = \omega_c = 0$ and $q_c = 0$) because $c_1 = c_2 = c_3 = 0$ and then $\dot{V} < 0$. However, the static PD controller (5.22) cannot guarantee the GAS either in the trajectory tracking or in the existence of external disturbance. This fact brings a performance limitation [18] of the inverse optimal controller.

The control performance is determined by the gain values of the controller. Therefore, it is important to set up a relation between the gain values and the system errors, which is found by examining points that satisfy $\dot{V} = 0$.

Theorem 5.5. *Choose $k_2 = 1$. Suppose that λ_c is the minimum eigenvalue of the matrix*

$$Q_c = \begin{bmatrix} (2k_1 + \frac{1}{\gamma^2})b^2 I_3 & (k_1 + \frac{1}{\gamma^2})bI_3 \\ (k_1 + \frac{1}{\gamma^2})bI_3 & (2k_1 + \frac{1}{\gamma^2} - \frac{b}{2}\lambda_j - \frac{\gamma^2}{4}\bar{c}_1)I_3 \end{bmatrix}. \tag{5.32}$$

Let the performance limitation $||\tilde{x}||_{PL}$ be defined as the Euclidean norm of the vector $\tilde{x}$ that satisfies $\dot{V} = 0$. If the inverse optimal control law (5.22) with $k_2 = 1$ is applied to the attitude tracking control system (5.4) and $\lambda_c > 0$ is satisfied, then its performance limitation is upper bounded by

$$||\tilde{x}||_{PL} \leq \frac{\gamma^2}{8\lambda_c}\Big[\bar{c}_2 + \sqrt{\bar{c}_2^2 + \frac{16}{\gamma^2}\lambda_c \bar{c}_3}\Big], \tag{5.33}$$

where $\bar{c}_1 = \sup\{c_1(t) : t \geq 0\}$, $\bar{c}_2 = \sup\{c_2(t) : t \geq 0\}$ and $\bar{c}_3 = \sup\{c_3(t) : t \geq 0\}$ with $c_1(t)$, $c_2(t)$ and $c_3(t)$ defined by (5.30).

Proof. Applying (5.25) with $k_2 = 1$, we can rewrite $\dot{V}$ in (5.28) as

$$\dot{V} \leq -\big(k_1 - \frac{b}{2}\lambda_j\big)||\omega_e||^2 - k_1 b^2||\epsilon||^2 - \big(k_1 + \frac{1}{\gamma^2}\big)||\omega_e + b\epsilon||^2 + \frac{\gamma^2}{4}||\hat{d}||^2$$

By (5.32) and (5.30), it follows that

$$\dot{V} \leq -x^T Q_c x + \frac{\gamma^2}{4}(c_2||\omega_e|| + c_3) \leq -\lambda_c||x||^2 + \frac{\gamma^2}{4}\bar{c}_2||x|| + \frac{\gamma^2}{4}\bar{c}_3, \tag{5.34}$$

where λ_c is the minimum eigenvalue of the matrix Q_c. By the definition of the performance limitation, the inequality (5.34) brings the performance limitation of (5.33). □

Remark 5.4. Either in the case of trajectory tracking or in the presence of external

disturbances, c_1, c_2 and c_3 are not always zeros and thus there exists a bound for the system error. The inequality (5.33) can be considered as an upper bound of the system error for all time and then can be used as a formula to predict the performance of the closed-loop system for various values of the controller gains. ⊗

Remark 5.5. Since the right-hand side of (5.33) is monotonically decreasing with λ_c, the inequality holds if λ_c is replaced by any smaller positive value. The minimum eigenvalue λ_c of the matrix Q_c in Theorem 5.5 satisfies

$$\lambda_c \geq \min\left\{b^2 k_1, \left(k_1 - \frac{b}{2}\lambda_j - \frac{\gamma^2}{4}\bar{c}_1\right)\right\}. \tag{5.35}$$

This can be seen by dividing the matrix Q_c into two parts expressed by

$$Q_c = \begin{bmatrix} k_1 b^2 I_3 & 0 \\ 0 & \left(k_1 - \frac{b}{2}\lambda_j - \frac{\gamma^2}{4}\bar{c}_1\right) I_3 \end{bmatrix} + \left(k_1 + \frac{1}{\gamma^2}\right)\begin{bmatrix} I_3 & 0 \\ \frac{1}{b} I_3 & I_3 \end{bmatrix}\begin{bmatrix} b^2 I_3 & b I_3 \\ 0 & 0 \end{bmatrix}.$$

Clearly, the minimum eigenvalue of the second part of Q_c is zero. Hence, λ_c satisfies the inequality (5.35). ⊗

Remark 5.6. Suppose that $||\omega_c(t)|| \leq \bar{c}_4$, where $\bar{c}_4 = \sup\{||\omega_c(t)|| : t \geq 0\}$ is a positive constant. Then it follows from (5.31) that $\beta_1 \leq \bar{\beta}_1 = 18\lambda_j^2 \bar{c}_4^2$ and

$$||\hat{d}||^2 \leq \beta_1 ||\omega_e||^2 + \beta_2 \leq \bar{\beta}_1 ||\omega_e||^2 + \beta_2.$$

Substituting these into $\dot{V}$ in (5.28), we have

$$\begin{aligned} \dot{V} &\leq -\left(k_1 - \frac{b}{2}\lambda_j\right)||\omega_e||^2 - k_1 b^2 ||\epsilon||^2 - \left(k_1 + \frac{1}{\gamma^2}\right)||\omega_e + b\epsilon||^2 + \frac{\gamma^2}{4}||\hat{d}||^2 \\ &\leq -\left(k_1 - \frac{b}{2}\lambda_j - \frac{\gamma^2}{4}\bar{\beta}_1\right)||\omega_e||^2 - k_1 b^2 ||\epsilon||^2 + \frac{\gamma^2}{4}\beta_2. \end{aligned} \tag{5.36}$$

As shown in (5.31), β_2 consists of the magnitude of the reference signals $\omega_c(t)$ and $\dot{\omega}_c(t)$ and the external disturbance $d(t)$. If

$$k_1 - \frac{b}{2}\lambda_j - \frac{\gamma^2}{4}\bar{\beta}_1 > 0,$$

it can be deduced from (5.36) that the closed-loop system is $(\omega_c, \dot{\omega}_c, d)$-to-$(\epsilon, \omega_e)$ stable in the sense of input-to-state stability. In addition, if $\omega_c(t)$, $\dot{\omega}_c(t)$, $d(t) \in \mathcal{L}_2[0, \infty)$, then the $\mathcal{L}_2$-gain from β_2 to (ϵ, ω_e) is finite and ϵ, $\omega_e \in \mathcal{L}_2[0, \infty)$. ⊗

5.5.2 Selecting Control Gains

After analyzing the performance estimates of the closed-loop system with the inverse optimal controller (5.22), we turn to present some guidelines for selecting the control gains. Without loss of generality, we can always choose $k_2 = 1$. The parameter b is chosen small enough to assure that the Lyapunov function V in (5.10) is positive definite. By appropriately choosing k_1 and b, we can choose $\lambda_c \geq b^2 k_1$ as follows.

Suppose that $||\omega_c|| \leq \bar{c}_4$. It follows $c_1 \leq \bar{c}_1 = 9\lambda_j^2\bar{c}_4^2$. If we choose the gain k_1 to satisfy the constraint condition

$$k_1 > \frac{\gamma^2}{4}\bar{c}_1 = \frac{9}{4}\gamma^2\lambda_j^2\bar{c}_4^2 \geq \frac{\gamma^2}{4}c_1, \tag{5.37}$$

and the inequality

$$k_1 - \frac{b}{2}\lambda_j - \frac{\gamma^2}{4}\bar{c}_1 \geq b^2 k_1, \tag{5.38}$$

then, it follows from (5.35) that

$$\lambda_c \geq b^2 k_1, \tag{5.39}$$

and the following constraint of the parameter b should be imposed:

$$b \leq \frac{1}{2k_1}\Big[-\frac{\lambda_j}{2} + \sqrt{\frac{\lambda_j^2}{4} + 4k_1\Big(k_1 - \frac{\gamma^2}{4}\bar{c}_1\Big)}\Big]. \tag{5.40}$$

The choice of (5.38) is reasonable as the gain b can be chosen sufficiently small.

From (5.37), we note that (k_1/γ^2) should be larger as the supremum of $||\omega_c||^2$ goes up, which means that $(\sqrt{k_1}/\gamma)$ should be proportional to $\bar{c}_4 = \sup\{||\omega_c(t)|| : \forall t \geq 0\}$, that is,

$$\sqrt{k_1}/\gamma \;\propto\; \bar{c}_4. \tag{5.41}$$

If we choose k_1 large enough such that $4k_1(k_1 - \frac{\gamma^2}{4}\bar{c}_1) \gg \frac{\lambda_j^2}{4}$, the constraint (5.40) can be approximated by

$$b \leq \frac{1}{2k_1}\sqrt{4k_1^2 - k_1\gamma^2\bar{c}_1} \approx 1,$$

which gives an upper bound for the gain b, albeit such choices are too conservative for both b and k_1. In general, it is unnecessary to require k_1 sufficiently large such that $4k_1(k_1 - \frac{\gamma^2}{4}\bar{c}_1) \gg \frac{1}{4}\lambda_j^2$. Since the gain b can be chosen sufficiently small, together with (5.38) we could choose

$$b \;\propto\; (2/\lambda_j)k_1 \tag{5.42}$$

with a scale that is less than 1, which implies that the gain b is chosen proportional to the gain k_1. With an appropriate choice of the scale for (5.42), $\lambda_c \geq b^2 k_1$ can be assured.

Using the inequality $\sqrt{x_1^2 + x_2^2} \leq ||x_1|| + ||x_2||$ for all $x_1, x_2 \in \mathcal{R}$ and substituting (5.39) into (5.33), we can rewrite the performance limitation (5.33) as follows:

$$||\tilde{x}||_{PL} \;\leq\; \frac{\gamma^2}{8b^2k_1}\Big(2\bar{c}_2 + \frac{4}{\gamma}\sqrt{b^2k_1\bar{c}_3}\Big)$$

which implies

$$||\tilde{x}||_{PL} \leq \frac{\bar{c}_2}{4}\left(\frac{1}{b}\right)^2\left(\frac{\gamma}{\sqrt{k_1}}\right)^2 + \frac{\sqrt{\bar{c}_3}}{2}\left(\frac{1}{b}\right)\left(\frac{\gamma}{\sqrt{k_1}}\right), \tag{5.43}$$

from which we can conclude that the performance limitation $||\tilde{x}||_{PL}$ in (5.33) can be considered as a performance estimate with respect to the magnitudes of the gains k_1 and γ: For a fixed γ, a bigger k_1 results in a smaller error $\tilde{x}$. A smaller γ also brings a smaller error $\tilde{x}$. A small $\mathcal{L}_2$-gain γ effects the performance by increasing the attenuation of the external disturbances and reference inputs.

Therefore, conditions (5.37), (5.41), (5.42) and (5.43) establish the relations between the attitude tracking error $\tilde{x}$ and the controller parameters k_1, γ and b. Hence, we can consider (5.41) and (5.42) as guidelines for selecting the gains k_1 and b in the inverse optimal control law (5.22).

5.6 Simulation Results

In this section, a micro-satellite is assumed rigid and simulated to demonstrate the performance of the H_∞ inverse optimal tracking controller (5.22). The structure of the attitude control system of the microsatellite is illustrated as in Figure 4.1 and the related main parameters are listed as in Table 5.1. Detailed specifications of the reaction wheel *MicroWheel 1000* (Dynacon Inc.) and the magnetorquer *MT-5-2* (Microcosm Inc.), respectively, can be found at *http://www.dynacon.ca/pdf/files/productpdf_14.pdf* and *http://www.smad.com/ie/ieframessr3.html*.

5.6.1 External Disturbance Estimation

With the moments of inertia listed in Table 5.1, the product terms J_{12}, J_{13} and J_{23} are much smaller than J_1, J_2 and J_3 so the effects induced by these product terms on gravity-gradient torque (4.20) can be neglected. Applying the expression (4.20) yields the worst-case gravity-gradient torque as

$$T_{g1} = 1.62 \times 10^{-5}\text{Nm}, \quad T_{g2} = 6.47 \times 10^{-6}\text{Nm}, \quad T_{g3} = 0.98 \times 10^{-5}\text{Nm}.$$

According to the values listed in Table 5.1, the distance from the center of the earth to the spacecraft is $r = 7178$km; the velocity of the microsatellite is $v = 7451.8$m/s and the atmospheric density $\rho = 1.17 \times 10^{-14}\text{kg/m}^3$, see [53] [126, pp.820] [118, pp.58]; the area of the center body is $A_b = 0.6 \times 0.8 = 0.48\text{m}^2$; the area of the solar panels is assumed to be $A_a = 1.5\text{m}^2$; the offset from the center of mass to the center of pressure is conservatively taken to be $L_{cp} = 0.1$m; the drag coefficient is $C_d = 2.0$. Thus, by (4.21), the worst-case aerodynamic disturbance becomes

$$T_a = 0.5 \times 1.17 \times 10^{-14} \times 7452^2 \times (1.5 + 0.48) \times 2 \times 0.1 = 1.3 \times 10^{-7}\text{Nm}.$$

Table 5.1: Microsatellite main parameters

Mission	Hyper-spectral imaging for earth observation
Mass	< 100kg
Inertia moments (kg·m^2)	(*Initial estimates*)
Principal moments of inertia	$\bar{J}_1 = 16.0$, $\bar{J}_2 = 10.0$, $\bar{J}_3 = 20.0$
Products of inertia	$\bar{J}_{12} = 0.1$, $\bar{J}_{13} = 0.3$, $\bar{J}_{23} = 0.5$
Variation range	10%
Size (cm)	$60 \times 60 \times 80$
Orbit	Sun-synchronous orbit (Circular)
Altitude	800 km
Inclination	87.0 deg
Orbital rate	0.00104 rad/s
Attitude control type	Three-axis control by three reaction wheels
Reaction wheel	Danacon MicroWheel 1000
Speed range	$\pm$10000 rpm
Momentum capacity	$0.2 \sim 1.0$ Nms (configurable)
Wheel torque	$\pm$0.03 Nm
Operation mode	Torque control mode
Magnetorquer	MT5-2 (Microcosm Inc.)
Linear dipole moment	5.0 A·m^2
Saturation moment	6.5 A·m^2
Voltage	5 V

With the assumption of the geomagnetic field as a dipole and by (4.27), the maximal magnitude of the geomagnetic field turns out to be $B = 4.38 \times 10^{-5}$T. Assume that the residual magnetic moment of the microsatellite is $\Delta M = 1.0$A·m^2 in each axis. From (4.22) the worst-case magnetic disturbance torque is given by

$$T_{md} = \Delta M \times B = 4.38 \times 10^{-5}\text{Nm}.$$

The magnetic field B is cyclic that appears in a summation of sinusoids with basic frequency n_0 and other higher-order frequencies kn_0 for some other integers $k > 1$ [118, 126]. (All values of k are always hard to completely determined.) Hence the residual magnetic torque T_{md} is also almost periodic because the residual magnetic moment ΔM can always be assumed constant when a satellite is manufactured.

By the fact that $c_a + c_{rs} + c_{rd} = 1$ and by choosing both A_p and A_{pp} in (4.23) to be its maximum $A \approx 2\text{m}^2$, the worst-case solar radiation pressure in (4.23) can be conservatively estimated as $F_s = \sqrt{5}pA = 2.0 \times 10^{-5}$N. The offset from the center of mass to the center of solar pressure is taken to be $L_{sp} = 0.1$m (which is often too conservative for a well-designed microsatellite). Thus, by (4.24), the worst-case solar-radiation disturbance is estimated as

$$T_s = 0.1 \times 2.0 \times 10^{-5} = 2.0 \times 10^{-6}\text{Nm}.$$

From the worst-case analysis above, it is observed that the predominant sources

of external disturbances for a LEO spacecraft with altitude 800km are the gravity-gradient torque and the residual magnetic torque, while the solar radiation torque and the aerodynamic torque are much smaller than the former two disturbances.

On the other hand, as a result of the operation of some payloads, the induced load disturbances are intense but of exceedingly short duration, which are properly considered as impulsive disturbances with strength 0.1Nm and duration 0.2second acting on all the three axes, which will correspondingly result in an increment of angular momentum by about 0.02Nms onto each wheel.

Therefore, we use the sum of the worst-case disturbances as the external disturbances $d(t)$ considered in the numerical simulations

$$d(t) = \begin{bmatrix} 3.2 \times 10^{-5} + 3.0 \times 10^{-5} \sin n_0 t + 0.1\delta(180, 0.2) \\ 2.2 \times 10^{-5} + 3.0 \times 10^{-5} \sin n_0 t - 0.1\delta(180, 0.2) \\ 2.6 \times 10^{-5} + 3.0 \times 10^{-5} \sin n_0 t + 0.1\delta(180, 0.2) \end{bmatrix} \text{Nm}, \tag{5.44}$$

where $\delta(t_0, \Delta t)$ denotes an impulsive disturbance with magnitude 1 and duration Δt, activated at the time t_0.

As analyzed in Section 4.4.4, the magnetic unloading torque T_m is designed for the control purpose of removing the excess angular momentum of the wheels, which is accumulated by external disturbances. In this sense, we may say that the magnetic unloading torque T_m cancels or rejects a part of external disturbances, especially the constant terms, to improve the system performance.

In practice, the magnetic unloading algorithm is designed for the long-term management of the wheels' angular momentum. In most cases, attitude tracking and attitude maneuver are carried out in a short time. Wheels can afford the accumulation of the angular momentum for a short time. Therefore, in the simulations of this chapter, we do not take this unloading algorithm into account and thus the magnetorquers are disenabled.

5.6.2 Numerical Simulations

Using the moments of inertia listed in Table 5.1, it follows that $\lambda_j = ||J|| = 20.05$. The desired angular velocity ω_c of the spacecraft is designed as

$$\omega_c = \begin{bmatrix} 0.03 \sin(2\pi t/400) \\ -0.03 \sin(3\pi t/400) \\ -0.02 \sin(2\pi t/400) \end{bmatrix} \cdot \text{rad/s} \tag{5.45}$$

with $\bar{c}_4 = \sup\{||w_c(t)||\} = 0.047$ and is plotted in black lines in Figure 5.2. The target quaternion q_c can then be computed by integrating (4.31) with the initial condition $q_c(0) = [0,\ 0,\ 0,\ 1]^T$ and is plotted in black line in Figure 5.3.

The initial conditions of the quaternion q and the angular velocity w are given by

$$q(0) = [0.3, -0.2, 0.3, 0.8832]^T, \qquad w(0) = [0.01, -0.01, 0.01]^T \text{rad/s}. \tag{5.46}$$

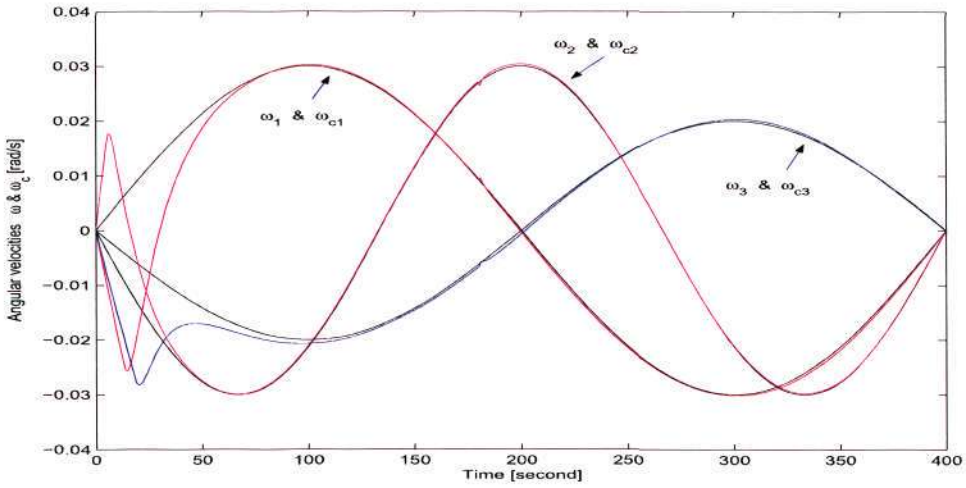

Figure 5.2: Time responses of the angular velocities ω and ω_c. The black lines stand for the target angular velocity ω_c, the colored lines denote ω

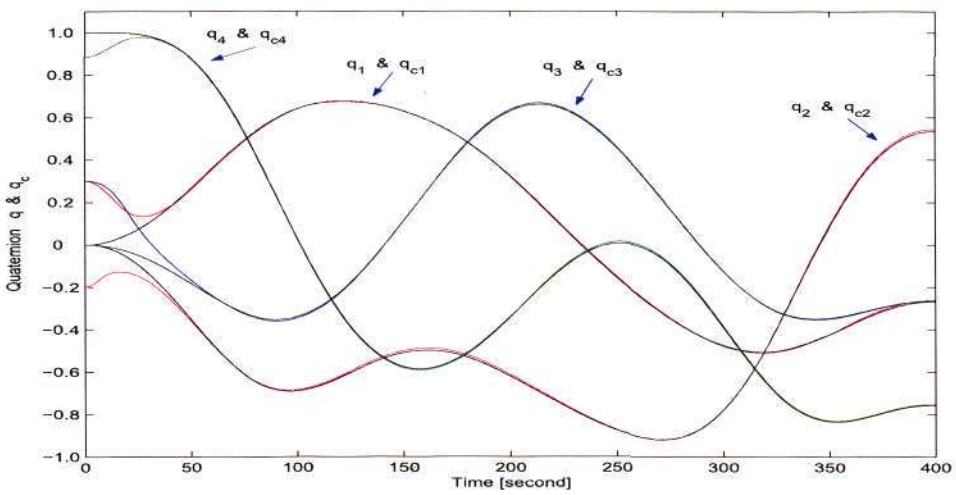

Figure 5.3: Time responses of the unit quaternions q and q_c. The black lines stand for the target quaternion q_c, the colored lines denote q.

The gain k_2 in the controller (5.22) is chosen as $k_2 = 1$. The gain k_1 is chosen such that $k_1 \gg \frac{9}{4}\gamma^2\lambda_j^2\bar{c}_4^2$, the value of b is then determined by (5.40) and (5.42).

Firstly, we choose a set of gains, $\gamma = 1$, $k_1 = 4.0$, $k_2 = 1$ and $b = 0.13$, to demonstrate the tracking performance of the H_∞ inverse optimal controller (5.22). Figures 5.2 and 5.3 depict the time responses of the angular velocities ω, ω_c and the unit quaternions q and q_c, from which it is observed that under the control law (5.22), the actual angular velocity ω and quaternion q track the target attitude motion (described by ω_c and q_c) well with satisfactory tracking errors, shown in Figure 5.4. Figure 5.5(a) shows the convergence of the scalar part η of the error quaternion. The control effort u calculated by the control algorithm (5.22) is plotted in Figure 5.5(b). The actual control torque that is provided by the reaction wheels and fed into the attitude control system is depicted in Figure 5.6(a), in which the control torque T_{wi}, i=1,2,3, is bounded by a restricted range $[-0.03, 0.03]$Nm that is the torque capacity of the wheels listed in Table

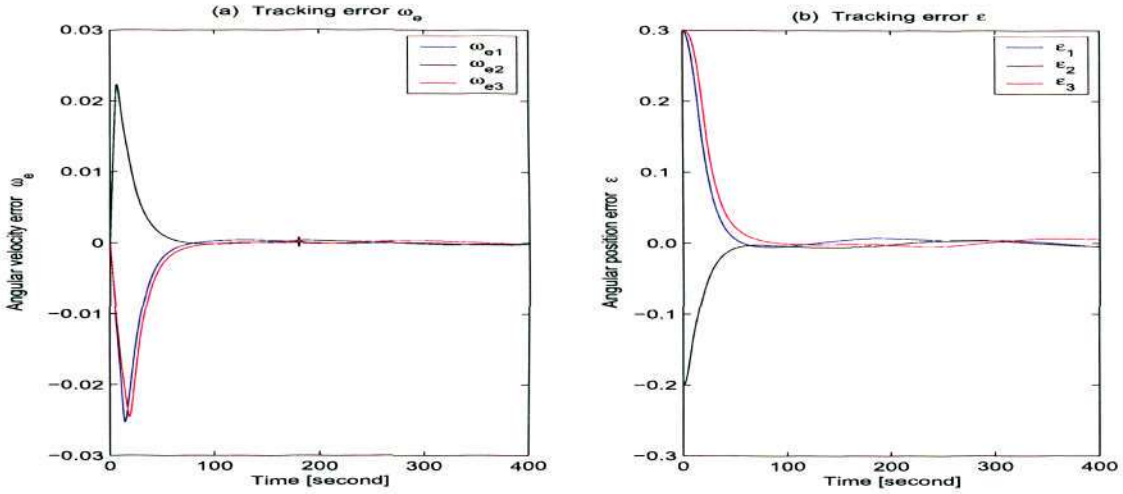

Figure 5.4: Tracking errors ω_e and ϵ with $\gamma = 1$, $k_1 = 4$.

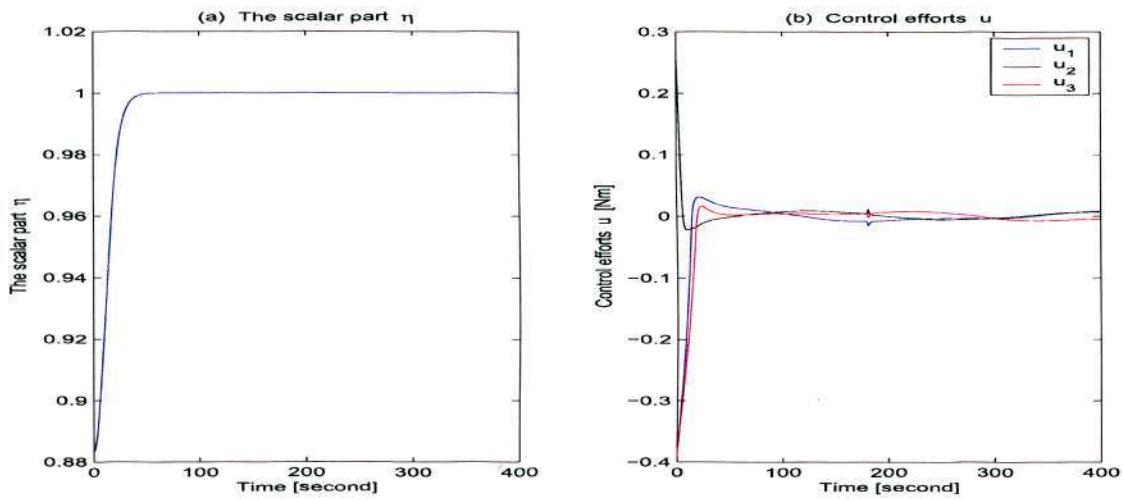

Figure 5.5: The error η and the control effort u given by (5.22) with $\gamma = 1$, $k_1 = 4$.

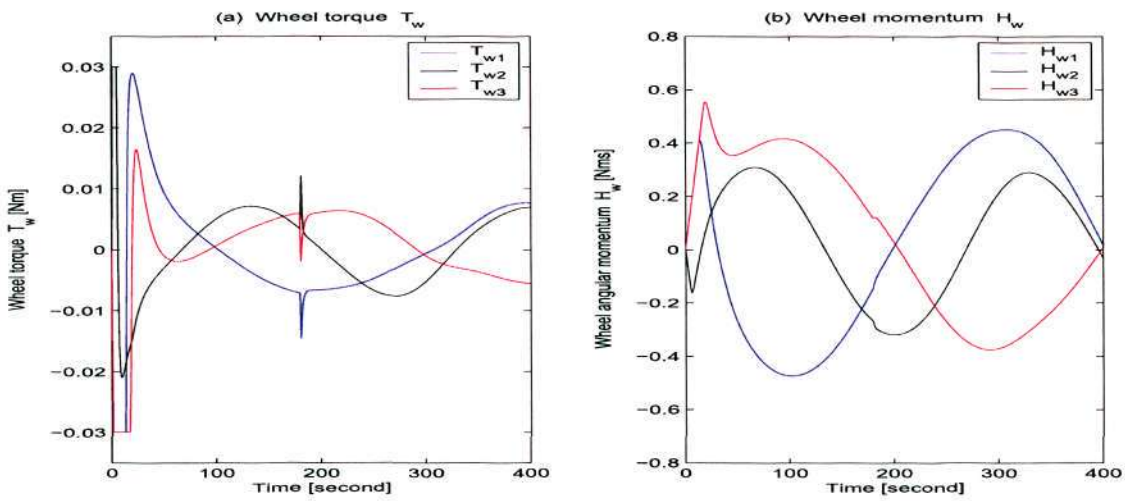

Figure 5.6: Wheel torque T_w and wheel angular momentum H_w with $\gamma = 1$, $k_1 = 4$.

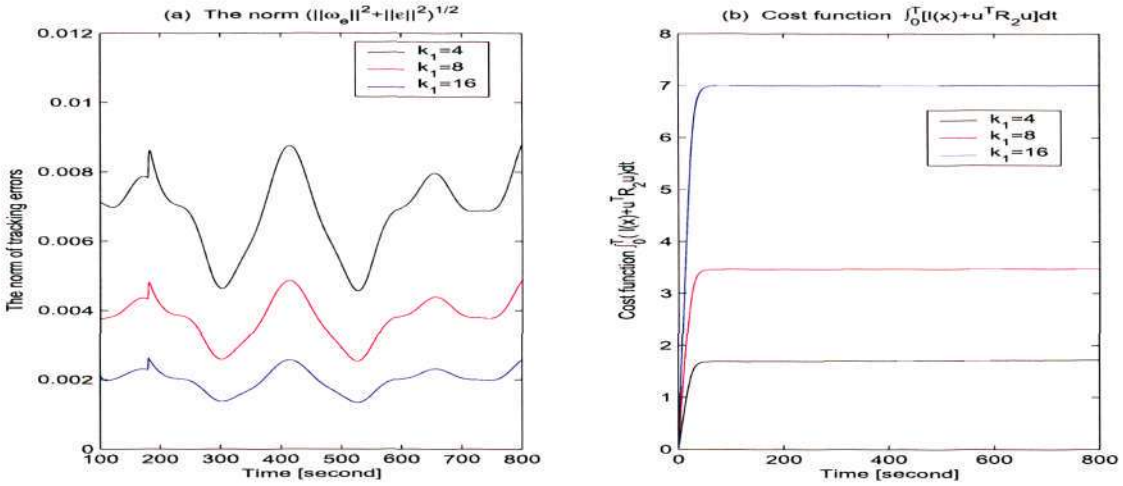

Figure 5.7: The norm $||\tilde{x}||$ and the cost function $\int_0^T [l(x) + u^T R_2 u]dt$ with different k_1.

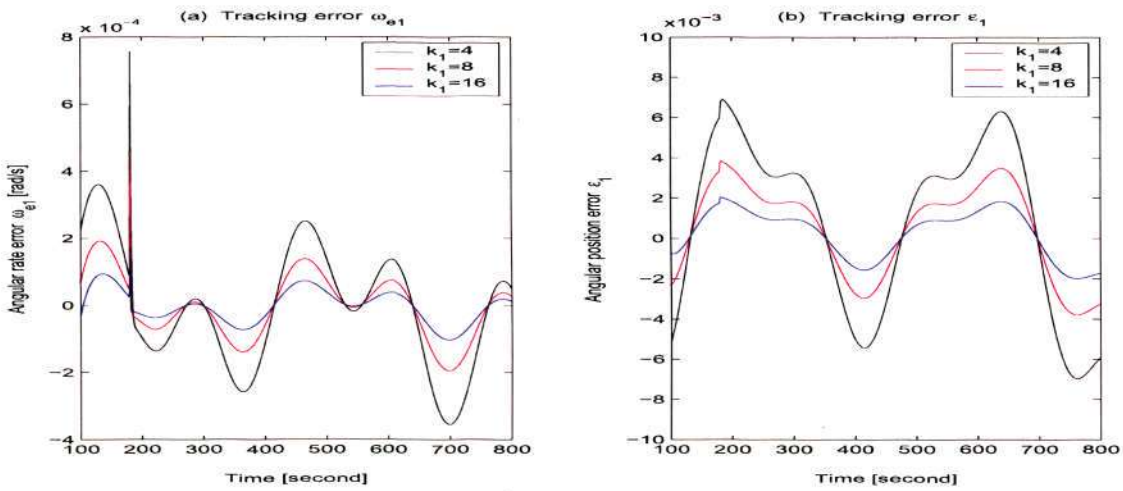

Figure 5.8: Errors ω_{e1} and ϵ_1 in the interval [100, 800]seconds with different k_1

5.1. The time history of the angular momentum of the reaction wheels is illustrated in Figure 5.6(b).

Next, we fix the $\mathcal{L}_2$-gain $\gamma = 1.0$ and change the magnitude of the gain k_1 from 4.0 to 8.0 and finally to 16.0 to show the relationship between the gain k_1 and the system error. After the conditions (5.40) and (5.42) are applied, we prefer to fix $b = 0.13$ to illustrate the direct relationship between the system performance and the control gain k_1. Under the control law (5.22) and with these values of k_1 and b, the closed-loop system enters into the steady tracking within 100 seconds as before. The norm of the tracking errors $||\tilde{x}|| = \sqrt{\epsilon^T \epsilon + \omega_e^T \omega_e}$ and the cost function $\int_0^t [l(x) + u^T R_2^T u]ds$ are plotted in Figure 5.7. The steady tracking error ϵ_1 and ω_{e1} in the interval [100, 800] seconds for different values of the gain k_1 are depicted as in Figure 5.8. From Figures 5.7(a) and 5.8, it is observed that the norm $||\tilde{x}||$, the steady-state tracking errors ϵ_1 and ω_{e1} decrease considerably as the gain k_1 increases. A larger gain k_1 results in a smaller tracking error $\tilde{x}$. For example, as k_1 increases as $4.0 \rightarrow 8.0 \rightarrow 16.0$, the maximum

value of the norm $||\tilde{x}||$ is reduced as $0.0089 \rightarrow 0.0049 \rightarrow 0.0025$ and the maximum of ϵ_1 as $0.0069 \rightarrow 0.0038 \rightarrow 0.0020$. From Remark 5.2, larger value of k_1 brings a larger state weighting matrix $Q(x)$ and a smaller control weighting matrix $R_2(x)$. For the systems with the same nonzero initial condition (5.46), this brings a larger cost function $\int_0^t [l(x) + u^T R_2 u] ds$, as depicted in Figure 5.7(b).

Lastly, we fix the gain $k_1 = 4$, and change the magnitude of the $\mathcal{L}_2$ gain γ from 1.0 to 0.5 and finally to 0.25 to show the relationship between the $\mathcal{L}_2$ gain γ and the system error $\tilde{x}$. By the tuning rule (5.42), the value of b is kept unchanged, $b = 0.13$. With the controller (5.22), the closed-loop system achieves steady tracking within 100 seconds as in the previous case. The norm of the tracking errors $||\tilde{x}||$ and the cost function $\int_0^t [l(x) + u^T R u] ds$ are plotted in Figure 5.9; the steady-state tracking errors ϵ_1 and ω_{e1} in the interval $[100, 800]$ seconds are plotted as in Figure 5.10. From Figures 5.9 and 5.10 it is seen that the steady-state tracking error $\tilde{x}$ decreases considerably as γ decreases, which brings a smaller cost $\int_0^t [l(x) + u^T R u] ds$. For example, as γ is reduced from 1.0 to 0.5 and then to 0.25, the maximum of the norm $||\tilde{x}||$ is reduced from 0.0089 to 0.0055 and then to 0.0023 and the attitude error ϵ_1 from 0.0069 to 0.0042 and finally to 0.0017.

5.6.3 A Comparison

Compared with the existing techniques for attitude control, one advantage of our approach is the flexible trade-off between the tracking performance and the control effort, which usually leads to a more economical control for a good tracking performance. To further illustrate this point, a computer simulation is presented to compare our H_∞ inverse optimal controller with the variable structure controller (VSC) in [9], where the attitude tracking problem was also considered with external disturbances, and the VSC was proved to be globally stable under certain conditions and was proposed as

$$\begin{aligned} u &= -u_m \text{sgn}(s), \qquad s = \omega_e + k\epsilon, \\ \dot{k} &= -\gamma_k u_m \sum_{i=1}^{3} [\text{sgn}(k)|\epsilon_i| + \epsilon_i \text{sgn}(s_i)], \end{aligned} \tag{5.47}$$

where s is the sliding surface; u_m is the maximum control torque with the constraint $u_m \geq \bar{d} + \lambda_j \bar{\nu}$, where $\bar{\nu} = \sup_t\{||\omega_c(t)||^2 + ||\dot{w}_c(t)||\}$ and $\bar{d} = \max\{\sup_t\{||d_i(t)||\}\}$ for $i = 1, 2, 3$. With this VSC control law, $\lim_{t\rightarrow\infty} \omega_e(t) \rightarrow 0$ and $\lim_{t\rightarrow\infty} k(t)\epsilon(t) \rightarrow 0$. To avoid the convergence of $\epsilon(t)$ to a nonzero constant, one needs to choose γ_k sufficiently small such that $\lim_{t\rightarrow\infty} k(t)$ is nonzero. The adaptation of the control gain k is to avoid imposing a stringent and conservative constraint on k. In simulations, we let $\gamma_k = 0.001$ and $k(0) = 0.132$ for the VSC (5.47). To avoid too much chattering, the sign function $\text{sgn}(s_i)$ is replaced by an approximate sign function $\frac{s_i}{|s_i|+\delta}$ with $\delta = 1.0 \times 10^{-7}$.

It should be noted that the constraint on u_m is indeed conservative in practice. For example, for the disturbance model (5.44), we have that $\bar{d} = 0.1$ and $\bar{\nu} = 0.0023$. As such, u_m should be larger than 0.147, which is beyond the control capability of the reaction wheels listed in Table 5.1. From simulations it is observed that the control

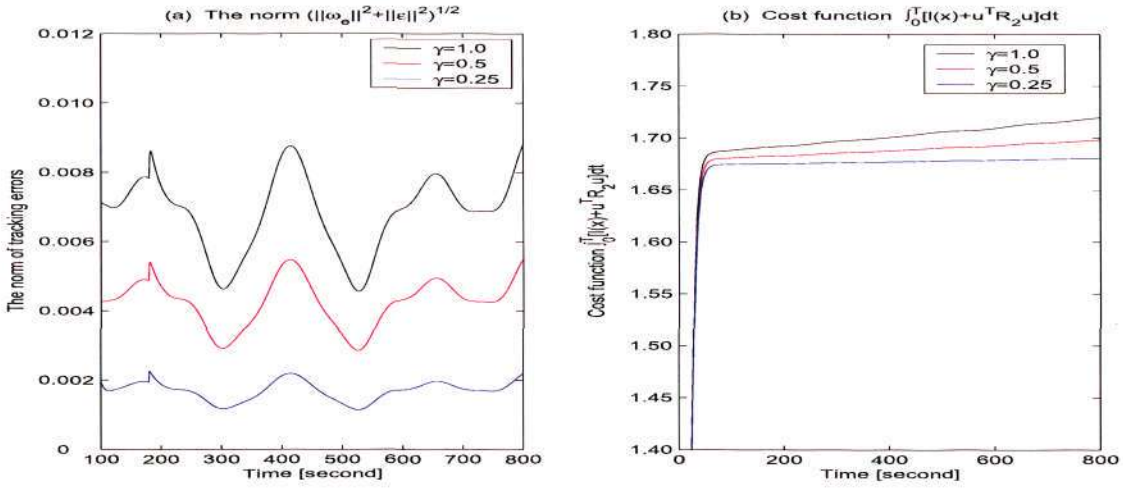

Figure 5.9: The norm $||\tilde{x}||$ and the cost function $\int_0^T [l(x) + u^T R_2 u]dt$ with different γ.

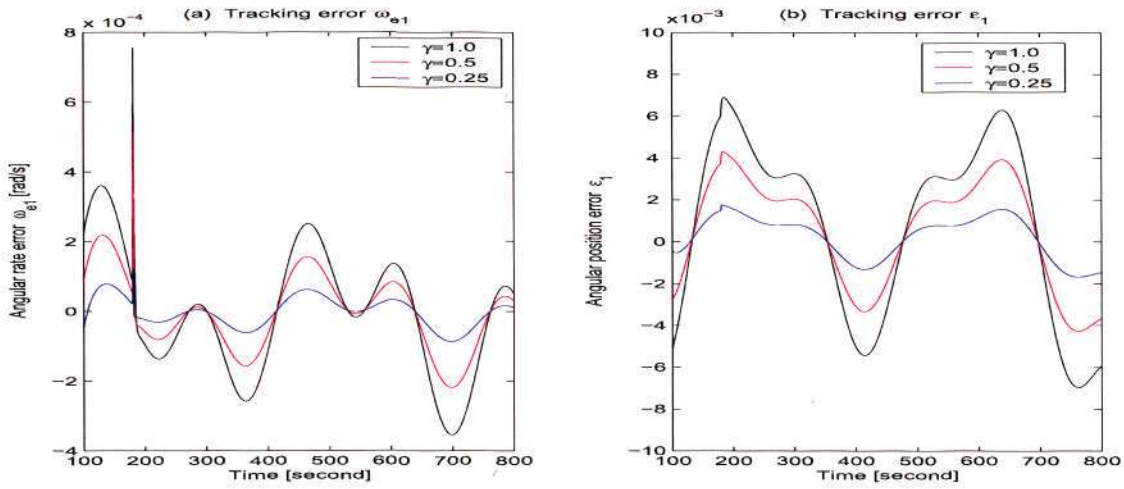

Figure 5.10: Tracking errors ω_{e1} and ϵ_1 in the interval $[100, 800]$ seconds for different γ

(5.47) with a smaller u_m, for instance, $u_m = 0.04$, can eventually achieve the attitude tracking of the target angular velocity subject to the external disturbances modelled by (5.44) and the initial conditions given by (5.46), but needs a much longer settling time t_s. To illustrate this point, we let $b = 0.13$, $k_1 = 16$ and $\gamma = 1$ for our H_∞ inverse optimal control (5.22). If we choose the initial conditions (5.46) for the tracking control problem, the VSC (5.47) with $u_m = 0.04$ can achieve attitude tracking with a horribly long settling time, $t_s = 1170$ seconds, while the VSC (5.47) with $u_m = 0.03$ cannot work well, as shown in Figure 5.11(a). However, if we reduce the initial condition $q(0)$ in (5.46) to $q(0) = [0.15, -0.10, 0.15, 0.972]$, the VSC (5.47) with $u_m = 0.03$ can achieve attitude tracking with a much longer setting time ($t_s = 764$seconds) than our H_∞ inverse optimal control ($t_s = 70$seconds), as shown in Figure 5.11(b). Note that the H_∞ inverse optimal control is bounded by $u_m = 0.03$ in the simulations for a fair comparison. Therefore, we can say that the VSC (5.47) is sensitive to initial conditions.

Next, we choose zero initial conditions for $\omega(0)$ and $q(0)$, i.e., $\omega(0) = [0, 0, 0]^T$

and $q(0) = [0, 0, 0, 1]^T$, to make a further comparison on the tracking errors. It is known [102] that by frequently switching the control torque between $\pm u_m$, the variable structure control achieves extremely high performance. For our H_∞ inverse optimal controller, we can make the flexible trade-off between the tracking performance and the control power. For example, let $u_m = 0.03$Nms for the VSC (5.47), let $b = 0.13$, $\gamma = 0.1$ and $k_1 = 850$ for our H_∞ inverse optimal control (5.22) and let the H_∞ inverse optimal control be bounded by $u_m = 0.03$ too for a fair comparison. Figure 5.12 plots the norm of the tracking error $||\tilde{x}||$ and the control effort u, from which we see that the VSC has a slightly better tracking performances than the H_∞ inverse optimal control (the mean values of $||\tilde{x}||$ under the VSC control is 1.7×10^{-5} and that under the H_∞ control is 2.2×10^{-5}), while the VSC would require a control power of $3u_m^2$, which is much higher than that required by the H_∞ inverse optimal controller. From further simulations we also notice that the H_∞ control (5.22) with a smaller γ or a larger k_1 will be saturated more often, which brings the H_∞ control (5.22) with a smaller γ or a larger k_1 closer to the VSC control (5.47).

Another advantage of our H_∞ inverse optimal controller over the VSC is that the PD controller (5.22) is of a simpler form and thus easier to be implemented in practice.

5.6.4 Some Comments

1. For a large-angle maneuver or an attitude tracking to be achieved in a short time, the magnetic unloading algorithm can be disconnected, as the wheels can afford the accumulation of momentum for a short time without destabilizing the control system. However, for long-term operations, the unloading is necessary.

2. In practice, when we design the target motions to be tracked, we should take into account the input saturation of the reaction wheels. Also, we should try to avoid long-time saturations of the wheel's angular momentum.

3. If a large-angle maneuvers are required to be achieved in the shortest time, one can design a time-optimal or a time-suboptimal trajectory for the attitude maneuver to take full advantage of the control torques. For example, one-axis time-optimal trajectory can be designed as the figure below:

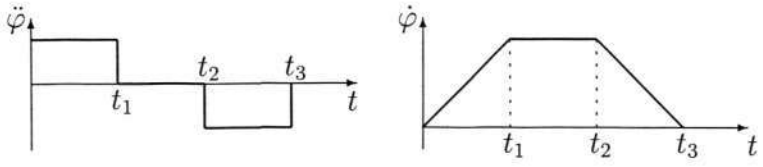

The motion of $\dot{\varphi}$ is divided into three stages: acceleration, holding and deceleration. This idea of trajectory planning is motivated by the work [56], where a near-time-optimal trajectory was planned in this way.

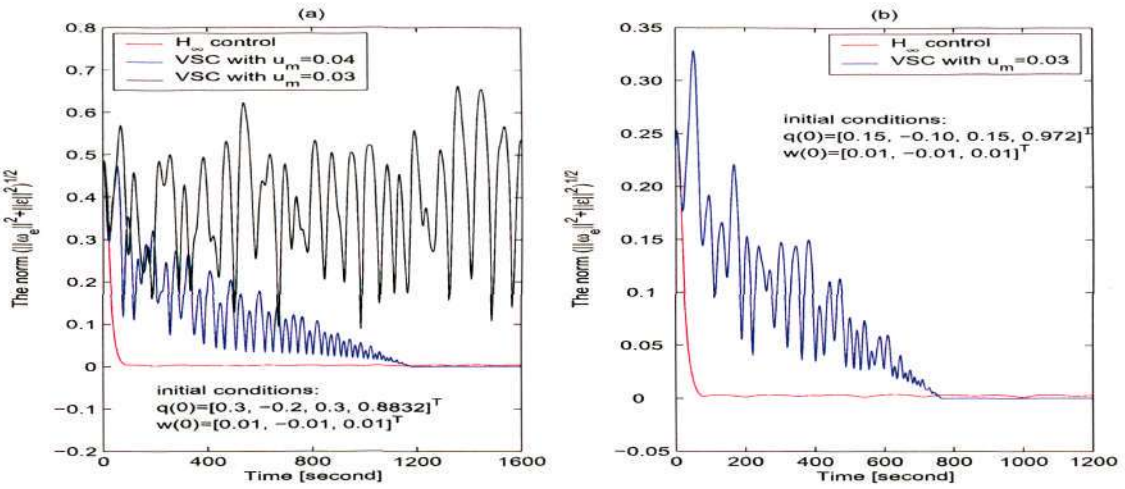

Figure 5.11: Convergence comparison between VSC control and H_∞ inverse optimal control for different initial conditions.

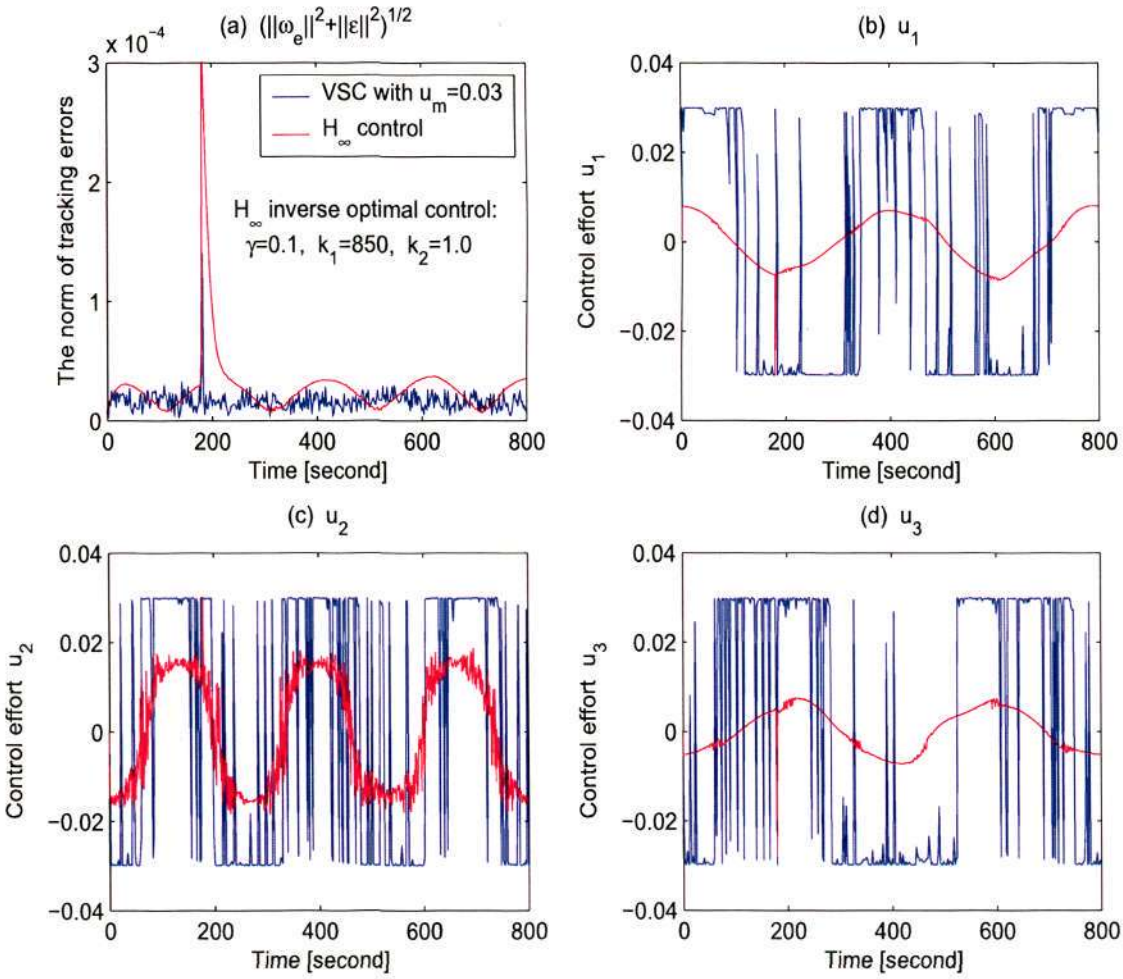

Figure 5.12: A comparison between VSC control and H_∞ inverse optimal control for zero initial conditions.

5.7 Conclusions

With the introduction of the concept of extended disturbance, the robust inverse optimal control method has been applied to the attitude tracking control problem of rigid spacecraft with external disturbances. The proposed state-feedback control law is inverse optimal with respect to a meaningful cost functional that involves penalties on tracking errors and control efforts. The associated control Lyapunov function solves a Hamilton-Jacobi-Isaacs (HJI) partial differential equation, thus, nonlinear H_∞ optimality with respect to the extended disturbance is achieved without obtaining a direct solution to the associated HJI equation and H_∞ disturbance attenuation is also achieved. Such a state-feedback law is in the form of a Proportional-Derivative state-feedback controller, which is easy to be implemented in practice. Performance estimates have been given in terms of the performance limitation. Based on the performance analysis, tuning rules have been established as guidelines for selecting the proportional and derivative gains. Numerical simulations have been carried out to demonstrate the control algorithms and the tuning rules.

Chapter 6

H_∞ Inverse Optimal Adaptive Attitude Tracking Control

6.1 Introduction

In most practical situations, the inertia matrix of a spacecraft may be uncertain or may change due to the motion of onboard payload, the rotation of solar arrays or the fuel consumption, etc. Thus, we would like the nonlinear attitude control system to be able to adapt to parameter uncertainties in the mass properties and have a robust capability to reject or attenuate external disturbances. As stated in Remark 5.3, the H_∞ inverse optimal control law proposed in Chapter 5 is robust to parametric uncertainties because no complete information of the inertia matrix is required in the H_∞ inverse optimal controller. In this chapter, we address these parametric uncertainties directly by applying the adaptive control method, and design an inverse optimal adaptive controller for the attitude tracking control problem with external disturbances and a constant but uncertain inertia matrix.

Adaptive control [45, 62, 66] has been applied successfully to the attitude tracking control problem of spacecraft by many scholars, for example, [1,9,10,33,34,56,103,125]. Authors of [34, 103] developed adaptive control schemes for the attitude tracking problem; however, due to the use of Rodriguez parameters, singularities appeared in the attitude representation so global results were not obtained. Based on the attitude representation using singularity-free modified Rodriguez parameters, an adaptive control algorithm was developed in [56] for attitude maneuvers. Using the singularity-free unit quaternion to represent the attitude of spacecraft, [1, 33, 125] presented adaptive controllers. It was shown by Lyapunov functions that these adaptive controllers achieved a global convergence of the attitude tracking errors to zero. In [125], only scalar control gains could be used. Also, it is not straightforward to extend the result [125] to other adaptive control schemes. In [33], the control scheme was designed using passivity theory and it allowed the control gain to be of a matrix form, but the controller was not for the case of an uncertain inertia matrix. By applying nonlinearity cancellation technique, an adaptive controller [1] was designed to identify the inertia matrix and to achieve asymptotic attitude tracking. All these adaptive tracking controllers above-

mentioned were designed for spacecraft without external disturbances. Moreover, the degree of optimality of these adaptive controllers was not stated explicitly.

As stated in the previous chapters, nonlinear H_∞ optimal control [123] is a potential approach for solving the attitude tracking control problem due to its inherent robustness with respect to external disturbances and uncertainties, while its practical applications remain open due to the difficulty in solving the associated Hamilton-Jacobi-Isaacs partial differential equation. On the other hand, *inverse optimal control approach* [35,63] is an alternative approach to circumvent the hard task of solving the HJI equation and results in the proposed feedback controllers optimal with respect to a family of meaningful cost functionals.

In this chapter, we combine both the adaptive control method and the inverse optimal control approach to account for the parametric uncertainties on the inertia matrix of the spacecraft and the optimality of the attitude controller for the the attitude tracking control problem with disturbances. The method of backstepping [35] is used to construct a control Lyapunov function and stabilizing control laws of particular forms. For the zero-disturbance case, the proposed inverse optimal adaptive controller achieves globally asymptotic attitude tracking for all initial conditions. In comparison with the results reported in [1,33,103,125], the adaptive feedback control laws in this chapter are optimal with respect to a family of meaningful cost functionals involving tracking errors and control efforts. When external disturbances are considered, an adaptive attitude tracking control law is proposed that is optimal and achieves H_∞ disturbance attenuation without solving the associated HJI equation directly.

This chapter is organized as follows. In Section 6.2 theoretical results on the inverse optimal adaptive control are proposed. In Section 6.3, the theoretical results in Section 6.2 are utilized to design inverse optimal adaptive control law to solve the attitude tracking problem with disturbances and an uncertain inertia matrix. Numerical simulations are carried out in Section 6.4 to demonstrate the performance of the optimal adaptive control algorithms. Finally, conclusions follow in Section 6.5.

6.2 Inverse Optimal Adaptive Control

6.2.1 Stable Adaptive Control

We consider the nonlinear uncertain system

$$\dot{x} = f(x) + F(x)\theta + g(x)u \tag{6.1}$$

where $x \in \mathcal{R}^n$, $u \in \mathcal{R}^m$, the mappings $f(x) \in \mathcal{R}^n$, $F(x) \in \mathcal{R}^{n\times p}$ and $g(x) \in \mathcal{R}^{n\times m}$ are smooth, and $\theta \in \mathcal{R}^p$ is a constant unknown parameter vector. Let $\hat{\theta}$ denote an estimate of θ with an error $\tilde{\theta} = \theta - \hat{\theta}$.

Definition 6.1 (Adaptive Control Problem). *We say that adaptive control problem of the system (6.1) is solvable if there exist a function $\alpha(x,\hat{\theta})$ smooth on $(\mathcal{R}^n \setminus \{0\}) \times \mathcal{R}^p$ with $\alpha(0,\hat{\theta}) \equiv 0$, a smooth function $\tau(x,\hat{\theta})$ and a positive definite symmetric*

matrix $\Gamma \in \mathcal{R}^{p\times p}$ *such that the dynamic feedback controller*

$$u = \alpha(x, \hat{\theta}) \tag{6.2}$$

$$\dot{\hat{\theta}} = \Gamma\tau(x, \hat{\theta}) \tag{6.3}$$

guarantees that the solution $(x(t), \hat{\theta}(t))$ *is globally bounded, and* $x(t) \to 0$ *as* $t \to \infty$, *for any value of the unknown parameter vector* $\theta \in \mathcal{R}^p$.

The approach adopted here to stabilize (6.1) is to replace first the problem of adaptive stabilization of (6.1) by a problem of non-adaptive stabilization of an auxiliary system and then design an adaptive controller based on the results obtained from the auxiliary system. This allows us to study adaptive stabilization in the framework of control Lyapunov functions.

Definition 6.2. *[61] A smooth function* $V_a(x, \theta) : \mathcal{R}^n \times \mathcal{R}^p \to \mathcal{R}_+$, *positive definite, decrescent, and radially unbounded in* x *for each* θ, *is called an adaptive control Lyapunov function (ACLF) for (6.1) if there exist a positive definite symmetric matrix* $\Gamma \in \mathcal{R}^{p\times p}$ *and a continuous function* $W(x, \theta)$ *positive definite in* x *for each* $\theta \in \mathcal{R}^p$ *such that* $V_a(x, \theta)$ *satisfies*[1]

$$\inf_{u\in\mathcal{R}^m} \left\{ \frac{\partial V_a}{\partial x}\left[f(x) + F(x)\left(\theta + \Gamma\left(\frac{\partial V_a}{\partial \theta}\right)^T\right) + g(x)u\right]\right\} \le -W(x, \theta) \tag{6.4}$$

for the auxiliary system

$$\dot{x} = f(x) + F(x)\left(\theta + \Gamma\left(\frac{\partial V_a}{\partial \theta}\right)^T\right) + g(x)u. \tag{6.5}$$

Lemma 6.1. *[61] A function* $V_a(x, \theta) : \mathcal{R}^n \times \mathcal{R}^p \to \mathcal{R}_+$, *positive definite, decrescent, and radially unbounded in* x *for each* $\theta \in \mathcal{R}^p$, *is an ACLF for (6.1) if and only if, for all* $x \neq 0$, *it follows that*

$$\frac{\partial V_a}{\partial x} g(x) = 0 \Longrightarrow \frac{\partial V_a}{\partial x}\left[f(x) + F(x)\left(\theta + \Gamma\left(\frac{\partial V_a}{\partial \theta}\right)^T\right)\right] \le -W(x, \theta) \tag{6.6}$$

When an adaptive control Lyapunov function is known, the next theorem [62, Theorem 4.3] shows how to design an adaptive controller.

Theorem 6.2. *The following two statements are equivalent:*

1. *There exists a triple* $\{\alpha, V_a, \Gamma\}$ *such that* $\alpha(x, \theta)$ *globally uniformly asymptotically stabilizes (6.5) at* $x = 0$ *for each* $\theta \in \mathcal{R}^p$ *with respect to the Lyapunov function* $V_a(x, \theta)$.

2. *There exists an ACLF* $V_a(x, \theta)$ *for (6.1) with a small control property.*

Moreover, if an ACLF $V_a(x, \theta)$ *exists, then (6.1) is globally adaptively stabilizable.*

[1] Throughout the chapter, we will drop the arguments in $\frac{\partial V_a(x,\theta)}{\partial x}$ and $\frac{\partial V_a(x,\theta)}{\partial \theta}$, and write shortly $\frac{\partial V_a}{\partial x}$ and $\frac{\partial V_a}{\partial x}$. However, we will keep the arguments in $f(x)$, $F(x)$, $g_1(x)$ and $g_2(x)$.

In the proof of Theorem 6.2, if $V_a(x,\theta)$ is an ACLF, a Sontag-type control law

$$\alpha = \begin{cases} -\frac{\frac{\partial V_a}{\partial x}\bar{f}+\sqrt{\left|\left|\frac{\partial V_a}{\partial x}\bar{f}\right|\right|^2+\left|\left|\frac{\partial V_a}{\partial x}g\right|\right|^4}}{||\frac{\partial V_a}{\partial x}g||^2}(\frac{\partial V_a}{\partial x}g)^T, & \frac{\partial V_a}{\partial x}g \neq 0, \\ 0, & \frac{\partial V_a}{\partial x}g = 0 \end{cases} \tag{6.7}$$

is designed, where $\bar{f}(x,\theta) = f(x)+F\theta+F\Gamma(\frac{\partial V_a}{\partial \theta})^T$ with a constant matrix $\Gamma = \Gamma^T > 0$. With the control (6.7), it is easy to verify that (6.4) is satisfied with the continuous function $W(x,\theta) = \sqrt{\left|\left|\frac{\partial V_a}{\partial x}\bar{f}\right|\right|^2 + \left|\left|\frac{\partial V_a}{\partial x}g\right|\right|^4}$, which, by Lemma 6.1, is positive definite in x for each θ. By the results in [107] and the small control property, the control (6.7) is smooth on $(\mathcal{R}^n \setminus \{0\}) \times \mathcal{R}^p$ and continuous everywhere on $\mathcal{R}^n \times \mathcal{R}^p$.

Consider the following Lyapunov function candidate

$$V(x,\hat{\theta}) = V_a(x,\hat{\theta}) + \frac{1}{2}(\theta-\hat{\theta})^T\Gamma^{-1}(\theta-\hat{\theta}). \tag{6.8}$$

With the control law (6.7) in which θ is replaced by $\hat{\theta}$, and choosing $\tau(x,\hat{\theta})$ in (6.3) as

$$\tau(x,\hat{\theta}) = \left[\frac{\partial V_a}{\partial x}F(x)\right]^T, \tag{6.9}$$

it follows that $\dot{V} \leq -W(x,\hat{\theta})$ for all $\theta \in \mathcal{R}^p$. Thus the equilibrium $x = 0$, $\tilde{\theta} = 0$ of the closed-loop system (6.1), (6.2) and (6.3) is globally uniformly stable, $\hat{\theta}$ and x are bounded for all $t \geq 0$, and by Theorems 3.2 and 3.3, $x \to 0$ as $t \to \infty$.

The adaptive control law constructed in Theorem 6.2 consists of a continuous state-feedback control law $u = \alpha(x,\hat{\theta})$ given by (6.7) and a parameter update law $\dot{\hat{\theta}} = \Gamma\tau(x,\hat{\theta})$ with the tuning function (6.9).

The control law $\alpha(x,\theta)$ stabilizes the auxiliary system (6.5) but may not stabilize the original system (6.1). However, its certainty equivalence[2] form $\alpha(x,\hat{\theta})$ is a globally adaptively stabilizing control law for the original system (6.1). Hence, if the certainty equivalence approach is to be applied to a nonlinear system, the system should be modified to require a control law which *anticipates* parameters estimation transients. This is achieved by incorporating the *tuning function* τ into the control law α. Indeed, the formula (6.7) for α depends on τ via $\frac{\partial V_a}{\partial x}\bar{f}(x,\theta) = \frac{\partial V_a}{\partial x}f(x) + \tau(x,\theta)^T\left[\theta + \Gamma(\frac{\partial V_a}{\partial \theta})^T\right]$. Using (6.9) to rewrite the inequality (6.4) as

$$\frac{\partial V_a}{\partial x}\left[f(x) + F(x)\theta + g(x)\alpha(x,\theta)\right] + \frac{\partial V_a}{\partial x}\Gamma\tau(x,\theta) \leq -W(x,\theta),$$

it is not difficult to see that the control (6.7) containing $\frac{\partial V_a}{\partial x}\bar{f}(x,\theta)$ prevents τ from destroying the nonpositivity of the Lyapunov derivative.

[2]The "*certainty equivalence*" thinking [62] in adaptive control is divided into two steps. One first performs a design for the case when the exact value of θ is known to get a feedback control $\alpha_c(x,\theta)$ with respect to a known CLF $V_c(x,\theta)$. The certainty equivalence idea is to replace θ by an estimate $\hat{\theta}$ obtained from the parameter update law $\dot{\hat{\theta}} = \Gamma\tau(x,\hat{\theta})$ for an adaptation matrix $\Gamma > 0$. The goal is to select u and τ with respect to a CLF candidate $V(x,\hat{\theta}) = V_c(x,\hat{\theta}) + \frac{1}{2}\tilde{\theta}^T\Gamma^{-1}\tilde{\theta}$.

6.2.2 Inverse Optimal Adaptive Control

Definition 6.3. *The **inverse optimal adaptive control problem** for the system (6.1) is solvable if there exist a positive constant β, a smooth nonnegative function $E(x) \geq 0$, a positive definite symmetric matrix $R(x,\hat{\theta})$, a real-valued function $l(x,\hat{\theta})$ positive definite in x for each $\hat{\theta}$, and a dynamic feedback controller (6.2)(6.3) that solves the adaptive problem and also minimizes the cost functional*

$$J_a(u) = \lim_{t\to\infty}\Big\{\big[\beta||\tilde{\theta}||^2_{\Gamma^{-1}} + E(x)\big] + \int_0^t \Big(l(x,\hat{\theta}) + u^T R(x,\hat{\theta})u\Big)d\tau\Big\}, \tag{6.10}$$

for each $\theta \in \mathcal{R}^p$.

Definition 6.3 is a bit different from Definition 5.12 in [61] in that a smooth nonnegative function $E(x(t))$ that penalizes the terminal state $x(\infty)$ is introduced in (6.10). This definition of optimality puts penalty on x and u as well as on the terminal values of $\hat{\theta}(\infty)$ and $x(\infty)$. Even though $\tilde{\theta}$ is not guaranteed to have a limit in the general adaptive case, the existence of $\lim_{t\to\infty}||\tilde{\theta}||^2_{\Gamma^{-1}}$ is assumed implicitly if the adaptive control problem is solvable. The absence of an integral penalty on $\tilde{\theta}$ in (6.10) should not be surprising because adaptive feedback controls, in general, do not guarantee the parameter convergence to the true value. In the next theorem, we present such an inverse optimal adaptive controller for the uncertain nonlinear system (6.1) in the sense of Definition 6.3.

Theorem 6.3. *Suppose that there exist an ACLF $V_a(x,\theta)$ for (6.1), a positive definite symmetric matrix $R(x,\theta)$ for all θ, a positive definite symmetric matrix $\Gamma \in \mathcal{R}^{p\times p}$ and a feedback control law*

$$\tilde{u} = \tilde{\alpha}(x,\theta) = -R^{-1}(x,\theta)\Big(\frac{\partial V_a}{\partial x}g(x)\Big)^T$$

that stabilizes the auxiliary system (6.5). Then the dynamic feedback control law

$$u = \tilde{\alpha}^*(x,\hat{\theta}) = \beta\tilde{\alpha}(x,\hat{\theta}), \quad \forall\beta \geq 2$$

together with the parameter update law

$$\dot{\hat{\theta}} = \Gamma\tau(x,\hat{\theta}) = \Gamma\Big(\frac{\partial V_a}{\partial x}F(x)\Big)^T$$

minimizes the cost functional J_a in (6.10) with $E(x) \equiv 0$, where

$$l(x,\hat{\theta}) = -2\beta\Big[\frac{\partial V_a}{\partial x}f + \frac{\partial V_a}{\partial x}F\Big(\hat{\theta} + \Gamma\Big(\frac{\partial V_a}{\partial\hat{\theta}}\Big)^T\Big) + \frac{\partial V_a}{\partial x}g\tilde{\alpha}\Big] + \beta(\beta-2)\frac{\partial V_a}{\partial x}gR^{-1}\Big(\frac{\partial V_a}{\partial x}g\Big)^T.$$

Proof. It is a straightforward extension of Theorem 5.13 in [61] to the MIMO case with some necessary modifications. Therefore, we omit the proof here. □

Remark 6.1. The freedom in selecting the parameter $\beta \geq 2$ in Theorem 6.3 means that the inverse optimal adaptive controller has an infinite gain margin. The ACLF V_a

solves the following family of Hamilton-Jacobi-Bellman partial differential equations parameterized in $\beta \geq 2$:

$$\frac{\partial V_a}{\partial x}\Big[f(x) + F(x)\hat{\theta} + F(x)\Gamma\Big(\frac{\partial V_a}{\partial \hat{\theta}}\Big)^T\Big] - \frac{1}{2}\Big(\frac{\partial V_a}{\partial x}g(x)\Big)R^{-1}\Big(\frac{\partial V_a}{\partial x}g(x)\Big)^T + \frac{l(x,\hat{\theta})}{2\beta} = 0.$$

The role of the term $F(x)\Gamma\big(\frac{\partial V_a}{\partial \hat{\theta}}\big)^T$ is to take into account the time-varying parameter adaptation and make the control law optimal in the presence of an update law. $\otimes$

Corollary 6.4. *If there exists an ACLF $V_a(x,\theta)$ for the system (6.1), then the inverse optimal adaptive control problem is solvable.*

With Theorem 6.3, the problem of inverse optimal adaptive control is reduced to the problem of finding an ACLF for the nonlinear uncertain system (6.1). As stated in [35, 61, 62], the recursive Lyapunov design known as *robust backstepping* helps to alleviate the difficulty in constructing such an ACLF for a nonlinear system. Moreover, it helps to design a controller that is smooth everywhere.

Theorem 6.5. *Suppose the nonlinear system (6.1) is globally adaptively stabilizable with an ACLF $V_a(x,\theta)$, a smooth control law $\alpha(x,\theta)$ and a smooth tuning function $\tau(x,\theta)$, and (6.4) is satisfied with $W(x,\theta) = x^T\Omega(x,\theta)x$, where $\Omega(x,\theta) \in \mathcal{R}^{n\times n}$ is positive definite and symmetric for all x and θ. Assume that $f(x)$, $F(x)$ and $F_1(x,\xi)$ are smooth and vanish for $x = 0$. Then the inverse optimal adaptive control problem with $E(x,\xi) = 0$ for the augmented system*

$$\begin{aligned} \dot{x} &= f(x) + F(x)\theta + g(x)\xi, \\ \dot{\xi} &= u + F_1(x,\xi)\theta, \end{aligned} \tag{6.11}$$

is also solvable with a smooth dynamic feedback control law.

It should be noted the augmented system in [61, Lemma 5.20] is augmented only by an integrator $\dot{\xi} = u$ and can be considered as a special case of the more general system (6.11). A stable adaptive controller was designed for the augmented system (6.11) in [62, Lemma 4.7 and Corollary 4.9] using the nonlinearity cancellation technique, which is, in general, not guaranteed to be optimal. Applying the "nonlinear damping" technique [59], Theorem 6.5 establishes the inverse optimality for a class of adaptive control systems. It is obtained by extending both [61, Lemma 5.20] and [62, Lemma 4.7 and Corollary 4.9] to the MIMO case with certain necessary modifications, and the proof is outlined as follows.

Proof. Since the system (6.1) is globally adaptively stabilizable, then there exist an ACLF $V_a(x,\theta)$ and a positive definite symmetric matrix $\Omega(x,\theta)$ such that the continuous function $W(x,\theta) = x^T\Omega(x,\theta)x$ is positive definite in x for each θ and (6.4) is satisfied with a smooth control law $\alpha(x,\theta)$.

Choose a control Lyapunov function $V_1(x,\xi,\theta)$ as

$$V_1(x,\xi,\theta) = V_a(x,\theta) + \frac{1}{2}(\xi - \alpha(x,\theta))^2 \tag{6.12}$$

to design the control law $\tilde{\alpha}_1$ and the tuning function τ_1 for the augmented system (6.11). Consider the auxiliary non-adaptive system

$$\begin{aligned}\dot{x} &= f(x) + F(x)\Big(\theta + \Gamma\big(\frac{\partial V_1}{\partial \theta}\big)^T\Big) + g(x)\xi,\\ \dot{\xi} &= \alpha_1 + F_1(x,\xi)\Big(\theta + \Gamma\big(\frac{\partial V_1}{\partial \theta}\big)^T\Big),\end{aligned} \tag{6.13}$$

and define $z = \xi - \alpha(x,\theta)$. Letting two matrices $\Psi_1(x,\theta)$ and $\Psi_2(x,\theta)$ satisfy

$$\begin{aligned}\Psi_1(x,\theta)^T\Omega(x,\theta)^{1/2}x = {}& \frac{\partial V_a}{\partial x}g - \frac{\partial \alpha}{\partial x}[f + F\theta + g\alpha] - \frac{\partial V_a}{\partial \theta}\Gamma\Big(\frac{\partial \alpha}{\partial x}F\Big)^T\\ & - \frac{\partial \alpha}{\partial \theta}\Gamma\Big(\frac{\partial V_a}{\partial x}F\Big)^T + F_1\theta + F_1\Gamma\Big(\frac{\partial V_a}{\partial \theta}\Big)^T,\\ \Psi_2(x,\theta) = {}& -\frac{1}{2}\frac{\partial \alpha}{\partial x}g + \frac{1}{2}\frac{\partial \alpha}{\partial \theta}\Gamma\Big(\frac{\partial \alpha}{\partial x}F\Big)^T - \frac{1}{2}F_1\Gamma\Big(\frac{\partial \alpha}{\partial \theta}\Big)^T,\end{aligned}$$

along the solution of the system (6.13) we can express the derivative of V_1 as

$$\dot{V}_1 \le -W(x,\theta) + z^T\Psi_1(x,\theta)^T\Omega(x,\theta)^{1/2}x + z^T[\Psi_2(x,\theta)^T + \Psi(x,\theta)]z.$$

Since $\alpha(x,\hat{\theta})$, $f(x)$, $F(x)$, $F_1(x,\xi)$, $\frac{\partial V_a}{\partial x}(x,\hat{\theta})$, $\frac{\partial V_a}{\partial \theta}(x,\hat{\theta})$ are smooth in x for all $\hat{\theta}$ and vanish for $x = 0$, we conclude that $\Psi_1(x,\theta)$ and $\Psi_2(x,\theta)$ are also smooth. Then, the choice of the smooth dynamic feedback controller

$$u = \alpha_1(x,\xi,\theta) = -R^{-1}(x,\xi,\theta)\frac{\partial V_1}{\partial(x,\xi)}\begin{bmatrix}0\\1\end{bmatrix}, \tag{6.14}$$

$$\dot{\hat{\theta}} = \Gamma\tau_1(x,\xi,\theta) = \Gamma\Big(\frac{\partial V_1}{\partial(x,\xi)}\begin{bmatrix}F\\F_1\end{bmatrix}\Big)^T = \Gamma\Big(\frac{\partial V_1}{\partial x}F + \frac{\partial V_1}{\partial \xi}F_1\Big)^T \tag{6.15}$$

with the matrix $R(x,\xi,\theta)$ satisfying

$$R^{-1}(x,\xi,\theta) = cI_n + \frac{\Psi_1^T\Psi_1}{2} + \frac{(\Psi_2 + \Psi_2^T)^2}{2c} > 0, \quad \forall c > 0, x, \xi, \theta,$$

renders

$$\dot{V}_1 \le -\frac{1}{2}||\Omega^{1/2}x||^2 - \frac{c}{2}z^2.$$

By Theorem 6.3, it is seen that the smooth dynamic feedback control

$$u_1 = \alpha_1^* = \beta\alpha_1(x,\xi,\hat{\theta}), \qquad \forall \beta \ge 2, \tag{6.16}$$

together with the parameter update law (6.15), is inverse optimal and minimizes the cost functional

$$J_a(u) = \beta \lim_{t\to\infty}\Big\{\big[||\tilde{\theta}||^2_{\Gamma^{-1}} + 2V_1(x(t),\xi(t),\hat{\theta}(t))\big] + \int_0^t \big[l(x,\xi,\hat{\theta}) + u_1^T R(x,\xi,\hat{\theta})u_1\big]\Big\}d\tau$$

for each $\theta \in R^p$, where

$$l(x,\xi,\hat{\theta}) = \beta(\beta-2)(\xi-\alpha)^T R^{-1}(\xi-\alpha) - 2\beta\frac{\partial V_1}{\partial x}\Big[f + F\hat{\theta} + F\Gamma\Big(\frac{\partial V_1}{\partial \hat{\theta}}\Big)^T + g\xi\Big] - 2\beta\frac{\partial V_1}{\partial \xi}\Big[\alpha_1 + F_1\hat{\theta} + F_1\Gamma\Big(\frac{\partial V_1}{\partial \hat{\theta}}\Big)^T\Big].$$

Thus, we conclude that the inverse optimal adaptive control problem for the augmented system (6.11) is also solvable with the smooth dynamic feedback control law (6.16) and the parameter update law (6.15). □

A repeated application of Theorem 6.5 leads to the following result for a class of single-input parametric strict-feedback systems.

Corollary 6.6. *The inverse optimal adaptive control problem for the parametric strict-feedback systems is solvable,*

$$\begin{aligned} \dot{x}_i &= x_{i+1} + \phi_i(x_1,\cdots,x_i)^T\theta, \qquad i = 1,2,\cdots,n-1,\\ \dot{x}_n &= u + \phi_n(x_1,\cdots,x_n)^T\theta. \end{aligned} \tag{6.17}$$

6.2.3 Robust Inverse Optimal Adaptive Control

In Theorems 6.3 and 6.5, we have addressed the inverse optimal adaptive control problem for the zero-disturbance nonlinear system (6.1). We then extend these results to nonlinear uncertain systems with disturbances and proceed to consider the inverse optimal adaptive control problem for the nonlinear uncertain system

$$\dot{x} = f(x) + F(x)\theta + g_1(x)d + g_2(x)u, \tag{6.18}$$

where the state $x \in \mathcal{R}^n$, the control effort $u \in \mathcal{R}^m$ and the disturbances $d \in \mathcal{R}^q$; the mappings $f(x) \in \mathcal{R}^n$, $F(x) \in \mathcal{R}^{n\times p}$, $g_1(x) \in \mathcal{R}^{n\times q}$ and $g_2(x) \in \mathcal{R}^{n\times m}$ are smooth in C^k, $k \geq 1$; $\theta \in \mathcal{R}^p$ is a constant, unknown parameter vector.

Definition 6.4. *The **inverse optimal adaptive gain-assignment problem** for the system (6.18) is solvable if there exist a positive constant β, a class $\mathcal{K}_\infty$ function ρ whose derivative ρ' is also a class $\mathcal{K}_\infty$ function, a positive definite symmetric matrix $R(x,\hat{\theta})$, a smooth nonnegative function $E(x,\hat{\theta}) \geq 0$ for each $\hat{\theta}$, a real-valued function $l(x,\hat{\theta})$ positive definite in x for each $\hat{\theta}$, and a dynamic feedback controller (6.2), (6.3) that is continuous everywhere and minimizes the cost functional*

$$J_a(u) = \sup_{d\in\mathcal{D}} \lim_{t\to\infty} \Big\{\beta||\tilde{\theta}(t)||^2_{\Gamma^{-1}} + E(x(t),\hat{\theta}(t)) + \int_0^t \big[l(x,\hat{\theta}) + u^T R(x,\hat{\theta})u - \rho(||d||)\big]d\tau\Big\}$$

for each $\theta \in \mathcal{R}^p$, where $\mathcal{D}$ is the set of locally bounded functions of x.

Definition 6.4 is analogous to Definition 3.1 in [63] and the difference lies in that the parameter adaptation for θ is considered in Definition 6.4. The next theorem provides a sufficient condition for the solvability of the inverse optimal adaptive gain-assignment problem for the system (6.18) in the sense of Definition 6.4.

Theorem 6.7. *Consider the auxiliary system*

$$\dot{x} = f(x) + F(x)\Big(\theta + \Gamma\Big(\frac{\partial V}{\partial \theta}\Big)^T\Big) + g_1(x)\ell\rho(2||L_{g_1}V||)\frac{(L_{g_1}V)^T}{||L_{g_1}V||^2} + g_2(x)u, \tag{6.19}$$

where $V(x,\theta)$ is a CLF candidate; the function ρ is a class $\mathcal{K}_\infty$ function whose derivative ρ' is also a class $\mathcal{K}_\infty$ function and $\ell\rho$ is defined by (3.28). Suppose that there exists a matrix $R_2(x,\theta) = R_2^T(x,\theta) > 0$ for all $\theta \in \mathcal{R}^p$ such that the feedback control law

$$u = \alpha(x,\theta) = -R_2(x,\theta)^{-1}(L_{g_2}V)^T \tag{6.20}$$

asymptotically stabilizes the auxiliary system (6.19) with respect to $V(x,\theta)$. Then, the dynamic feedback control

$$\begin{aligned} u &= \alpha^*(x,\hat{\theta}) = -\beta R_2(x,\hat{\theta})^{-1}(L_{g_2}V)^T, \quad \forall \beta \geq 2 \\ \dot{\hat{\theta}} &= \Gamma\tau(x,\hat{\theta}) = \Gamma(L_F V)^T \end{aligned} \tag{6.21}$$

solves the inverse optimal adaptive control problem for the nonlinear uncertain system (6.18) by minimizing the cost functional

$$\begin{aligned} J_a(u) = \sup_{d\in\mathcal{D}}\Big\{ \lim_{t\to\infty} \Big[\beta||\tilde{\theta}(t)||^2_{\Gamma^{-1}} + 2\beta V(x(t),\hat{\theta}(t)) \\ + \int_0^t \Big(l(x,\hat{\theta}) + u^T R_2(x,\hat{\theta})u - \beta\lambda\rho(\frac{||d||}{\lambda})\Big)d\tau\Big]\Big\} \end{aligned} \tag{6.22}$$

for any $\lambda \in (0,2]$ and for all $\theta \in \mathcal{R}^p$, where $\mathcal{D}$ is the set of locally bounded functions of x and the state weight $l(x,\hat{\theta})$ is given by

$$l(x,\hat{\theta}) = \beta^2 L_{g_2}V R_2^{-1}(L_{g_2}V)^T - 2\beta L_f V - 2\beta L_F V\Big[\hat{\theta} + \Gamma\Big(\frac{\partial V}{\partial \hat{\theta}}\Big)^T\Big] - \beta\lambda\ell\rho(2||L_{g_1}V||). \tag{6.23}$$

Theorem 6.7 is an important extension of Theorem 3.1 in [63], as the adaptive control problem of uncertain parameters is also considered here to form an inverse optimal adaptive control problem. When $\Gamma = 0$, the parameter θ is assumed known and the problem defined in Definition 6.4 is reduced to a non-adaptive inverse optimal problem, which was already studied in [63]. The proof is based on that of [63, Theorem 3.1], with certain significant modifications for the adaptive case.

Proof. Since the feedback control law $u = \alpha(x,\theta)$ in (6.20) stabilizes the auxiliary system (6.19), it follows from Definition 6.2 that there exists a continuous function $W(x,\theta)$ positive definite in x for each $\theta \in \mathcal{R}^p$ such that

$$L_f V + L_F V\Big[\theta + \Gamma\Big(\frac{\partial V}{\partial \theta}\Big)^T\Big] + \ell\rho(2||L_{g_1}V||) - L_{g_2}V R_2^{-1}(L_{g_2}V)^T \leq -W(x,\theta) \leq 0,$$

which brings

$$l(x,\hat{\theta}) \geq W(x,\hat{\theta}) + \beta(2-\lambda)\ell\rho(2||L_{g_1}V||) + \beta(\beta-2)L_{g_2}VR_2^{-1}\big(L_{g_2}V\big)^T.$$

Since $\beta \geq 2$, $R_2(x,\hat{\theta}) > 0$ and $W(x,\hat{\theta})$ is positive definite, $l(x,\hat{\theta})$ is also positive definite in x for each $\hat{\theta} \in \mathcal{R}^p$. Therefore, the cost functional $J_a(u)$ defined in (6.22) with $l(x,\hat{\theta})$ of (6.23) is a meaningful cost functional, which puts penalties on the state $x(t)$, the control input $u(t)$ and the disturbance $d(t)$.

Substituting $l(x,\hat{\theta})$ into $J_a(u)$ defined in (6.22) and applying the dynamic feedback control law (6.21), along the trajectories of (6.18) we get

$$\begin{aligned}
J_a(u) = \sup_d \Big\{ \lim_{t\to\infty} \Big[& \beta||\tilde{\theta}(t)||^2_{\Gamma^{-1}} + 2\beta V(x(t),\hat{\theta}(t)) \\
& - 2\beta \int_0^t \Big[L_f V + L_F V\theta + L_{g_1}Vd + L_{g_2}Vu - L_F V\tilde{\theta} + L_F V\Gamma\Big(\frac{\partial V}{\partial\hat{\theta}}\Big)^T\Big] d\tau \\
& + \int_0^t \Big(\beta^2 L_{g_2}VR_2^{-1}(L_{g_2}V)^T + 2\beta L_{g_2}Vu + u^T R_2 u\Big) d\tau \\
& + \int_0^t \Big(2\beta L_{g_1}Vd - \beta\lambda\ell\rho(2||L_{g_1}V||) - \beta\lambda\rho(\frac{||d||}{\lambda})\Big) d\tau \Big] \Big\} \\
= \sup_d \Big\{ \lim_{t\to\infty} \Big[& \beta||\tilde{\theta}||^2_{\Gamma^{-1}} + 2\beta V(x(t),\hat{\theta}(t)) - 2\beta\int_0^t \Big(\frac{\partial V}{\partial x}\dot{x} + \frac{\partial V}{\partial\hat{\theta}}\dot{\hat{\theta}} - L_F V\tilde{\theta}\Big) d\tau \\
& + \int_0^t v^T R_2 v d\tau + \int_0^t \Big(2\beta L_{g_1}Vd - \beta\lambda\ell\rho(2||L_{g_1}V||) - \beta\lambda\rho(\frac{||d||}{\lambda})\Big) d\tau \Big] \Big\} \\
= \beta||\tilde{\theta}(0)||^2_{\Gamma^{-1}} & + 2\beta V(x(0),\hat{\theta}(0)) + \int_0^\infty v^T R_2 v d\tau \\
& + \beta \sup_d \Big\{ \int_0^\infty \Big(2L_{g_1}Vd - \lambda\rho'(\frac{||d^*||}{\lambda})\frac{||d^*||}{\lambda} + \lambda\rho(\frac{||d^*||}{\lambda}) - \lambda\rho(\frac{||d||}{\lambda})\Big) d\tau \Big\},
\end{aligned}$$

where $v = u - \alpha^*$ and $d^* = \lambda(\rho')^{-1}(2||L_{g_1}V||)\frac{(L_{g_1}V)^T}{||L_{g_1}V||}$ is the "worst-case" disturbance and we have made use of the property $\ell\rho(r) = r(\rho')^{-1}(r) - \rho((\rho')^{-1}(r))$. (See the proof of Theorem 3.12 and Appendix C.) It was also shown in the proof of Theorem 3.12 that (see also [63, Theorem 3.1])

$$\sup_d \Big\{ \int_0^\infty \Big[2L_{g_1}Vd - \lambda\rho'(\frac{||d^*||}{\lambda})\frac{||d^*||}{\lambda} + \lambda\rho(\frac{||d^*||}{\lambda}) - \lambda\rho(\frac{||d||}{\lambda})\Big] d\tau \Big\} \leq 0$$

and the equal sign "=" is satisfied if and only if $d = d^*$. Hence, the minimum of the cost functional $J_a(u)$ in (6.22) is reached with $u = \alpha^*(x,\hat{\theta})$, and the dynamic feedback control law (6.21) minimizes the cost functional (6.22). The value function of (6.22) is $J_a^*(x) = \beta||\tilde{\theta}(t)||^2_{\Gamma^{-1}} + 2\beta V(x(t),\hat{\theta}(t))$. □

Remark 6.2. The Lyapunov function $V(x,\hat{\theta})$ indeed solves the following family of Hamilton-Jacobi-Isaacs partial differential equation

$$L_f V + L_F V\Big[\hat{\theta} + \Gamma\Big(\frac{\partial V}{\partial\hat{\theta}}\Big)^T\Big] + \frac{\lambda}{2}\ell\rho(2||L_{g_1}V||) - \frac{\beta}{2}L_{g_2}VR_2^{-1}(L_{g_2}V)^T + \frac{l(x,\hat{\theta})}{2\beta} = 0$$

parameterized by $(\beta, \lambda) \in [2, \infty) \times (0, 2]$. It is seen from the proof of Theorem 6.7 that the achieved disturbance attenuation level is

$$\int_0^T \left[l(x, \hat{\theta}) + u^T R_2(x, \hat{\theta}) u\right] \leq \beta\lambda \int_0^T \rho\left(\frac{||d||}{\lambda}\right) d\tau + \beta||\tilde{\theta}(0)||^2_{\Gamma^{-1}} + 2\beta V(x(0), \hat{\theta}(0))$$

for all $T \geq 0$. ⊗

With the inverse optimal adaptive control (6.21), the next theorem establishes that the closed-loop system is integral-input-to-state stable (IISS).

Theorem 6.8. *If the inverse optimal adaptive gain assignment problem is solvable for the system (6.18), then (6.18) is integral-input-to-state stabilizable.*

Proof. Let $\beta = \lambda = 2$. For the adaptive control Lyapunov function

$$V_2(x, \hat{\theta}) = V(x, \hat{\theta}) + \frac{1}{2}\tilde{\theta}^T \Gamma^{-1} \tilde{\theta},$$

applying (6.23), along the solutions of the system (6.18) with the inverse optimal adaptive control law (6.21) we have

$$\begin{aligned} \dot{V}_2 &= L_f V + L_{g_1} V d + L_{g_2} V u + L_F V \theta + \frac{\partial V}{\partial \hat{\theta}} \Gamma (L_F V)^T - \tilde{\theta}^T (L_F V)^T \\ &= -\frac{1}{4} l(x, \hat{\theta}) - L_{g_2} V R_2^{-1} (L_{g_2} V)^T + \rho\left(\frac{||d||}{2}\right). \end{aligned}$$

Since $l(x, \hat{\theta})$ is positive definite in x for each $\hat{\theta} \in \mathcal{R}^p$ and radially unbounded, and $\rho(\cdot)$ is a class $\mathcal{K}_\infty$ function, by Definition 3.11, Remark 3.1 and the results in [4,69], we can conclude that the closed-loop system with the inverse optimal adaptive control (6.21) is integral input-to-state (d-to-x) stable for each θ. □

6.3 Inverse Optimal Adaptive Control for Attitude Tracking Problem

In this section, we present inverse optimal adaptive feedback control laws that solve the attitude tracking control problem of spacecraft. The inverse optimality approach requires the knowledge of a control Lyapunov function and a feedback control law of a particular form. We construct both of them via the method of *backstepping* [35,62].

6.3.1 Problem reformulation via backstepping

Observe that the error system in (4.38)–(4.40) is indeed a nonlinear cascade interconnection, that is, the kinematics subsystem (4.38)–(4.39) is stabilized only indirectly through the angular velocity vector ω_e. Stabilizing control laws for such cascade structures can be efficiently designed using the method of *backstepping*. By this method, ω_e in (4.38)–(4.39) is considered as a *virtual control* input and a control law ω_d is designed

to stabilize the kinematics subsystem. Subsequently, the actual control u is designed to stabilize the dynamics subsystem (4.40) without destabilizing the kinematics subsystem (4.38)–(4.39) by forcing $\omega_e \to \omega_d$.

Step 1. *Control of the kinematics subsystem:* Consider ω_e in the kinematics subsystem (4.38) and (4.39) as a virtual control input and design the control law

$$\omega_d = -K\epsilon, \tag{6.24}$$

where $K \in \mathcal{R}^{3\times 3}$ is symmetric and positive definite. With this control law, the vector ϵ converges to zero asymptotically for all initial conditions $\epsilon(0)$, and the scalar $\eta \to 1$ as $t \to \infty$ whenever the initial condition $\eta(0) \neq -1$.

We first proceed to show that $\eta \to 1$ as $t \to \infty$ whenever $\eta(0) \neq -1$. Let k_1 and k_2 be the minimum and maximum eigenvalues of K, i.e., $k_1 = \lambda_{\min}(K)$ and $k_2 = \lambda_{\max}(K)$. Applying the virtual control law (6.24) to (4.39) and using the constraint condition $\epsilon^T\epsilon + \eta^2 = 1$, we have

$$\frac{1}{2}k_1(1-\eta^2) \leq \dot{\eta} = \frac{1}{2}\epsilon^T K\epsilon \leq \frac{1}{2}k_2(1-\eta^2).$$

By Lemma 2.4 (the comparison principle), it follows that $\eta(t)$ satisfies the following inequalities

$$1 - \frac{2[1-\eta(0)]e^{-k_1 t}}{1+\eta(0)+[1-\eta(0)]e^{-k_1 t}} \leq \eta(t) \leq 1 - \frac{2[1-\eta(0)]e^{-k_2 t}}{1+\eta(0)+[1-\eta(0)]e^{-k_2 t}}$$

for all $t \geq 0$. (The first one is obtained from $\dot{\tilde{\eta}} \leq -\frac{1}{2}k_1(1-\tilde{\eta}^2)$ by letting $\tilde{\eta} = -\eta$.) When $\eta(0) = -1$, it follows that $\eta(t) \equiv -1$ for all $t \geq 0$. Whenever $\eta(0) \neq -1$, we conclude that $\eta(t) > -1$ for all $t \geq 0$ and $\eta(t) > 0$ for all $t \geq \max\{0, \frac{1}{k_1}\ln\frac{1-\eta(0)}{1+\eta(0)}\}$ with $\lim_{t\to\infty}\eta(t) = 1$. In particular, when $k_1 = k_2$ and $\eta(0) \neq -1$, $\eta(t)$ is strictly increasing for all $t \geq 0$, i.e., $\eta(t_1) < \eta(t_2)$ for all $0 \leq t_1 < t_2$.

Applying the fact that $\eta(t) \to 1$ as $t \to \infty$ whenever $\eta(0) \neq -1$, we continue to show the global asymptotic stability of $\epsilon = 0$ under the control law (6.24). We select the following Lyapunov function with a constant $c > 0$ for the kinematics subsystem

$$V_a = c\epsilon^T\epsilon + c(1-\eta)^2 \tag{6.25}$$

whose derivative is

$$\dot{V}_a = c\epsilon^T\omega_d = -c\epsilon^T K\epsilon \leq -ck_1||\epsilon||^2 \leq 0. \tag{6.26}$$

Then the global asymptotic stability of $\epsilon = 0$ follows for all initial conditions $\epsilon(0)$.

Both $(\epsilon, \eta) = (0, +1)$ and $(\epsilon, \eta) = (0, -1)$ stand for exactly the same physical attitude orientation. Therefore, we can conclude that the attitude motion under the control law (6.24) is globally asymptotically stable.

Step 2. *Control of the full rigid-body models:* We consider that the inertia matrix $J \in \mathcal{R}^{3\times 3}$ is constant, but is unknown or poorly known. In this case, we can replace

it with an estimate and update the estimate by an adaptive scheme. To isolate the uncertain parameter, a linear operator $L : \mathcal{R}^3 \to \mathcal{R}^{3\times 6}$ acting on the vector $a = [a_1,\ a_2,\ a_3]^T$ is defined by

$$L(a) = \begin{bmatrix} a_1 & 0 & 0 & 0 & a_3 & a_2 \\ 0 & a_2 & 0 & a_3 & 0 & a_1 \\ 0 & 0 & a_3 & a_2 & a_1 & 0 \end{bmatrix} \tag{6.27}$$

and the parameter vector $\theta \in \mathcal{R}^6$ is defined as

$$\theta := \begin{bmatrix} J_{11} & J_{22} & J_{33} & J_{23} & J_{13} & J_{12} \end{bmatrix}^T, \tag{6.28}$$

then it follows that

$$Ja = L(a)\theta. \tag{6.29}$$

Let $\hat{\theta}$ denote the parameter estimate of θ and $\tilde{\theta}$ be the estimation error defined by

$$\tilde{\theta} = \theta - \hat{\theta}. \tag{6.30}$$

We also adopt the following notations:

$$z = \omega_e - \omega_d = \omega_e + K\epsilon, \tag{6.31}$$
$$u_c = H(\omega_c, \dot{\omega}_c)\hat{\theta}, \tag{6.32}$$
$$u_e = u + u_c = u + H(\omega_c, \dot{\omega}_c)\hat{\theta}, \tag{6.33}$$
$$H(\omega_c, \dot{\omega}_c) = -\omega_c^{\times} L(\omega_c) - L(\dot{\omega}_c) \tag{6.34}$$

Then it follows that

$$J\dot{z} = \left[F(\epsilon, \eta, \omega_e, \omega_c, \dot{\omega}_c) + G(\epsilon, \eta, \omega_e)\right]\theta + H(\omega_c, \dot{\omega}_c)\tilde{\theta} + u_e + d, \tag{6.35}$$
$$\dot{\epsilon} = \tfrac{1}{2}[\eta I_3 + \epsilon^{\times}](z - K\epsilon), \tag{6.36}$$
$$\dot{\eta} = -\tfrac{1}{2}\epsilon^T(z - K\epsilon), \tag{6.37}$$

where the matrix-valued functions $F(\epsilon, \eta, \omega_e, \omega_c, \dot{\omega}_c) \in \mathcal{R}^{3\times 6}$ and $G(\epsilon, \eta, \omega_e) \in \mathcal{R}^{3\times 6}$ are given by

$$\begin{aligned} F = {} & L(\omega_e^{\times} C\omega_c) - L(C_1\dot{\omega}_c) - (\omega_e + C\omega_c)^{\times} L(\omega_e) - \omega_c^{\times} L(C_1\omega_c) \\ & - (\omega_e + C_1\omega_c)^{\times} L(C\omega_c), \end{aligned} \tag{6.38}$$
$$G = \tfrac{1}{2} L(K(\eta I_3 + \epsilon^{\times})\omega_e), \tag{6.39}$$

$C(\epsilon, \eta) \in \mathcal{R}^{3\times 3}$ is defined by (4.35), and $C_1(\epsilon, \eta) \in \mathcal{R}^{3\times 3}$ is given by

$$C_1(\epsilon, \eta) = C(\epsilon, \eta) - I_3 = -2\epsilon^T\epsilon I_3 + 2\epsilon\epsilon^T - 2\eta\epsilon^{\times}. \tag{6.40}$$

Thus, the stabilizing control problem of ω_e in (4.40) with the control input u is trans-

formed into the control problem of stabilizing z defined in (6.35) with an auxiliary control input u_e. When $z \to 0$, we have that $\omega_e \to \omega_d$ and then the kinematics subsystem (6.36) and (6.37) is asymptotically stable as analyzed in Step 1, that is, $\epsilon \to 0$ and subsequently $\omega_e \to 0$ as $t \to \infty$ according to (6.31).

The control effort u_c in (6.32) is called the adaptive feedforward compensation, which is independent of the tracking errors ϵ and ω_e. Once u_e is designed, we can also obtain the actual control input $u = u_e - u_c$ by (6.33).

In summary, we need to design a dynamic feedback control law

$$u_e = \alpha(\epsilon, \eta, \omega_e, \hat{\theta}, \omega_c, \dot{\omega}_c)$$

and an adaptive parameter update law

$$\dot{\hat{\theta}} = \Gamma\tau(\epsilon, \eta, \omega_e, \hat{\theta}, \omega_c, \dot{\omega}_c)$$

to stabilize the full-model system (6.35), (6.36) and (6.37) with an uncertain parameter vector $\theta \in \mathcal{R}^6$.

6.3.2 Control design: zero-disturbance case

First, we consider the zero-disturbance case, $d = 0$, which is a special case, but has some interesting and important properties such as optimality, asymptotic property and global convergence. Compared to the nonzero-disturbance case discussed in Section 6.3.3, under the inverse optimal adaptive controller proposed in Theorem 6.10, the attitude tracking problem without external disturbances is solvable asymptotically in the sense of Definition 4.2 with a global convergence of tracking errors to zero for all initial conditions. Next theorem presents an adaptive feedback controller that achieves globally asymptotic attitude tracking in the sense of Definition 4.2.

Theorem 6.9. *Suppose that Assumption 4.1 is satisfied and the external disturbance $d(t)$ in (6.35) is $d \equiv 0$. Let the constant matrices $K \in \mathcal{R}^{3\times3}$, $K_1 \in \mathcal{R}^{3\times3}$ and $\Gamma \in \mathcal{R}^{6\times6}$ be symmetric and positive definite and let $c > 0$. Then the dynamic feedback control*

$$u_e = \alpha(\epsilon, \eta, \omega_e, \hat{\theta}, \omega_c, \dot{\omega}_c) = -R(\epsilon, \eta, \omega_e, \hat{\theta}, \omega_c, \dot{\omega}_c)^{-1}(\omega_e + K\epsilon), \tag{6.41}$$

$$\dot{\hat{\theta}} = \Gamma[F(\epsilon, \eta, \omega_e, \omega_c, \dot{\omega}_c) + G(\epsilon, \eta, \omega_e) + H(\omega_c, \dot{\omega}_c)]^T(\omega_e + K\epsilon), \tag{6.42}$$

with $R(\epsilon, \eta, \omega_e, \hat{\theta}, \omega_c, \dot{\omega}_c)$ satisfying

$$R^{-1}(\epsilon, \eta, \omega_e, \hat{\theta}, \omega_c, \dot{\omega}_c) = K_1 + \tfrac{1}{2}\Psi_1^T\Psi_1 + \tfrac{1}{2}\bar{\Psi}_2 K_1^{-1}\bar{\Psi}_2, \tag{6.43}$$

solves the adaptive attitude tracking control problem asymptotically, that is, $\epsilon \to 0$ and $\omega_e \to 0$ as $t \to \infty$. Furthermore, $\hat{\theta}$ is bounded for all $t \geq 0$ and $\dot{\hat{\theta}} \to 0$ as $t \to \infty$.

Here, the symmetric matrix-valued function $\bar{\Psi}_2(\epsilon, \eta, \omega_e, \hat{\theta}) \in \mathcal{R}^{3\times3}$ is given by

$$\bar{\Psi}_2(\epsilon, \eta, \omega_e, \hat{\theta}) = \Psi_2^T(\epsilon, \eta, \omega_e, \hat{\theta}) + \Psi_2(\epsilon, \eta, \omega_e, \hat{\theta});$$

the smooth functions $\Psi_1(\epsilon,\eta,\omega_e,\hat{\theta},\omega_c,\dot{\omega}_c) \in \mathcal{R}^{3\times 3}$, $\Psi_2(\epsilon,\eta,\omega_e,\hat{\theta}) \in \mathcal{R}^{3\times 3}$, $C_2(\epsilon,\eta,\omega_c) \in \mathcal{R}^{3\times 3}$ *and* $C_3(\epsilon,\eta,\dot{\omega}_c) \in \mathcal{R}^{3\times 3}$ *are defined by*

$$\begin{aligned}\Psi_1^T = c^{-1/2}\big[&(\omega_e + C\omega_c)^\times \hat{J} + \hat{J}(C\omega_c)^\times - (\hat{J}C\omega_c)^\times - \tfrac{1}{2}\hat{J}K(\eta I_3 + \epsilon^\times)\\ &+ cK^{-1} + (\hat{J}C\omega_c)^\times C_2K^{-1} - \omega_c^\times \hat{J}C_2K^{-1} - \hat{J}C_3K^{-1}\big]K^{1/2}, \qquad (6.44)\\ \Psi_2 = \tfrac{1}{4}\hat{J}K(\eta I_3 + \epsilon^\times) - \tfrac{1}{2}\omega_e^\times \hat{J}, \qquad &(6.45)\\ C_2 = 2\epsilon^T\omega_c I_3 - 2\omega_c\epsilon^T + 2\eta\omega_c^\times, \qquad &(6.46)\\ C_3 = 2\epsilon^T\dot{\omega}_c I_3 - 2\dot{\omega}_c\epsilon^T + 2\eta\dot{\omega}_c^\times; \qquad &(6.47)\end{aligned}$$

the matrix $\hat{J}$ *is of the form (4.30), obtained from the estimate* $\hat{\theta}$*; the matrices* $H(\omega_c,\dot{\omega}_c)$, $F(\epsilon,\eta,\omega_e,\omega_c,\dot{\omega}_c)$ *and* $G(\epsilon,\eta,\omega_e)$ *are given as in (6.34), (6.38) and (6.39) respectively.*

Proof. Define an adaptive control Lyapunov function candidate for the nonlinear system (6.35)(6.36) and (6.37) with an unknown parameter θ as follows:

$$V_2 = c\epsilon^T\epsilon + c(1-\eta)^2 + \tfrac{1}{2}z^TJz + \tfrac{1}{2}\tilde{\theta}^T\Gamma^{-1}\tilde{\theta}. \qquad (6.48)$$

Along the trajectories of (6.35), (6.36), (6.37) and (6.42) we have

$$\begin{aligned}\dot{V}_2 &= 2c\epsilon^T\dot{\epsilon} - 2c(1-\eta)\dot{\eta} + z^TJ\dot{z} - \tilde{\theta}^T\Gamma^{-1}\dot{\hat{\theta}}\\ &= c\epsilon^T(z - K\epsilon) + z^T\big[u_e + (F+G)\hat{\theta}\big] + \tilde{\theta}^T\big[(F+G+H)^Tz - \tau\big]\\ &= -c\epsilon^TK\epsilon + z^T\big[c\epsilon + u_e + (F+G)\hat{\theta}\big]. \qquad (6.49)\end{aligned}$$

To render $\dot{V}_2$ negative, one natural choice like the adaptive feedback control laws in [1, 125] is

$$u_e = -K_2z - (F+G)\hat{\theta} - c\epsilon,$$

which cancels all the nonlinear terms in the right-hand side of (6.49), where $K_2 \in \mathcal{R}^{3\times 3}$ is a positive definite symmetric matrix. However, this feedback control law based on nonlinearity cancellation is not guaranteed to be inverse optimal in general. In fact, some information in these nonlinear terms is useful to facilitate us to design an optimal controller. To solve the attitude tracking control problem with an inverse optimal adaptive controller, we employ the "nonlinear damping" technique as follows.

Suppose that the matrices $C_2(\epsilon,\eta,\omega_c)$ and $C_3(\epsilon,\eta,\dot{\omega}_c)$ are defined as in (6.46) and (6.47) respectively such that

$$C_1\omega_c = C_2\epsilon, \quad C_1\dot{\omega}_c = C_3\epsilon.$$

From (6.28) and (6.29), it follows that $L(a)\hat{\theta} = \hat{J}a$ for all $a \in \mathcal{R}^3$. Applying the matrix $F(\epsilon,\eta,\omega_e,\omega_c,\dot{\omega}_c)$ in (6.38), the matrix $G(\epsilon,\eta,\omega_e)$ in (6.39) and the properties of $a^\times$ in Lemma 4.1, we can rewrite (6.49) as

$$\begin{aligned}\dot{V}_2 = -c\epsilon^TK\epsilon + z^T\big[&c\epsilon + u_e - (\omega_e + C\omega_c)^\times\hat{J}(z - K\epsilon) + (\hat{J}C\omega_c)^\times(z - K\epsilon) - \hat{J}C_1\dot{\omega}_c\\ &- \hat{J}(C\omega_c)^\times(z - K\epsilon) + \tfrac{1}{2}\hat{J}K(\eta I_3 + \epsilon^\times)(z - K\epsilon) - \omega_c^\times\hat{J}C_1\omega_c + (\hat{J}C\omega_c)^\times C_1\omega_c\big]\end{aligned}$$

$$= -c\epsilon^T K\epsilon + z^T\Big\{u_e + \Big[cK^{-1} + (\omega_e + C\omega_c)^\times \hat{J} - (\hat{J}C\omega_c)^\times - \frac{1}{2}\hat{J}K(\eta I_3 + \epsilon^\times)$$
$$+ \hat{J}(C\omega_c)^\times + (\hat{J}C\omega_c)^\times C_2K^{-1} - \omega_c^\times \hat{J}C_2K^{-1} - \hat{J}C_3K^{-1}\Big]K\epsilon$$
$$+ \Big[\frac{1}{2}\hat{J}K(\eta I_3 + \epsilon^\times) - \omega_e^\times \hat{J}\Big]z\Big\} + z^T H_1 z,$$

where $H_1 = (\hat{J}\omega_c)^\times - (C\omega_c)^\times \hat{J} - \hat{J}(C\omega_c)^\times$. It can be easily shown that $H_1 = -H_1^T$ due to the fact that $\hat{J}$ is symmetric and $(\hat{J}\omega_c)^\times$ and $(C\omega_c)^\times$ are skew-symmetric. Therefore, $z^T H_1 z = 0$ for all $z \in \mathcal{R}^3$.

Introducing the smooth matrices $\Psi_1(\epsilon, \eta, \omega_e, \hat{\theta}, \omega_c, \dot{\omega}_c) \in \mathcal{R}^{3\times 3}$ as in (6.44) and $\Psi_2(\epsilon, \eta, \omega_e, \hat{\theta}) \in \mathcal{R}^{3\times 3}$ as in (6.45) and letting $\bar{\Psi}_2 = \Psi_2^T + \Psi_2$, we have

$$\dot{V}_2 = -c\epsilon^T K\epsilon + z^T u_e + \sqrt{c}z^T\Psi_1^T K^{1/2}\epsilon + z^T\bar{\Psi}_2 z. \tag{6.50}$$

Then, the choice

$$u_e = \alpha(\epsilon, \eta, \omega_e, \hat{\theta}, \omega_c, \dot{\omega}_c) = -R(\epsilon, \eta, \omega_e, \hat{\theta}, \omega_c, \dot{\omega}_c)^{-1}z$$

with $R(\epsilon, \eta, \omega_e, \hat{\theta}, \omega_c, \dot{\omega}_c)$ satisfying (6.43) renders

$$\dot{V}_2 = -\frac{c}{2}\epsilon^T K\epsilon - \frac{1}{2}z^T K_1 z - \frac{1}{2}\Big\|\sqrt{c}K^{1/2}\epsilon - \Psi_1 z\Big\|^2 - \frac{1}{2}z^T(K_1 - \bar{\Psi}_2)^T K_1^{-1}(K_1 - \bar{\Psi}_2)z$$
$$\leq -\frac{c}{2}\epsilon^T K\epsilon - \frac{1}{2}z^T K_1 z, \tag{6.51}$$

which shows that $\dot{V}_2$ is negative semidefinite. Since $K_1 \in \mathcal{R}^{3\times 3}$ is a positive definite symmetric matrix, the smooth matrix $R(\epsilon, \eta, \omega_e, \hat{\theta}, \omega_c, \dot{\omega}_c) \in \mathcal{R}^{3\times 3}$ is also positive definite and symmetric. As $V_2(\epsilon, \eta, \omega_e, \tilde{\theta})$ is nonincreasing and bounded below, i.e., for all $t \geq 0$,

$$0 \leq V_2(\epsilon(t), \eta(t), \omega_e(t), \tilde{\theta}(t)) \leq V_2(\epsilon(0), \eta(0), \omega_e(0), \tilde{\theta}(0)),$$

and θ is a constant, it follows that the signals $\epsilon(t)$, $\eta(t)$, $\omega_e(t)$, $z(t)$, $\tilde{\theta}(t)$ and $\hat{\theta}(t)$ are all bounded for all $t \geq 0$. Also, $\omega_c(t)$ and $\dot{\omega}_c(t)$ are bounded by Assumption 4.1. Therefore, $H(\omega_c, \dot{\omega}_c)$, $G(\epsilon, \eta, \omega_e)$ and $F(\epsilon, \eta, \omega_e, \omega_c, \dot{\omega}_c)$ are bounded and consequently $\dot{\epsilon}(t)$ and $\dot{z}(t)$ are bounded for all $t \geq 0$, which implies that $\epsilon(t)$ and $z(t)$ are continuous functions. Integrating both sides of (6.51) with respect to t from 0 to ∞ and applying $V_2(\epsilon, \eta, \omega_e, \tilde{\theta}) \geq 0$, we have

$$\int_0^\infty (c\epsilon^T K\epsilon + z^T K_1 z)dt \leq 2V_2(\epsilon(0), \eta(0), \omega_e(0), \tilde{\theta}(0)).$$

Using the *Barbalat's Lemma* 2.2, we conclude that $\epsilon \to 0$ and $z \to 0$ as $t \to \infty$. As a result, $\omega_e \to 0$ as $t \to \infty$. Hence, the dynamic feedback control law (6.41) and the adaptive parameter update law (6.42) stabilize the attitude error system (4.38), (4.39) and (6.35) with an uncertain parameter θ and zero external disturbance, $d = 0$, and thus the adaptive attitude tracking control problem is solved and asymptotic tracking

is achieved with the tracking errors ϵ, ω_e converging to zeros.

As the matrices $H(\omega_c, \dot{\omega}_c)$, $G(\epsilon, \eta, \omega_e)$ and $F(\epsilon, \eta, \omega_e, \omega_c, \dot{\omega}_c)$ are bounded and $z \to 0$, it follows that $\dot{\hat{\theta}} \to 0$ as $t \to \infty$, which means that there exists a finite constant limit for $\hat{\theta}$ as $t \to \infty$, i.e., $\lim_{t\to\infty} \hat{\theta}(t) = \bar{\theta}$ for a finite constant $\bar{\theta}$. □

Remark 6.3. In the absence of external disturbances, $d = 0$, both $(\epsilon, \eta, \omega_e, \tilde{\theta}) = (0, \pm 1, 0, 0)$ are the equilibrium points of the system (6.35), (6.36), (6.37), and (6.42), which describes the adaptive attitude tracking control problem. Both of them stand for exactly the same physical attitude orientation. However, it was shown in [125] that the point $(\epsilon, \eta, \omega_e, \tilde{\theta})_e = (0, -1, 0, 0)$ is an unstable equilibrium point. On the other hand, it can be seen from the proof of Theorem 6.9 that the equilibrium point $(\epsilon, \eta, \omega_e, \tilde{\theta})_e = (0, 1, 0, 0)$ is uniformly stable [102, Theorem 4.1] under the dynamic adaptive control laws (6.41) and (6.42). ⊗

Remark 6.4. Under the assumption that $d = 0$ and with the control laws (6.41) and (6.42), the tracking errors ϵ and ω_e converge to zeros asymptotically, which ensure that the attitude tracking is achieved with a global convergence for any initial conditions. As analyzed in Step 1, $z \to 0$ implies that $\omega_e \to \omega_d$ as $t \to \infty$. The parameter update law (6.42) represents a scheme for adjusting the adaptive parameter $\hat{\theta}$. Although the derivative value of the adaptive parameter $\dot{\hat{\theta}} \to 0$ as $t \to \infty$, $\tilde{\theta} = \theta - \hat{\theta}$ does not necessarily converge to zero as $t \to \infty$. ⊗

Replacing K by $k_1 I_3$ in (6.42), R^{-1} by $k_2 I_3$ and K by $k_3 I_3$ in (6.41), where the scalars $k_1, k_2, k_3 > 0$, and omitting some high-order terms in the states ϵ and ω_e, we obtain a simplified adaptive attitude tracking controller as those in [1, 125]:

$$\begin{aligned} \dot{\hat{\theta}} &= \Gamma H(\omega_c, \dot{\omega}_c)^T(\omega_e + k_1\epsilon) \\ u_e &= -k_2(\omega_e + k_3\epsilon) \end{aligned} \tag{6.52}$$

Using the control Lyapunov function

$$V = k_2(k_1 + k_3)[(1-\eta)^2 + \epsilon^T\epsilon] + k_1\epsilon^T J\omega_e + \frac{1}{2}\omega_e^T J\omega_e + \frac{1}{2}\tilde{\theta}^T\Gamma^{-1}\tilde{\theta}$$

and the Schwartz inequality

$$|w^T J(\eta I_3 \pm \epsilon^\times)w| \le ||J|| \cdot ||w||^2,$$

and making full use of the properties of $a^\times$ in Lemma 4.1, we have the following derivative of $V(x)$ along the solutions of the system (6.35), (6.36), (6.37) and (6.42):

$$\begin{aligned} \dot{V} &= k_2(k_1 + k_3)\epsilon^T\omega_e + (\omega_e + k_1\epsilon)^T(F\theta + u_e) + \frac{1}{2}k_1\omega_e^T J(\eta I_3 + \epsilon^\times)\omega_e \\ &= -k_2||\omega_e||^2 - k_1k_2k_3||\epsilon||^2 + \frac{1}{2}k_1\omega_e^T J(\eta I_3 + \epsilon^\times)\omega_e + (\omega_e + k_1\epsilon)^T\big[J\omega_e^\times C\omega_c \\ &\quad - (\omega_e + C\omega_c)^\times J\omega_e - (\omega_e + C_2\epsilon)^\times JC\omega_c - \omega_c^\times JC_2\epsilon - JC_3\epsilon\big] \end{aligned}$$

$$
\begin{aligned}
&= -k_2||\omega_e||^2 + \frac{k_1}{2}\omega_e^T J(\eta I_3 - \epsilon^\times)\omega_e + \omega_e^T\big[(JC\omega_c)^\times C_2 - \omega_c^\times JC_2 - JC_3\big]\epsilon \\
&\quad + k_1\epsilon^T\big[(JC\omega_c)^\times - J(C\omega_c)^\times - (C\omega_c)^\times J\big]\omega_e - k_1k_2k_3||\epsilon||^2 \\
&\quad + k_1\epsilon^T\big[(JC\omega_c)^\times C_2 - \omega_c^\times JC_2 - JC_3\big]\epsilon \\
&\le -\begin{bmatrix}||\omega_e|| \\ ||\epsilon||\end{bmatrix}^T\begin{bmatrix}k_2 - \frac{1}{2}k_1\lambda_j & -\frac{1}{2}\lambda_j(2\mu\lambda_{c2} + \lambda_{c3} + 3\mu k_1) \\ -\frac{1}{2}\lambda_j(2\mu\lambda_{c2} + \lambda_{c3} + 3\mu k_1) & k_1k_2k_3 - k_1\lambda_j(2\mu\lambda_{c2} + \lambda_{c3})\end{bmatrix}\begin{bmatrix}||\omega_e|| \\ ||\epsilon||\end{bmatrix}
\end{aligned}
$$

where λ_j is the largest eigenvalue of J, $\lambda_{c2} = \sup\{||C_2(\epsilon(t), \eta(t), \omega_c(t))|| : \forall t \ge 0\}$, $\lambda_{c3} = \sup\{||C_3(\epsilon(t), \eta(t), \dot{\omega}_c(t))|| : \forall t \ge 0\}$, $\mu = \sup\{||\omega_c(t)|| : \forall t \ge 0\}$ and C_2, C_3 are defined by (6.46) and (6.47) respectively. If let

$$
\begin{aligned}
&2k_2 - k_1\lambda_j > 0, \\
&k_2k_3 - \lambda_j(2\mu\lambda_{c2} + \lambda_{c3}) > 0, \\
&4(k_2 - \tfrac{1}{2}k_1\lambda_j)[k_1k_2k_3 - k_1\lambda_j(2\mu\lambda_{c2} + \lambda_{c3})] - \lambda_j^2(3\mu k_1 + 2\mu\lambda_{c2} + \lambda_{c3})^2 > 0,
\end{aligned}
$$

then $\dot{V} < 0$. Thus, asymptotic attitude tracking is achieved for this simplified controller (6.52). From the foregoing derivations, we see that the adaptive attitude tracking control laws (6.41) and (6.42) relax these constraints on the gains of the simplified controller (6.52) and allow the gains K and K_1 to be some matrices rather than some scalars, hence the designer has much more freedom in selecting K and K_1. Furthermore, knowledge of the largest eigenvalue λ_j of the inertia matrix J is not required in designing the controller (6.41)(6.42). In fact, few priori information of the inertia matrix J is required in designing the dynamic feedback controller (6.41)(6.42) and the inverse optimal adaptive controllers in Theorems 6.10 and 6.11.

With the dynamic feedback control law (6.41) (6.42) and by applying Theorems 6.3 and 6.5, we can easily construct a dynamic feedback control law that solves the inverse optimal adaptive control problem for the spacecraft attitude tracking by the following theorem:

Theorem 6.10. *Suppose that the external disturbance $d \equiv 0$ and Assumption 4.1 is satisfied. Together with the adaptive parameter update law (6.42), the dynamic feedback control law*

$$
u_e = \alpha^*(\epsilon, \eta, \omega_e, \hat{\theta}, \omega_c, \dot{\omega}_c) = \beta\alpha(\epsilon, \eta, \omega_e, \hat{\theta}, \omega_c, \dot{\omega}_c) = -\beta R^{-1}(\omega_e + K\epsilon), \tag{6.53}
$$

with any $\beta \ge 2$, solves the inverse optimal control problem for the attitude tracking control system (6.35), (6.36) and (6.37) by minimizing the cost functional

$$
J_a = \beta\lim_{t\to\infty}\Big(||\tilde{\theta}(t)||^2_{\Gamma^{-1}} + 4c[1 - \eta(t)]\Big) + \int_0^\infty \Big(l(\epsilon, \eta, \omega_e, \hat{\theta}, \omega_c, \dot{\omega}_c) + u_e^T R u_e\Big)dt \tag{6.54}
$$

for each $\theta \in R^6$, where the state weight $l(\epsilon, \eta, \omega_e, \hat{\theta}, \omega_c, \dot{\omega}_c)$ is defined by

$$
\begin{aligned}
l(\epsilon, \eta, \omega_e, \hat{\theta}, \omega_c, \dot{\omega}_c) &= -2\beta\big[c\epsilon^T\omega_e + (\omega_e + K\epsilon)^T(F(\epsilon, \eta, \omega_e, \omega_c, \dot{\omega}_c) + G(\epsilon, \eta, \omega_e))\hat{\theta}\big] \\
&\quad + \beta^2(\omega_e + K\epsilon)^T R(\epsilon, \eta, \omega_e, \hat{\theta}, \omega_c, \dot{\omega}_c)^{-1}(\omega_e + K\epsilon),
\end{aligned} \tag{6.55}
$$

and $R(\epsilon,\eta,\omega_e,\hat{\theta},\omega_c,\dot{\omega}_c)$ *is defined by (6.43);* $\Gamma \in \mathcal{R}^{6\times 6}$ *is symmetric and positive definite;* $H(\omega_c,\dot{\omega}_c)$, $F(\epsilon,\eta,\omega_e,\omega_c,\dot{\omega}_c)$ *and* $G(\epsilon,\eta,\omega_e)$ *are given as in (6.34), (6.38) and (6.39) respectively.*

Proof. From the proof of Theorem 6.9, we have that

$$c\epsilon^T\omega_e + z^T[(F+G)\hat{\theta} - R^{-1}z] \leq -W(\epsilon,\eta,\omega_e)$$

with $W(\epsilon,\eta,\omega_e) = \frac{c}{2}\epsilon^T K\epsilon + \frac{1}{2}z^T K_1 z$ positive definite in ϵ and z, which implies that

$$l(\epsilon,\eta,\omega_e,\hat{\theta},\omega_c) \geq 2\beta W(\epsilon,\eta,\omega_e) + \beta(\beta-2)z^T R^{-1}z,$$

from which it is observed that $l(\epsilon,\eta,\omega_e,\hat{\theta},\omega_c,\dot{\omega}_c)$ is positive definite in ϵ and ω_e, and positive whenever $(\epsilon,\omega_e) \neq (0,0)$ for each $\hat{\theta} \in \mathcal{R}^6$. Therefore, the cost functional $J_a(u)$ in (6.54) is a meaningful cost functional, penalizing the tracking errors ϵ and ω_e as well as the control effort u_e.

Substituting $l(\epsilon,\eta,\omega_e,\hat{\theta},\omega_c,\dot{\omega}_c)$ in (6.55), $z = \omega_e + K\epsilon$ and

$$v = u_e - \alpha^* = u_e - \beta\alpha = u_e + \beta R^{-1}z$$

into the cost functional $J_a(u)$ in (6.54) and applying the fact that $2(1-\eta) = ||\epsilon||^2 + (1-\eta)^2$, we have the following expression of the cost functional $J_a(u)$ along the solutions of the attitude tracking error system (6.35), (6.36), (6.37) and the adaptive parameter update law (6.42):

$$\begin{aligned}
J_a &= \beta \lim_{t\to\infty}\Big(||\tilde{\theta}(t)||^2_{\Gamma^{-1}} + 4c[1-\eta(t)]\Big) + \int_0^\infty \Big\{\beta^2 z^T R^{-1}z - 2\beta z^T(F+G)\hat{\theta} \\
&\quad - 2\beta c\epsilon^T\omega_e + (v-\beta R^{-1}z)^T R(v-\beta R^{-1}z)\Big\}dt \\
&= \beta \lim_{t\to\infty}\Big(||\tilde{\theta}(t)||^2_{\Gamma^{-1}} + 4c[1-\eta(t)]\Big) + \int_0^\infty v^T R v dt \\
&\quad - 2\beta\int_0^\infty \Big\{c\epsilon^T\omega_e + z^T[(F+G)\theta + H\tilde{\theta} + u_e] - z^T(F+G+H)\tilde{\theta}\Big\}dt \\
&\quad + 2\beta\int_0^\infty \Big\{z^T(v-\beta R^{-1}z) + \beta z^T R^{-1}z - v^T z\Big\}dt \\
&= \beta \lim_{t\to\infty}\Big(||\tilde{\theta}(t)||^2_{\Gamma^{-1}} + 4c[1-\eta(t)]\Big) \\
&\quad - 2\beta\int_0^\infty \frac{d}{dt}\Big(c(1-\eta)^2 + c\epsilon^T\epsilon + \frac{1}{2}z^T Jz + \frac{1}{2}\tilde{\theta}^T\Gamma^{-1}\tilde{\theta}\Big)dt + \int_0^\infty v^T R v dt \\
&= \beta||\tilde{\theta}(0)||^2_{\Gamma^{-1}} + 4c\beta[1-\eta(0)] + \beta z(0)^T Jz(0) - \beta\lim_{t\to\infty} z(t)^T Jz(t) + \int_0^\infty v^T R v dt.
\end{aligned}$$

Substituting $u_e = \beta\alpha(\epsilon,\eta,\omega_e,\hat{\theta},\omega_c,\dot{\omega}_c)$ into $\dot{V}_2$ in (6.50), we can conclude that the dynamic feedback control law (6.53) and the adaptive parameter update law (6.42) also solve the adaptive attitude tracking problem of the system (6.35), (6.36) and (6.37), i.e., $\lim_{t\to\infty}\epsilon(t) = 0$, $\lim_{t\to\infty} z(t) = 0$ and $\lim_{t\to\infty}\omega_e(t) = 0$. It follows that $\lim_{t\to\infty} z(t)^T Jz(t) = 0$. Hence, we conclude that the minimum of the cost functional

$J_a(u_e)$ is reached only if $v = 0$, that is, the control law $u_e = \alpha^* = \beta\alpha$ in (6.53) is inverse optimal and minimizes the cost functional (6.54). The value function of (6.54) is $J_a^*(\epsilon, \eta, \omega_e, \tilde{\theta}) = 2\beta V_2(\epsilon, \eta, \omega_e, \tilde{\theta})$. □

When the external disturbance $d(t)$ is assumed zero, under the adaptive feedback control laws (6.42) and (6.53), the attitude tracking errors ϵ and ω_e converge to zeros asymptotically for any initial conditions, which ensure that asymptotic attitude tracking is achieved with a global convergence.

Remark 6.5. The parameter $\beta \geq 2$ in Theorem 6.10 represents a degree of freedom for the design. From the proof of Theorem 6.10, we can also obtain an $\mathcal{L}_2$ bound on the attitude tracking errors ϵ, ω_e and the control efforts u_e for the inverse optimal adaptive attitude tracking control laws (6.42) and (6.53) by the following inequality

$$\int_0^\infty \left[c\epsilon^T K\epsilon + z^T K_1 z + \frac{2(\beta-1)}{\beta^2} u_e^T R u_e\right] dt \leq ||\tilde{\theta}(0)||^2_{\Gamma^{-1}} + 4c[1-\eta(0)] + ||z(0)||^2_J,$$

which implies that the attitude tracking errors ϵ, $\omega_e \in \mathcal{L}_2[0, \infty)$. ⊗

6.3.3 Control design: with external disturbances

In Theorem 6.10, we presented an inverse optimal adaptive control law to solve the adaptive attitude tracking control problem without external disturbances, $d = 0$. When the external disturbance $d(t)$ exists, employing the inverse optimal approach and *Theorems 6.3, 6.5* and *6.7*, we can present a dynamic feedback control law that solves a robust inverse optimal assignment problem by the following theorem.

Theorem 6.11. *Suppose that Assumption 4.1 is satisfied. Let the constant matrices $K \in \mathcal{R}^{3\times3}$, $K_1 \in \mathcal{R}^{3\times3}$ and $\Gamma \in \mathcal{R}^{6\times6}$ be symmetric and positive definite, and $c > 0$. Suppose the matrices $H(\omega_c, \dot{\omega}_c)$, $F(\epsilon, \eta, \omega_e, \omega_c, \dot{\omega}_c)$, $G(\epsilon, \eta, \omega_e)$ and $\Psi_1(\epsilon, \eta, \omega_e, \hat{\theta}, \omega_c, \dot{\omega}_c)$ are as defined in (6.34), (6.38), (6.39) and (6.44) respectively. The matrix $\Psi_2(\epsilon, \eta, \omega_e, \hat{\theta})$ of (6.45) is redefined as*

$$\Psi_2(\epsilon, \eta, \omega_e, \hat{\theta}) = \frac{1}{4}\hat{J}(\eta I_3 + \epsilon^\times) - \frac{1}{2}\omega_e^\times \hat{J} + \frac{1}{2\gamma^2} I_3. \tag{6.56}$$

for some given $\gamma > 0$. Then the state-feedback control

$$u_e = \alpha(\epsilon, \eta, \omega_e, \hat{\theta}, \omega_c, \dot{\omega}_c) = -R(\epsilon, \eta, \omega_e, \hat{\theta}, \omega_c, \dot{\omega}_c)^{-1}(\omega_e + K\epsilon), \tag{6.57}$$

together with the adaptive parameter update law (6.42), globally adaptively stabilizes an auxiliary system that consists of (6.36), (6.37) and the following equation

$$J\dot{z} = [F(\epsilon, \eta, \omega_e, \omega_c, \dot{\omega}_c) + G(\epsilon, \eta, \omega_e)]\theta + H(\omega_c, \dot{\omega}_c)\tilde{\theta} + u_e + z/\gamma^2 \tag{6.58}$$

with respect to the adaptive control Lyapunov function

$$V_2(\epsilon, \eta, \omega_e, \tilde{\theta}) = c\epsilon^T\epsilon + c(1-\eta)^2 + \frac{1}{2}z^T J z + \frac{1}{2}\tilde{\theta}^T\Gamma^{-1}\tilde{\theta},$$

that is, $\epsilon \to 0$ and $\omega_e \to 0$ as $t \to \infty$ for all initial conditions. Then, the dynamic feedback control law

$$\begin{aligned} u_e &= \alpha^*(\epsilon, \eta, \omega_e, \hat{\theta}, \omega_c, \dot{\omega}_c) = \beta R(\epsilon, \eta, \omega_e, \hat{\theta}, \omega_c, \dot{\omega}_c)^{-1}(\omega_e + K\epsilon), \quad \forall \beta \geq 2, \\ \dot{\hat{\theta}} &= \Gamma[F(\epsilon, \eta, \omega_e, \omega_c, \dot{\omega}_c) + G(\epsilon, \eta, \omega_e) + H(\omega_c, \dot{\omega}_c)]^T(\omega_e + K\epsilon) \end{aligned} \tag{6.59}$$

solves an adaptive inverse optimal control problem for the attitude tracking control system (6.35), (6.36), (6.37) and (6.42) by minimizing the cost functional

$$\begin{aligned} J_a(u_e) = \sup_{d \in \mathcal{D}} \Big\{ \lim_{t \to \infty} \big[& 2\beta V_2(\epsilon(t), \eta(t), \omega_e(t), \tilde{\theta}(t)) \\ & + \int_0^t \Big(l(\epsilon, \eta, \omega_e, \hat{\theta}, \omega_c, \dot{\omega}_c) + u_e^T R u_e - \frac{\beta \gamma^2}{2} ||d||^2 \Big) dt \big] \Big\} \end{aligned} \tag{6.60}$$

for each $\theta \in R^6$, where $\mathcal{D}$ is the set of locally bounded functions of z; the weight matrix $R(\epsilon, \eta, \omega_e, \hat{\theta}, \omega_c, \dot{\omega}_c)$ is of the same form as (6.43) with the smooth matrix $\Psi_2(\epsilon, \eta, \omega_e, \hat{\theta})$ being replaced by (6.56); and the state weight $l(\epsilon, \eta, \omega_e, \hat{\theta}, \omega_c, \dot{\omega}_c)$ is given by

$$l(\epsilon, \eta, \omega_e, \hat{\theta}, \omega_c, \dot{\omega}_c) = -2\beta \big[c\epsilon^T \omega_e + z^T (F + G)\hat{\theta} \big] + \beta^2 z^T R^{-1} z - \frac{2\beta}{\gamma^2} z^T z. \tag{6.61}$$

Proof. The first part of the proof is similar to that of Theorem 6.9 and the second part is analogous to that of Theorem 6.7. We outline the proof briefly. Along the solutions of the system (6.36), (6.37), (6.58) and (6.42) we have

$$\dot{V}_2 = -c\epsilon^T K \epsilon + z^T \big[c\epsilon + u_e + (F + G)\hat{\theta} + \frac{1}{\gamma^2} z \big].$$

Applying the matrices $F(\epsilon, \eta, \omega_e, \omega_c, \dot{\omega}_c)$ in (6.38), $G(\epsilon, \eta, \omega_e)$ in (6.39), defining the smooth matrices $\Psi_1(\epsilon, \eta, \omega_e, \hat{\theta}, \omega_c, \dot{\omega}_c)$ as in (6.44) and $\Psi_2(\epsilon, \eta, \omega_e, \hat{\theta})$ as in (6.56) and letting $\bar{\Psi}_2 = \Psi_2^T + \Psi_2$, we can rewrite $\dot{V}_2$ as

$$\dot{V}_2 = -c\epsilon^T K \epsilon + z^T u_e + \sqrt{c} z^T \Psi_1^T K^{1/2} \epsilon + z^T \bar{\Psi}_2 z.$$

Then the feedback control law

$$u_e = \alpha(\epsilon, \eta, \omega_e, \hat{\theta}, \omega_c, \dot{\omega}_c) = -\Big(K_1 + \frac{\Psi_1^T \Psi_1}{2} + \frac{\bar{\Psi}_2 K_1^{-1} \bar{\Psi}_2}{2} \Big) z$$

yields $\dot{V}_2 \leq -\frac{c}{2} \epsilon^T K \epsilon - \frac{1}{2} z^T K_1 z = W(\epsilon, z) \leq 0$.

Hence, as analyzed in Theorem 6.9, we can conclude that, under the adaptive feedback control laws (6.57) and (6.42), the auxiliary system (6.36), (6.37) and (6.58) is asymptotically adaptively stable, i.e., $\epsilon \to 0$, $\omega_e \to 0$ and $z \to 0$ as $t \to \infty$ for any initial condition. It follows that

$$c\epsilon^T \omega_e + z^T [(F + G)\hat{\theta} + \frac{1}{\gamma^2} z - R^{-1} z] \leq -W(\epsilon, z)$$

which implies that

$$l(\epsilon, \eta, \omega_e, \hat{\theta}, \omega_c, \dot{\omega}_c) \geq 2\beta W(\epsilon, z) + \beta(\beta - 2) z^T R^{-1} z,$$

from which we conclude that $l(\epsilon, \eta, \omega_e, \hat{\theta}, \omega_c, \dot{\omega}_c)$ is positive definite in ϵ and ω_e for each $\hat{\theta} \in \mathcal{R}^6$. Therefore, the cost functional $J_a(u_e)$ in (6.60) is a meaningful cost functional for the attitude tracking control problem, penalizing both the attitude tracking errors ϵ, ω_e and the control effort u_e as well as the external disturbance $d(t)$.

Substituting $l(\epsilon, \eta, \omega_e, \hat{\theta}, \omega_c, \dot{\omega}_c)$ in (6.61), $z = \omega_e + K\epsilon$ and $v = u_e - \alpha^* = u_e - \beta\alpha = u_e + \beta R^{-1} z$ into the cost functional $J_a(u_e)$ in (6.60), we obtain the following expression of $J_a(u_e)$ along the trajectories of the system (6.35), (6.36), (6.37) and (6.59):

$$\begin{aligned}
J_a(u_e) = \sup_d \Big\{ \lim_{t\to\infty} \Big[& 2\beta V_2(\epsilon(t), \eta(t), \omega_e(t), \tilde{\theta}(t)) + \int_0^t v^T R v d\tau \\
& - 2\beta \int_0^t \Big(c\epsilon^T \omega_e + z^T [F\theta + G\theta + H\tilde{\theta} + u_e + d] - z^T (F + G + H)\tilde{\theta} \Big) d\tau \\
& - \int_0^t \Big(\frac{2\beta}{\gamma^2} z^T z - 2\beta z^T d + \frac{\beta\gamma^2}{2} ||d||^2 \Big) d\tau \Big] \Big\} \\
= \sup_d \Big\{ \lim_{t\to\infty} \Big[& 2\beta V_2(\epsilon(t), \eta(t), \omega_e(t), \tilde{\theta}(t)) - \frac{\beta\gamma^2}{2} \int_0^t \Big|\Big| \frac{2z}{\gamma^2} - d \Big|\Big|^2 d\tau \\
& - 2\beta \int_0^t \frac{d}{dt} \Big(c(1-\eta)^2 + c\eta^2 + \frac{1}{2} z^T J z + \frac{1}{2} \tilde{\theta}^T J \tilde{\theta} \Big) dt + \int_0^t v^T R v d\tau \Big] \Big\} \\
= 2\beta V_2(\epsilon(0), \eta(0), \omega_e(0), \tilde{\theta}(0)) & + \int_0^\infty v^T R v dt - \frac{\beta\gamma^2}{2} \sup_d \Big[\int_0^\infty \Big|\Big| \frac{2z}{\gamma^2} - d \Big|\Big|^2 dt \Big].
\end{aligned}$$

It is clear that

$$\sup_d \Big[- \int_0^\infty \Big|\Big| \frac{2}{\gamma^2} z - d \Big|\Big|^2 dt \Big] = 0$$

and the "worst-case" disturbance $d^*(\epsilon, \omega_e)$ is given by

$$d^*(\epsilon, \omega_e) = \frac{2}{\gamma^2} z = \frac{2}{\gamma^2} (\omega_e + K\epsilon). \tag{6.62}$$

Hence, the minimum of the cost functional $J_a(u_e)$ is reached only if $v = 0$, that is, the dynamic feedback control law $u_e = \alpha^*(\epsilon, \eta, \omega_e, \hat{\theta}, \omega_c, \dot{\omega}_c)$ in (6.59) is inverse optimal and minimizes the cost functional (6.60). The value function of (6.60) is $J_a^*(\epsilon, \eta, \omega_e, \tilde{\theta}) = 2\beta V_2(\epsilon, \eta, \omega_e, \tilde{\theta})$. □

Remark 6.6. The parameter $\beta \geq 2$ in Theorem 6.11 represents a degree of freedom for the design. Also, applying the inverse optimal attitude control law (6.59) and the adaptive parameter update law (6.42), along the trajectories of the system (6.35), (6.36) and (6.37) we obtain the derivative value $\dot{V}_2$ as

$$\dot{V}_2 \leq -\frac{c}{2} \epsilon^T K \epsilon - z^T \Big[\frac{I_3}{\gamma^2} + \frac{K_1}{2} + (\beta - 1) R^{-1} \Big] z + z^T d.$$

It follows from the Young's inequality [41] that $z^T d \leq \frac{\gamma^2}{4} ||d||^2 + \frac{1}{\gamma^2} z^T z$, where the equal

sign is satisfied only if $d(t) = d^*(\epsilon, \omega_e) = \frac{2}{\gamma^2} z$. From (6.43) it follows that $R^{-1} \geq K_1$. Therefore,

$$\dot{V}_2 \leq -\frac{c}{2}\epsilon^T K \epsilon - \frac{2\beta - 1}{2} z^T K_1 z + \frac{\gamma^2}{4}||d||^2.$$

Then there must exist finite constants $c_5 > 0$ and $c_6 > 0$ such that

$$\dot{V}_2 \leq -c_5||\epsilon||^2 - c_6||\omega_e||^2 + \frac{\gamma^2}{4}||d||^2, \tag{6.63}$$

which implies that the closed-loop system under the adaptive control law (6.59)(6.42) is d-to-(ϵ, ω_e)-stable in the sense of input-to-state stability [59]. In turn, it follows from the definition of input-to-state stability that the inverse optimal adaptive control law (6.59)(6.42) guarantees the boundedness of the tracking errors ω_e and ϵ for any bounded (and persistent) external disturbance. We emphasize that the inverse optimal adaptive control (6.59)(6.42) is not restricted to disturbances with bounded energy $\int_0^\infty ||d(t)||dt < \infty$ but any bounded (and persistent) external disturbances are allowed.

Integrating both sides of (6.63) with respect to t from 0 to ∞, we can present an $\mathcal{L}_2$ bound on the tracking errors ϵ and ω_e for the attitude tracking control problem by the following inequality

$$\int_0^T [4c_5||\epsilon||^2 + 4c_6||\omega_e||^2]dt \leq \gamma^2 \int_0^T ||d||^2 dt + 4V_2(\epsilon(0), \eta(0), \omega_e(0), \tilde{\theta}(0)) \tag{6.64}$$

for all $T \geq 0$. Hence, the dynamic control laws (6.59) and (6.42) are robust to external disturbances and the $\mathcal{L}_2$ gain from the external disturbance $d(t)$ to a block vector of the attitude tracking errors (ϵ, ω_e) is bounded by $\frac{\gamma}{2\sqrt{\min\{c_5, c_6\}}}$.

Since $J_a = 2\beta V_2(\epsilon(0), \eta(0), \omega_e(0), \tilde{\theta}(0))$, it follows

$$\int_0^T \left[l(\epsilon, \eta, \omega_e, \hat{\theta}, \omega_c, \dot{\omega}_c) + u_e^T R u_e\right]dt \leq \frac{\beta\gamma^2}{2} \int_0^T ||d||^2 dt + 2\beta V_2(\epsilon(0), \eta(0), \omega_e(0), \tilde{\theta}(0))$$

for all $T \geq 0$. If we let $\beta = 2$ and define an output vector $h(\epsilon, \eta, \omega_e, \hat{\theta}, \omega_c, \dot{\omega}_c)$ such that

$$h^T h = l(\epsilon, \eta, \omega_e, \hat{\theta}, \omega_c, \dot{\omega}_c)$$

then the $\mathcal{L}_2$ gain of the closed-loop attitude control system from the external disturbance $d(t)$ to the output block $\begin{pmatrix} h \\ R^{1/2} u_e \end{pmatrix}$ is not greater than γ in the sense of Definition 3.15. Thus, H_∞ disturbance attenuation is achieved for any given attenuation level $\gamma > 0$ at the cost of a larger control u_e for a smaller γ.

Furthermore, if $d(t) \in \mathcal{L}_2[0, \infty)$, we conclude that ϵ, $\omega_e \in \mathcal{L}_2[0, \infty)$. It follows from (4.38) and (4.40) that $\dot{\epsilon}$, $\dot{\omega}_e \in \mathcal{L}_2[0, \infty)$. Using *Barbalat's Lemma* 2.2, we conclude that $\epsilon \to 0$ and $\omega_e \to 0$ as $t \to \infty$. As such, asymptotic attitude tracking is achieved with a global convergence for all initial conditions. $\otimes$

6.3.4 Convergence of Adaptive Parameters

As stated in Remark 6.4, the parameter update law (6.42) represents a scheme for adjusting the adaptive parameter $\hat{\theta}$ and the estimation error $\tilde{\theta} = \theta - \hat{\theta}$ does not necessarily converge to zero as $t \to \infty$. However, $\hat{\theta}$ can converge to θ under certain conditions on the reference inputs $\omega_c(t)$ and $\dot{\omega}_c(t)$.

Consider the dynamic feedback controller (6.41) and (6.42) in the zero-disturbance case, $d = 0$. Expanding (6.42) and only keeping one-order terms in the error states ϵ and ω_e (and ignoring those high-order terms in ϵ and ω_e), we can simplify the adaptive parameter update law (6.42) to that given by (6.52), i.e.,

$$\dot{\hat{\theta}} = \Gamma H(\omega_c, \dot{\omega}_c)^T(\omega_e + K\epsilon), \qquad H(\omega_c, \dot{\omega}_c) = -\omega_c^{\times} L(\omega_c) - L(\dot{\omega}_c).$$

Lemma 6.12. *Assume that ω_c is periodic and let*

$$G = \{\chi : H(\omega_c(t), \dot{\omega}_c(t))\chi = 0 \quad \forall t \geq 0\}.$$

Under the control laws (6.41)(6.42), $\theta - \hat{\theta} \to G$ as $t \to \infty$.

Proof. Its proof was done in [1] and we reproduce it here for comprehension. Let $x = [z^T, \epsilon^T, \eta, \tilde{\theta}^T]^T$ and let $E_0 = \{x : \dot{V}_2 = 0\}$ with $V_2(\epsilon, \eta, \omega_e, \tilde{\theta})$ given by (6.48). Let $x(t; x_0, t_0)$ denote the solution of the system (6.35), (6.36) and (6.37) with the adaptive update law (6.42) at time $t \geq t_0$, where $x_0 \equiv x(t_0)$ is the initial condition at time t_0. Let $L = \{(\hat{x}, \hat{t}) \in E_0 \times [0, \infty) : x(t, \hat{x}, \hat{t} \in E_0 \text{ for all } t \geq \hat{t}\}$ and $N = \{x(t; \hat{x}, \hat{t}) : (\hat{x}, \hat{t}) \in L, t \geq \hat{t}\}$. Note that $N \subset E_0$. By the fact that $\epsilon^T\epsilon + \eta^2 = 1$, it follows from (6.35), (6.36), (6.37) and (6.42) that N is given by

$$N = \{(z, \epsilon, \eta, \hat{\theta}) : z = 0, \epsilon = 0, \eta = \{-1, 1\}, \tilde{\theta} \in G\}.$$

It now follows from Theorem 2.8 of [82] that $\theta - \hat{\theta} \to G$ as $t \to \infty$. □

Direct applications of Lemma 6.12 lead to the following two propositions [1] to partially or completely identify the inertia matrix J.

Proposition 6.13. *Assume that ω_c is constant. If $\omega_c = [0,\ \omega_{c2},\ 0]^T$, where $\omega_{c2} \neq 0$, then, under the dynamical control laws (6.41) and (6.42), $\hat{\theta}_4 \to \theta_4$, and $\hat{\theta}_6 \to \theta_6$ as $t \to \infty$. Furthermore, if $\omega_c = [0,\ 0,\ \omega_{c3}]^T$, where $\omega_{c3} \neq 0$, then, under the control laws (6.41) and (6.42), $\hat{\theta}_4 \to \theta_4$, and $\hat{\theta}_5 \to \theta_5$ as $t \to \infty$.*

Proposition 6.14. *Assume that ω_c is periodic. Let $0 \leq t_1 \leq t_2 \leq \cdots \leq t_n$ and suppose that*

$$\text{rank}\begin{bmatrix} H(\omega_c(t_1), \dot{\omega}_c(t_1)) \\ \vdots \\ H(\omega_c(t_n), \dot{\omega}_c(t_n)) \end{bmatrix} = 6 \text{ (dimensions of } \theta). \tag{6.65}$$

Then, under the control laws given by (6.41) and (6.42), $\hat{\theta} \to \theta$ as $t \to \infty$.

Hence, the inertia matrix J can be completely identified if the reference signal $\omega_c(t)$ is periodic and the condition (6.65) is satisfied. Note that Propositions 6.13 and 6.14 on the convergence of $\hat{\theta}$ is certainly valid for Theorems 6.9 and 6.10 where the external disturbances are assumed zero, $d = 0$. When in the presence of external disturbances, the tracking errors ϵ and ω_e are not necessarily guaranteed to converge to zeros globally as $t \to \infty$, which results in that the adaptive parameter $\hat{\theta}$ might not converge to its true value θ even though the condition (6.65) is satisfied. However, when the external disturbance $d(t) \in \mathcal{L}_2[0, \infty)$, the inertia matrix J may also be finally identified if the condition (6.65) is satisfied for a periodic signal $\omega_c(t)$, that is, $\hat{\theta} \to \theta$ as $t \to \infty$.

6.4 Simulation Results

A microsatellite is simulated to demonstrate the performance of the inverse optimal adaptive controllers for the attitude tracking control problem. The structure of the attitude control system is illustrated in Figure 4.1, with the controller block substituted by the inverse optimal adaptive controller proposed in this chapter. Without considerations of the attitude determination, the control chart to simulate the adaptive attitude tracking control problem is shown as in Figure 6.1.

The desired attitude motion of the spacecraft is described in the body frame $\mathcal{F}_{bc}$. We assume that the desired angular velocity $\omega_c(t)$ to be tracked is given in the body frame $\mathcal{F}_{bc}$ by

$$\omega_c(t) = \begin{bmatrix} 0.03\sin(2\pi t/200) \\ 0.03\sin(3\pi t/200) \\ 0.03\sin(1\pi t/200) \end{bmatrix} \text{rad/s},$$

plotted in dotted lines in Figure 6.2. Then the target unit quaternion q_c is obtained by integrating (4.31) with the initial condition $q_c(0) = [0,\ 0,\ 0,\ 1]^T$. With this choice of the reference signal $\omega_c(t)$, it is easy to check that the rank condition (6.65) is satisfied so that it is possible to identify completely the inertia matrix J from the adaptive parameter $\hat{\theta}$, according to Proposition 6.14 .

With the values of moments of inertia listed in Table 5.1, the spacecraft is assumed to have the inertia matrix

$$J = \begin{bmatrix} 16.0 & 0.10 & 0.30 \\ 0.10 & 10.0 & 0.50 \\ 0.30 & 0.50 & 20.0 \end{bmatrix} \text{kg}\cdot\text{m}^2,$$

which is unknown to the controller in the body frame $\mathcal{F}_b$. So we construct an adaptive parameter vector $\hat{\theta}$ as in (6.28) with the true value

$$\theta = [16.0,\ 10.0,\ 20.0,\ 0.50,\ 0.30,\ 0.10]. \tag{6.66}$$

In the numerical simulations of the inverse optimal adaptive attitude tracking con-

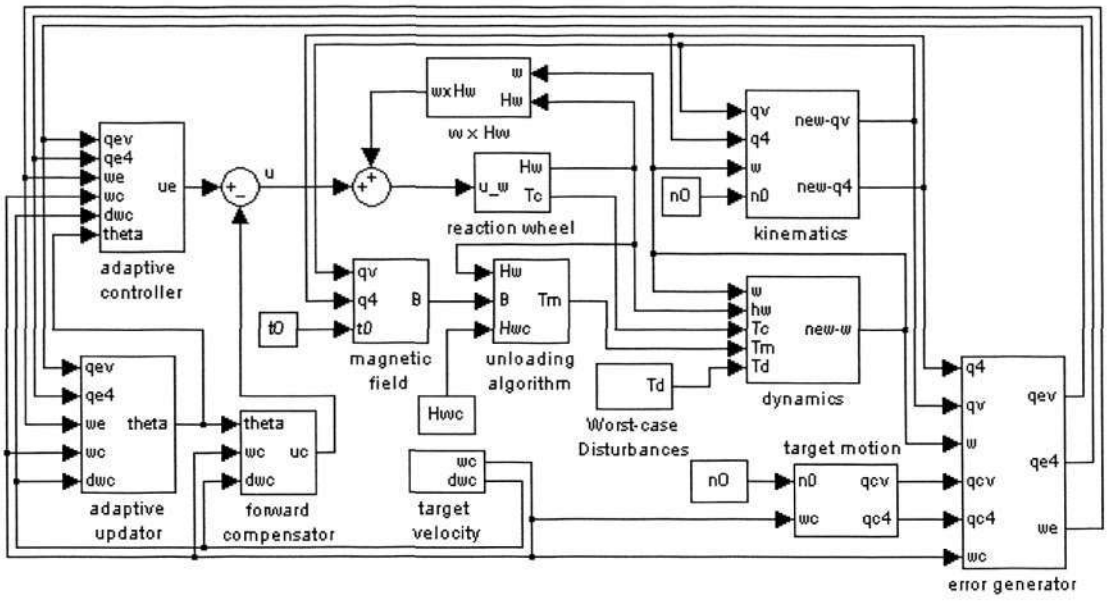

Figure 6.1: SIMULINK chart for adaptive attitude tracking control.

trollers, we assume that the initial attitude orientation and the initial angular velocity of the rigid spacecraft in the body frame $\mathcal{F}_b$, and the initial value of the adaptive parameter $\hat{\theta}$ are given by

$$
\begin{aligned}
q(0) &= [0.15,\ -0.15,\ 0.15,\ 0.9657]^T, \\
\omega(0) &= [0.01,\ -0.01,\ 0.01]^T \text{ rad/s}, \\
\hat{\theta}(0) &= [15,\ 15,\ 15,\ 0,\ 0,\ 0]^T \text{kg} \cdot \text{m}^2.
\end{aligned}
$$

The convergence rate and the transient performance of the adaptive parameter $\hat{\theta}$ depend mainly on the magnitude of the gain matrix Γ in the adaptive update law (6.42). For a larger gain Γ, the estimate $\hat{\theta}$ has a shorter converging time, but due to the initial error conditions $q_e(0)$, $\omega_e(0)$ and $\tilde{\theta}(0)$, its transient performance is also worse with larger overshoots, which not only deteriorates the performance of ϵ and ω_e, but may also fail to guarantee that the estimate $\hat{J}$ constructed from $\hat{\theta}$ is always positive definite (as we expected). For a smaller gain Γ, although the transient of $\hat{\theta}$ is mild, it will take much more time for $\hat{\theta}$ to converge to its true value. On the other hand, in numerical simulations we find out that the input saturation will also degrade the transient performance of $\hat{\theta}$ since the control torques provided by the reaction wheels are limited. By the "trial-and-error" method, we choose the matrix Γ as $\Gamma = 8000 I_6$.

At first, we consider the zero-disturbance case and thus disenable the magnetic unloading algorithm for the angular momentum management of reaction wheels. Applying the inverse optimal feedback control law (6.53) and the adaptive parameter update law (6.42) with the following controller gains

$$
\beta = 2.0, \quad c = 0.5, \quad K = 0.15 I_3, \quad K_1 = 2.0 I_3, \quad \Gamma = 8000 I_6, \tag{6.67}
$$

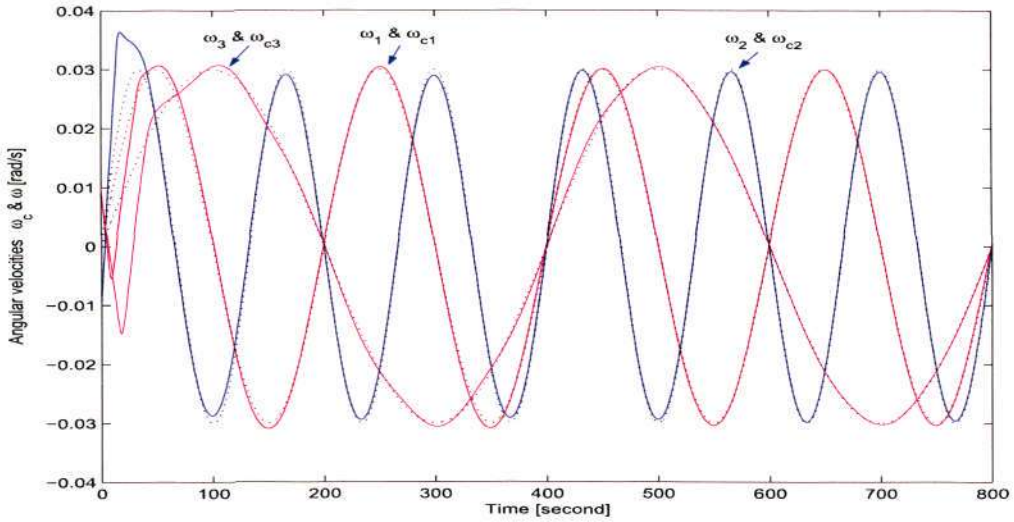

Figure 6.2: Angular velocities ω and ω_c. Solid lines denote ω, and dotted lines stand for ω_c.

we illustrate the simulation results as in Figures 6.2—6.7, from which we conclude that asymptotic attitude tracking can be achieved when the inertia matrix J in the body frame $\mathcal{F}_b$ is uncertain. Figure 6.2 depicts the time histories of the angular velocities ω and ω_c, Figure 6.3 plots the time trajectories of the attitude tracking errors ϵ and ω_e, from which it is seen that the inverse optimal adaptive controller (6.53) and (6.42) achieves asymptotic attitude tracking with satisfactory tracking errors ω_e and ϵ and with a rapid convergence of the tracking errors to zero. Figure 6.4 plots the time histories of the control efforts u_e and $u = u_e - u_c$, which are given by the inverse optimal controller (6.53) and (6.33) respectively and thus have no bounds on their magnitudes. Using the control signals $u_w = u + \omega \times H_w$ to drive the reactions wheels, the actual wheel torque $T_w = \dot{H}_w$ is shown in Figure 6.5(a), which is applied for controlling the attitude. The resulting angular momentum of the reactions wheels H_w is plotted in Figure 6.5(b). Figures 6.6 indicates that the estimate of the adaptive parameter $\hat{\theta}$ converges to its nominal value θ, i.e., $\hat{\theta} \to \theta$ in accordance with Lemma 6.14. The largest and the smallest eigenvalues of the estimated inertia matrix $\hat{J}$ are shown in Figure 6.7(a), converging to their true values $\lambda_{\max}(J) = 20.048$ and $\lambda_{\min}(J) = 9.974$. With the inverse optimal controller (6.53), the resulting control matrix R^{-1} in (6.43) is shown in Figure 6.7(b) by its largest and smallest eigenvalues $\lambda_{\max}(R^{-1})$ and $\lambda_{\min}(R^{-1})$. It is seen from these numerical simulations that the attitude tracking is achieved rapidly, while the convergence of the adaptive parameter takes a much longer time.

Next, we consider the tracking control problem in the presence of external disturbances $d(t)$ defined by (5.44) in Section 5.6. Disenabling the magnetic unloading algorithm proposed in Section 4.4.4 and applying the robust inverse optimal adaptive control laws (6.59) and (6.42) with the control gains given by (6.67) and $\gamma = 1$, we present the simulation results as in Figures 6.8 and 6.9. The time histories of the tracking errors ϵ and ω_e and the parameter estimate $\hat{\theta}$ are plotted in Figure 6.8, from

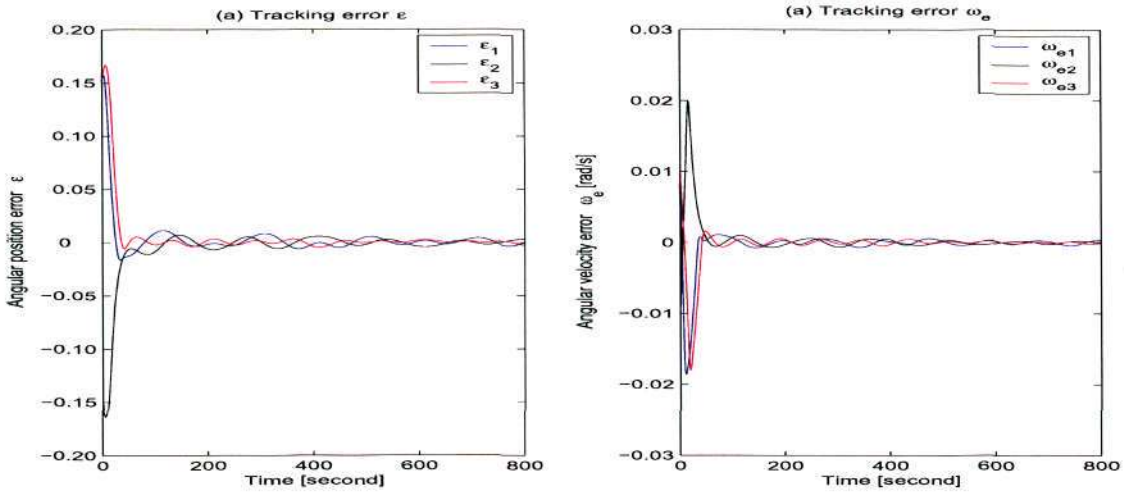

Figure 6.3: Tracking errors ϵ and ω_e in the zero-disturbance case.

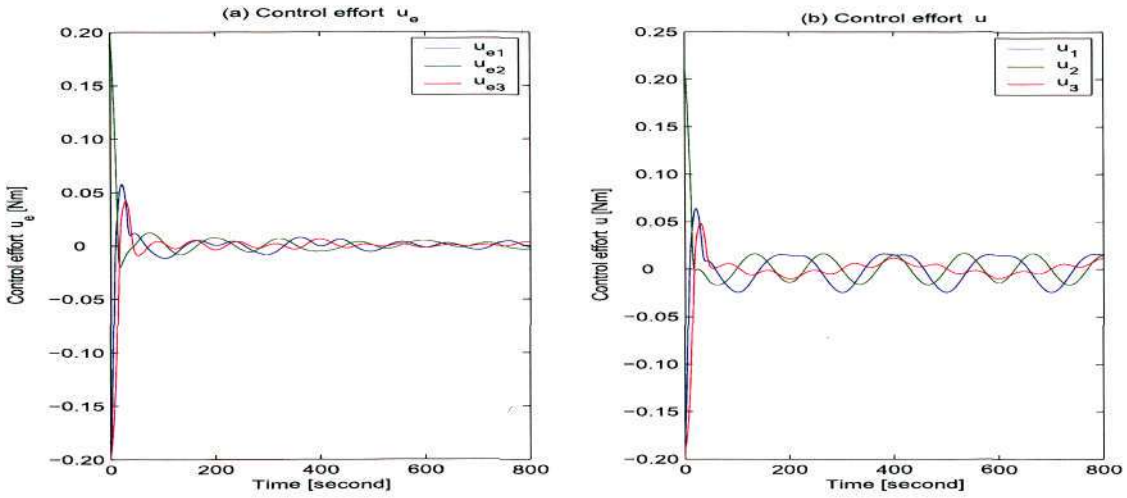

Figure 6.4: Control efforts u_e given by (6.53) and $u = u_e - u_c$ by (6.33).

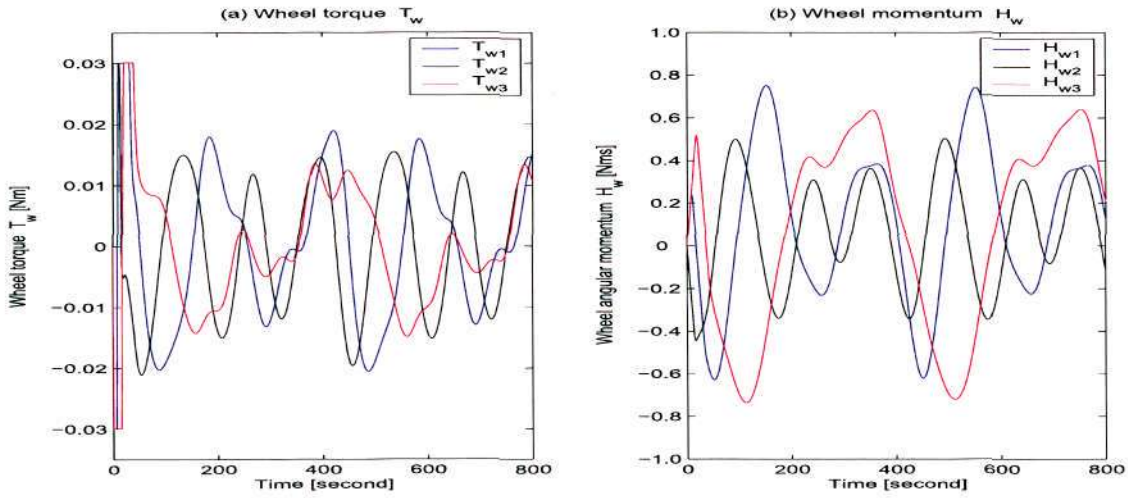

Figure 6.5: Wheels' torque T_{cw} and momentum H_w in the zero-disturbance case.

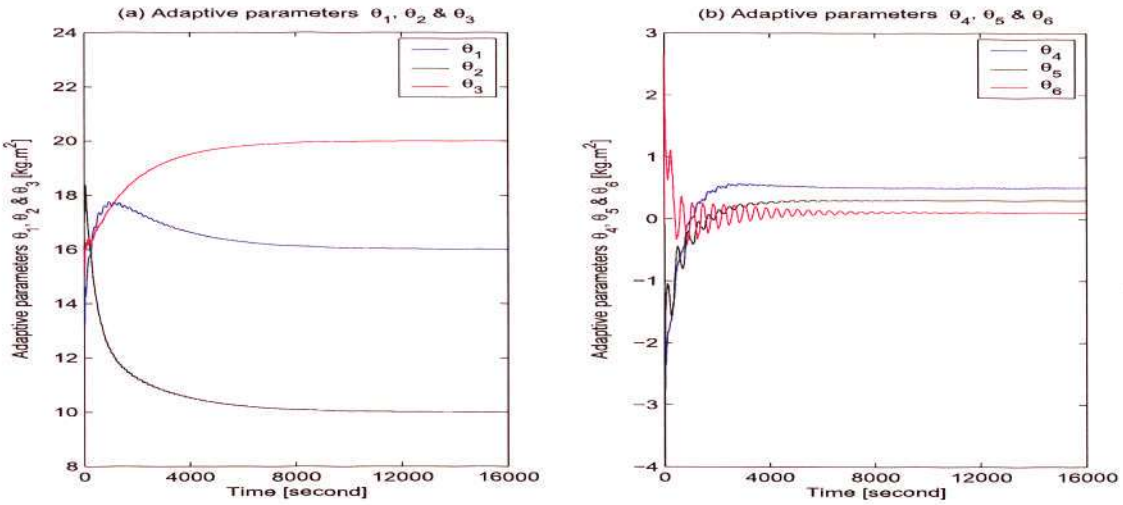

Figure 6.6: Adaptive parameter vector $\hat{\theta}$ in the zero-disturbance case.

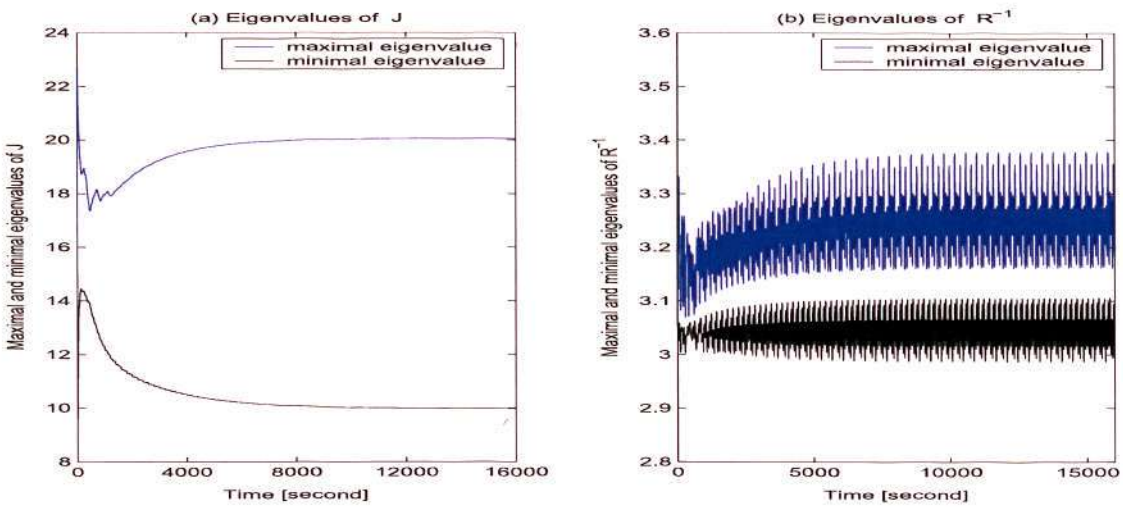

Figure 6.7: Eigenvalues of the estimated inertia matrix $\hat{J}$ and the control gain R^{-1}.

which it is observed that the system is finally destabilized. This is due to the fact that the presence of external disturbances results in an accumulation of angular momentum of reaction wheels to their saturating limits shown in Figure 6.9(a), and finally make the wheels saturated at most time, depicted as in Figure 6.9(b), such that the wheels provide insufficient torques to control the attitude and eliminate the gyroscopic effects. Therefore, it is necessary to activate the magnetic unloading algorithm for the wheel's angular momentum management in the presence of external disturbances. When the magnetic unloading algorithm is enabled, the simulation results are shown as in Figures 6.10 and 6.11, from which we conclude that 1)the magnetic unloading alleviates the accumulation of the wheels' angular momentum and thus enhance the stability, and 2)the adaptive feedback tracking control laws (6.59) and (6.42) can achieve the adaptive attitude tracking with satisfactory tracking errors ω_e and ϵ and with a good convergence in the presence of external disturbances. Further analysis of Figure 6.11 shows that

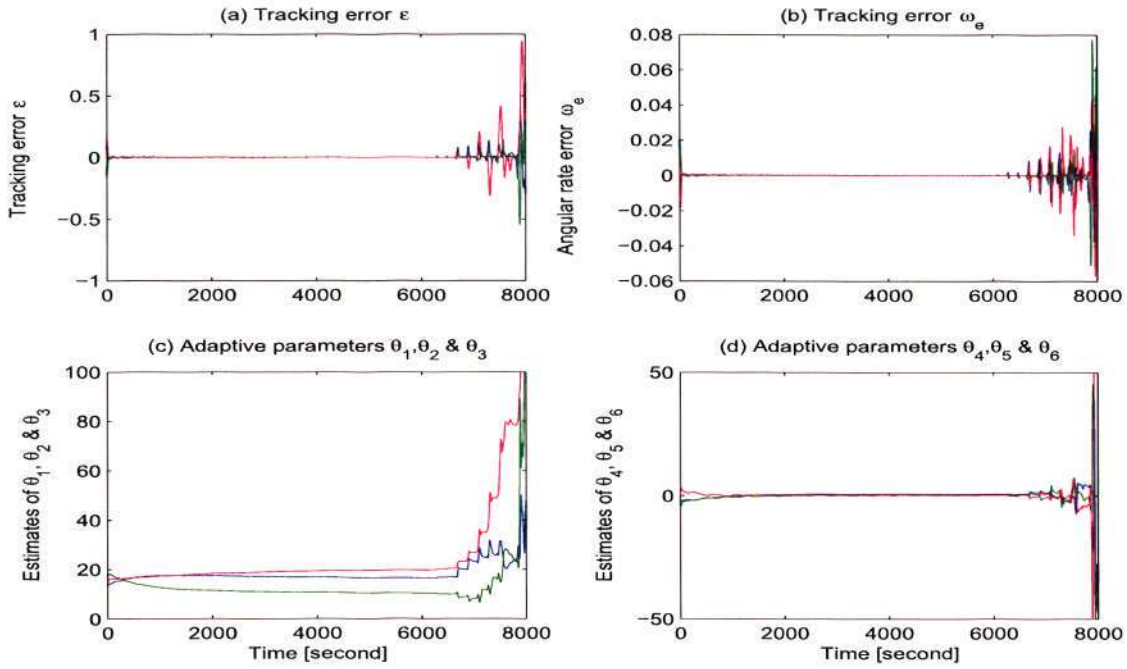

Figure 6.8: Tracking errors ϵ, ω_e and the adaptive parameter vector $\hat{\theta}$ under external disturbances without magnetic unloading.

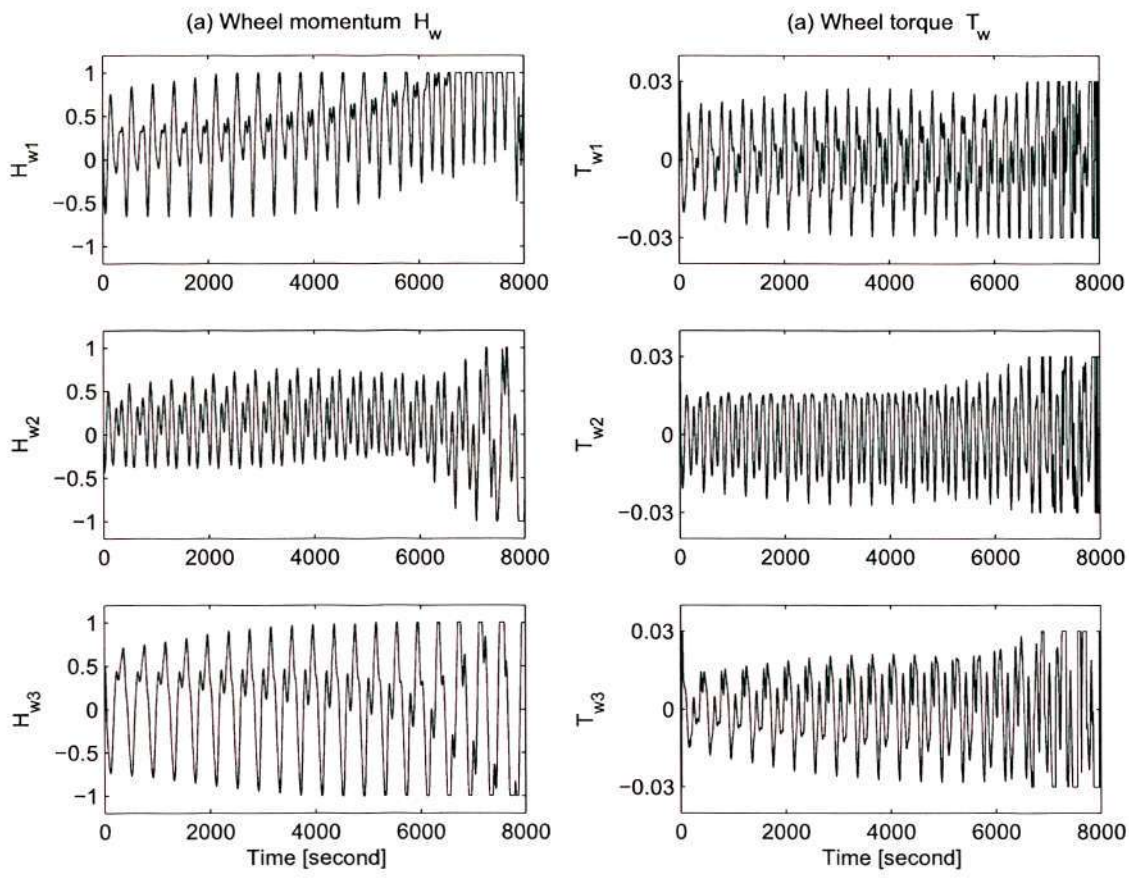

Figure 6.9: Wheel angular momentum H_w and wheel torque T_w under external disturbances without magnetic unloading.

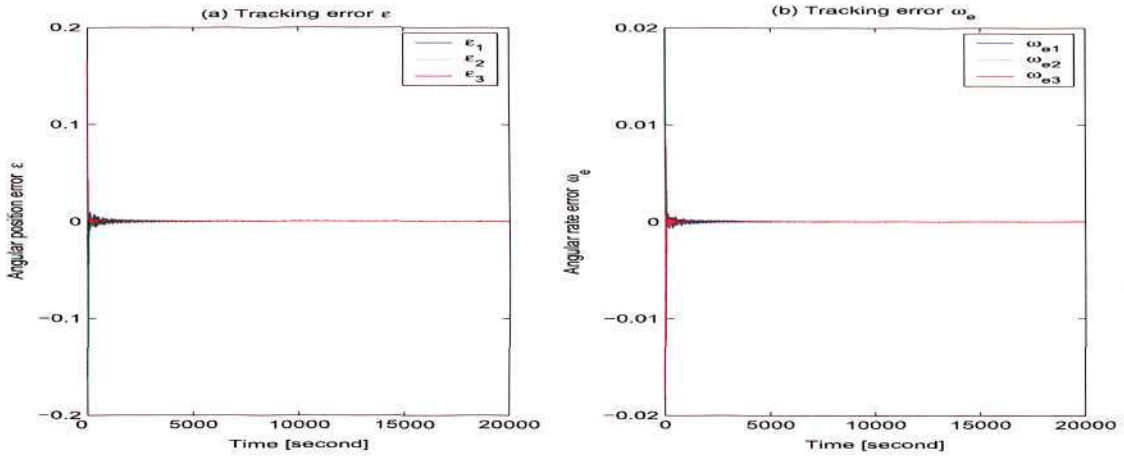

Figure 6.10: Errors ϵ and ω_e under external disturbances with magnetic unloading.

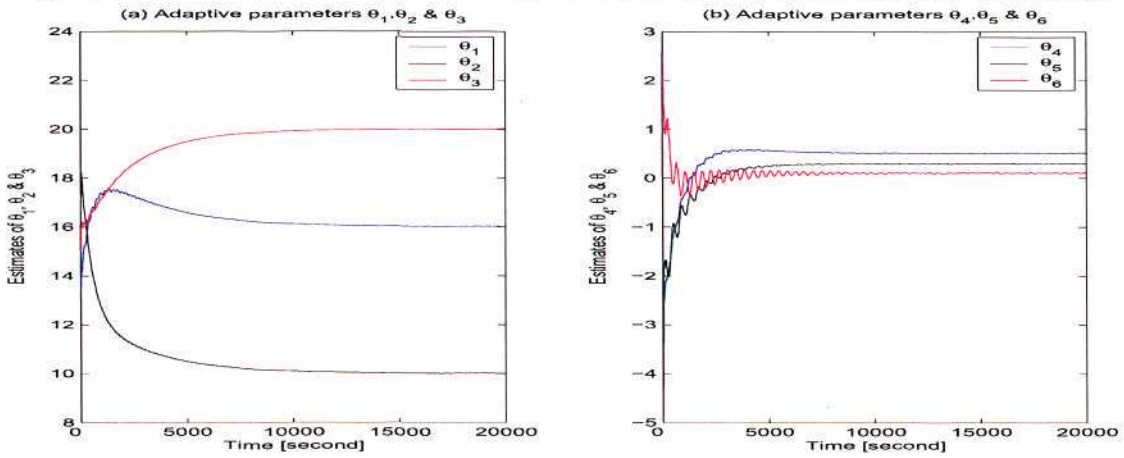

Figure 6.11: Parameter $\hat{\theta}$ under external disturbances with magnetic unloading.

due to the external disturbances, there is a steady-state error between the estimate $\hat{\theta}$ and the true value θ in (6.66), given by $\tilde{\theta}_{ss} = [0.025, 0.015, 0.018, 0.010, 0.002, 0.001]^T$.

Finally, to illustrate the capacity of disturbance attenuation, three different attenuation levels are considered, $\gamma = 1.0$, $\gamma = 0.5$ and $\gamma = 0.25$. Figure 6.12 plots the histories of ω_{e1} and ϵ_1, the first components of the tracking errors ω_e and ϵ respectively. Figure 6.13(a) shows the control effort u_1, the first element of u given by (6.33). Figure 6.13(b) evaluates the control gain R^{-1} in (6.43) by its minimal eigenvalue $\lambda_{\min}(R^{-1})$. As expected, a smaller γ yields a better performance of attenuating the external disturbance $d(t)$ at the cost of a larger control effort and a larger control gain R^{-1}.

6.5 Conclusions

An attitude tracking control system is indeed a nonlinear cascade system. Therefore, stabilizing such a system can be efficiently achieved using the method of backstepping. Employing the adaptive control method and the inverse optimal control approach, this

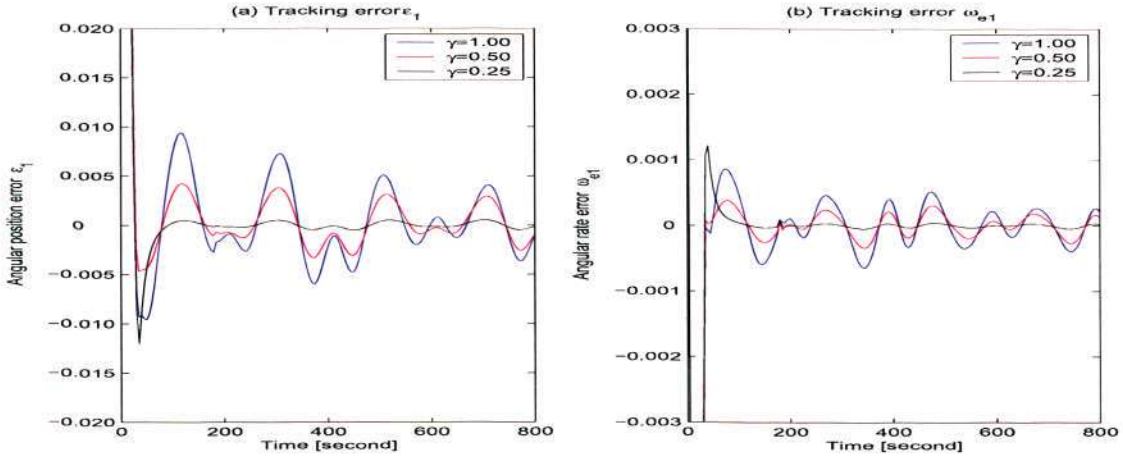

Figure 6.12: The tracking errors ω_{e1} and ϵ_1 for different attenuation levels.

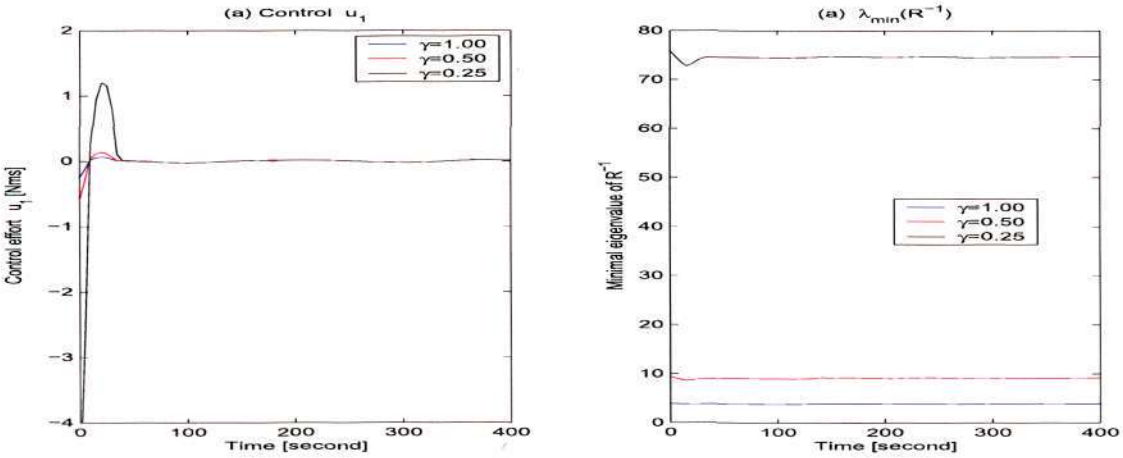

Figure 6.13: Control effort u_1 and the value $\lambda_{\min}(R^{-1})$ for different attenuation levels.

chapter has presented two inverse optimal adaptive feedback control laws to solve the attitude tracking control problem of rigid spacecraft with an uncertain inertia matrix. In the zero-disturbance case, the proposed inverse optimal adaptive controller achieves asymptotic attitude tracking of the desired attitude motions, which has a global convergence of the tracking errors to zero for all initial conditions. The control law is inverse optimal with respect to a family of meaningful cost functionals that consist of penalties on both the tracking errors ϵ, ω_e and the control effort u_e. When external disturbances are considered, we have presented a robust adaptive attitude tracking control law which is not only inverse optimal with respect to a set of meaningful cost functionals that include penalties on the tracking errors, control efforts as well as external disturbances, but also forms a closed-loop attitude control system that has a finite $\mathcal{L}_2$ gain from the external disturbances to the tracking errors. Any given level of H_∞ disturbance attenuation can be achieved with an appropriate control effort. Such optimal control laws have been obtained without solving the associated Hamilton-Jacobi-Isaacs equation directly. Numerical simulations have been carried out to illustrate the performance of the proposed attitude tracking algorithms.

Chapter 7

Local Synthesis of Linear Systems with Actuator Saturations

7.1 Introduction

Using the nonlinear attitude equations, by far we have designed robust optimal controllers in Chapters 5 and 6, respectively, for the attitude tracking control problem of spacecraft with disturbances and uncertainties. In designing these controllers, actuator's saturation nonlinearity is not taken into account explicitly in the synthesis because a nonlinear control problem involving input saturation nonlinearities, however, turns out to be very hard to obtain an analytic result. On the other hand, it has been well known that, when the actuator's saturations occur, the system performance under the controller designed without considering input saturations may seriously deteriorate.

For general nonlinear systems without disturbances, Sontag [70] proposed a universal formula on designing a bounded control law, and then this universal formula was extended to ISS (and integral-ISS) disturbance attenuation problems with bounded controls [67]. However, it should be noted that in [67, 70] the input saturation constraint $||u||_\infty \leq 1$ was restricted into a spherical constraint $||u|| < 1$ to avoid the actuator's saturation and therefore only a small part of the available control capacity is used, which leads to a low-gain controller and thus a slower response of the closed-loop system. Analogously, by restricting the saturation nonlinearity into $||u|| \leq 1$ to avoid the saturation, the SDRE technique was applied to nonlinear systems with bounded controls [52, 74] to design a locally stable low-gain controller.

Thus, one may ask: for a given stabilizing controller obtained without the consideration of the input saturation nonlinearity, whether is it still stabilizing when the saturation occurs in the inputs and then how large is the region of attraction for the closed-loop system? Furthermore, whether can we synthesize robust controllers that allow the saturation to make a full use of the actuator's control capability? Unfortunately, it seems impossible to describe analytically and exactly the region of attraction and obtain analytical results on designing robust controllers for high-order nonlinear systems with saturated controls. However, even when an analytical solution is not available, we may use numerical approaches (such as the LMI approach) and the lin-

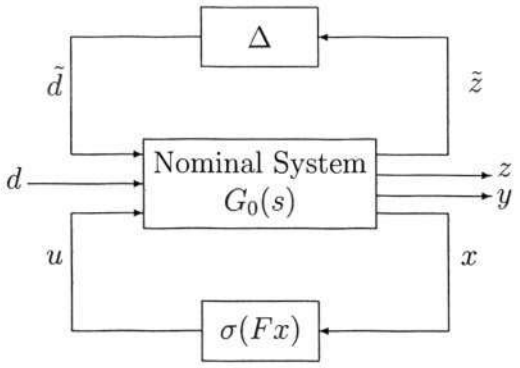

Figure 7.1: Interconnection of linear systems with saturations and uncertainties.

earized system models to estimate the region of attraction and design locally robust controllers for the system interconnection shown in Figure 7.1, where $\sigma(\cdot)$ denotes the saturation nonlinearity and the operator $\Delta(\cdot)$ denotes uncertainties.

There are several tools for robust stability analysis/synthesis of systems with nonlinearities and uncertainties shown in Figure 7.1. μ-analysis [29] was developed in the frequency domain and therefore can be applied to uncertainties Δ that have a frequency domain description but is not suitable for nonlinearities, such as a saturation, which cannot be described in the frequency domain. Nonlinearities can be analyzed in the framework of Integral Quadratic Constraints (IQC) [76, 77, 87], which provides a powerful tool for the analysis of robust stability of systems with uncertainties, nonlinearities and time-varying parameters and can be used in both of the frequency and the time domains. However, within the IQC framework, it is required that the nonlinear/uncertain operator be bounded and the LTI transfer function $G_0(s)$ be a stable proper transfer function without poles in the closed right half plane, i.e., $G_0(s) \in RH_\infty$. For our problem, it is shown later that the linearized attitude control system has unstable poles in the right half-plane such that there are no global results with bounded controls, and it is not suitable to use the IQC theory for stability analysis. Basing on the dissipative theory, Romanchuk [89] developed a less conservative condition on the computation of the induced L_2-norm for linear systems subjects to disturbances and input saturations. However, the problem of searching for a valid dissipative function remains open for high-order systems. Some other methods on robust stability analysis, such as the small gain theorem, the circle criterion and the Popov criterion and so on, can be referred to [59, 86, 89, 102] and the references therein.

In the face of disturbances and parametric uncertainties, robust control theory provides engineers a systematical approach for analysis and synthesis of attitude controllers. It is well known that H_2 control and H_∞ control are two main streams of robust control theory [95, 138]. The time-domain interpretation of H_2 norm is a measure of the root-mean-square value of the performance output driven by unit impulse or unit intensity white noise, and H_∞ norm is a measure of the robust stability with respect to disturbances and uncertainties. For linear systems without input constraints, the H_2 and H_∞ control theories have been applied to the attitude control problem successfully,

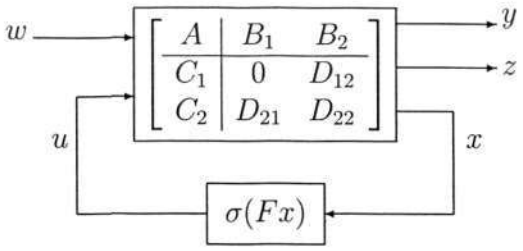

Figure 7.2: Linear Systems with actuator saturations.

for examples, [95, 129, 130, 136]. When the saturation nonlinearity is considered, these problems become much more complicated. However, they can be formulated in the time domain in terms of linear matrix inequalities for some local results.

In this chapter, we will study the linear attitude control problem subject to external disturbances, structured moment-of-inertia uncertainties and actuator saturation nonlinearities. We attempt to estimate the region of attraction of the origin and formulate the analysis/synthesis problem of local H_2- and H_∞-performance in terms of LMIs for linear systems with saturated controls by applying the properties of the saturation nonlinearity. Using the LMI software, the results obtained are applied to the linear attitude control problem of a microsatellite.

This chapter is organized as follows. In Section 7.2, set invariance conditions are presented for a local stability analysis. In Sections 7.3 and 7.4, respectively, the analysis/synthesis problems for the local H_2- and H_∞-performance are formulated in terms of LMIs. The synthesis models are formulated in Section 7.5 for the linear attitude control problem with disturbances and structured uncertainties of moments of inertia. Local analysis and local synthesis are performed in Section 7.6 for the linear attitude control problem with saturated controls, disturbances and structured parametric uncertainties. Conclusions follow in Section 7.7.

7.2 Stability Analysis

Consider the linear system with a saturated control input shown in Figure 7.2:

$$\dot{x} = Ax + B_1 w + B_2 u, \tag{7.1}$$
$$u = \sigma(Fx), \tag{7.2}$$
$$y = C_1 x + D_{12} u, \tag{7.3}$$
$$z = C_2 x + D_{21} w + D_{22} u, \tag{7.4}$$

where $x \in \mathcal{R}^n$, $u \in \mathcal{R}^m$, $w \in \mathcal{R}^q$, $y \in \mathcal{R}^{n_y}$ and $z \in \mathcal{R}^{n_z}$; the feedback matrix F is designed such that $A+BF$ is Hurwitz. Let f_i be the ith row of the matrix F, $i \in [1, m]$, and let $\bar{u}$ denote the maximal control capability. Then, $\sigma(Fx)$ denotes the saturation function vector

$$\sigma(Fx) = [\sigma(f_1 x),\ \sigma(f_2 x), \cdots, \sigma(f_m x)]^T,$$

and the scalar $\sigma(f_i x)$ is a saturation function defined by

$$\sigma(f_i x) = \text{sgn}(f_i x) \min\{\bar{u}, |f_i x|\}, \quad i = 1, \cdots, m. \tag{7.5}$$

Assumption 7.1. *The following assumptions are made:*

(A1). (A, B_1) *is stabilizable and* (C_1, A) *is detectable;*

(A2). (A, B_2) *is stabilizable and* (C_2, A) *is detectable;*

(A3). D_{12} *has full column rank;*

(A4). D_{21} *has full row rank.*

The assumption $D_{11} = 0$ in the output y guarantees that the closed-loop linear transfer matrix is in $\mathcal{H}_2$ (recall that a real rational stable transfer matrix is in $\mathcal{H}_2$ if and only if it is strictly proper), thus making H_2 performance synthesis feasible. Assumption (A1) is clearly necessary for the existence of stabilizing controllers. Assumption (A2) is made for technique reasons. Assumptions (A1) and (A2) together guarantee that the control and the filtering Riccati equations associated with the standard H_2 problem of linear system admit positive semidefinite solution. Assumption (A3) is actually a restatement that $R_{12} = D_{12}^T D_{12} > 0$, which guarantees that the H_2 problem is nonsingular. Assumption (A4) guarantees that the H_∞ problem is nonsingular with $D_{21} D_{21}^T > 0$. A special choice $D_{22} = 0$ will simplify the analysis of the output z. The resulting linear systems were extensively studied in the literature, for example [95,138], without considerations of saturations. In this chapter, we will consider the general case: $D_{22} \neq 0$. Assume that D_{22} has full column rank, i.e., $R_{22} = D_{22}^T D_{22} > 0$.

For a matrix $H \in \mathcal{R}^{m \times n}$, let h_i denote the ith row of H and then define a region as

$$\mathcal{L}(H, \bar{u}) = \{x \in \mathcal{R}^n : |h_i x| \leq \bar{u}, i \in [1, m]\}, \tag{7.6}$$

Let $r \in \mathcal{R}_+^m$ be a vector whose components specify the allowable input amplitudes to the actuators. Then, we define a region $\mathcal{R}_r$ as

$$\mathcal{R}_r = \{x : \ |f_i x| \leq r_i, \ i = 1, \cdots, m\} = \mathcal{L}(F, r) \tag{7.7}$$

Definition 7.1. *Any set* $\hat{\mathcal{D}} \subset \mathcal{R}_r$ *such that whenever* $x(0) \in \hat{\mathcal{D}}$ *and* $w \equiv 0$ *we have* $x(t) \in \mathcal{R}_r$ *and* $\lim_{t \to \infty} x(t) = 0$ *will be called an* r*-level guaranteed region of attraction. The largest set* $\mathcal{D} \subset \mathcal{R}^n$ *for which* $x(t) \to 0$ *as* $t \to \infty$ *whenever* $x(0) \in \mathcal{D}$ *and* $w \equiv 0$ *is called the region of attraction*[1].

Finding the exact region of attraction analytically might be difficult or even impossible. However, Lyapunov function can be used to estimate the region of attraction. Let $P \in \mathcal{R}^{n \times n}$ be a positive definite matrix and define the Lyapunov function candidate as $V(x) = x^T P x$. Denote an ellipsoid as

$$\mathcal{E}(P, \rho) = \{x \in \mathcal{R}^n : x^T P x \leq \rho\}. \tag{7.8}$$

[1]The region of attraction is also called the region of asymptotic stability, the domain of attraction or the basin [59, pp.109].

The ellipsoid $\mathcal{E}(P,\rho)$ is said to be a (contractively) *invariant* set if the derivative $\dot{V}(x) \leq (<)0$ for all $x \in \mathcal{E}(P,\rho)\backslash\{0\}$.

7.2.1 A set invariant based on the circle criterion

A multivariable circle criterion was presented in [59] in the frequency domain via the transfer function. In [86], it was represented in terms of some matrix inequalities and applied to estimate the region of attraction of the origin for system (7.1) with $w \equiv 0$.

Lemma 7.1 (Stability region via circle criterion). *Assume that (F, A, B) is controllable and observable. Given an ellipsoid $\mathcal{E}(P,\rho)$, if there exist positive diagonal matrices $K_1, K_2 \in \mathcal{R}^{n\times n}$ with $K_1 < I$ and $K_1 + K_2 \geq I$ such that*

$$(A + BK_1F)^T P + P(A + BK_1F) + \tfrac{1}{2}(F^T K_2 + PB)(K_2F + B^T P) < 0 \qquad (7.9)$$

and $\mathcal{E}(P,\rho) \subset \mathcal{L}(K_1F, \bar{u})$, then $\mathcal{E}(P,\rho)$ is a contractively invariant set and hence inside the region of attraction.

A similar condition based on the circle criterion was presented in [44] and solved with the LMI software. Since the matrix inequality (7.9) in Lemma 7.1 is not jointly convex in K_1, K_2 and P, these matrices have to be optimized separately by fixing some of them and thus there is no guarantee to obtain a globally optimal solution.

7.2.2 An improved estimation of the region of attraction

Denote the ith column of B_2 as b_{2i} and the ith row of F as f_i. Then $B_2F = \sum_{i=1}^{m} b_{2i} f_i$. Consider an *auxiliary* feedback matrix $H \in \mathcal{R}^{m\times n}$ and denote the ith row of H as h_i. For two matrices F, $H \in \mathcal{R}^{m\times n}$ and a vector $\nu \in \mathcal{R}^m$, denote

$$M(\nu, F, H) = \begin{bmatrix} \nu_1 f_1 + (1-\nu_1)h_1 \\ \vdots \\ \nu_m f_m + (1-\nu_m)h_m \end{bmatrix}, \quad \nu \in \mathcal{V}, \qquad (7.10)$$

where $\mathcal{V} = \{\nu \in \mathcal{R}^m : \nu_i = 0 \text{ or } 1,\ i \in [1, m]\}$.

With the introduction of an auxiliary matrix $H \in \mathcal{R}^{m\times n}$ such that $|h_i x| \leq \bar{u}$ for all $i \in [1, m]$, an improved estimate of the region of attraction is presented as an invariant set by the following lemma.

Lemma 7.2. [48] *Assume that $w \equiv 0$. Given an ellipsoid $\mathcal{E}(P,\rho)$, if there exists a real matrix $H \in \mathcal{R}^{m\times n}$ such that*

$$P(A + B_2M(\nu, F, H)) + (A + B_2M(\nu, F, H))^T P < 0, \quad \forall \nu \in \mathcal{V}, \qquad (7.11)$$

and $\mathcal{E}(P,\rho) \subseteq \mathcal{L}(H, \bar{u})$ for all $x \in \mathcal{E}(P,\rho)$, then $\mathcal{E}(P,\rho)$ is a contractively invariant set and hence inside the region of attraction.

Proof. Although given in [48], we repeat the proof here for comprehension. Let the Lyapunov function be $V = x^T Px$. It follows that

$$\dot{V} = x^T(PA + A^T P)x + 2x^T PB_2\sigma(Fx) = x^T(PA + A^T P)x + 2\sum_{i=1}^{m} x^T Pb_{2i}\sigma_i(f_i x)$$

For each term $x^T Pb_{2i}$,

- if $x^T Pb_{2i} \geq 0$ and $f_i x \leq -\bar{u}$, then $x^T Pb_{2i}\sigma_i(f_i x) = -x^T Pb_{2i}\bar{u} \leq x^T Pb_{2i}h_i x$. Here we note that $-\bar{u} \leq h_i x$ for all $x \in \mathcal{E}(P, \rho)$;
- if $x^T Pb_{2i} \geq 0$ and $f_i x \geq -\bar{u}$, then $\sigma_i(f_i x) \leq f_i x$ and $x^T Pb_{2i}\sigma_i(f_i x) \leq x^T Pb_{2i}f_i x$;
- if $x^T Pb_{2i} \leq 0$ and $f_i x \geq \bar{u}$, then $x^T Pb_{2i}\sigma_i(f_i x) = x^T Pb_{2i}\bar{u} \leq x^T Pb_{2i}h_i x$. Here we note that $h_i x \leq 1$ for all $x \in \mathcal{E}(P, \rho)$;
- if $x^T Pb_{2i} \leq 0$ and $f_i x \leq \bar{u}$, then $\sigma_i(f_i x) \geq f_i x$ and $x^T Pb_{2i}\sigma_i(f_i x) \leq x^T Pb_{2i}f_i x$.

Combing all the four cases, we have

$$x^T Pb_{2i}\sigma_i(f_i x) \leq \max\{x^T Pb_{2i}f_i x, x^T Pb_{2i}h_i x\}$$

for every $x \in \mathcal{E}(P, \rho)$ and each $i \in [1, m]$. Choose a vector $\nu \in \mathcal{V}$ as follows: if $x^T Pb_{2i}h_i x < x^T Pb_{2i}f_i x$, then let $\nu_i = 1$, otherwise we let $\nu_i = 0$. It follows that

$$\begin{aligned}\dot{V} &\leq x^T(PA + A^T P)x + 2\sum_{i=1}^{m} x^T Pb_{2i}[\nu_i f_i + (1 - \nu_i)h_i]x \\ &\leq x^T(P(A + B_2 M(\nu, F, H) + (A + B_2 M(\nu, F, H))^T P)x.\end{aligned}$$

If (7.11) is satisfied, it follows that in the region $\mathcal{E}(P, \rho)$, $\dot{V} < 0$ for all $x \neq 0$. □

It is evident from [48,59] that the condition (7.9) in Lemma 7.1 is more conservative than (7.11) in Lemma 7.2 and thus leads to a less conservative estimation of the region of attraction of the origin.

The estimation of the largest region of attraction in Lemma 7.2 can be formulated as a convex optimization problem by maximizing the volume of the ellipsoid $\mathcal{E}(P, \rho)$, but usually we should also take its shape into consideration. Let X_R be a prescribed bounded convex set. For a set $N \subset \mathcal{R}^n$, define

$$\alpha_R(N) = \sup\{\alpha > 0 : \alpha X_R \subset N\}. \tag{7.12}$$

Clearly, if $\alpha_R(N) \geq 1$, then $X_R \subset N$. Choose the shape X_R as the ellipsoids

$$X_R = \mathcal{E}(R, 1) = \{x \in \mathcal{R}^n : \ x^T Rx \leq 1\}.$$

Among all ellipsoids satisfying the sufficient conditions given in Lemma 7.2, we would like to choose the solution such that $\alpha_R(\mathcal{E}(P, \rho))$ is maximized. This convex optimiza-

tion problem can be formulated as

$$\begin{aligned} \sup_{P>0,H,\rho,\alpha} \quad & \alpha \\ s.t. \quad & (a)\ P(A+B_2M(\nu,F,H))+(A+B_2M(\nu,F,H))^TP\le 0, \quad \forall \nu\in\mathcal{V} \\ & (b)\ \alpha X_R\subset\mathcal{E}(P,\rho)\subset\mathcal{L}(H,\bar{u}). \end{aligned} \tag{7.13}$$

7.2.3 Enlargement of the region of attraction

Taking the control gain as an additional optimization parameter, we can choose a feedback matrix F to maximize the region of attraction. Similar to (7.13), the convex optimization problem to enlarge the region of attraction for (7.1) with $w(t)\equiv 0$ is formulated as follows.

$$\begin{aligned} \sup_{P>0,H,F,\rho,\alpha} \quad & \alpha \\ s.t. \quad & (a)\ P(A+B_2M(\nu,F,H))+(A+B_2M(\nu,F,H))^TP\le 0, \quad \forall \nu\in\mathcal{V} \\ & (b)\ \alpha X_R\subset\mathcal{E}(P,\rho)\subset\mathcal{L}(H,\bar{u}). \end{aligned} \tag{7.14}$$

Remark 7.1. As stated in [46, 48], the optimal value of (7.14) is the same as that obtained by a simpler optimization problem

$$\begin{aligned} \sup_{P>0,F,\rho,\alpha} \quad & \alpha \\ s.t. \quad & (a)\ P(A+B_2F)+(A+B_2F)^TP\le 0, \\ & (b)\ \alpha X_R\subset\mathcal{E}(P,\rho)\subset\mathcal{L}(F,\bar{u}). \end{aligned} \tag{7.15}$$

Therefore, if our only purpose is to enlarge the region of attraction, we might as well solve the simpler optimization problem (7.15). The resulting invariant ellipsoid will lie in the linear region of the saturation function $\sigma(Fx)$. If other performance requirements are involved, we might choose the optimization parameter H in (7.14) equal to the optimal value of (7.15), namely $H=F^*$, and then with a known domain $\mathcal{L}(H,\bar{u})$, we may choose the controller from all the F's that satisfy (7.14) to optimize the other performance requirements. ⊗

7.2.4 Disturbance rejection bound

Due to the saturation nonlinearity, the system (7.1) with saturated control $\sigma(Fx)$ cannot reject all kinds of disturbances. In robust control, the disturbance inputs are usually described by their energy. Therefore, we would like to estimate the largest disturbance rejection bound in a finite region.

Definition 7.2. *The number $\hat{\beta}_w\in\mathcal{R}_+$ will be called an r-level disturbance rejection bound if whenever $||w||_{L_2}^2\le\hat{\beta}_w$ and $x(0)=0$, we have $\lim_{t\to\infty}x(t)=0$ and $x(t)\in\mathcal{R}_r$ for all $t\ge 0$. The largest such number will be denoted by β_w.*

Via the LMI optimization approach, next proposition establishes an estimate of the bound $\hat{\beta}_w$ for the system (7.1) with saturated input $\sigma(Fx)$.

Proposition 7.3. *For the system (7.1) with $x \in \mathcal{L}(F,r)$, i.e., $|f_i x| \le r_i$ for $i \in [1,m]$, a disturbance rejection bound $\hat{\beta}_w$ can be computed as $\hat{\beta}_w = 1/t_r^*$, where t_r^* is the optimal value of the following LMI optimization problem in the variables $P = P^T$, H and t_r:*

$$\begin{aligned} \min_{t_r>0,P>0,H} \quad & t_r \\ s.t.\ (a)\quad & P(A + B_2M(\nu,F,H)) + (A + B_2M(\nu,F,H))^T P + PB_1B_1^T P \le 0,\ \forall \nu \in \mathcal{V}, \\ (b)\quad & \mathcal{E}(P,1/t_r) \subset \mathcal{L}(F,r), \qquad \mathcal{E}(P,1/t_r) \subset \mathcal{L}(H,\bar{u}). \end{aligned} \tag{7.16}$$

Furthermore, whenever $||w||_{L_2}^2 \le 1/t_r$ and $x(0) = 0$, $x(t)$ will never leave $\mathcal{E}(P,1/t_r)$.

Proof. Let $V = x^T Px$. With the result in Lemma 7.2, it follows that there exists a real matrix H such that for all $x \in \mathcal{E}(P,1/t_r) \subset \mathcal{L}(H,\bar{u})$, we have

$$\dot{V} \le x^T[P(Ax + B_2M(\nu,F,H)) + (Ax + B_2M(\nu,F,H))^T P + PB_1B_1^T P]x + w^T w,$$

where $\nu \in \mathcal{V}$ with ν_i taking values 0 or 1. If $x(0) = 0$ and $||w||_{L_2}^2 \le 1/t_r$, (7.16a) implies that

$$V(x(t)) = x^T Px \le ||P_t w||_{L_2}^2 \le 1/t_r$$

for all $t \ge 0$, where P_t is the truncation operator defined by (2.4). Hence, $x(t) \in \mathcal{E}(P,1/t_r)$ for all $t \ge 0$.

Then, we determine the minimum of $x^T Px$ subject to the constraints $|f_i x| = r_i$ for $i \in [1,m]$, which is a convex optimization problem and has a unique minimum. Using the Lagrange multiplier method, we obtain

$$\min_x \{x^T Px :\ f_i x = r_i\} = r_i^2 (f_i P^{-1} f_i^T)^{-1}.$$

Consequently, we can choose the maximal disturbance rejection bound $\hat{\beta}_w$ as

$$\hat{\beta}_w = 1/t_r = \min_{i\in[1,m]} r_i^2 (f_i P^{-1} f_i^T)^{-1}$$

by minimizing the value of t_r with respect to P, which implies that

$$\forall i \in [1,m],\ \ f_i P^{-1} f_i^T \le r_i^2 t_r \iff \forall i \in [1,m],\ \ 1/t_r \le \min_x \{x^T Px :\ f_i x = r_i\}.$$

On the other hand, we have the equivalence:

$$\forall i \in [1,m],\ \ 1/t_r \le \min_x \{x^T Px :\ f_i x = r_i\} \iff \mathcal{E}(P,1/t_r) \subset \mathcal{L}(F,r). \tag{7.17}$$

To see this, note that $\mathcal{E}(P,1/t_r) \subset \mathcal{L}(F,r)$ if and only if all the hyperplanes $f_i x = r_i$, $\forall i \in [1,m]$, lie completely outside the ellipsoid $\mathcal{E}(P,1/t_r)$, i.e., at each point x on the hyperplanes $f_i x = \pm r_i$, we have $x^T Px \ge 1/t_r$. □

Corollary 7.4. *If $|f_i x| \le \bar{u}$ for each $i = 1, \ldots, m$, the largest disturbance reject bound $\hat{\beta}_w$ for the system (7.1) can be computed as*

$$\hat{\beta}_w = \min_{i\in[1,m]} \bar{u}^2 (f_i P^{-1} f_i^T)^{-1},$$
$$P(A + B_2F) + (A + B_2F)^T P + PB_1B_1^T P \le 0, \quad \mathcal{E}(P, \hat{\beta}_w) \subset \mathcal{L}(F, \bar{u})$$

7.3 Local H_2 Performance Analysis and Synthesis

7.3.1 H_2 performance analysis

In most applications, it is desirable to keep the peak amplitude of the output $y(t)$ below a certain level. For linear systems without input saturations, the H_2 performance can be formulated by $||T_{yw}(s)||_2$, where $T_{yw}(s)$ is the linear transfer matrix from the generalized disturbances w to the performance output y,

$$T_{yw}(s) = \left[\begin{array}{c|c} A + B_2F & B_1 \\ \hline C_1 + D_{12}F & 0 \end{array}\right].$$

It is well known [95, 138] that the norm $||T_{yw}(s)||_2$ can be computed as

$$||T_{yw}(s)||_2 = \text{Trace}((C_1 + D_{12}F)S_1(C_1 + D_{12}F)^T),$$

where $S_1 = S_1^T > 0$ solves the Lyapunov equation

$$(A + B_2F)S_1 + S_1(A + B_2F)^T + B_1B_1^T = 0. \tag{7.18}$$

The solvability of (7.18) by a positive definite symmetric matrix S_1 is a sufficient and necessary condition for the existence of the norm $||T_{yw}(s)||_2$. (See [30, 138, 139].)

However, for linear systems with saturated inputs as in (7.1), it is not feasible to use the transfer matrix $T_{yw}(s)$ to define the H_2 performance. If the disturbance input $w(t)$ is still quantified by its finite energy, we can consider the so-called generalized H_2-norm [91, 92, 97] defined by

$$||T_{yw}||_2 \triangleq \sup\left\{\frac{||y(t)||}{||w||_{L_2}} : x(0) = 0, t \ge 0, \int_0^t ||w(\tau)||^2 d\tau \le \beta_w\right\}. \tag{7.19}$$

This measures the peak amplitude of the output signal $y(t)$ over all energy-bounded inputs $w(t)$ in the time-domain. We define our H_2 optimal problem as follows.

Definition 7.3 (Local generalized H_2-norm bound). *Any number $\hat{\alpha}_2 \in \mathcal{R}_+$ such that whenever $||w||_{L_2}^2 \le \beta_w$ and $x(0) = 0$ we have $x(t) \in \mathcal{D}$ for all $t \ge 0$, $\lim_{t\to\infty} x(t) = 0$ and $||y(t)||^2 \le \hat{\alpha}_2 \int_0^t ||w(\tau)||^2 d\tau$ for all $t \ge 0$, is called a generalized H_2-norm bound in the finite region $\mathcal{D}$. The smallest such number is denoted by α_2.*

Exploiting the slope condition of the saturation function, the next theorem presents a sufficient condition for the local existence of the generalized H_2 performance.

Lemma 7.5. *Suppose that $\beta_w = \rho$, i.e., $||w||_{L_2}^2 \leq \rho$. If there exist a positive definite symmetric matrix P, a positive diagonal matrix S_1, two real matrices H and $\tilde{H}$, and a positive constant α_2 satisfying the inequalities*

$$P(A + B_2M(\nu, F, H)) + (A + B_2M(\nu, F, H))^T P + PB_1B_1^T P \leq 0, \quad \nu \in \mathcal{V}, \tag{7.20}$$

$$\begin{bmatrix} (C_1 + D_{12}\tilde{H})^T(C_1 + D_{12}\tilde{H}) - \alpha_2 P & * \\ D_{12}^T(C_1 + D_{12}\tilde{H}) + S_1(F - \tilde{H}) & D_{12}^T D_{12} - 2S_1 \end{bmatrix} \leq 0, \tag{7.21}$$

$\mathcal{E}(P, \rho) \subset \mathcal{L}(H, \bar{u})$ and $\mathcal{E}(P, \rho) \subset \mathcal{L}(\tilde{H}, \bar{u})$, then α_2 is a generalized H_2-norm for the system (7.1)–(7.3) in the finite region $\mathcal{E}(P, \rho)$.

Proof. Let $V = x^T Px$. With the result in Lemma 7.2, it follows that

$$\begin{aligned} \dot{V} &= 2x^T P(Ax + B_1w + B_2\sigma(Fx)) \\ &\leq x^T[P(Ax + B_2M(\nu, F, H)) + (Ax + B_2M(\nu, F, H))^T P + PB_1B_1^T P]x + w^T w, \end{aligned}$$

where $\nu \in \mathcal{V}$ with ν_i taking values 0 or 1. If (7.20) is satisfied, it follows that

$$V(x(t)) = x^T Px \leq ||P_t w||_{L_2}^2 \leq \rho, \quad \forall t \geq 0,$$

where P_t is the truncation operator defined by (2.4). Since $\mathcal{E}(P, \rho) \subset \mathcal{L}(\tilde{H}, \bar{u})$, it follows that $\sigma(\tilde{H}x) = \tilde{H}x$ for all $x \in \mathcal{E}(P, \rho)$. Thus, we can rewrite the output y as

$$y = (C_1 + D_{12}\tilde{H})x + D_{12}[\sigma(Fx) - \sigma(\tilde{H}x)].$$

Obviously,

$$y^T y - \alpha_2 x^T Px = \begin{bmatrix} x \\ \Delta\sigma \end{bmatrix}^T \begin{bmatrix} (C_1 + D_{12}\tilde{H})^T(C_1 + D_{12}\tilde{H}) - \alpha_2 P & * \\ D_{12}^T(C_1 + D_{12}\tilde{H}) & D_{12}^T D_{12} \end{bmatrix} \begin{bmatrix} x \\ \Delta\sigma \end{bmatrix}$$

with the notation $\Delta\sigma = \sigma(Fx) - \sigma(\tilde{H}x)$. Since the saturation function $\sigma(Fx)$ defined by (7.5) belongs to sector$[0, 1]$ and is monotonically non-decreasing, the inequality

$$[\sigma(Fx) - \sigma(\tilde{H}x)]^T S_1[\sigma(Fx) - \sigma(\tilde{H}x)] \leq [\sigma(Fx) - \sigma(\tilde{H}x)]^T S_1(F - \tilde{H})x$$

is satisfied for any positive diagonal matrix S, implying

$$\begin{bmatrix} x \\ \Delta\sigma \end{bmatrix}^T \begin{bmatrix} 0 & -(F - \tilde{H})^T S_1 \\ -S_1(F - \tilde{H}) & 2S_1 \end{bmatrix} \begin{bmatrix} x \\ \Delta\sigma \end{bmatrix} \leq 0.$$

Hence, if (7.21) is satisfied for some positive diagonal matrix S, we have

$$||y(t)||^2 \leq \alpha_2 x(t)^T Px(t) = \alpha_2 V(x(t)) \leq \alpha_2 ||P_t w||_{L_2}^2$$

for all $t \geq 0$, where P_t is the truncation operator. Therefore, we conclude that the peak amplitude of the output $y(t)$ is under a certain level for all $t \geq 0$. □

Remark 7.2. If $C_1^T D_{12} = 0$ and $D_{12}^T D_{12}$ is positive diagonally dominant, using the properties of the pdd matrices[2], it is easy to verify that (7.21) can be replaced by

$$(C_1 + D_{12}F)^T(C_1 + D_{12}F) \leq \alpha_2 P. \tag{7.22}$$

These two additional constraints that $C_1^T D_{12} = 0$ and $D_{12}^T D_{12}$ is pdd are achievable if the designer has the freedom to select the matrices C_1 and D_{12}. However, such a replacement brings some conservatism to the performance analysis because a more conservative inequality $\sigma(Fx)^T D_{12}^T D_{12}\sigma(Fx) \leq x^T F^T D_{12}^T D_{12} Fx$, instead of the less conservative one $\sigma(Fx)^T D_{12}^T D_{12}\sigma(Fx) \leq \sigma(Fx)^T D_{12}^T D_{12} Fx$, is applied to derive (7.22).

Remark 7.3. When the system (7.1) works in its linear region, $|f_i x| \leq \bar{u}$, it is obvious that $M(\nu, F, H)$ can then be reduced to F by choosing $H = F$. Furthermore, if the system (7.1) is linear without input constraints, it was shown in [91, 97] that the sufficient condition (7.20)(7.22) is also a necessary condition for the generalized H_2 performance $||y(t)||_2^2 \leq \alpha_2 ||w||_{L_2}^2$ to hold. However, when there exist input saturations, constraint (7.20)(7.21) is only a sufficient condition, but not a necessary condition.

7.3.2 LMI of H_2 performance analysis

When $\rho \to 0$, the constraint $\mathcal{E}(P, \rho) \subset \mathcal{L}(H, \bar{u})$ will be removed and the region of attraction will be covered by the linear region of the system, which is not our major concerns. Since the energy level β_w of the disturbances is usually predetermined by the designer and the largest disturbance rejection bound of the system (7.1) is limited by the saturated controls, we could in this case fix the value of ρ to be such a bound in the analysis. Among all the ellipsoids satisfying the H_2 performance conditions, we would like to search for the positive definite solution P to (7.20)(7.21) such that the H_2 performance α_2 is minimized, which is formulated as an optimization problem:

$$\begin{aligned}
&\min_{P,H,\tilde{H},S_1,\alpha_2} \quad \alpha_2 \\
&s.t.\ (a)\quad P = P^T > 0,\ \alpha_2 > 0,\ S_1 > 0 \text{ is diagonal,} \\
&\quad (b)\quad P(A + B_2 M(\nu, F, H)) + (A + B_2 M(\nu, F, H))^T P + P B_1 B_1^T P \leq 0,\ \forall \nu \in \mathcal{V}, \\
&\quad (c)\quad \begin{bmatrix} (C_1 + D_{12}\tilde{H})^T(C_1 + D_{12}\tilde{H}) - \alpha_2 P & * \\ D_{12}^T(C_1 + D_{12}\tilde{H}) + S_1(F - \tilde{H}) & D_{12}^T D_{12} - 2S_1 \end{bmatrix} \leq 0, \\
&\quad (d)\quad \mathcal{E}(P, \rho) \subset \mathcal{L}(H, \bar{u}),\quad \mathcal{E}(P, \rho) \subset \mathcal{L}(\tilde{H}, \bar{u})
\end{aligned} \tag{7.23}$$

By the Schur Complements, the LMI (7.23c) is equivalent to

$$\begin{bmatrix} -P & (F - \tilde{H})^T S_1/\alpha_2 & (C_1 + D_{12}\tilde{H})^T \\ S_1(F - \tilde{H})/\alpha_2 & -2S_1/\alpha_2 & D_{12}^T \\ C_1 + D_{12}\tilde{H} & D_{12} & -\alpha_2 I \end{bmatrix} \leq 0. \tag{7.24}$$

[2]It was shown in [19–21] that the inequalities $\sigma(x)^T S\sigma(x) \leq \sigma(x)Sx \leq x^T Sx$ are satisfied for all x if and only if S is positive diagonally dominant (pdd for short), where $\sigma(x)$ is a saturation function, monotonically non-decreasing.

If $C_1^T D_{12} = 0$ and $D_{12}^T D_{12}$ is positive diagonally dominant, (7.23c) can be replaced by (7.22). By the Schur complements, (7.22) is equivalent to

$$\begin{bmatrix} P & (C_1 + D_{12}F)^T \\ (C_1 + D_{12}F) & \alpha_2 I \end{bmatrix} \geq 0, \quad C_1^T D_{12} = 0, \quad D_{12}^T D_{12} \text{ is pdd.} \tag{7.25}$$

The constraint $\mathcal{E}(P,\rho) \subset \mathcal{L}(H,\bar{u})$ is equivalent to a minimization problem

$$\min\{x^T P x : \ h_i x = \bar{u}\} \geq \rho, \qquad i = 1, 2, \cdots, m.$$

To see this, note that $\mathcal{E}(P,\rho) \subset \mathcal{L}(H,\bar{u})$ if and only if all the hyperplanes $h_i x = \pm\bar{u}$, $i = 1, 2, \cdots, m$, lie completely outside the ellipsoid $\mathcal{E}(P,\rho)$, i.e., at each point x on the hyperplanes $h_i x = \pm\bar{u}$, we have $x^T P x \geq \rho$. The minimization $\min\{x^T P x : \ h_i x = \bar{u}\}$ is a convex optimization problem and has a unique minimum. Applying the Lagrange multiplier method, we obtain

$$\min\{x^T P x : \ h_i x = \bar{u}\} = \bar{u}^2 (h_i P^{-1} h_i^T)^{-1}.$$

Consequently, the constraint $\mathcal{E}(P,\rho) \subset \mathcal{L}(H,\bar{u})$ is equivalent to

$$\rho h_i P^{-1} h_i^T \leq \bar{u}^2 \iff \begin{bmatrix} \bar{u}^2/\rho & h_i P^{-1} \\ P^{-1} h_i^T & P^{-1} \end{bmatrix} \geq 0, \qquad \forall i \in [1, m]. \tag{7.26}$$

Similarly, the constraint $\mathcal{E}(P,\rho) \subset \mathcal{L}(\tilde{H},\bar{u})$ is equivalent to

$$\rho \tilde{h}_i P^{-1} \tilde{h}_i^T \leq \bar{u}^2 \iff \begin{bmatrix} \bar{u}^2/\rho & \tilde{h}_i P^{-1} \\ P^{-1} \tilde{h}_i^T & P^{-1} \end{bmatrix} \geq 0, \qquad \forall i \in [1, m], \tag{7.27}$$

where $\tilde{h}_i$ is the i-row of the matrix $\tilde{H}$.

Denote $\tilde{\rho} = 1/\rho$. To make the LMI optimization problem (7.23) more tractable, let

$$Q = P^{-1}, \qquad G = HQ, \qquad \tilde{G} = \tilde{H}Q, \qquad T_1 = (S_1/\alpha_2)^{-1}.$$

Also let the ith row of G be g_i and the ith row of $\tilde{G}$ be $\tilde{g}_i$, i.e.,

$$g_i = h_i Q = h_i P^{-1}, \qquad \tilde{g}_i = \tilde{h}_i Q = \tilde{h}_i P^{-1}.$$

Thus, we can transform (7.23) into a convex LMI optimization problem as

$$\min_{Q, T_1, G, \tilde{G}, \alpha_2} \ \alpha_2$$

$$s.t. \ (a) \ \ Q = Q^T > 0, \ \alpha_2 > 0, \ T_1 > 0 \text{ is diagonal},$$

$$(b) \ \ AQ + QA^T + B_2 M(\nu, FQ, G) + M(\nu, FQ, G)^T B_2^T + B_1 B_1^T \leq 0, \quad \forall \nu \in \mathcal{V},$$

$$(c) \ \ \begin{bmatrix} -Q & QF^T - \tilde{G}^T & QC_1^T + \tilde{G}^T D_{12}^T \\ FQ - \tilde{G} & -2T_1 & T_1 D_{12}^T \\ C_1 Q + D_{12}\tilde{G} & D_{12} T_1 & -\alpha_2 I \end{bmatrix} \leq 0,$$

$$(d)\quad \begin{bmatrix} \bar{u}^2\tilde{\rho} & g_i \\ g_i^T & Q \end{bmatrix} \geq 0, \quad \begin{bmatrix} \bar{u}^2\tilde{\rho} & \tilde{g}_i \\ \tilde{g}_i^T & Q \end{bmatrix} \geq 0, \quad i \in [1, m]. \tag{7.28}$$

If $C_1^T D_{12} = 0$ and $D_{12}^T D_{12}$ is a pdd matrix, (7.28c) can be replaced by

$$(c')\quad \begin{bmatrix} Q & Q(C_1 + D_{12}F)^T \\ (C_1 + D_{12}F)Q & \alpha_2 I \end{bmatrix} \geq 0. \tag{7.29}$$

Remark 7.4. When the system (7.1) is linear without input constraints, the LMI (7.28d) is removed and the matrix $M(\nu, FQ, G)$ in (7.28b) is reduced to FQ. Thus, the optimization problem (7.28) becomes a standard generalized H_2-optimal problem. In this case, it was shown in [97] that the solvability of (7.28) is a necessary and sufficient condition for the existence of the generalized H_2-norm performance α_2. ⊗

7.3.3 Local H_2 Performance Synthesis

Having analyzed the H_2 performance when the feedback matrix F is given, we may ask: can we design a H_2 optimal controller F^* to minimize the H_2 performance level? To answer this question, we take the controller gain F as an additional optimization parameter and choose an optimal feedback matrix F^* that corresponds to the minimal H_2 performance level α_2^*. Similar to (7.28), by using a new parameter Y to replace FQ, the resulting optimization problem is formulated as follows.

$$\begin{aligned} &\min_{Q,\tilde{G},G,Y,T_1,\alpha_2} \quad \alpha_2 \\ &s.t.\ (a)\ \ Q = Q^T > 0,\ \alpha_2 > 0,\ T_1 > 0 \text{ is diagonal}, \\ &\quad (b)\ \ AQ + QA^T + B_2 M(\nu, Y, G) + M(\nu, Y, G)^T B_2^T + B_1 B_1^T \leq 0, \quad \forall \nu \in \mathcal{V}, \\ &\quad (c)\ \ \begin{bmatrix} -Q & Y^T - \tilde{G}^T & QC_1^T + \tilde{G}^T D_{12}^T \\ Y - \tilde{G} & -2T_1 & T_1 D_{12}^T \\ C_1 Q + D_{12}\tilde{G} & D_{12}T_1 & -\alpha_2 I \end{bmatrix} \leq 0, \\ &\quad (d)\ \ \begin{bmatrix} \bar{u}^2\tilde{\rho} & g_i \\ g_i^T & Q \end{bmatrix} \geq 0, \quad \begin{bmatrix} \bar{u}^2\tilde{\rho} & \tilde{g}_i \\ \tilde{g}_i^T & Q \end{bmatrix} \geq 0, \quad i \in [1, m]. \end{aligned} \tag{7.30}$$

The H_2 optimal control matrix F^* will be recovered by $F = YQ^{-1}$.

If $C_1^T D_{12} = 0$ and $D_{12}^T D_{12}$ is pdd, (7.30c) can be replaced by

$$(c'')\quad \begin{bmatrix} Q & QC_1 + Y^T D_{12}^T \\ C_1 Q + D_{12} Y & \alpha_2 I \end{bmatrix} \geq 0, \quad C_1^T D_{12} = 0, \quad D_{12}^T D_{12} \text{ is pdd}. \tag{7.31}$$

Remark 7.5. When (7.1) is linear without input saturations, the constraint (7.30d) is removed and the matrix $M(\nu, Y, G)$ in (7.30b) can be reduced to Y. Thus, the LMI problem (7.30) becomes a standard H_2-optimal control problem [97]. In this linear case, it was shown in [91, 92, 138] that the existence of an H_2 optimal control F for the system (7.1) with the control inputs $u = Fx$ is a necessary and sufficient condition for

the solvability of the following LMI optimization problem:

$$\begin{aligned} \min_{Q>0,Y,\alpha_2>0} \quad & \alpha_2 \\ s.t.\ (a) \quad & AQ + QA^T + B_2Y + Y^TB_2^T + B_1B_1^T \le 0, \\ (b) \quad & \begin{bmatrix} -Q & (C_1Q + D_{12}Y)^T \\ C_1Q + D_{12}Y & -\alpha_2 I \end{bmatrix} \le 0. \end{aligned} \tag{7.32}$$

Then, the optimal control F^* is recovered by $F^* = YQ^{-1}$. ⊗

7.4 Local H_∞ Performance Analysis and Synthesis

The H_∞ norm γ is a measure of robust stability of input-to-output systems with respect to disturbances and uncertainties. Let T_{zw} denote an operator from the disturbances w to the output z. Then, the constraint $||T_{zw}||_\infty < \gamma$ can be interpreted as a disturbance rejection performance and is also useful to enhance robust stability. Specially, it guarantees that the closed-loop system remains robustly stable for all perturbations $w = \Delta(z)$ with $||\Delta||_\infty < 1/\gamma$. A smaller H_∞ gain γ implies better disturbance attenuation performance and better robust stability.

7.4.1 Analysis: A sufficient condition

Definition 7.4. *Any number $\hat{\gamma} \in \mathcal{R}_+$ such that whenever $||w||_{L_2}^2 \le \beta_w$ and $x(0) = 0$, we have $x(t) \in \mathcal{D}$ for all $t \ge 0$, $\lim_{t\to\infty} x(t) = 0$ and $||z||_{L_2} \le \hat{\gamma}^2||w||_{L_2}^2$ will be called a local L_2-gain in the finite region $\mathcal{D}$. The smallest such number will be denoted by γ.*

The next lemma establishes a sufficient condition for the existence of the local $\mathcal{L}_2$-gain in the finite region $\mathcal{E}(P,\rho) \subset \mathcal{L}(H,\bar{u})$.

Lemma 7.6. *Given $\gamma^2 > ||D_{21}^TD_{21}||$. If there exist a positive definite symmetric matrix P, a positive diagonal matrix S_2 and two real matrices H and $\hat{H}$ satisfying*

$$\begin{bmatrix} P\bar{A} + \bar{A}^TP + \gamma^{-2}\bar{C}_2^T\bar{C}_2 & * & * \\ B_1^TP + \gamma^{-2}D_{21}^T\bar{C}_2 & -I + \gamma^{-2}D_{21}^TD_{21} & * \\ \gamma^{-2}D_{22}^T\bar{C}_2 + S_2(F - \hat{H}) & \gamma^{-2}D_{22}^TD_{21} & -2S_2 + \gamma^{-2}D_{22}^TD_{22} \end{bmatrix} \le 0, \tag{7.33}$$

$$\mathcal{E}(P,\rho) \subset \mathcal{L}(H,\bar{u}), \qquad \mathcal{E}(P,\rho) \subset \mathcal{L}(\hat{H},\bar{u}), \tag{7.34}$$

where $\bar{C}_2 = C_2 + D_{22}\hat{H}$ and $\bar{A} = A + B_2M(\nu,F,H)$, $\forall\nu \in \mathcal{V}$, then, $||z||_{L_2}^2 \le \gamma^2||w||_{L_2}^2$ in the finite region $\mathcal{E}(P,\rho) \subset \mathcal{L}(H,\bar{u})$.

Proof. Since $\mathcal{E}(P,\rho) \subset \mathcal{L}(\hat{H},\bar{u})$, it follows that $\sigma(\hat{H}x) = \hat{H}x$ for all $x \in \mathcal{E}(P,\rho)$. Thus, we can represent the output function z as

$$z = (C_2 + D_{22}\hat{H})x + D_{21}w + D_{22}[\sigma(Fx) - \sigma(\hat{H}x)].$$

Let $V = x^T P x$, and denote $\bar{C}_2 = C_2 + D_{22}F_2$ and $\hat{\Delta}\sigma = \sigma(Fx) - \sigma(\hat{H}x)$. With the results in Lemma 7.2, for all $x \in \mathcal{E}(P,\rho) \subset \mathcal{L}(H,\bar{u})$, it follows that

$$\begin{aligned}
\dot{V} &= x^T(PA + A^TP + \gamma^{-2}\bar{C}_2^T\bar{C}_2)x + 2x^T(PB_1 + \gamma^{-2}\bar{C}_2^T D_{21})w + 2x^T PB_2\sigma(Fx) \\
&\quad + 2\gamma^{-2}w^T D_{21}^T D_{22}\hat{\Delta}\sigma + w^T(\gamma^{-2}D_{21}^T D_{21} - I)w + 2\gamma^{-2}x^T\bar{C}_2^T D_{22}\hat{\Delta}\sigma \\
&\quad + 2\gamma^{-2}(\hat{\Delta}\sigma)^T D_{22}^T D_{22}\hat{\Delta}\sigma - \gamma^{-2}||z||^2 + ||w||^2 \\
&\leq \begin{bmatrix} x \\ w \\ \hat{\Delta}\sigma \end{bmatrix}^T \begin{bmatrix} P\bar{A} + \bar{A}^TP + \gamma^{-2}\bar{C}_2^T\bar{C}_2 & * & * \\ B_1^TP + \gamma^{-2}D_{21}^T\bar{C}_2 & \gamma^{-2}D_{21}^TD_{21} - I & * \\ \gamma^{-2}D_{22}^T\bar{C}_2 + S_2(F-\hat{H}) & \gamma^{-2}D_{22}^TD_{21} & \gamma^{-2}D_{22}^TD_{22} - 2S_2 \end{bmatrix} \begin{bmatrix} x \\ w \\ \hat{\Delta}\sigma \end{bmatrix} \\
&\quad + 2(\hat{\Delta}\sigma)^T S_2\hat{\Delta}\sigma - 2(\hat{\Delta}\sigma)^T S_2(F-\hat{H})x - \gamma^{-2}||z||^2 + ||w||^2,
\end{aligned}$$

where $\bar{A} = A + B_2M(\nu,F,H)$ for all $\nu \in \mathcal{V}$. Since the saturation function $\sigma(Fx)$ defined by (7.5) belongs to sector$[0,1]$ and is monotonically non-decreasing, it follows that the inequality

$$[\sigma(Fx) - \sigma(\hat{H}x)]^T S_2[\sigma(Fx) - \sigma(\hat{H}x)] \leq [\sigma(Fx) - \sigma(\hat{H}x)]^T S_2(F-\hat{H})x$$

is always satisfied for any positive diagonal matrix S_2. Hence, if (7.33) is satisfied, it follows that in the region $\mathcal{E}(P,\rho) \subset \mathcal{L}(H,\bar{u})$,

$$\dot{V} \leq -\gamma^{-2}||z||^2 + ||w||^2,$$

which means that the closed-loop system is locally $\mathcal{L}_2$ stable in the finite region $\mathcal{E}(P,\rho)$ from the input w to the output z with a finite $\mathcal{L}_2$-gain γ, i.e., there exists a finite $\gamma > 0$ such that $||z||_{L_2}^2 \leq \gamma^2||w||_{L_2}^2$ in the finite region $\mathcal{E}(P,\rho)$. □

Remark 7.6. *If $D_{21}^TD_{22} = 0$, $C_2^TD_{22} = 0$ and $D_{22}^TD_{22}$ is pdd, then it is easy to verify that (7.33) can be replaced by*

$$\begin{bmatrix} P\bar{A} + \bar{A}^TP + \gamma^{-2}C_2^TC_2 + \gamma^{-2}F^TD_{22}^TD_{22}F & PB_1 + \gamma^{-2}C_2^TD_{21} \\ B_1^TP + \gamma^{-2}D_{21}^TC_2 & -I + \gamma^{-2}D_{21}^TD_{21} \end{bmatrix} \leq 0. \qquad (7.35)$$

This is possible if the designer has the freedom to choose the matrices C_2, D_{21} and D_{22}. However, such a replacement brings some conservatism to the local H_∞ performance analysis because a more conservative inequality $\sigma(Fx)^TD_{22}^TD_{22}\sigma(Fx) \leq x^TF^TD_{22}^TD_{22}Fx$, instead of the less conservative one $\sigma(Fx)^TD_{22}^TD_{22}\sigma(Fx) \leq \sigma(Fx)^TD_{22}^TD_{22}Fx$, is used to derive (7.35) if $D_{22}^TD_{22}$ is pdd.

7.4.2 Optimization using LMI approach

The sufficient condition (7.33) can be rewritten as

$$\begin{bmatrix} P\bar{A} + \bar{A}^TP & PB_1 & (F-\hat{H})^TS_2 \\ B_1^TP & -I & 0 \\ S_2(F-\hat{H}) & 0 & -2S_2 \end{bmatrix} - \frac{1}{\gamma^2}\begin{bmatrix} \bar{C}_2^T \\ D_{21}^T \\ D_{22}^T \end{bmatrix}\begin{bmatrix} \bar{C}_2 & D_{21} & D_{22} \end{bmatrix} \leq 0. \qquad (7.36)$$

By Schur complements, the inequality (7.36) is equivalent to

$$\begin{bmatrix} P(A+B_2M(\nu,F,H))+(A+B_2M(\nu,F,H))^TP & * & * & * \\ B_1^TP & -I & 0 & * \\ S_2(F-\hat{H}) & 0 & -2S_2 & * \\ (C_2+D_{22}\hat{H}) & D_{21} & D_{22} & -\gamma^2 I \end{bmatrix} \le 0. \quad (7.37)$$

Let

$$Q=P^{-1}, \qquad G=HP^{-1}, \qquad \hat{G}=\hat{H}P^{-1}, \qquad T_2=S_2^{-1},$$

and let the ith row of G be g_i and the ith row of $\hat{G}$ be $\hat{g}_i$, i.e.,

$$g_i=h_iQ, \qquad \hat{g}_i=\hat{h}_iQ.$$

Then, we can represent the H_∞ optimization problem as a convex LMI problem

$$\begin{aligned} &\min_{Q,T_2,G,\hat{G},\gamma} \quad \gamma \\ &s.t.\ (a)\ Q=Q^T>0,\ \gamma>0,\ T_2>0 \text{ is diagonal}, \\ &(b)\ \begin{bmatrix} AQ+QA^T+B_2M+M^TB_2^T & * & * & * \\ B_1^T & -I & 0 & * \\ FQ-\hat{G} & 0 & -2T_2 & * \\ C_2Q+D_{22}\hat{G} & D_{21} & D_{22}T_2 & -\gamma^2 I \end{bmatrix} \le 0, \\ &(c)\ \begin{bmatrix} \bar{u}^2\tilde{\rho} & g_i \\ g_i^T & Q \end{bmatrix} \ge 0, \qquad \begin{bmatrix} \bar{u}^2\tilde{\rho} & \hat{g}_i \\ \hat{g}_i^T & Q \end{bmatrix} \ge 0, \qquad i\in[1,m] \end{aligned} \quad (7.38)$$

with $M=M(\nu,FQ,G)$ for all $\nu\in\mathcal{V}$.

Remark 7.7. If $D_{21}^TD_{22}=0$, $C_2^TD_{22}=0$ and $D_{22}^TD_{22}$ is pdd, the LMI (7.38b) could be replaced by

$$\begin{bmatrix} AQ+B_2M(\nu,FQ,G))+QA^T+M(\nu,FQ,G)^TB_2^T & * & * \\ B_1^T & -I & * \\ C_2Q+D_{22}FQ & D_{21} & -\gamma^2 I \end{bmatrix} \le 0, \quad \forall \nu\in\mathcal{V}.$$

Remark 7.8. If the system is linear without input saturation, namely $u=Fx$, (7.38c) is removed and then the H_∞ performance analysis can be done by solving the LMI in Remark 7.7 with the matrix $M(\nu,FQ,G)$ being replaced by FQ. ⊗

7.4.3 Synthesis

Having analyzed the H_∞ performance when the feedback matrix F is given, we turn to the design of an H_∞ controller to minimize the local L_2-gain. Taking the controller gain F as an additional optimization parameter, we can choose a feedback matrix F to minimize the L_2-gain γ.

Similar to (7.28), by using a new parameter Y to replace FQ, the resulting opti-

mization problem is formulated as follows.

$$\begin{aligned}
&\min_{Q,T_2,Y,G,\hat{G},\gamma} \quad \gamma \\
&s.t.\ (a)\ \ Q = Q^T > 0,\ \gamma > 0,\ T_2 > 0 \text{ is diagonal,} \\
&(b)\ \ \begin{bmatrix} AQ + QA^T + B_2M(\nu,Y,G) + M(\nu,Y,G)^TB_2^T & * & * & * \\ B_1^T & -I & 0 & * \\ Y - \hat{G} & 0 & -2T_2 & * \\ C_2Q + D_{22}\hat{G} & D_{21} & D_{22}T_2 & -\gamma^2 I \end{bmatrix} \leq 0, \\
&\qquad \nu \in \mathcal{V}, \\
&(c)\ \ \begin{bmatrix} \bar{u}^2\tilde{\rho} & g_i \\ g_i^T & Q \end{bmatrix} \geq 0, \qquad \begin{bmatrix} \bar{u}^2\tilde{\rho} & \hat{g}_i \\ \hat{g}_i^T & Q \end{bmatrix} \geq 0, \qquad i \in [1,m].
\end{aligned} \tag{7.39}$$

The H_∞-optimal control gain F will be recovered by $F = YQ^{-1}$.

Remark 7.9. If $D_{21}^TD_{22} = 0$, $C_2^TD_{22} = 0$ and $D_{22}^TD_{22}$ is pdd. Then, (7.39b) can be replaced by

$$\begin{bmatrix} AQ + B_2M(\nu,Y,G)) + QA^T + M(\nu,Y,G)^TB_2^T & * & * \\ B_1^T & -I & * \\ C_2Q + D_{22}Y & D_{21} & -\gamma^2 I \end{bmatrix} \leq 0,\ \forall \nu \in \mathcal{V}. \tag{7.40}$$

Remark 7.10. If the system is linear without input saturation, (7.39c) is removed and then the H_∞ optimal control can be obtained by solving the LMI (7.40) with the matrix $M(\nu,Y,G)$ being replaced by Y. ⊗

7.4.4 Mixed H_2/H_∞ suboptimal controller

The LMI formulations of closed-loop system specifications under H_2 and H_∞ performance considerations have been summarized as above with different matrices P's. The LMI formulation of the mixed H_2/H_∞ suboptimal controller synthesis is based on the *Lyapunov shaping paradigm* [97] by seeking for a common Lyapunov matrix P to fulfill the LMI constraints. Undoubtedly, it brings some conservatism. However, such conservatism is paid by the following merits. First, it makes a large set of LMIs become more easily tractable. Second, the common Lyapunov matrix P is shaped by the LMI optimization until either all specifications are met or all degrees of freedom are exhausted. The mixed H_2/H_∞ suboptimal control problem is defined in a local region as follows.

Definition 7.5. *Assume that* $||w||_{L_2}^2 \leq \beta_w$ *and* $x(0) = 0$. *The mixed* H_2/H_∞ *control problem is to find a control* F *to minimize* α_2 *such that* $||y(t)||^2 \leq \alpha_2||w||_{L_2}^2$ *subject to the constraint* $||z||_{L_2}^2 \leq \gamma^2||w||_{L_2}^2$ *for a given* $\gamma^2 > ||D_{21}^TD_{21}||$.

Combing the optimization problems (7.30) and (7.39), in the finite region $\mathcal{E}(P,\rho) \subset \mathcal{L}(H,\bar{u})$, we can formulate the local mixed H_2/H_∞ suboptimal control problem into

the following LMI optimization problem:

$$\begin{aligned} \min_{Q,\tilde{G},G,Y,T_1,T_2,\alpha_2} \quad & \alpha_2 \\ s.t. \quad & Q = Q^T > 0,\ \alpha_2 > 0,\ T_1 \text{ and } T_2 \text{ is positive diagonal}, \qquad (7.41) \\ & (7.30c),\quad (7.39b),\quad (7.39c), \qquad (7.42) \end{aligned}$$

in which γ is given. With this optimization, the mixed H_2/H_∞ suboptimal controller is recovered by $F = YQ^{-1}$. Note that (7.30b) is implied by (7.39b).

Specially, if $C_1^T D_{12} = 0$, $C_2^T D_{22} = 0$, $D_{21}^T D_{22} = 0$, $D_{12}^T D_{12}$ and $D_{22}^T D_{22}$ are pdd, the optimization problem (7.41) is replaced by

$$\begin{aligned} \min_{Q,G,Y,\alpha_2} \quad & \alpha_2 \\ s.t. \quad & (7.31),\quad (7.40),\quad (7.39c),\quad Q = Q^T > 0,\quad \alpha_2 > 0. \qquad (7.43) \end{aligned}$$

When the input/output system (7.1)–(7.4) is linear without input saturation nonlinearity, the constraints $\mathcal{E}(P,\rho) \subset \mathcal{L}(H,\bar{u})$ and $\mathcal{E}(P,\rho) \subset \mathcal{L}(\hat{H},\bar{u})$ are removed and thus it is obvious that $M(\nu,Y,G)$ is reduced to Y. Then, the optimization problem (7.43) becomes a standard mixed H_2/H_∞ optimal control problem [30, 91, 92, 97] for linear systems, i.e., to find a positive definite symmetric matrix Q and a matrix Y such that for a given γ, the control law $F = YQ^{-1}$ minimizes

$$\begin{aligned} \min_{Q>0,Y,\alpha_2} \quad & \alpha_2 \\ s.t.\ (a) \quad & \begin{bmatrix} Q & QC_1^T + Y^T D_{12}^T \\ C_1 Q + D_{12} Y & \alpha_2 I \end{bmatrix} > 0, \\ (b) \quad & \begin{bmatrix} AQ + QA^T + B_2 Y + Y^T B_2^T & B_1 & QC_2^T + Y^T D_{22}^T \\ B_1^T & -I & D_{21}^T \\ C_2 Q + D_{22} Y & D_{21} & -\gamma^2 I \end{bmatrix} \le 0. \end{aligned} \qquad (7.44)$$

7.5 Synthesis Models of Linear Attitude Control

7.5.1 Structured uncertainty modelling

The following procedure for modelling structured uncertainty is motivated by the works of [129, 130, 136]. Consider a dynamical system described by

$$E\dot{x} = Fx + G_d d + G_u u$$

where x, d, and u are the state, disturbance input and control input vectors respectively; G_d is the disturbance input distribution matrix; G_u is the control input distribution matrix; and the matrices E and F are subject to structured parameter variations.

Suppose that there are l independent, uncertain parameters variations δ_i, and as-

sume that the perturbed matrices E and F can be linearly decomposed as follows:

$$E = E_0 + \Delta E = E_0 + \sum_{i=1}^{l} \Delta E_i \delta_i = E_0 + \sum_{i=1}^{l} M_E^{(i)} \delta_i I_{\varsigma_i} N_E^{(i)} = E_0 + M_E \Pi_E N_E,$$
$$F = F_0 + \Delta F = F_0 + \sum_{i=1}^{l} \Delta F_i \delta_i = F_0 + \sum_{i=1}^{l} M_F^{(i)} \delta_i I_{\upsilon_i} N_F^{(i)} = F_0 + M_F \Pi_F N_F,$$

where ς_i is the rank of ΔE_i, υ_i is the rank of ΔF_i, Π_E and Π_F are diagonal matrices with δ_i as their diagonal elements. Let

$$\Pi = \text{diag}\{\Pi_E, \Pi_F\}, \qquad \tilde{z} = \begin{bmatrix} N_E \dot{x} \\ N_F x \end{bmatrix}, \qquad \tilde{d} = -\Pi \tilde{z},$$

where $\tilde{d}$ is called the fictitious disturbance input, $\tilde{z}$ the fictitious output, and Π the gain matrix of the fictitious internal feedback loop, which are caused by the uncertainties in the matrices E and F. Then it follows

$$E_0 \dot{x} = F_0 x + G_{\tilde{d}} \tilde{d} + G_d d + G_u u,$$

where the matrix $G_{\tilde{d}}$ is the fictitious disturbance distribution matrix and defined by

$$G_{\tilde{d}} = [M_E \quad -M_F].$$

7.5.2 Linearized dynamical models of spacecraft

Taking the three principal axes of the spacecraft as the three axes of the body frame $\mathcal{F}_b$ and ignoring those (much smaller) off-diagonal elements, we assume, for simplicity of analysis, that the inertia matrix is of a diagonal form

$$J = \text{diag}\{J_1, J_2, J_3\}.$$

Suppose that three reaction wheels that are mounted along the three principal axes of the spacecraft are identical and the fourth wheel is installed as a backup and used only in the fault cases. The dynamic model of the reaction wheels had been presented in Section 4.4.2 as a first-order low-pass model (4.19), where the time constant τ_w is very small. The bounded wheel torques $\dot{H}_{wi}$ are fed into the attitude control system to control the attitude, where $\dot{H}_{wi} \in [-u_m, u_m]$ with $u_m = 0.03\text{Nm}$, $i = 1, 2, 3$.

To linearize the attitude dynamics, we assume that the roll angle φ, the pitch angle ϑ and the yaw angle ψ are small such that $\sin\vartheta \approx \vartheta$, $\sin\varphi \approx \varphi$ and $\sin\psi \approx \psi$. With this small-angle assumption, the angular velocity ω can be linearized as

$$\begin{aligned} \omega_1 &= \dot{\varphi} - n_0 \psi, \\ \omega_2 &= \dot{\vartheta} - n_0, \\ \omega_3 &= \dot{\psi} + n_0 \varphi, \end{aligned} \tag{7.45}$$

and the gravity-gradient torque T_{gd} in (4.20) can be approximated as

$$\begin{aligned} T_{gx} &= 3n_0^2(J_3 - J_2)\varphi, \\ T_{gy} &= 3n_0^2(J_3 - J_1)\vartheta, \\ T_{gz} &= 3n_0^2(J_2 - J_1)\vartheta\psi \approx 0. \end{aligned} \tag{7.46}$$

Assume that the microsatellite is rigid. As such, we ignore the dynamic equations of flexible modes. Substituting (7.45) and (7.46) into (4.17) and neglecting the motion of the flexure modes yields a linearized attitude dynamics as follows [53, 101]:

$$\begin{aligned} &J_1\ddot{\varphi} - n_0(J_1 - J_2 + J_3)\dot{\psi} + 4n_0^2(J_2 - J_3)\varphi = -\dot{H}_{w1} + T_{d1} + n_0 H_{w_3}, \\ &J_2\ddot{\vartheta}_2 + 3n_0^2(J_1 - J_3)\vartheta = -\dot{H}_{w2} + T_{d2}, \\ &J_3\ddot{\psi}_3 + n_0(J_1 - J_2 + J_3)\dot{\varphi} + n_0^2(J_2 - J_1)\psi = -\dot{H}_{w3} + T_{d3} - n_0 H_{w_1}, \end{aligned} \tag{7.47}$$

where the disturbance vector $T_d = [T_{d1}, T_{d2}, T_{d3}]^T$ is defined by

$$T_d = \begin{bmatrix} T_{md1} + T_{ad1} + T_{sd1} + T_{m1} - H_{w3}\dot{\vartheta} + H_{w2}(\dot{\psi} + n_0\varphi) \\ T_{md2} + T_{ad2} + T_{sd2} + T_{m2} - H_{w1}(\dot{\psi} + n_0\varphi) + H_{w3}(\dot{\varphi} - n_0\psi) \\ T_{md3} + T_{ad3} + T_{sd3} + T_{m3} + H_{w1}\dot{\vartheta} - H_{w2}(\dot{\varphi} - n_0\psi) \end{bmatrix}.$$

We denote $\dot{H}_w = [\dot{H}_{w1}, \dot{H}_{w2}, \dot{H}_{w3}]^T$ and define the vector $T_c = [T_{c1}, T_{c2}, T_{c3}]^T$ as

$$T_c = -\dot{H}_w + \hat{u}, \quad \text{with} \quad \hat{u} = \begin{bmatrix} 0 & 0 & n_0 \\ 0 & 0 & 0 \\ -n_0 & 0 & 0 \end{bmatrix} \begin{bmatrix} H_{w1} \\ H_{w2} \\ H_{w3} \end{bmatrix}. \tag{7.48}$$

Then, our objective is to design a feedback control T_c to stabilize the attitude control system (7.47). Once T_c is known, we could use $u_w = \hat{u} - T_c$ to drive the reaction wheels.

According to the parameters listed in Table 5.1, the angular momentum H_{wi} is bounded by ± 1Nms and the wheel torque $\dot{H}_{wi}$ is constrained into the limit $[-u_m, u_m]$ with $u_m = 0.03$Nm for $i = 1, 2, 3$. Since the orbital angular velocity n_0 is given by $n_0 = 1.038 \times 10^{-3}$rad/s, the term $n_0 H_{wi}$ is much smaller than the limit u_m and thus we can use $\pm u_m$ as the limits of the attitude controls T_{ci}, $i = 1, 2, 3$.

It is observed from (7.47) that the linear pitch dynamics decouples from the linear roll/yaw dynamics. Therefore, the control laws for the pitch channel and the roll/yaw channel could be designed independently.

7.5.3 Synthesis model of roll/yaw channel

For the roll/yaw channel, define the state vector x_1, the control input vector u_1 and the disturbance input d_1 as

$$x_1 = \begin{bmatrix} \varphi \\ \psi \end{bmatrix}, \qquad d_1 = \begin{bmatrix} T_{d1} \\ T_{d3} \end{bmatrix}, \qquad u_1 = \begin{bmatrix} T_{c1} \\ T_{c3} \end{bmatrix}. \tag{7.49}$$

Thus, we can represent the dynamic model of the roll/yaw attitude channel (φ–ψ channel) into the following matrix form:

$$E_1\ddot{x}_1 = D_1\dot{x}_1 + F_1x_1 + G_{11}d_1 + G_{12}u_1 \tag{7.50}$$

where the matrices E_1, D_1, F_1, G_{11} and G_{12} are given by

$$E_1 = \begin{bmatrix} J_1 & 0 \\ 0 & J_3 \end{bmatrix}, \quad D_1 = \begin{bmatrix} 0 & n_0(J_1+J_3-J_2) \\ -n_0(J_1+J_3-J_2) & 0 \end{bmatrix},$$
$$F_1 = \begin{bmatrix} 4n_0^2(J_3-J_2) & 0 \\ 0 & n_0^2(J_1-J_2) \end{bmatrix}, \quad G_{12} = \begin{bmatrix} 1 & 0 \\ 0 & 1 \end{bmatrix}, \quad G_{11} = \begin{bmatrix} 1 & 0 \\ 0 & 1 \end{bmatrix}.$$

Besides the external disturbances, moment-of-inertia variations are the major source of uncertainty for microsatellite attitude control design. The principal moment of inertia J_i can be expressed as a nominal value $\bar{J}_i$ plus a perturbation matrix $\Delta J_i\delta_i$,

$$J_i = \bar{J}_i + \Delta J_i\delta_i, \quad |\delta_i| \le 1, \quad i = 1,2,3 \tag{7.51}$$

where ΔJ_i is the variation envelope of J_i and δ_i is the normalized uncertainty. The variations $\Delta J_i\delta_i$ will cause perturbations in the matrices E_1 and F_1, which will be expressed as addition-type uncertainties:

$$\begin{aligned} E_1 &= E_{10} + \Delta E_1 = E_{10} + M_{E1}\Pi_{E1}N_{E1}, \\ D_1 &= D_{10} + \Delta D_1 = D_{10} + M_{D1}\Pi_{D1}N_{D1}, \\ F_1 &= F_{10} + \Delta F_1 = F_{10} + M_{F1}\Pi_{F1}N_{F1}, \end{aligned} \tag{7.52}$$

with the following matrices

$$E_{10} = \begin{bmatrix} \bar{J}_1 & 0 \\ 0 & \bar{J}_3 \end{bmatrix}, \quad M_{E1} = \begin{bmatrix} \Delta J_1 & 0 \\ 0 & \Delta J_3 \end{bmatrix}, \quad \Pi_{E1} = \begin{bmatrix} \delta_1 & 0 \\ 0 & \delta_3 \end{bmatrix}, \quad N_{E1} = \begin{bmatrix} 1 & 0 \\ 0 & 1 \end{bmatrix},$$
$$\Pi_{D1} = \mathrm{diag}\{\delta_1,\delta_1,\delta_2,\delta_2,\delta_3,\delta_3\}, \quad \Pi_{F1} = \mathrm{diag}\{\delta_1,\delta_2,\delta_2,\delta_3\},$$
$$N_{F1} = \begin{bmatrix} 0 & 4 & 0 & 1 \\ 1 & 0 & 1 & 0 \end{bmatrix}^T, \quad M_{D1} = n_0\begin{bmatrix} 0 & \Delta J_1 & 0 & -\Delta J_2 & 0 & \Delta J_3 \\ -\Delta J_1 & 0 & \Delta J_2 & 0 & -\Delta J_3 & 0 \end{bmatrix},$$
$$N_{D1} = \begin{bmatrix} 1 & 0 & 1 & 0 & 1 & 0 \\ 0 & 1 & 0 & 1 & 0 & 1 \end{bmatrix}^T, \quad M_{F1} = n_0^2\begin{bmatrix} 0 & -\Delta J_2 & 0 & 4\Delta J_3 \\ \Delta J_1 & 0 & -\Delta J_2 & 0 \end{bmatrix},$$
$$D_{10} = \begin{bmatrix} 0 & n_0(\bar{J}_1+\bar{J}_3-\bar{J}_2) \\ n_0(\bar{J}_2-\bar{J}_1-\bar{J}_3) & 0 \end{bmatrix}, \quad F_{10} = \begin{bmatrix} 4n_0^2(\bar{J}_3-\bar{J}_2) & 0 \\ 0 & n_0^2(\bar{J}_1-\bar{J}_2) \end{bmatrix}.$$

For the roll/yaw attitude control channel, let

$$\Delta_1 = \begin{bmatrix} \Pi_{E1} & 0 & 0 \\ 0 & \Pi_{D1} & 0 \\ 0 & 0 & \Pi_{F1} \end{bmatrix}, \quad \tilde{z}_1 = \begin{bmatrix} N_{E1}\ddot{x}_1 \\ N_{D1}\dot{x}_1 \\ N_{F1}x_1 \end{bmatrix}, \quad \tilde{d}_1 = -\Delta_1\tilde{z}_1. \tag{7.53}$$

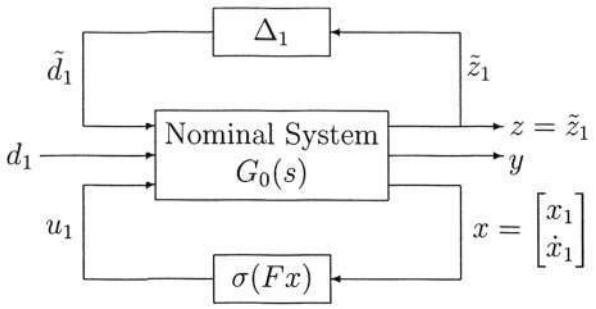

Figure 7.3: Systematical configuration of perturbed system.

Substituting (7.52) into (7.50) and applying (7.53) yields

$$E_{10}\ddot{x}_1 = D_{10}\dot{x}_1 + F_{10}x_1 + G_{\tilde{d}1}\tilde{d}_1 + G_{11}d_1 + G_{12}u_1 \tag{7.54}$$

where $G_{\tilde{d}1}$ is the fictitious disturbance distribution matrix and defined by

$$G_{\tilde{d}1} = [M_{E1} \quad -M_{D1} \quad -M_{F1}]. \tag{7.55}$$

It is noted that all the momentum-of-inertia uncertainties are modelled into the fictitious disturbances $\tilde{d}_2$ and there are no uncertainties contained in the matrices E_{10} and F_{10}. The interconnection of the nominal system, the uncertainties and saturations is shown in Figure 7.3, where Δ_1 is the normalized gain matrix of the moment-of-inertia uncertainties, $\tilde{z}_1$ is the output from the nominal system to the uncertainty block Δ_1, $\tilde{d}_1 = \Delta(\tilde{z}_1)$ is the input from the uncertainty block Δ_1 to the nominal system.

The robust stability requirement with respect to the uncertainty Δ_1 is represented by $\tilde{z}_1$. Therefore, we can choose the H_∞ measurement as

$$z = \tilde{z}_1. \tag{7.56}$$

The effect of the moment-of-inertia uncertainties appears in the perturbation $\tilde{d}_1$. (7.53) shows the relation of the H_∞ constraint (measure of robust stability) z, perturbation $\tilde{d}_1$ and uncertainty block Δ_1. According to the small gain theorem [59,95,138], if there exists a controller satisfying $||z/\tilde{d}_1||_\infty < \gamma$, then the closed-loop system will be robustly stable for any uncertainty $||\Delta||_\infty < 1/\gamma$. If a smaller γ exists, the closed-loop system remains stable for a larger uncertainty.

On the other hand, in a viewpoint of H_2 control, we hope to keep another output vector below a certain level. To reach this goal, we define a controlled output vector (the H_2 cost) of the form

$$y = \begin{bmatrix} C_{x/z} \\ 0 \end{bmatrix} \begin{bmatrix} x_1 \\ \dot{x}_1 \end{bmatrix} + \begin{bmatrix} 0 \\ D_{x/z} \end{bmatrix} u_1 \triangleq C_1 \begin{bmatrix} x_1 \\ \dot{x}_1 \end{bmatrix} + D_{12}u_1, \tag{7.57}$$

where the matrices C_1 and D_{12} are chosen such that $C_1^T D_{12} = 0$ and $D_{12}^T D_{12} = R_u$ is positive definite. If the system state vector x, the disturbance input w and the control

input u for the roll/yaw attitude channel are chosen as

$$x = \begin{bmatrix} x_1 \\ \dot{x}_1 \end{bmatrix}, \qquad w = \begin{bmatrix} \tilde{d}_1 \\ d_1 \end{bmatrix}, \qquad u = u_1,$$

together with (7.54), (7.56) and (7.57), we have the following input/output interconnection (as shown in Figure 7.2) for the roll/yaw system

$$\begin{aligned} \dot{x} &= Ax + B_1 w + B_2 u, \\ y &= C_1 x + D_{12} u, \\ z &= C_2 x + D_{21} w + D_{22} u \end{aligned} \tag{7.58}$$

with the matrices

$$A = \begin{bmatrix} 0 & I \\ E_{10}^{-1} F_{10} & E_{10}^{-1} D_{10} \end{bmatrix}, \quad B_1 = \begin{bmatrix} 0 & 0 \\ E_{10}^{-1} G_{\tilde{d}1} & E_{10}^{-1} G_{11} \end{bmatrix}, \quad B_2 = \begin{bmatrix} 0 \\ E_{10}^{-1} G_{12} \end{bmatrix},$$

$$C_1 = \begin{bmatrix} C_{x/z} \\ 0 \end{bmatrix}, \qquad D_{12} = \begin{bmatrix} 0 \\ D_{x/z} \end{bmatrix},$$

$$C_2 = \begin{bmatrix} N_{E1} E_{10}^{-1} F_{10} & N_{E1} E_{10}^{-1} D_{10} \\ 0 & N_{D1} \\ N_{F1} & 0 \end{bmatrix}, D_{21} = N_{E1} E_{10}^{-1} \begin{bmatrix} G_{\tilde{d}1} & G_{11} \\ 0 & 0 \\ 0 & 0 \end{bmatrix}, D_{22} = \begin{bmatrix} N_{E1} E_{10}^{-1} G_{12} \\ 0 \\ 0 \end{bmatrix}.$$

By straightforward computations, it is obvious that $C_2^T D_{21} \neq 0$, $C_2^T D_{22} \neq 0$ and $D_{22}^T D_{22}$ is a positive diagonal matrix given by $D_{22}^T D_{22} = \text{diag}\{\bar{J}_1^{-2}, \bar{J}_3^{-2}\}$.

Note that the disturbance w contains not only the external disturbances T_{d1} and T_{d3} but also the perturbations $\tilde{d}_1$ caused by parametric uncertainties. Then, our objective is to perform an analysis/synthesis for a saturated state-feedback control $u = \sigma(Fx)$.

7.5.4 Synthesis model of pitch channel

Define the control input u_2, the disturbance d_2 and the state vector x_2 for the pitch attitude control as follows:

$$u_2 = T_{c2}, \qquad d_2 = T_{d2}, \qquad x_2 = \begin{bmatrix} \vartheta & \dot{\vartheta} \end{bmatrix}^T, \tag{7.59}$$

Then, we have the following model of the pitch attitude control

$$E_2 \dot{x}_2 = F_2 x_2 + G_{21} d_2 + G_{22} u_2, \tag{7.60}$$

where the matrices E_2, F_2, G_{21} and G_{22} are given by

$$E_2 = \begin{bmatrix} 1 & 0 \\ 0 & J_2 \end{bmatrix}, \quad F_2 = \begin{bmatrix} 0 & 1 \\ 3n_0^2(J_3 - J_1) & 0 \end{bmatrix}, \quad G_{21} = \begin{bmatrix} 0 \\ 1 \end{bmatrix}, \quad G_{22} = \begin{bmatrix} 0 \\ 1 \end{bmatrix}.$$

Under the uncertain variations (7.51), perturbations exists in the matrices E_2 and

F_2, which is expressed as addition-type uncertainties:

$$\begin{aligned} E_2 &= E_{20} + \Delta E_2 = E_{20} + M_{E2}\Pi_{E2}N_{E2}, \\ F_2 &= F_{20} + \Delta F_2 = F_{20} + M_{F2}\Pi_{F2}N_{F2} \end{aligned} \tag{7.61}$$

with the following matrices

$$\begin{aligned} &E_{20} = \begin{bmatrix} 1 & 0 \\ 0 & \bar{J}_2 \end{bmatrix}, \quad M_{E2} = \begin{bmatrix} 0 \\ \Delta J_2 \end{bmatrix}, \quad F_{20} = \begin{bmatrix} 0 & 1 \\ 3n_0^2(\bar{J}_3 - \bar{J}_1) & 0 \end{bmatrix}, \\ &N_{E2} = \begin{bmatrix} 0 & 1 \end{bmatrix}, \qquad \Pi_{E2} = \delta_2, \\ &M_{F2} = \begin{bmatrix} 0 & 0 \\ -3n_0^2\Delta J_1 & 3n_0^2\Delta J_3 \end{bmatrix}, \quad \Pi_{F2} = \begin{bmatrix} \delta_1 & 0 \\ 0 & \delta_3 \end{bmatrix}, \quad N_{F2} = \begin{bmatrix} 1 & 0 \\ 1 & 0 \end{bmatrix}. \end{aligned}$$

Letting

$$\Delta_2 = \begin{bmatrix} \Pi_{E2} & 0 \\ 0 & \Pi_{F2} \end{bmatrix}, \qquad \tilde{z}_2 = \begin{bmatrix} N_{E2}\dot{x}_2 \\ N_{F2}x_2 \end{bmatrix}, \qquad \tilde{d}_2 = -\Delta_2\tilde{z}_2, \tag{7.62}$$

and substituting (7.61) and (7.62) into (7.60) yields

$$\dot{x}_2 = E_{20}^{-1}F_{20}x_2 + E_{20}^{-1}G_{\tilde{d}2}\tilde{d}_2 + E_{20}^{-1}G_{21}d_2 + E_{20}^{-1}G_{22}u_2, \tag{7.63}$$

where $G_{\tilde{d}2}$ is the fictitious disturbance distribution matrix and defined by

$$G_{\tilde{d}_2} = [M_{E2} \quad -M_{F2}]. \tag{7.64}$$

Analogous to the derivations of the roll/yaw channel, defining

$$x = x_2, \qquad z = -\tilde{z}_2, \qquad w = \begin{bmatrix} \tilde{d}_2^T & d_2^T \end{bmatrix}^T,$$

we obtain the following synthesis model for the attitude control of pitch channel

$$\begin{aligned} \dot{x} &= Ax + B_1w + B_2u, \qquad u = \sigma(Fx), \\ y &= C_1x + D_{12}u \\ z &= C_2x + D_{21}w + D_{22}u \end{aligned} \tag{7.65}$$

where the corresponding matrices are given by

$$\begin{aligned} &A = E_{20}^{-1}F_{20}, \qquad B_1 = E_{20}^{-1}[G_{\tilde{d}2} \;\; G_{21}], \qquad B_2 = E_{20}^{-1}G_{22}, \\ &C_1 = \begin{bmatrix} C_y \\ 0 \end{bmatrix}, \qquad D_{12} = \begin{bmatrix} 0 \\ D_y \end{bmatrix}, \quad D_{12}^TD_{12} \text{ is pdd}, \\ &C_2 = \begin{bmatrix} N_{E2}E_{20}^{-1}F_{20} \\ N_{F2} \end{bmatrix}, \quad D_{21} = N_{E2}E_{20}^{-1}\begin{bmatrix} G_{\tilde{d}2} & G_{21} \\ 0 & 0 \end{bmatrix}, \quad D_{22} = \begin{bmatrix} N_{E2}E_{20}^{-1}G_{22} \\ 0 \end{bmatrix}. \end{aligned}$$

Similarly, it is quite easy to verify that $C_2^TD_{21} \neq 0$, $C_2^TD_{22} \neq 0$ and $D_{22}^TD_{22} = \bar{J}_2^{-2}$.

7.6 Attitude Performance Analysis and Synthesis

7.6.1 Analysis of system models

For the open-loop linear system model (7.65) of the pitch channel, the characteristic equation is given by

$$\bar{J}_2 s^2 - 3n_0^2(\bar{J}_3 - \bar{J}_1) = 0. \tag{7.66}$$

By the nominal parameters listed in Table 5.1, it follows that the eigenvalues of A in (7.65) are given by $s = \pm 1.0955 n_0$, where $n_0 = \frac{3\mu}{r^3} = 1.038 \times 10^{-3}$rad/s is the mean orbital rate of the microsatellite. Clearly, the open-loop system (7.65) has an exponentially unstable eigenvalues, $s = 1.0955 n_0$, and therefore it is not globally asymptotically controllable with any bounded control inputs.

Similarly, it is easy to find out that the open-loop characteristic equation for the roll/yaw channel (7.58) is given by

$$\bar{J}_1\bar{J}_3 s^4 + \left(2\bar{J}_1\bar{J}_3 + 2\bar{J}_2\bar{J}_3 - \bar{J}_1\bar{J}_2 + \bar{J}_2^2 - 3\bar{J}_3^2\right)n_0^2 s^2 + 4(\bar{J}_1 - \bar{J}_2)(\bar{J}_3 - \bar{J}_2)n_0^4 = 0. \tag{7.67}$$

With the nominal parameters listed in Table 5.1, the four eigenvalues of A in (7.58) are given by $s = -0.7778 n_0 \pm 0.5110 n_0 j$ and $s = 0.7778 n_0 \pm 0.5110 n_0 j$. Clearly, the system (7.58) has a pair of unstable poles, $s = 0.7778 n_0 \pm 0.5110 n_0 j$, and thus it is also not globally asymptotically controllable with any bounded control inputs.

Any bounded feedback laws designed for control systems having unstable poles would not work globally. However, there is a bounded and convex null controllable region for such a system. Hu and Lin [46] exploited the null controllable region, the reachable set and the region of attraction for such systems with bounded controls and concluded that for a first- or second-order system, the region of attraction can be exactly determined, but an exact description of the region of attraction seems impossible for a general high-order system. Our objective is to estimate the region of attraction, with least conservatism, for our linearized attitude control system with bounded controls and then to analyze robust performance within a subset of the estimated domain.

Remark 7.11. The moments of inertia given in Table 5.1 have the following physical interpretations. For many earth-observation satellites, solar arrays are installed along the pitch axis ($\mathbf{y}_b$) so that they can track the Sun while the payloads such as the camera can point toward the earth (along the $\mathbf{z}_b$ axis) with a clear field of view for observing the earth. Therefore, when the solar arrays are deployed, the value of J_2 is the smallest among the three principal moments of inertia J_1, J_2 and J_3. For a gravity-gradient stabilized satellite, $J_1 \geq J_3$. However, it is not necessarily the case for a three-axis stabilized satellite [53, 101], allowing more flexibility in the satellite design. In our example in Table 5.1, we have chosen $J_1 \leq J_3$ because, as analyzed in (7.66), this corresponds to a more interesting control problem: there are unstable poles in the linearized attitude models so that any bounded control laws are not global. Nevertheless, the theoretical results in the previous sections remain useful for other

choices of the inertia matrix in obtaining local results. ⊗

Pitch channel analysis

Thus far, we have formulated the synthesis models for the pitch channel and the roll/yaw channel independently. The H_2 penalty y and the H_∞ penalty z for pitch channel (7.65) are given by

$$\begin{aligned} y &= \left[\begin{array}{ccc} c_q\vartheta & c_{\dot{q}}\dot{\vartheta} & c_u u \end{array}\right]^T, \\ z &= \left[\begin{array}{ccc} \ddot{\vartheta} & \vartheta & \vartheta \end{array}\right]^T. \end{aligned} \tag{7.68}$$

It is stated in Section 7.5 that the output function z is used to measure the robust stability with respect to parametric uncertainties and external disturbances and the output function y to estimate the generalized H_2-norm performance. We use the $Q(x)$ and $R(x)$ in Remark 5.2 with $k_1 = 4$, $b = 0.15$ and $\gamma = 1$ (it is not the same as the γ defined in this chapter) to formulate the H_2 performance output y in (7.65) and obtain the coefficients c_q, $c_{\dot{q}}$ and c_u as

$$c_q = 0.30, \qquad c_{\dot{q}} = 3.6056, \qquad c_u = 0.4472. \tag{7.69}$$

The uncertainties of the moments of inertia are considered to be within $\pm 10\%$ of the nominal values and are penalized into z through the matrix $G_{\tilde{d}_2}$ in (7.64).

With the parameters listed in Table 5.1, the matrices in (7.65) are given by

$$\begin{aligned} A &= \left[\begin{array}{cc} 0 & 1 \\ 1.2n_0^2 & 0 \end{array}\right], \quad B_1 = \left[\begin{array}{cccc} 0 & 0 & 0 & 0 \\ 0.1 & -0.48n_0^2 & -0.6n_0^2 & 0.1 \end{array}\right], \quad B_2 = \left[\begin{array}{c} 0 \\ 0.1 \end{array}\right], \\ C_1 &= \left[\begin{array}{cc} c_q & 0 \\ 0 & c_{\dot{q}} \\ 0 & 0 \end{array}\right] = \left[\begin{array}{cc} 0.30 & 0 \\ 0 & 3.6056 \\ 0 & 0 \end{array}\right], \quad D_{12} = \left[\begin{array}{c} 0 \\ 0 \\ c_u \end{array}\right] = \left[\begin{array}{c} 0 \\ 0 \\ 0.4472 \end{array}\right], \\ C_2 &= \left[\begin{array}{cc} 1.2n_0^2 & 0 \\ -1 & 0 \\ 1 & 0 \end{array}\right], \quad D_{21} = \left[\begin{array}{cccc} 0.1 & -0.48n_0^2 & -0.6n_0^2 & 0.1 \\ 0 & 0 & 0 & 0 \\ 0 & 0 & 0 & 0 \end{array}\right], \quad D_{22} = \left[\begin{array}{c} 0.1 \\ 0 \\ 0 \end{array}\right]. \end{aligned} \tag{7.70}$$

Corresponding to the choices of c_q, $c_{\dot{q}}$ and c_u, the controller is given by

$$u_2 = -0.75\vartheta - 10\dot{\vartheta} \quad \Longrightarrow \quad F = \left[\begin{array}{cc} -0.75 & -10.0 \end{array}\right], \tag{7.71}$$

which is the linear form of the inverse optimal controller (5.22) in the pitch channel. Obviously, $A + BF$ is Hurwitz with eigenvalues -0.0817 and -0.9183.

Roll/yaw channel analysis

Similarly, we take the components, which correspond to the roll/yaw channel, of the weighting matrices $Q(x)$ and $R(x)$ in Remark 5.2 with $k_1 = 4$, $b = 0.15$ and $\gamma = 1$ to formulate the H_2 output function y in (7.57) and obtain the matrix coefficients c_q, $c_{\dot{q}}$

and c_u as

$$c_q = \begin{bmatrix} 0.3 & 0 \\ 0 & 0.3 \end{bmatrix}, \quad c_{\dot{q}} = \begin{bmatrix} 3.3466 & 0 \\ 0 & 3.1623 \end{bmatrix}, \quad c_u = \begin{bmatrix} 0.4472 & 0 \\ 0 & 0.4472 \end{bmatrix}. \tag{7.72}$$

The H_2 penalty y and the H_∞ penalty z for the roll/yaw channel (7.58) are then expressed as

$$\begin{aligned} y &= \begin{bmatrix} c_{q_1}\vartheta & c_{q_3}\psi & c_{\dot{q}_1}\dot{\vartheta} & c_{\dot{q}_3}\dot{\psi} & c_{u_1}u_1 & c_{u_3}u_3 \end{bmatrix}^T, \\ z &= \begin{bmatrix} \ddot{\varphi} & \ddot{\psi} & \dot{\psi} & \dot{\varphi} & \dot{\psi} & \dot{\varphi} & \dot{\psi} & \dot{\varphi} & \psi & \varphi & \psi & \varphi \end{bmatrix}^T. \end{aligned} \tag{7.73}$$

It is stated in Section 7.5 that z is used to measure the robust stability with respect to parametric uncertainties and external disturbances. The uncertainties of the moments of inertia are considered to be within $\pm 10\%$ of the nominal values and are penalized into z through the fictitious disturbance distribution matrix $G_{\tilde{d}_2}$ in (7.55).

The controller F is given by

$$\begin{cases} u_1 = -0.75\vartheta - 10\dot{\vartheta} \\ u_3 = -0.75\psi - 10\dot{\psi} \end{cases} \implies F = \begin{bmatrix} -0.75 & 0 & -10 & 0 \\ 0 & -0.75 & 0 & -10 \end{bmatrix}, \tag{7.74}$$

which is the linear form of the inverse optimal control (5.22) in the roll/yaw channel. With this control law F, the matrix $A + B_2F$ is Hurwitz with eigenvalues -0.53783, -0.40814, -0.08717 and -0.09186.

7.6.2 Performance analysis

Region of attraction

Let $w \equiv 0$. It is known that solving the LMI problem (7.13) with different shape references $X_R = \mathcal{E}(R, 1)$ yields different invariant ellipsoids $\mathcal{E}(P/\rho, 1)$. Our objective is to develop a union of invariant ellipsoids for different shapes R's, which forms a larger invariant set within the region of attraction [47].

For the pitch channel (7.65) with the control F in (7.71), we first choose $R = R_1 = I$ to solve the LMI problem (7.13) and get

$$\alpha^* = 0.0606, \quad P/\rho = \begin{bmatrix} 1.6707 & 12.6992 \\ 12.6992 & 272.1434 \end{bmatrix}, \quad H = -\begin{bmatrix} 0.0288 & 0.4853 \end{bmatrix}$$

such that $\alpha_R(\mathcal{E}(\frac{P}{\rho}, 1))$ defined by (7.12) is maximized and the ellipsoid $\mathcal{E}(\frac{P}{\rho}, 1)$ is an invariant set, which is plotted in the red line in Figure 7.4. If we choose $R = R_2 = \frac{P}{\rho}$, solving the LMI (7.13) yields $\alpha^* = 1$ and the same ellipsoid $\mathcal{E}(\frac{P}{\rho}, 1)$. To make a difference, we choose $R = R_2 = \left(\begin{smallmatrix} 1 & 16 \\ 16 & 260 \end{smallmatrix}\right)$ near this ellipsoid $\mathcal{E}(\frac{P}{\rho}, 1)$ to form a new shape X_R to solve the LMI (7.13) again and obtain a new invariant ellipsoid, as shown in the blue line in Figure 7.4. To form the envelop, we define $R = aR_1 + (1-a)R_2$ with $1 \geq a \geq 0$. If choose $a = 0.3, 0.4, 0.5, 0.6, 0.7$, the resulting ellipsoids are plotted in

black lines in Figure 7.4. Thus, the union of all ellipsoids in Figure 7.4 forms a larger invariant set for the pitch channel.

Similarly, for the roll/yaw channel (7.58) with the control F in (7.74), solving the LMI problem (7.13) with the shape reference $X_R = \mathcal{E}(R, 1)$, $R = I$, we get $\alpha^* = 0.0343$ such that the ellipsoid $\mathcal{E}(\frac{P}{\rho}, 1)$ is an invariant set and $\alpha_R(\mathcal{E}(\frac{P}{\rho}, 1))$ is maximized with

$$P/\rho = \begin{bmatrix} 3.2138 & -0.3478 & 24.9054 & 0.4358 \\ -0.3478 & 4.2459 & -0.1052 & 33.8153 \\ 24.9054 & -0.1052 & 595.2041 & -1.8057 \\ 0.4358 & 33.8153 & -1.8057 & 850.8455 \end{bmatrix},$$

$$H = -\begin{bmatrix} 0.0403 & -0.0017 & 0.7101 & 0.0067 \\ 0.0003 & 0.0464 & -0.0011 & 0.8475 \end{bmatrix}.$$

Since the roll/yaw channel is of 4-dimensional and coupled, the graphics like Figure 7.4 is not presented. However, we can also choose different R's to form a union of different invariant ellipsoids for the roll/yaw channel.

Disturbance rejection bound

Corresponding to the control F's in (7.71) and (7.74) respectively, solving the LMI optimization problem (7.16) with the saturation level $u_m = 0.03$ yields the estimated largest disturbance reject bound $\beta_w = 1/t_r^*$ with $t_r^* = 217.1883$ for the pitch channel and $t_r^* = 477.9661$ for the roll/yaw channel. To work out these maximal disturbance rejection bounds $\beta_w = 1/t_r^*$, we solve the LMI (7.16) by fixing r for each iteration to get a value t_r and then repeat solving the LMI problem (7.16) for another larger r until t_r approaches a limit t_r^*, as shown in Figure 7.5.

From Figure 7.5, we also observe that when the actuators are forced to work in the linear region, that is, $r = u_m$, the LMI problem in Corollary 7.4 can be solved to obtain $t_r^* = 1194.4463$ for the pitch channel and $t_r^* = 1597.2254$ for the roll/yaw channel, meaning that the results got from Corollary 7.4 are much more restrictive than those values obtained from Proposition 7.3.

More computations on solving (7.16) show that the maximal disturbance rejection bound β_w increases as the saturation level u_m goes up, as shown in Figure 7.6. Using fitting techniques, the relationship between β_w and u_m can be evaluated as quadratic: $\beta_w = 5.1155u_m^2$ for the pitch channel (7.65) with the control F in (7.71) and $\beta_w = 2.3245u_m^2$ for the roll/yaw channel (7.58) with the control F in (7.74).

Generalized H_2 performance analysis

If the actuator's saturation nonlinearity is not considered in the system, i.e., $u = Fx$, by solving the LMI problem in Remark 7.4, the optimal value of the generalized H_2-norm bound α_2 is given by $\alpha_2 = 0.3394$ for the pitch channel (7.65) with the control F in (7.71) and $\alpha_2 = 0.4029$ for the roll/yaw channel (7.58) with the control F in (7.74).

However, the input saturation nonlinearity will seriously deteriorate the generalized

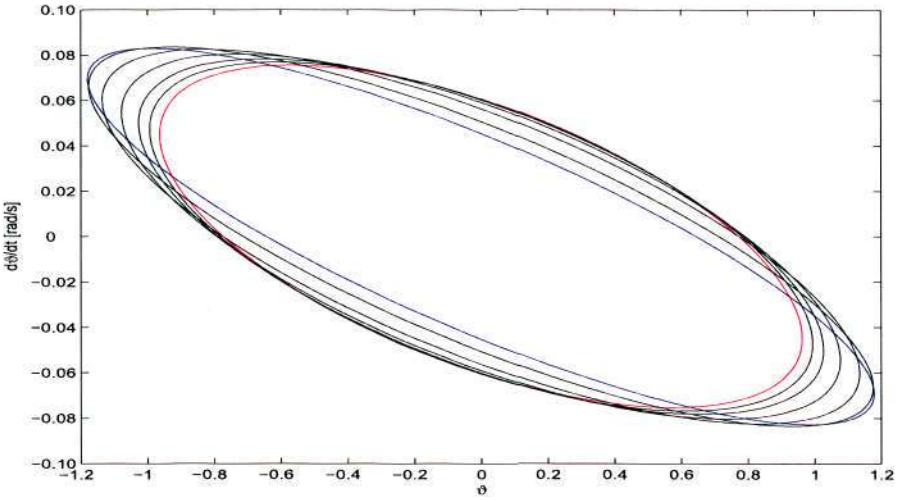

Figure 7.4: Union of the invariant ellipsoids for the pitch attitude channel (ϑ–$\dot{\vartheta}$).

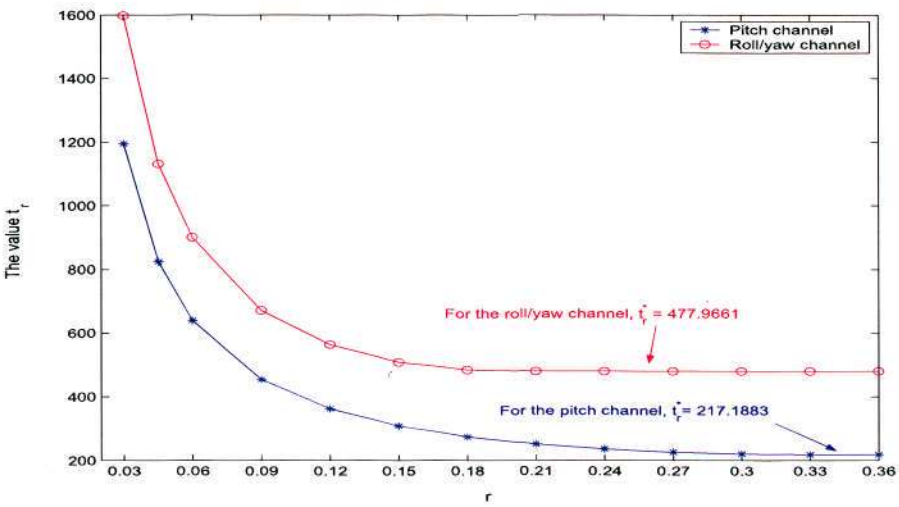

Figure 7.5: The value t_r vs the input amplitude r, where $u_m = 0.03$.

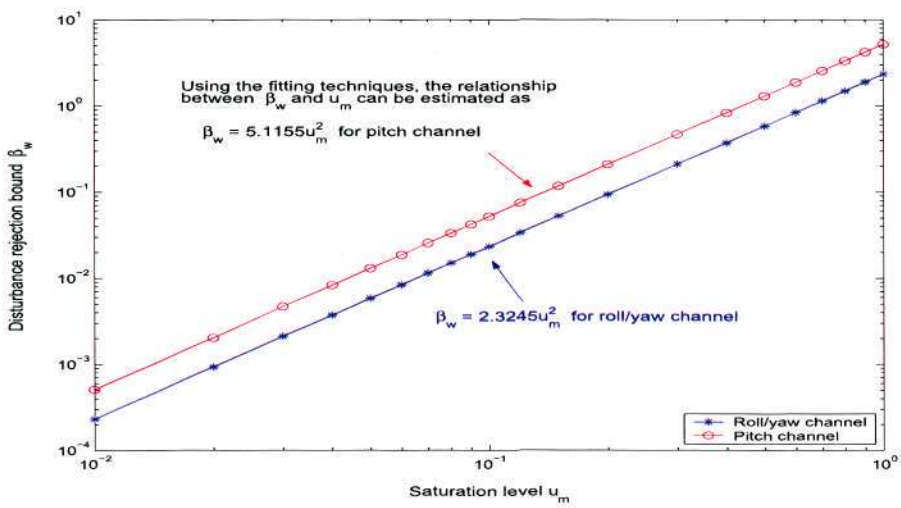

Figure 7.6: Disturbance rejection bound β_w vs the saturation level u_m.

H_2 performance α_2. For instance, if letting $\rho = \beta_w = 5.1155u_m^2$ for the pitch channel to solve the LMI optimization problem (7.28), we have $\alpha_2^* = 6.4598$ and

$$P = \begin{bmatrix} 0.0344 & 0.2280 \\ 0.2280 & 5.1111 \end{bmatrix}, \quad H = -\begin{bmatrix} 0.0560 & 0.9776 \end{bmatrix}, \quad \tilde{H} = \begin{bmatrix} 0.0024 & 0.0467 \end{bmatrix}, \quad S = 0.0308.$$

For the roll/yaw attitude channel, choosing $\rho = \beta_w = 2.3245u_m^2$ and solving the LMI problem (7.28) again with the control F in (7.74) yields $\alpha_2^* = 5.0508$ and

$$P = \begin{bmatrix} 0.2220 & -0.0007 & 0.4254 & 0.0017 \\ -0.0007 & 0.0407 & 0.0001 & 0.2676 \\ 0.4254 & 0.0001 & 18.5214 & -0.0451 \\ 0.0017 & 0.2676 & -0.0451 & 7.2629 \end{bmatrix},$$

$$H = \begin{bmatrix} -0.1934 & 0.0006 & -2.5221 & -0.0145 \\ -0.0005 & -0.0938 & 0.0028 & -1.7023 \end{bmatrix},$$

$$\tilde{H} = \begin{bmatrix} 0.0004 & 0.0001 & 0.0060 & 0.0005 \\ 0.0001 & 0.0185 & 0.0005 & 0.1735 \end{bmatrix}, \quad S = \begin{bmatrix} 0.0387 & 0 \\ 0 & 0.0387 \end{bmatrix}.$$

It is easy to check that $C_1^T D_{12} = 0$ and $D_{12}^T D_{12}$ is pdd for both the pitch channel channel and the roll/yaw channel. Replacing (7.28c) by (7.29) and solving the LMI problem, we have that $\alpha_2^* = 6.4597$ in the pitch channel and $\alpha_2^* = 5.0506$ in the roll/yaw channel, both of which are very close to the results got from (7.28).

More computations show that if we reduce the value of $\rho = \beta_w$, the H_2 performance α_2 is getting better, as shown in Figures 7.7(a) and 7.7(c) for the pitch channel and the roll/yaw channel respectively. As a matter of fact, when ρ is sufficiently small, the attitude control system will work in the linear region, that is, $|f_i x| \leq u_m$ for $i = 1, 2, 3$. This happens when $\rho \leq 0.9302u_m^2$ for the pitch channel and $\rho \leq 0.6957u_m^2$ for the roll/yaw channel, which are obtained by solving the LMI problem in Corollary 7.4. On the other hand, if we fix the value of ρ and allows a larger saturation level u_m, the H_2 performance will also be improved, as shown in Figures 7.7(b) and 7.7(d).

H_∞ performance analysis

If the actuator's saturation nonlinearity is not considered, i.e., $u = Fx$, solving the LMI in Remark 7.8 gives the minimum of the H_∞-performance as $\gamma = 2.6667$ for the pitch channel (7.65) with the control F of (7.71) and $\gamma = 4.2164$ for the roll/channel channel (7.58) with the control F given by (7.74). However, when the input saturation is included, the saturation nonlinearity will degrade the H_∞ performance γ.

If let $\gamma \to \infty$, we note that (7.33) implies (7.16a). Therefore, we conclude that the largest value $\rho^* = 5.1155u_m^2$ for the pitch channel is the critical choice of ρ corresponding to $\gamma = \infty$. It is shown in Figure 7.8(a) that when the magnitude of ρ approaches the maximal value $\rho^* = 5.1155u_m^2$, the local H_∞-norm γ will tend to ∞; if the magnitude of ρ decreases, the H_∞ norm γ decreases and thus the robust stability of the pitch channel is enhanced for the control F in (7.71).

Similarly, the maximum $\rho^* = 2.3245u_m^2$ for the roll/yaw channel is the critical choice of ρ corresponding to $\gamma = \infty$. It is shown in Figure 7.8(b) that when the magnitude of ρ approaches the maximum $\rho^* = 2.3245u_m^2$, the local H_∞-norm γ will finally explode; if the magnitude of ρ is reduced, the H_∞ performance is better and thus the robust stability are improved for the control (7.74).

7.6.3 Attitude Control Synthesis

Thus far, we have analyzed the robust performance for a given controller F. In general, the predesigned control is not guaranteed to be optimal for the linear attitude control problem subject to the input saturation. For such systems, it is hard to obtain an optimal control analytically. However, we could search for some "optimal" controls via the numerical approaches to further improve the system performance. As such, we turn to perform control synthesis using the LMI approach for the synthesis models (7.58) and (7.65) with some coefficients given in Subsection 7.6.1.

Enlargement of the region of attraction

To enlarge the region of attraction, we let $w \equiv 0$. With the shape reference $X_R = \mathcal{E}(R, 1)$, $R = I$, we solve the LMI problem (7.15) for the pitch channel (7.65) and get $\alpha^* = 2.6363$ such that the ellipsoid $\mathcal{E}(\frac{P}{\rho}, 1)$ is invariant and αX_R is maximized with

$$P/\rho = \begin{bmatrix} 1.8658 \times 10^{-7} & 1.6341 \times 10^{-4} \\ 1.6341 \times 10^{-4} & 1.4389 \times 10^{-1} \end{bmatrix}, \quad F = -\begin{bmatrix} 1.2950 \times 10^{-5} & 1.1372 \times 10^{-2} \end{bmatrix}.$$

Again, solving the LMI problem (7.15) with the shape reference $X_R = \mathcal{E}(I, 1)$ for the roll/yaw channel (7.58) gives $\alpha^* = 1.7465$ such that the ellipsoid $\mathcal{E}(\frac{P}{\rho}, 1)$ is an invariant set and αX_R is maximized with

$$\frac{P}{\rho} = \begin{bmatrix} 8.2377 \times 10^{-7} & -1.2208 \times 10^{-8} & 3.5604 \times 10^{-4} & 3.6380 \times 10^{-8} \\ -1.2208 \times 10^{-8} & 5.7416 \times 10^{-8} & -6.9697 \times 10^{-5} & 6.6642 \times 10^{-5} \\ 3.5604 \times 10^{-4} & -6.9697 \times 10^{-5} & 2.4606 \times 10^{-1} & 7.7929 \times 10^{-2} \\ 3.6380 \times 10^{-4} & 6.6642 \times 10^{-5} & 7.7929 \times 10^{-2} & 2.5358 \times 10^{-1} \end{bmatrix},$$

$$F = \begin{bmatrix} -2.4189 \times 10^{-5} & 3.5198 \times 10^{-6} & -1.4547 \times 10^{-2} & -6.7160 \times 10^{-3} \\ -2.5139 \times 10^{-5} & -1.9199 \times 10^{-6} & -9.1711 \times 10^{-3} & -1.4114 \times 10^{-2} \end{bmatrix}.$$

Remark 7.12. The enlarged region of attraction is only meaningful in a mathematical sense, while, in practice, it is not very useful because the linearization of the attitude dynamics and kinematics on the basis of the small-angle assumption is not valid any more and we have to use nonlinear attitude models directly to design an attitude controller in such a large region. ⊗

Remark 7.13. Since the system is not globally stabilizable with bounded controls and the estimate of the region of attraction $\mathcal{E}(P, \rho)$ has the constraint $\mathcal{E}(P, \rho) \subset \mathcal{L}(F, u_m)$, F will be made small to enlarge the region of attraction under the requirement that

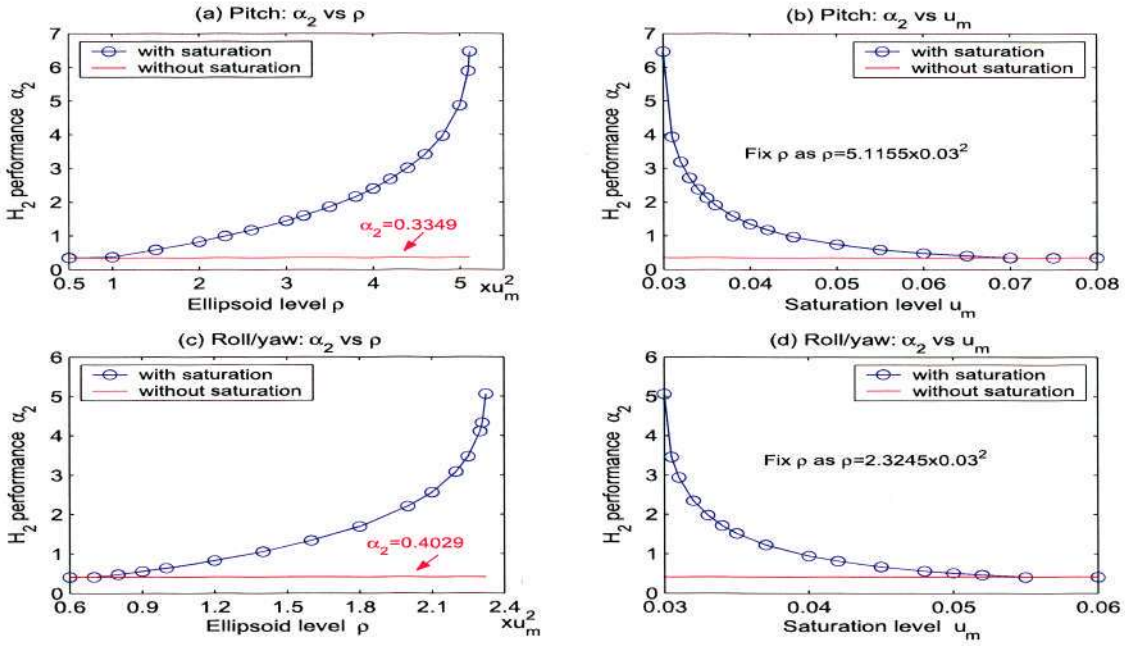

Figure 7.7: Local H_2 performance analysis.

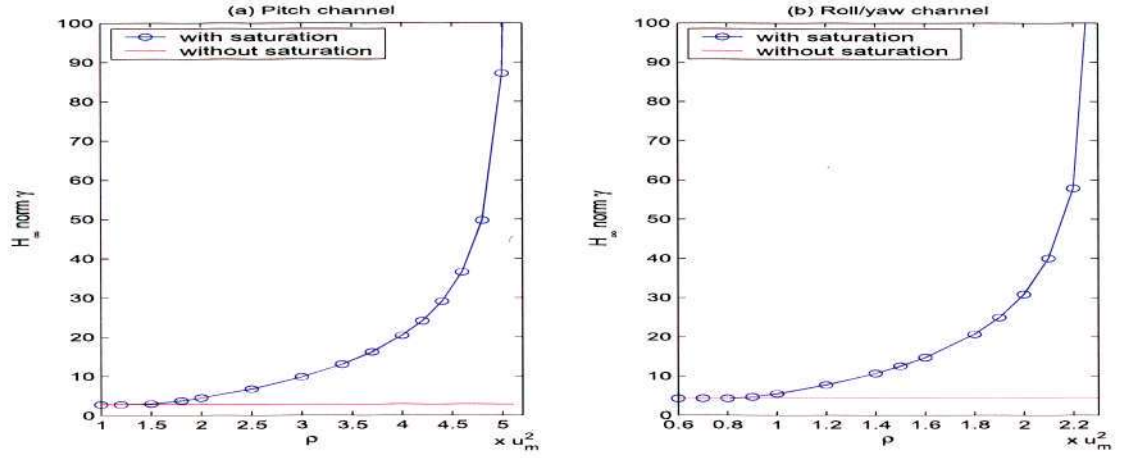

Figure 7.8: Local H_∞ performance analysis with different ρ.

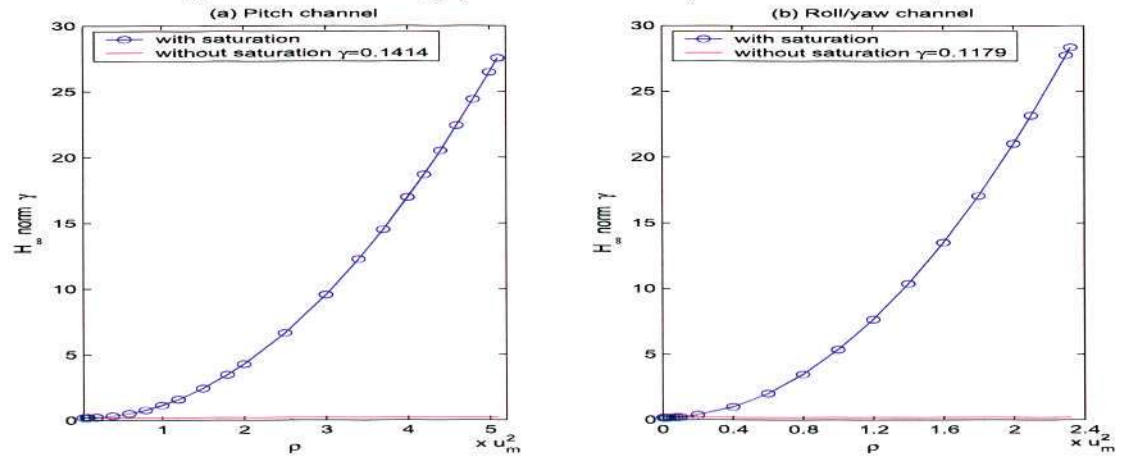

Figure 7.9: Local H_∞-performance synthesis for different ρ.

$A + B_2F$ is Hurwitz. As the positive real part of the eigenvalues of A is very small, such an enlargement of the region of attraction will bring an extremely low-gain control F. To avoid such small F's, we could make an additional requirement that all the eigenvalues of $A + B_2F$ have real parts smaller than $-\delta$, i.e., $Re(\lambda(A + B_2F)) \leq -\delta$, which can be represented into an LMI as

$$P(A + B_2F) + (A + B_2F)^T P + 2\delta P \leq 0,$$

where δ is a positive real number given by the designer. $\otimes$

Generalized H_2 performance synthesis

If the actuator's saturation nonlinearity is not considered in the system, $u = Fx$, by solving the LMI problem (7.32), the optimal value of the generalized H_2-norm bound α_2 is given by $\alpha_2 = 0.3241$ for the pitch channel and $\alpha_2 = 0.3660$ for the roll/yaw channel. However, the input saturation nonlinearity will deteriorate the H_2 performance α_2. For instance, letting $\rho = 5.1155u_m^2$ for the pitch channel to solve the LMI optimization problem (7.30), we have $\alpha_2 = 0.9097$ and

$$P = \begin{bmatrix} 0.1021 & 0.0000 \\ 0.0000 & 15.0272 \end{bmatrix}, \quad F = -\begin{bmatrix} 0.0679 & 1.5027 \end{bmatrix}.$$

Note that similarly to the enlargement of the region of attraction, we may set $H = \tilde{H} = F$ in the H_2 synthesis problem to achieve the same optimal α_2. There is a need to have different F, H and $\tilde{H}$ only if there are some additional requirements on F.

For the roll/yaw attitude channel, choosing $\rho = 2.3245u_m^2$ and solving the LMI problem (7.28) again yields $\alpha_2 = 0.7815$ with

$$P = \begin{bmatrix} 0.1220 & 0.0006 & 0.0175 & -0.0373 \\ 0.0006 & 0.1209 & 0.0604 & -0.0036 \\ 0.0175 & 0.0604 & 31.7241 & -1.7908 \\ -0.0373 & -0.0036 & -1.7908 & 18.8430 \end{bmatrix}$$

$$F = \begin{bmatrix} -0.0595 & -0.0128 & -3.5806 & 0.2722 \\ -0.0034 & -0.1290 & -0.0028 & -2.3388 \end{bmatrix}.$$

More computations show that, if we fix the value of ρ and increase the value of u_m, the H_2 performance will be improved. For example, if we fix $\rho = 5.1155 \times 0.03^2$ for the pitch channel and $\rho = 2.3245 \times 0.03^2$ for the roll/yaw channel respectively, the changes of the generalized H_2 performance via the saturation level u_m are shown below:

	u_m	0.03	0.031	0.032	0.033	0.035	0.04	0.05	0.06
roll/yaw	α_2	0.7815	0.6597	0.5748	0.5184	0.3817	0.3660	0.3660	0.3660
pitch	α_2	0.9097	0.8178	0.7469	0.6897	0.6021	0.4679	0.3539	0.3245

Alternatively, we could reduce the magnitude of ρ and the generalized H_2 perfor-

mance α_2 will also be improved. A smaller energy of the disturbance w is considered and therefore a better performance is obtained, as shown in the following table:

roll/yaw	ρ	$2.3u_m^2$	$2.2u_m^2$	$2.1u_m^2$	$2.0u_m^2$	$1.8u_m^2$	$1.6u_m^2$	$1.4u_m^2$	$1.0u_m^2$
	α_2	0.7595	0.6770	0.6078	0.5529	0.4765	0.4264	0.3927	0.3660
pitch	ρ	$5.0u_m^2$	$4.6u_m^2$	$4.2u_m^2$	$4.0u_m^2$	$3.5u_m^2$	$3.0u_m^2$	$2.0u_m^2$	$1.0u_m^2$
	α_2	0.8750	0.7708	0.6841	0.6455	0.5591	0.4846	0.3676	0.3245

H_∞ performance synthesis

For the systems (7.58) and (7.65) without input saturation, i.e., $u = Fx$, the minimums of H_∞-gain are given by $\gamma = 0.1414$ for the pitch channel (7.65) and $\gamma = 0.1179$ for the roll/yaw channel (7.58), by solving the LMI in Remark 7.10. However, when the input saturation is included, the H_∞ performance γ will be deteriorated by the saturation nonlinearity.

To see this, we choose $\rho = 5.1155u_m^2$ for the pitch channel[3] (7.65). Solving the LMI problem (7.39), we get that $\gamma = 27.5159$, which is much larger than 0.1414, implying a worse robustness to uncertainties. If the magnitude of ρ is reduced, the H_∞ performance would be better, as shown in Figure 7.9(a).

Similarly, we choose $\rho = 2.3245u_m^2$ for the roll/yaw channel (7.58). Solving the LMI problem (7.39), we have that $\gamma = 28.3126$. More computations show that the H_∞ performance would be better if ρ is smaller, as shown in Figure 7.9(b).

7.7 Conclusion

In this chapter, the analysis/synthesis of local robust performance under the H_2 and H_∞ norm considerations in a local region of attraction is studied for linear systems with saturated controls and disturbances. With the introduction of an auxiliary matrix H such that $||Hx||_\infty \leq \bar{u}$, the analysis and the synthesis are formulated in terms of linear matrix inequalities (LMIs) with a less conservatism. The theoretical results are then applied to the analysis/synthesis problems for the linear attitude control of a rigid spacecraft with disturbances, structured parameter uncertainties and saturated controls. All LMI optimization problems are solved using the LMI software.

[3]Note that the relation $\rho = 5.1155u_m^2$ has nothing to do with the synthesis problem. It is for a particular F given in (7.71). However, we keep using it here just to make a comparison to see how much robust stability could be improved by redesigning the control F.

Chapter 8

Conclusions and Recommendations

8.1 Conclusions of This Thesis

We will now summarize the results obtained in this thesis by highlighting my contributions. Suggestions for future work are proposed at the end.

In this thesis, we have studied the attitude control problem of microsatellites that are assumed rigid spacecraft with external disturbances and an uncertain inertia matrix, and achieved optimality of the proposed attitude controllers as well as the H_∞ disturbance attenuation.

The kinematic and dynamic equations of the attitude motion were derived in Chapter 4 for a wheel-based attitude control system. Using the unit quaternion to represent the attitude of spacecraft, the attitude tracking control problem was formulated for a rigid spacecraft with disturbances. Large-angle attitude maneuvers and attitude regulation problems can be considered as special cases of the attitude tracking control problem.

With the introduction of the concept of extended disturbances, the inverse optimal control method was applied in Chapter 5 to the attitude tracking control problem with external disturbances. The Lyapunov method was applied to construct a stabilizing control of a particular form and an optimal feedback controller that is optimal with respect to a meaningful cost functional involving tracking errors, control efforts and extended disturbances. By the arguments of the Lyapunov method, it was shown that the associated Lyapunov function satisfied a Hamilton-Jacobi-Isaacs partial differential equation and hence H_∞ disturbance attenuation was also achieved with an arbitrary attenuation level γ. On the basis of the system performance analysis of the inverse optimal controller in terms of performance limitation, rules were established for the selection of the controller gains.

The inverse adaptive control problem of nonlinear systems with disturbances was also examined and the results were applied to the attitude control problem. Under parametric uncertainties of inertia matrix and external disturbances, the adaptive control method and the inverse optimal control approach were combined in Chapter 6 to address the attitude tracking control problem. The inverse optimal adaptive control required the knowledge of a control Lyapunov function and a stabilizing control of a

particular form, both of which were constructed by using the method of integrator backstepping. The proposed adaptive feedback controllers are optimal with respect to a family of meaningful cost functionals involving the tracking errors and the control effort. Again, without solving the HJI inequality/equation directly, the controller achieved H_∞ disturbance attenuation with an arbitrary level γ. For the tracking control problem with $\mathcal{L}_2$-type disturbances, it was shown by the Lyapunov argument that the inverse optimal adaptive controller achieved asymptotic attitude tracking with a global convergence of tracking errors to zero for all initial conditions.

By the tools of linear matrix inequalities (LMIs), linear systems with the actuator's saturation nonlinearity were examined in Chapter 7 for local estimates of the system performance in terms of the domain of attraction, the local H_∞ performance and the local H_2 performance. With the help of an auxiliary matrix H such that $||Hx||_\infty \leq \bar{u}$ in a finite region, the analysis/synthesis problem was formulated as some LMI problems. Based on the small-angle assumption, the attitude models were linearized to derive an input-output system model for robust stability analysis and synthesis. Using the synthesis models and the LMI software, robust H_2 control and H_∞ control are analyzed and synthesized in a local domain of attraction via some convex LMI optimizations.

8.2 Recommendations for Future Work

Finally, we point out several related directions which deserve further investigations.

- If the structural dynamics of the flexible solar panels is considered in the attitude control system, the design of robust optimal state-feedback controllers becomes a more complicated task because, in general, the flexible modes are unmeasurable and therefore cannot be used in the state-feedback control. Also, the design might become more restrictive. However, it is still beneficial to carry out an investigation to such an optimal control in terms of the attitude error and the angular velocity error.

- The optimal adaptation problem of time-varying uncertain parameters is surely much more complicated than the case in this thesis where the uncertain parameters are assumed constant. This problem and its application to the attitude control have not been touched by this thesis, but are certainly worth looking at.

- Further investigations to linear systems with saturation nonlinearity for some less conservative local results is still a topic of interest. With the introduction of an auxiliary matrix H such that $||Hx||_\infty \leq \bar{u}$, it may be possible to formulate the analysis/synthesis via tractable LMIs for some quadratic functions of the saturation to get a less conservative estimate.

- For some choices of the principal moments of inertia, such as $J_1 > J_3$, it is verified [53, 101] that the linearized attitude control system of each control channel has two poles on the imaginary axis and input saturations, which forms an interconnection of a saturation nonlinearity and a neutrally stable system with poles

on the imaginary axis, as generalized by the interconnection 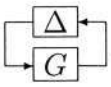

. Since the LTI part $G(s)$ is only neutrally stable, the analysis framework of integral quadratic constraints (IQC) cannot be applied directly for the (robustness and) stability analysis. By means of an appropriate feedback loop transformation, the neutrally stable part can be encapsulated with the saturation nonlinearity into a new bounded nonlinear operator, which also has an almost-continuous homotopy. The most challenging task is to derive a valid IQC, which is still under investigation.

Publications

1. Wencheng Luo, Yun-Chung Chu and Keck-Voon Ling, "H_∞ inverse optimal attitude tracking of rigid spacecraft", AIAA *Journal of Guidance, Control and Dynamics*, Vol. 28, No.3, May-June, 2005.

2. Wencheng Luo, Yun-Chung Chu and Keck-Voon Ling, "Inverse optimal adaptive control for attitude tracking of rigid spacecraft", *IEEE Transactions on Automatic Control*, accepted.

3. Wencheng Luo and Yun-Chung Chu, "Attitude control using the SDRE technique", in *Proceeding of the 7th International Conference on Control, Automation, Robotic and Vision*, Singapore, December 2002.

4. Wencheng Luo, Yun-Chung Chu and Keck-Voon Ling, "Optimal adaptive attitude tracking control of rigid spacecraft", in *Proceeding of the 12th Mediterranean Conference on Control and Automation*, Kusadasi, Turkey, June 2004.

5. Wencheng Luo, Yun-Chung Chu and Keck-Voon Ling, "H_∞ attitude tracking of rigid spacecraft", in *Proceedings of 2004 American Control Conference*, Boston, New York, USA, June-July 2004.

Bibliography

[1] J. Ahmed, V. T. Coppola, and D. S. Bernstein. Adaptive asymptotic tracking of spacecraft attitude motion with inertia matrix identification. *Journal of Guidance, Control and Dynamics*, 21(5):684–691, 1998.

[2] R. A. Alonsa, P. Anigstein, and R. Sanchez-Pena. SAC-A attitude control design. In *Proceedings of the AAS/GSFC Internation Symposium on Space Flight Dynamics*, vol. 100, Part I, pages 99–100. American Astronautical Society Publication, San Diego, 1998.

[3] B. D. O. Anderson and J. B. Moore. *Optimal Control: Linear Quadratic Methods*. NJ: Prentice Hall, 1990.

[4] D. Angeli, E. D. Sontag, and Y. Yang. A characterization of integral input-to-state stability. *IEEE Transactions on Automatic Control*, 45(6):1082–1097, 2000.

[5] Z. Artstein. Stabilization with relaxed controls. *Nonlinear Analysis*, 7:1163–1173, 1983.

[6] T. Bank. All stellar attitude estimation using a Ball CT-633 star tracker. In *Proceedings of the Annual AAS Rocky Mountain Guidance and Control Conference*, vol. 88, pages 59–66. American Astronautical Society Publication, San Diego, 1995.

[7] K. D. Bilimoria and B. Wie. Time-optimal three-axis reorientation of rigid spacecraft. *Journal of Guidance, Control and Dynamics*, 16(3):446–552, 1993.

[8] D. M. Bošković and M. Krstić. Global attitude/position regulation for underwater vehicles. *International Journal of Systems Science*, 30(9):939–946, 1999.

[9] J. D. Bošković, S.-M. Li, and R. K. Mehra. Globally stable adaptive tracking control design for spacecraft under input saturation. In *Proceedings of the 38th IEEE Conference on Decision and Control*, pages 1952–1957, Phoenex, Arizon USA, December 1999.

[10] J. D. Bošković, S.-M. Li, and R. K. Mehra. Robust adaptive variable structure control of spacecraft under input saturation. *Journal of Guidance, Control and Dynamics*, 24(1):14–22, 2001.

[11] H. Bourdache-Siguerdidjane. Futher results on the optimal regulation of spacecraft angular momentum. *Optimization, Control, Application and Methods*, 12:273–278, 1991.

[12] S. Boyd, L. El Ghaoui, E. Feron, and V. Balakrishnan. *Linear Matrix Inequalities in System and Control Theory*. SIAM studies in applied mathematics. SIAM, Philadelphia, 1994.

[13] R. G. Brown and P. Y. C. Hwang. *Introduction to Random Signals and Applied Kalman Filtering*. John Wiley & Sons, Inc., the 2nd edition, 1992.

[14] R. M. Byers and S. R. Vadali. Quasi closed-form solution to the time-optimal rigid spacecraft reorientation problem. AAS paper 91-120, 1991.

[15] C. K. Carrington and J. L. Junkins. Nonlinear optimal feedback control of spacecraft slew maneuver. *Journal of Astronautical Sciences*, 32(1), 1984.

[16] C. K. Carrington and J. L. Junkins. Optimal nonlinear feedback control for spacecraft attitude maneuver. *Journal of Guidance, Control and Dynamics*, 9(1):99–107, 1986.

[17] Y. Chitour, W. Liu, and E. D. Sontag. On the continuity and incremental-gain properties of certain saturated linear feedback loops. *International Journal of Robust and Nonlinear Control*, 5:413–440, 1995.

[18] Y. Choi, W.-K. Chung, and I. H. Suh. Performance and H_∞ optimality of PID trajectory tracking controller for Lagrange system. *IEEE Transactions on Robotics and Automation*, 17(6):857–869, 2001.

[19] Y.-C. Chu. *Control of Systems with Repeated Scalar Nonlinearities*. Ph.D. dissertation, University of Cambridge, 1996.

[20] Y.-C. Chu and K. Glover. Bounds of the induced norm and model reduction errors for systems with repeated scalar nonlinearities. *IEEE Transactions on Automatic Control*, 44(3):471–483, 1999.

[21] Y.-C. Chu and K. Glover. Stabilization and performance synthesis for systems with repeated scalar nonlinearities. *IEEE Transactions on Automatic Control*, 44(3):484–496, 1999.

[22] T.-W. Chua, C.-T. Phua, S.-H. Tan, K. Arichandran, and C.-L. Law. Merlion L&S band system. In *the 13th AIAA/UTAH State University Conference on Small Satellites*, Utah, USA, August 1999.

[23] J. R. Cloutier. State-dependent Riccati equation techniques: An overview. In *Proceedings of American Control Conference*, New Mexico, USA, June 1997.

[24] J. L. Crassidis and F. L. Markley. Sliding mode control using modified Rodriguez parameters. *Journal of Guidance, Control and Dynamics*, 19(6):1381–1383, 1996.

[25] M. Dalsmo and O. Egeland. State feedback H_∞-suboptimal control of a rigid spacecraft. *IEEE Transactions on Automatic Control*, 42(8):1186–1189, 1997.

[26] A. S. Debs and M. Athans. On the optimal angular velocity control of asymmetric space vehicles. *IEEE Transactions on Automatic Control*, 14(2):80–83, 1969.

[27] R. A. DeCarlo, S. H. Zak, and G. P. Matthews. Variable structure control of nonlinear multivariable systems: A tutorial. *Proceeding of the IEEE*, 76(3):212–232, 1988.

[28] M. V. Dixon, T. Edelbaum, J. E. Potter, and W. E. Vandervelde. Fuel optimal reorientation of axissymmetric spacecraft. *Journal of Spacecraft*, 7:1345–1351, 1970.

[29] J. Doyle. Analysis of feedback systems with structured uncertainties. *Proceedings of Inst. Elec. Eng.*, D-129:242–251, 1982.

[30] J. Doyle, K. Zhou, K. Glover, and B. Bodenheimer. Mixed H_2 and H_∞ performance objectives II: Optimal control. *IEEE Transactions on Automatic Control*, 39(8):1575–1587, 1994.

[31] T. A. W. Dwyer, M. S. Fadali, and N. Chen. Single step optimization of feedback-decoupled spacecraft attitude maneuvers. In *Proceedings of the 24th Conference on Decision and Control*, Florida, USA, December 1985.

[32] T. A. W. Dwyer and H. Sira-Ramirez. Variable structure control of spacecraft attitude maneuvers. *Journal of Guidance, Control and Dynamics*, 11(3):262–270, 1988.

[33] O. Egeland and J.-M. Godhavn. Passivity-based adaptive control of a rigid spacecraft. *IEEE Transactions on Automatic Control*, 39(4):848–852, 1994.

[34] T. I. Fossen. Comments on "Hamilton adaptive control of spacecraft". *IEEE Transactions on Automatic Control*, 38(4):671–672, 1993.

[35] R. A. Freeman and P. Kokotović. *Robust Nonlinear Control Design: State-Space and Lyapunov Techniques.* Birkäuser, 1996.

[36] B. Friedland. *Advanced Control System Design.* Prentice-Hall, Upper Saddle River, New Jersey, 1996.

[37] P. Gahinet, A. Nemirovski, A. J. Laub, and M. Chilali. *LMI Control Toolbox for Use with MATLAB.* The MATH WORKS Inc., 1995.

[38] M. Grossi, S Vetrella, and A. Moccia. Preliminary design of the attitude control system of a microsatellite for earth observation. *Space Technology*, 15(4):223–230, 1995.

[39] G. Gurevich, R. Bell, and J. R. Wertz. Autonomous on-board orbit control: Flight results and applications. *AIAA paper 2000-5226*, 2000.

[40] D. R. Haley, T. E. Strikwerda, J. C. Ray, H. L. Fisher, G. A. Heyler, and R. T. Pham. Performance of the MSX guidance and control system. In *Proceedings of the annual AAS Rocky Mountain Guidance and Control Conference*, vol. 94, pages 311–330. American Astronautical Society Publication, San Diego, 1997.

[41] G. Hardy, J. E. Littlewood, and G. Pólya. *Inequalities.* Cambridge University Press, the 2nd edition, 1991.

[42] R. R. Harman and I. Y. Bar-Itzhack. Pseudolinear and state-dependent Riccati equation filters for angular rate estimation. *Journal of Guidance, Control and Dynamics*, 22(5):723–725, 1999.

[43] D. Hill and P. Moylan. The stability of nonlinear dissipative systems. *IEEE Transactions on Automatic Control*, 21:708–711, 1976.

[44] H. Hindi and S. P. Boya. Analysis of linear systems with saturation using convex optimization. In *Proceedings of the 37th IEEE Conference on Decision and Control*, Tample, Florida, USA, December 1998.

[45] K. Howard, B.-K. Izhak, and S. Kenneth. *Direct Adaptive Control Algorithms: Theory and Applications.* Springer-Verlag, New York, 1994.

[46] T. Hu and Z.-L. Lin. *Control Systems with Actuator Saturation.* Boston: Birkhäuser, 2001.

[47] T. Hu and Z.-L. Lin. Composite quadratic Lyapunov functions for constrained control systems. *IEEE Transactions on Automatic Control*, 48(3):440–450, 2003.

[48] T. Hu, Z.-L. Lin, and B.-M. Chen. An analysis and design method for linear systems subject to actuator saturation and disturbances. *Automatica*, 38(2):351–359, 2002.

[49] J. Huang. An iterative method to solve a sequence of linear equations arising in nonlinear H_∞ control. *Applied Numerical Mathematics*, 26:293–306, 1998.

[50] J. Huang. An algorithm to solve the HJI equations arising in L_2 gain optimization problem. *International Journal of Control*, 72(1):49–57, 1999.

[51] J. Huang and C.-F. Lin. A numerical approach to computing nonlinear H_∞ control laws. *Journal of Guidance, Control and Dynamics*, 18(5):989–994, 1995.

[52] Y. Huang and W.-M. Lu. Nonlinear optimal control: Alternative to Hamilton-Jacobi equations. In *Proceedings of the 35th IEEE Conference on Decision and Control*, Kobe, Japan, December 1996.

[53] P. C. Hughes. *Spacecraft Attitude Dynamics.* John Wiley & Sons, Inc., 1986.

[54] J.-Y. Hung, W. Gao, and J.-C. Hung. Variable structure control: A survey. *IEEE Transactions on Industrial Electronics*, 40(1):2–22, 1993.

[55] A. Isidori. *Nonlinear Control Systems (II).* Spring-Verlag, New York, 1999.

[56] J. L. Junkins and M. R. Akella. Nonlinear adaptive control of spacecraft maneuvers. *Journal of Guidance, Control and Dynamics*, 20(6):1104–1110, 1997.

[57] W. Kang. Nonlinear H_∞ control and its applications to rigid spacecraft. *IEEE Transactions on Automatic Control*, 40(7):1281–1285, 1995.

[58] W. Kang and D. S. Bernstein. Nonlinear feedback control with global stabilization. *Dynamics and Control*, 5(4):321–346, 1995.

[59] H. K. Khalil. *Nonlinear Systems.* Prentice Hall, the 2nd edition, 1996.

[60] D. E. Koditschek. Application of new Lyapunov function to global adaptive attitude tracking. In *Proceedings of the 27th Conference on Decision and Control*, Austin, Texas, USA, December 1988.

[61] M. Krstić and H. Deng. *Stabilization of Nonlinear Uncertain Systems.* Springer-Verlag, New York, 1998.

[62] M. Krstić, I. Kanellakopoulos, and P. Kokotović. *Nonlinear and Adaptive Control Design.* John Wiley & Sons Inc., 1995.

[63] M. Krstić and Z.-H. Li. Inverse optimal design of Input-to-State stabilizing nonlinear controllers. *IEEE Transactions on Automatic Control*, 43(3):336–350, 1998.

[64] M. Krstić and P. Tsiotras. Inverse optimal stabilization of a rigid spacecraft. *IEEE Transactions on Automatic Control*, 44(5):1042–1049, 1999.

[65] J. Kuang and A. Y. T. Leung. H_∞ feedback for attitude control of liquid-filled spacecraft. *Journal of Guidance, Control and Dynamics*, 24(1):46–53, 2001.

[66] S. N. Kumpati and M. A. Anuradha. *Stable Adaptive Systems.* Prentice Hall, 1989.

[67] D. Liberzon. ISS and integral-ISS disturbance attenuation with bounded controls. In *Proceedings of the 38th IEEE Conference on Decision and Control*, pages 2501–2506, Phoenex, Arizon USA, December 1999.

[68] D. Liberzon, E. D. Sontag, and Y. Wang. On integral-input-to-state stabilization. In *Proceedings of the American Control Conference*, pages 1598–1602, San Diego USA, June 1999.

[69] D. Liberzon, E. D. Sontag, and Y. Wang. Universal construction of feedback laws achieving ISS and integral-ISS disturbance attenuation. *Systems and Control Letters*, 46:111–127, 2002.

[70] Y. Lin and E. D. Sontag. A universal formula for stabilization with bounded controls. *Systems and Control Letters*, 16:393–397, 1991.

[71] W. Liu, Y. Chitour, and E. D. Sontag. Remarks on finite gain stabilizability of linear systems subject to input saturation. In *Proceedings of the 32th IEEE Conference on Decision and Control*, San Antonic, Texas, December 1993.

[72] W. Liu, Y. Chitour, and E. D. Sontag. On finite gain stabilizability of linear systems subject to input saturation. *SIAM Journal of Optimization and Control*, 34(4):1190–1219, 1996.

[73] S.-C. Lo and Y.-P. Chen. Smooth sliding-mode control for spacecraft attitude tracking maneuvers. *Journal of Guidance, Control and Dynamics*, 18(6).

[74] W.-C. Luo and Y.-C. Chu. Attitude control using the SDRE technique. In *Proceedings of the 7th International Conference on Control, Automation, Robotic and Vision*, Singapore, December 2002.

[75] F. L Markley, J. R. O'Donnell, A. F. Andrews, and D. K. Ward. The Micromave Anisotropy Probe (MAP) missions. In *AIAA Guidance, Navigation, and Control Conference and Exhibit*, AIAA paper 2002-4578, Monterey, CA, August 2002.

[76] A. Megretski and A. Rantzer. System analysis via integral quadratic constraints. *IEEE Transaction on Automatic Control*, 42(6).

[77] A. Megretski and A. Rantzer. System analysis via integral quadratic constraints, Part I. *Technical report, Department of Automatic Control, Lund Institute of Technology*, September 1995.

[78] P. K. Menon and M. Yousefpor. Design of nonlinear autopilots for high angle of attack missiles. AIAA Paper 96-3913, July 1991.

[79] P. J. Moylan and B. D. O. Anderson. Nonlinear regulator theory and an inverse optimal control problem. *IEEE Transactions on Automatic Control*, 18:460–465, 1973.

[80] C. P. Mracek and J. R. Cloutier. Control design for the nonlinear benchmark problem via the state-dependent Riccati equation method. *International Journal of Robust and Nonlinear Control*, 8:401–433, 1998.

[81] S. Muncheberg, M. Krischke, and N. Lemke. Nanosatellites and micro systems technology: Capabilities, limitations and applications. *ACTA Astronautica*, 39(9-12):799–808, 1996.

[82] K. S. Narendra and A. M. Annaswamy. *Stable Adaptive Systems*. Prentice-Hall, Englewood Cliffs, NJ, 1989.

[83] J. Park and W.-K. Chung. Analytic nonlinear H_∞ inverse-optimal control for Euler-Lagrange system. *IEEE Transactions on Robotics and Automation*, 16(6):847–854, 2000.

[84] J. Park and W.-K. Chung. Design a robust H_∞ PID control for industrial manipulators. *ASME Journal of Dynamic Systems, Measurement, and Control*, 122(4):803–812, 2000.

[85] D. K. Parrish and D. B. Ridgely. Attitude control of a satellite using the SDRE method. In *Proceedings of American Control Conference*, Albuquerque, New Mexico, June 1997.

[86] C. Pittet, T. Tarbouriech, and C. Burgat. Stability regions for linear systems with saturatings controls via circle and Popov criteria. In *Proceedings of the 36th IEEE Conference on Decision and Control*, pages 4518–4523, San Diego, CA, December 1997.

[87] A. Rantzer and A. Megretski. System analysis via integral quadratic constraints, Part II. *Technical report, Department of Automatic Control, Lund Institute of Technology*, September 1997.

[88] F. P. J. Rimrott. *Introductory Attitude Dynamics.* Springer-Verlag New York Inc., 1988.

[89] B. G. Romanchuk. *Input-Output Analysis of Feedback Loops with Saturation Nonlinearities.* Ph.D. dissertation, University of Cambridge, 1995.

[90] M. Rotea, P. Tsiotras, and M. Corless. Suboptimal control of rigid body motion with a quadratic cost. *Dynamics and Control*, 8(1):55–81, 1998.

[91] M. A. Rotea. The generalized H_2 control problem. *Automatica*, 29(2):373–385, 1993.

[92] M. A. Rotea and P. P. Kharhonekar. Generalized H_2/H_∞ control via convex optimization. In *Proceedings of the 30th IEEE Conference on Decision and Control*, Brighton, England, December 1991.

[93] N. Rouche, P. Habets, and M. LaLoy. *Stability Theory by Lyapunov's Direct Method.* Spring-Verlag, New York, 1977.

[94] A. Saberi, Z.-L. Lin, and A. R. Teel. Control of linear systems with saturating actuators. *IEEE Transactions on Automatic Control*, 41(3).

[95] R. S. Sánchez-Pená and M. Sznaier. *Robsut Systems: Theory and Applications.* John-Wiley & Sons, Inc., 1998.

[96] H. Schaub, M. R. Akella, and J. L. Junkins. Adaptive control of nonlinear attitude motions realizing linear closed loop dynamics. *Journal of Guidance, Control and Dynamics*, 24(1):95–100, 2001.

[97] C. Scherer, P. Gahinet, and M. Chilali. Multiobjective output-feedback control via LMI optimization. *IEEE Transactions on Automatic Control*, 42(7):896–911, 1997.

[98] S. L. Scrivener and R. C. Thomson. Survey of time-optimal attitude maneuvers. *Journal of Guidance, Control and Dynamics*, 17(2):225–233, 1994.

[99] R. Sepulchre, M Janković, and P. V. Kokotović. *Constructive Nonlinear Control.* Springer-Verlag, New York, 1997.

[100] S.-P. Shue and R. K. Agarwal. Nonlinear H_∞ method for control of wing rock motions. *Journal of Guidance, Control and Dynamics*, 23(1):60–68, 2000.

[101] M. J. Sidi. *Spacecraft Dynamics and Control.* Cambridge University Press, 1997.

[102] J.-J. E. Slotine and W.-P. Li. *Applied Nonlinear Control.* Prentice Hall, 1991.

[103] J.-J. E. Slotine and D. M. Di Benedetto. Hamilton adaptive control of spacecraft. *IEEE Transactions on Automatic Control*, 35(7):848–852, 1990.

[104] V. S. Sohoni and D. R. Guild. Optimal attitude control systems for spinning aerospace vehicles. *Journal of Astronautical Science*, 18(2):86–100, 1970.

[105] E. D. Sontag. A Lyapunov-like characterization of asymptotic controllability. *SIAM Journal of Control and Optimization*, 21:462–471, 1983.

[106] E. D. Sontag. Smooth stabilization implies coprime factorization. *IEEE Transactions on Automatic Control*, 34:435–443, 1989.

[107] E. D. Sontag. A universal construction of Artstein's theorem on nonlinear stabilization. *Systems and Control Letters*, 13:117–123, 1989.

[108] E. D. Sontag. *Mathematical Control Theory.* Spring-Verlag, New York, 1990.

[109] E. D. Sontag. Comments on integral variants of ISS. *Systems and Control Letters*, 34:93–100, 1998.

[110] E. D. Sontag. State-space and I/O stability for nonlinear systems. In *Feedback Control, Nonlinear Systems and Complexity*, Francis, B. A. and Tannenbaum A. R., eds., Lecture Notes in Control and Information Sciences, pages 215–235. Springer-Verlag, Berlin, 1999.

[111] E. D. Sontag and Y. Wang. On characterizations of input-to-state stability property. *Systems and Control Letters*, 24:351–359, 1995.

[112] P. Soravia. H_∞ control of nonlinear systems: Differential games and viscosity solutions. *SIAM Journal of Control and Optimization*, 34(3):1071–1097, 1996.

[113] D. T. Stansberg and J. R. Cloutier. Position and attitude control of a spacecraft using the state-dependent Riccati equation techniques. In *Proceedings of American Control Conference*, Chicago, Illinois, June 2000.

[114] P. Tsiotras. Stabilization and optimality results for the attitude control problem. *Jounal of Guidance, Control and Dynamics*, 19(4):772–779, 1996.

[115] P. Tsiotras. On the optimal regulation of an axis-symmetric rigid body with two controls. In *AIAA Guidance, Navigation and Control Conference*, AIAA paper 96-3791, (San Diego, CA), July, 1996.

[116] P. Tsiotras, M. Corless, and M. Rotea. Optimal control of rigid body angular velocity with quadratic cost. In *Proceedings of the 35th Conference on Decision and Control*, Kobe, Japan, December 1996.

[117] S.-C. Tu, Y.-Q. Chen, L.-D. Liu, and J. Li. *Satellite Attitude Dynamics and Control: Part II.* Satellite engineering series (Chinese version). Astronautics Press, 1999.

[118] S.-C. Tu, Y.-Q. Chen, and G.-T. Yan. *Satellite Attitude Dynamics and Control: Part I.* Satellite engineering series (Chinese version). Astronautics Press, 1999.

[119] S. R. Vadali. Variable-structure control of spacecraft large-angle maneuvers. *Journal of Guidance, Control and Dynamics*, 9(2):235–239, 1986.

[120] S. R. Vadali and J. L. Junkins. Optimal open-loop and stable feedback control of rigid spacecraft attitude maneuver. *Journal of Astronautical Science*, 32(2):105–122, 1984.

[121] S. R. Vadali, L. G. Kraige, and J. L. Junkins. New results on the optimal spacecraft attitude maneuver problem. *Journal of Guidance, Control and Dynamics*, 7(3):378–380, 1984.

[122] A. J. Van der Schaft. On a state space approach to nonlinear H_∞ control. *Systems and Control Letters*, 16(1):1–8, 1991.

[123] A. J. Van der Schaft. L_2-gain analysis of nonlinear system and nonlinear state feedback H_∞ control. *IEEE Transactions on Automatic Control*, 37(6):770–784, 1992.

[124] A. J. Van der Schaft. Nonlinear state space H_∞ control theory. In *Essays on Control: Perspectives in the Theory and its Applications*, pages 153–190. Birkhäuser, 1993.

[125] J. T.-Y. Wen and K. Kreutz-Delgado. The attitude control problem. *IEEE Transactions on Automatic Control*, 36(10):1148–1162, 1991.

[126] J. R. Wertz. *Spacecraft Attitude Determination and Control.* D. Reidel Publishing Company, 1978.

[127] J. R. Wertz and W. J. Larson. *Spacecraft Mission Analysis and Design.* Microcosm Press, California, and Kluwer Academic Publishers, London, the 3rd edition, 1999.

[128] B. Wie and P. Barba. Quaternion feedback for spacecraft large angle maneuvers. *Journal of Guidance, Control and Dynamics*, 8(3):105–122, 1985.

[129] B. Wie and Q. Liu. Classical and robust H_∞ control redesign for the Hubble space telescope. *Journal of Guidance, Control and Dynamics*, 16(6):1069–1077, 1993.

[130] B. Wie and Q. Liu. Robust stabilization of the space station in the presence of inertia matrix uncertainty. *Journal of Guidance, Control and Dynamics*, 18(3):611–617, 1995.

[131] D. Wiemer. Attitude determination and control for the Global Imaging System 2000. In *Proceedings of the annual AAS Rocky Mountain Guidance and Control Conference*, vol. 98, pages 139–159. American Astronautical Society Publication, San Diego, 1998.

[132] J. C. Willems. Dissipative dynamical systems, part I: General theory. *Archive for Rational Mechanics and Analysis*, 45:321–351, 1972.

[133] S. M. Wolfe, K. T. Alfriend, and B. S. Leonard. A magnetic attitude control system for sun pointing satellites. In *Proceedings of the AAS/AIAA Astrodynamics Conference*, vol. 90, Part I, pages 1047–1064. American Astronautical Society Publication, San Diego, 1995.

[134] C.-S. Wu and B.-S. Chen. Adaptive attitude control of spacecraft: Mixed H_2/H_∞ approach. *Journal of Guidance, Control and Dynamics*, 24(4):755–766, 2001.

[135] C.-D. Yang and C.-C. Kung. Nonlinear H_∞ flight control of general six-degree-of-freedom motions. *Journal of Guidance, Control and Dynamics*, 23(2):278–288, 2000.

[136] C.-D. Yang and Y.-P. Sun. Mixed H_2/H_∞ state-feedback design for microsatellite attitude control. *Control Engineering Practice*, 10(9):951–970, 2002.

[137] J. S.-C. Yuan. Closed-loop manipulator control using quaternion feedback. *IEEE Transactions on Robotics and Automation*, 4(4):434–440, 1988.

[138] K. Zhou, J. Doyle, and K. Glover. *Robsut and Optimal Control.* Prentice Hall, New Jersy, 1995.

[139] K. Zhou, K. Glover, B. Bodenheimer, and J. Doyle. Mixed H_2 and H_∞ performance objectives I: Robust performance analysis. *IEEE Transactions on Automatic Control*, 39(8):1564–1574, 1994.

[140] D. Zimbelman and J. G. Watzin. On-orbit performance of the Transition Region and Coronal (TRACE) attitude control system. In *Proceedings of the annual AAS Rocky Mountain Guidance and Control Conference*, vol. 101, pages 437–455. American Astronautical Society Publication, San Diego, 1999.

Appendix

A. Angular Velocity and Rotational Kinematics [53]

If two reference frames $\mathcal{F}_a$ and $\mathcal{F}_b$ are rotating with respect to each other, the frame $\mathcal{F}_a$ has an angular velocity with respect to $\mathcal{F}_b$ and *vice versa*. We shall denote the former angular velocity by $\vec{\omega}_{ba}$ and define the latter by $\vec{\omega}_{ab}$ similarly. The order of the subscripts is important. By symmetry,

$$\vec{\omega}_{ba} + \vec{\omega}_{ab} = 0.$$

Let C_{ba} denote a rotation matrix for the angular rotations from the frame $\mathcal{F}_a$ to the frame $\mathcal{F}_b$. Then,

$$\mathcal{F}_a^T = \mathcal{F}_b^T C_{ba}^T. \tag{A.1}$$

Denoting time derivatives in $\mathcal{F}_a$ by an overdot, it follows that $\dot{\mathcal{F}}_a$ vanishes and that, from vector calculus [53, Section B.4],

$$\dot{\mathcal{F}}_b^T = \vec{\omega}_{ba} \times \mathcal{F}_b^T. \tag{A.2}$$

Let ω_{ba} be the component of $\vec{\omega}_{ba}$ in $\mathcal{F}_b$, that is,

$$\vec{\omega}_{ba} = \omega_{ba}^T \mathcal{F}_b. \tag{A.3}$$

Taking $\mathcal{F}_a$-derivatives of (A.1), we have

$$0 = \omega_{ba}^T \mathcal{F}_b^T \times \mathcal{F}_b^T C_{ba} + \mathcal{F}_b^T \dot{C}_{ba} = \mathcal{F}_b^T (\omega_{ba}^\times C_{ba} + \dot{C}_{ba}).$$

Therefore, we conclude that

$$\omega_{ba}^\times C_{ba} + \dot{C}_{ba} = 0 \quad \Longrightarrow \quad \omega_{ba}^\times = -\dot{C}_{ba} C_{ba}^T. \tag{A.4}$$

The last expression follows from the orthonormality condition $C_{ba}^T C_{ba} = I_3$.

There are three eigenvalues for the rotation matrix C_{ba}, namely, $\{1, e^{j\Phi}, e^{-j\Phi}\}$. Let the eigenvector corresponding to the eigenvalue 1 be $e = [e_1, e_2, e_3]^T$. By the Euler theorem, the rotation matrix C_{ba} is equivalent to an angular rotation about e over the

angle Φ and can be rewritten as [53, 101, 126]

$$C_{ba} = \cos\Phi I_3 + (1 - \cos\Phi)ee^T - \sin\Phi e^\times. \tag{A.5}$$

Starting from (A.4) and (A.5), we proceed to derive the expression of ω_{ba} in terms of $\dot{e}$ and $\dot{\Phi}$. The identities

$$\begin{aligned} &e^Te = 1; \quad e^T\dot{e} = 0; \quad e^\times e = 0; \quad \dot{e}^\times e = -e^\times\dot{e}; \quad \dot{e}^\times e^\times = e\dot{e}^T; \\ &e\dot{e}^Te^\times + e^\times\dot{e}e^T = -\dot{e}^\times; \qquad \dot{e}e^T - e\dot{e}^T = (e^\times\dot{e})^\times \end{aligned} \tag{A.6}$$

are very useful in reducing the expression (A.4) to its desired form:

$$\omega_{ba}^\times = \dot{\Phi}e^\times - (1 - \cos\Phi)(e^\times\dot{e})^\times + \sin\Phi\dot{e}^\times. \tag{A.7}$$

It follows immediately that

$$\omega_{ba} = \dot{\Phi}e - (1 - \cos\Phi)e^\times\dot{e} + \sin\Phi\dot{e}. \tag{A.8}$$

Next, we proceed to find the equations for $\dot{e}$ and $\dot{\Phi}$ when ω_{ba} is known. Premultiply (A.8) by e^T and use the identities for e to reduce the results to

$$\dot{\Phi} = e^T w_{ba}. \tag{A.9}$$

To complete the derivation, we need $\dot{e}$ in terms of ω_{ba}. By multiplying (A.8) with $e^\times$ and using the property $e^\times e^\times = ee^T - e^Tee^T$ in Lemma 4.1 and these identities in (A.6) again, it follows that

$$e^\times\omega_{ba} = (1 - \cos\Phi)\dot{e} + \sin\Phi e^\times\dot{e}. \tag{A.10}$$

Again, multiplying (A.10) by $e^\times$ gives

$$e^\times e^\times\omega_{ba} = (1 - \cos\Phi)e^\times\dot{e} - \sin\Phi\dot{e}. \tag{A.11}$$

The last two equations (A.10) and (A.11) can be viewed as two algebraic equations in the two unknowns $\dot{e}$ and $e^\times\dot{e}$. Solving (A.10) and (A.11) for $\dot{e}$ yields

$$\dot{e} = \frac{1}{2}\Big[e^\times - \frac{\sin\Phi}{1 - \cos\Phi}e^\times e^\times\Big]\omega_{ba} = \frac{1}{2}\Big[e^\times - \cot\frac{\Phi}{2}e^\times e^\times\Big]\omega_{ba}. \tag{A.12}$$

From the definition of the unit quaternion $q = [q_v^T, q_4]^T$,

$$q_v = e\sin\frac{\Phi}{2}, \qquad q_4 = \cos\frac{\Phi}{2}, \tag{A.13}$$

the rate of change of the unit quaternion is found by differentiating (A.13). Inserting $\dot{\Phi}$ of (A.9) and $\dot{e}$ of (A.12) into $\dot{q}_v$ and $\dot{q}_4$ and applying $e^\times e^\times = ee^T - e^Tee^T$ and those

identities in (A.6), we have

$$\begin{aligned} \dot{q}_v &= \dot{e}\sin\frac{\Phi}{2} + \frac{1}{2}\dot{\Phi}\cos\frac{\Phi}{2}e = \frac{1}{2}(q_v^\times + q_4 I_3)\omega_{ba}, \\ \dot{q}_4 &= -\frac{1}{2}\dot{\Phi}\sin\frac{\Phi}{2} = -\frac{1}{2}q_v^T\omega_{ba}. \end{aligned} \tag{A.14}$$

By explicitly inverting (A.14), it follows

$$\omega_{ba} = 2(q_4 I_3 - q_v^\times)\dot{q}_v - 2q_v\dot{q}_4. \tag{A.15}$$

From (A.5) and (A.13), it follows that the rotation matrix C_{ba} can be represented in terms of the quaternion q as

$$C_{ba}(q) = (q_4^2 - q_v^T q_v)I_3 + 2q_v q_v^T - 2q_4 q_v^\times. \tag{A.16}$$

B. Derivations of (4.13), (4.38) and (4.39)

Derivation of (4.13)

Let $\vec{\omega}_{ai}$ be the angular velocity of the frame $\mathcal{F}_a$ with respect to an inertia frame $\mathcal{F}_I$ and let ω_a be the components of $\vec{\omega}_{ai}$ in $\mathcal{F}_a$. Similarly, let $\vec{\omega}_{bi}$ be the angular velocity of the frame $\mathcal{F}_b$ with respect to an inertia frame $\mathcal{F}_I$ and let ω_b be the components of $\vec{\omega}_{bi}$ in $\mathcal{F}_b$. Then, it follows that

$$\omega_{ba} = \omega_b - C_{ba}(q)\omega_a. \tag{B.17}$$

Since $q_4^2 + q_v^T q_v = 1$, $q_v^\times q_v = 0$ and $q_v^\times q_v^\times = q_v q_v^T - q_v^T q_v I_3$, it follows that

$$\begin{aligned} (q_v^\times + q_4 I_3)C_{ba}(q) &= (q_v^\times + q_4 I_3)[(q_4^2 - q_v^T q_v)I_3 + 2q_v q_v^T - 2q_4 q_v^\times] \\ &= q_4(q_4^2 - q_v^T q_v)I_3 + 2q_4 q_v q_v^T - 2q_4^2 q_v^\times + (q_4^2 - q_v^T q_v)q_v^\times - 2q_4 q_v^\times q_v^\times \\ &= q_4(q_4^2 - q_v^T q_v)I_3 + 2q_4 q_v q_v^T - q_v^\times - 2q_4(q_v q_v^T - q_v^T q_v I_3) \\ &= q_4(q_4^2 - q_v^T q_v)I_3 + 2q_4 q_v^T q_v I_3 - q_v^\times = q_4 I_3 - q_v^\times, \end{aligned}$$

and

$$q_v^T C_{ba}(q) = q_v^T[(q_4^2 - q_v^T q_v)I_3 + 2q_v q_v^T - 2q_4 q_v^\times] = q_v^T(q_4^2 - q_v^T q_v)I_3 + 2q_v^T q_v q_v^T = q_v^T.$$

Therefore, substituting (B.17) and (A.16) into (A.14), we have

$$\begin{aligned} \dot{q}_v &= \frac{1}{2}(q_v^\times + q_4 I_3)[\omega_b - C_{ba}(q)\omega_a] = \frac{1}{2}(q_v^\times + q_4 I_3)\omega_b - \frac{1}{2}(q_v^\times - q_4 I_3)\omega_a, \\ \dot{q}_4 &= -\frac{1}{2}q_v^T[\omega_b - C_{ba}(q)\omega_a] = -\frac{1}{2}q_v^T\omega_b + \frac{1}{2}q_v^T\omega_a. \end{aligned} \tag{B.18}$$

Derivations of (4.38) and (4.39)

Let ω_{co} denote the angular velocity of the body frame $\mathcal{F}_{bc}$ with respect to the orbital frame $\mathcal{F}_o$ and be expressed in the frame $\mathcal{F}_{bc}$. Let C_{co} denote the rotation matrix for angular rotations from $\mathcal{F}_o$ to $\mathcal{F}_{bc}$. Clearly, $\omega_c = \omega_{co} + C_{co}(q_c)\omega_0$, with ω_0 defined by (4.5). By the implications (4.6) and (4.32), it is easy to verify that

$$\begin{aligned}\omega_e &= \omega - C_{bc}(q_e)\omega_c = \omega_{bo} + C_{bo}(q)\omega_0 - C_{bc}(q_e)\omega_{co} - C_{bc}(q_e)C_{co}(q_c)\omega_0\\ &= \omega_{bo} - C_{bc}(q_e)\omega_{co}.\end{aligned}$$

Since $\epsilon^T\epsilon + \eta^2 = 1$ and the rotational matrix $C_{bc}(q_e) = C_{bc}(\epsilon,\eta)$ is given by

$$C \triangleq C_{bc}(\epsilon,\eta) = (\eta^2 - \epsilon^T\epsilon)I_3 + 2\epsilon\epsilon^T - 2\eta\epsilon^\times,$$

it is easy to check that $\epsilon^T C = \epsilon^T$ and $(\eta I_3 + \epsilon^\times)C - (\eta I_3 - \epsilon^\times) = 0$. Therefore, differentiating (4.33) and applying (4.13), (4.31), (4.33) and Lemma 4.1 yields

$$\begin{aligned}\dot\eta =& q_v^T\dot q_{cv} + q_{cv}^T\dot q_v + q_{c4}\dot q_4 + q_4\dot q_{c4}\\ =& \tfrac{1}{2}\big[q_v^T(q_{cv}^\times + q_{c4}I_3) - q_4 q_{cv}^T\big]\omega_{co} + \tfrac{1}{2}\big[q_{cv}^T(q_v^\times + q_4 I_3) - q_{c4}q_v^T\big]\omega_{bo}\\ =& -\tfrac{1}{2}\epsilon^T(\omega_{bo} - C\omega_{co}) - \tfrac{1}{2}\epsilon^T(C - I_3)\omega_{co} = -\tfrac{1}{2}\epsilon^T\omega_e,\end{aligned} \tag{B.19}$$

and

$$\begin{aligned}\dot\epsilon =& (q_{c4}I_3 - q_{cv}^\times)\dot q_v - q_{cv}\dot q_4 - (q_4 I_3 - q_v^\times)\dot q_{cv} + q_v\dot q_{c4}\\ =& \tfrac{1}{2}\big[(q_{c4}I_3 - q_{cv}^\times)(q_4 I_3 + q_v^\times) + q_{cv}q_v^T\big]\omega_{bo} - \tfrac{1}{2}\big[(q_4 I_3 - q_v^\times)(q_{c4}I_3 + q_{cv}^\times) + q_v q_{cv}^T\big]\omega_{oc}\\ =& \tfrac{1}{2}\big[q_{c4}q_4 I_3 - q_4 q_{cv}^\times + q_{c4}q_v^\times - q_v q_{cv}^T + q_v^T q_{cv}I_3 + q_{cv}q_v^T\big]\omega_{bo}\\ & - \tfrac{1}{2}\big[q_{c4}q_4 I_3 + q_4 q_{cv}^\times - q_{c4}q_v^\times - q_{cv}q_v^T + q_v^T q_{cv}I_3 + q_v q_{cv}^T\big]\omega_{co}\\ =& \tfrac{1}{2}\big[(q_{c4}q_4 + q_v^T q_{cv})I_3 + (q_{c4}q_v - q_4 q_{cv} - q_{cv}^\times q_v)^\times\big]\omega_{bo}\\ & - \tfrac{1}{2}\big[(q_{c4}q_4 + q_v^T q_{cv})I_3 - (q_{c4}q_v - q_4 q_{cv} - q_{cv}^\times q_v)^\times\big]\omega_{co}\\ =& \tfrac{1}{2}(\eta I_3 + \epsilon^\times)\omega_{bo} - \tfrac{1}{2}(\eta I_3 - \epsilon^\times)\omega_{co}\\ =& \tfrac{1}{2}(\eta I_3 + \epsilon^\times)(\omega_{bo} - C\omega_{co}) + \tfrac{1}{2}\big[(\eta I_3 + \epsilon^\times)C - (\eta I_3 - \epsilon^\times)\big]\omega_{co}\\ =& \tfrac{1}{2}(\eta I_3 + \epsilon^\times)\omega_e.\end{aligned} \tag{B.20}$$

Thus, the differential equations (4.38) and (4.39) follow for the quaternion vectors.

C. Legendre-Fenchel Transform and Young's Inequality

For a class $\mathcal{K}_\infty$ function ρ whose derivative exists and is also a class $\mathcal{K}_\infty$ function, $\ell\rho$ denotes the *Legendre-Fenchel transform* [61,63]

$$\ell\rho(r) = r(\rho')^{-1}(r) - \rho\big((\rho')^{-1}(r)\big), \tag{C.21}$$

where $(\rho')^{-1}(r)$ stands for the inverse function of $\frac{d\rho(r)}{dr}$.

Lemma C.1. *If γ and its derivative ρ' are class $\mathcal{K}_\infty$ functions, then the Legendre-Fenchel transform satisfies the following properties:*

$$\text{(a)} \quad \ell\rho(r) = r(\rho')^{-1}(r) - \rho\big((\rho')^{-1}(r)\big) = \int_0^r (\rho')^{-1}(s)ds \tag{C.22}$$

$$\text{(b)} \quad \ell\ell\rho = \rho \tag{C.23}$$

$$\text{(c)} \quad \ell\rho \text{ is a class } \mathcal{K}_\infty \text{ function} \tag{C.24}$$

$$\text{(d)} \quad \ell\rho(\rho'(r)) = r\rho'(r) - \rho(r) \tag{C.25}$$

Proof. (a) Integrating by parts, we get

$$\begin{aligned}\int_0^r (\rho')^{-1}(s)ds &= r(\rho')^{-1}(r) - \int_0^r sd\big((\rho')^{-1}(s)\big) \\ &= r(\rho')^{-1}(r) - \int_0^r \rho\big((\rho')^{-1}(s)\big)d\big((\rho')^{-1}(s)\big) \\ &= r(\rho')^{-1}(r) - \int_0^r d\Big(\rho\big((\rho')^{-1}(s)\big)\Big),\end{aligned} \tag{C.26}$$

which completes the proof.

(b) Immediate by differentiating the second expression in (a), and then inverting and integrating the result.

(c) Obvious from the second expression in (a) because $(\rho')^{-1}$ is a class $\mathcal{K}_\infty$ function.

(d) Follows by direct substituting into (C.22). □

Lemma C.2 (Young's Inequality [41]). *For any two vectors x and y, the following inequality holds*

$$x^T y \le \rho(||x||) + \ell\rho(||y||), \tag{C.27}$$

and the equality is achieved if and only if

$$y = \rho'(||x||)\frac{x}{||x||}, \quad \textit{that is,} \quad x = (\rho')^{-1}(||y||)\frac{y}{||y||}. \tag{C.28}$$

Corollary C.3. *For any two vectors x and y, the following inequality holds*

$$x^T y \le \frac{\delta^p}{p}||x||^p + \frac{1}{q\delta^q}||y||^q, \tag{C.29}$$

where $\delta > 0$ and the constants $p > 1$ and $q > 1$ satisfy $(p-1)(q-1) = 1$.